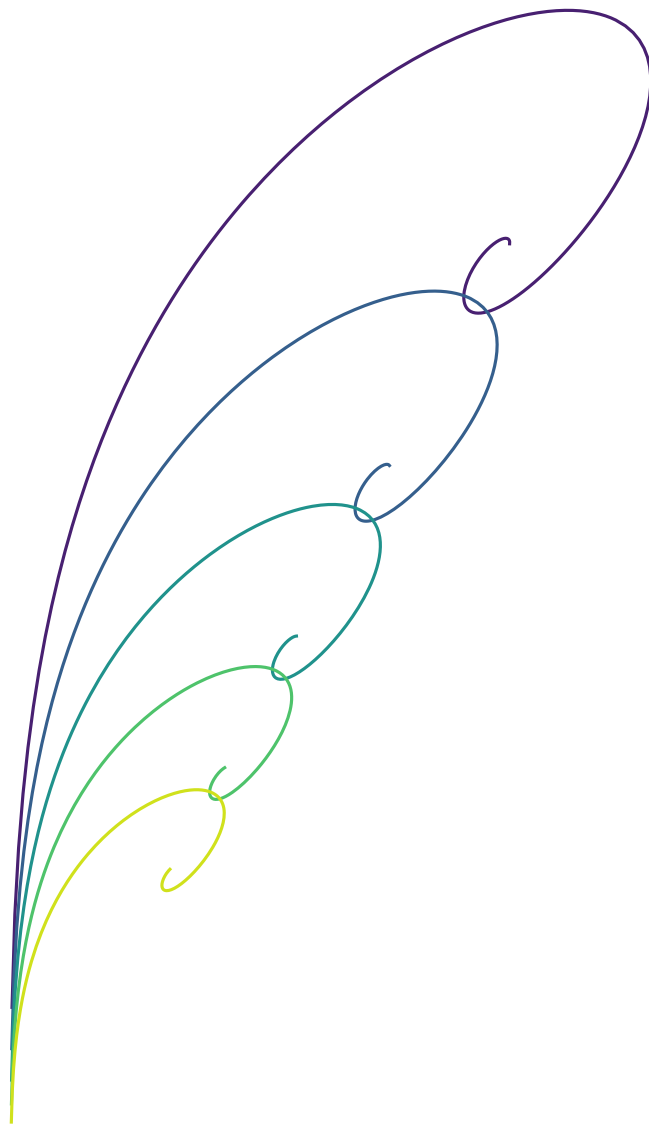


Master

Martin Kjøllesdal Johnsrud
Supervisor: Jens Oluf Andersen

September 21, 2022



Preface

This thesis is the concluding work of a 5-year Master of Science (“Sivilingeniør”) degree in Applied Physics (“Teknisk Fysikk”) at the Norwegian University of Science and Technology (NTNU), under the supervision of Professor Jens Oluf Andersen. It is the result of 20 weeks of work in the spring of 2022 and builds on work done in the specialization project (“Prosjektoppgave”) in the autumn of 2021. The topic of the thesis is the thermodynamic properties of the pion-condensed phase of quantum chromodynamics, which is investigated using three-flavor chiral perturbation theory, and the application of these results to the study of pion stars.

Conventions

In this thesis, we employ *natural units*, defined by $\hbar = c = k_B = 1$. Here, \hbar is Planck’s reduced constant, c is the speed of light, and k_B is Boltzmann’s constant. Dimensionful results are given in MeV or SI units and, unless otherwise stated, computed using the values given in section A.1. We use the “mostly minus” convention for the metric, in which $g_{\mu\nu} = \text{diag}(1, -1, -1, -1)$. Unless otherwise stated, we employ Einstein’s summation convention in which repeated indices are summed over, $a_i b_i = \sum_i a_i b_i = a_1 b_1 + a_2 b_2 + \dots$. Spacetime indices are denoted by μ, ν, ρ, η , or λ and should only be repeated once as a sub- and superscript, $a_\mu b^\mu = a^\mu b_\mu = g_{\mu\nu} a^\mu b^\nu$. The placement of other indices does not have any importance and is only chosen for readability.

Note to the reader

To make this thesis as self-contained as possible, and to ensure notation and definitions are clearly explained, parts of the specialization project have been included with only minor modifications. These parts should not be part of evaluating this thesis. They are marked with an asterisk (*) in their titles and in the table of contents. The parts are Appendix B and Appendix C; section A.4 and section A.5; from section 3.1 to and including section 3.4; subsection A.3.2, subsection A.3.2, subsection 5.2.2, subsection 5.2.1 and subsection A.3.2.

In addition, Chapter 1, section 5.1, section 6.5 are partially based on the specialization project, but contains substantial new work.

Acknowledgements

This thesis would never have been without all the help I have received, for which I am truly grateful. I want to thank my advisor, Jens Oluf Andersen, for his patience and mentorship. The guidance, hints and comments I have received have been invaluable, and without all the red ink spilled on older versions of this thesis it would have been far less coherent. I thank B. Brandt, G. Endrődi, and S. Schmalzbauer for providing their lattice data, and for helpful discussion. I thank Martin Mojahed, *in absentia*, as his excellent master’s thesis was a great help both as theoretical background and as a guide on how to write a thesis. Lastly, I want to thank my friends and family back home in Bø, as well as here in Trondheim for all their time and support.

Sammendrag

Muligheten for en ny type kompakte stjerner, navngitt pionstjerner, er nylig foreslått på teoretisk grunnlag. Pionstjerner er massive astrofysiske objekter bestående av et pionkondensat og holdt sammen av tyngdekraften. I denne masteroppgaven bruker vi kiral perturbasjonsteori med tre kvarktyper for å regne ut de termodynamiske egenskapene til pionkondensatet, som så blir brukt til å modellere pionstjerner. Vi gjennomgår det teoretiske fundamentet til kiral perturbasjonsteori og konstruksjonen av en effektiv Lagrange-tetthet bestående av pseudoskalare mesoner, blant dem pionene. Vi undersøker de termodynamiske egenskapene til denne modellen ved null temperatur, og med kjemisk potensial for isospin og strangeness, μ_I og μ_S , forskjellige fra null. Vi kartlegger fasediagrammet i $\mu_I - \mu_S$ -planet, hvor det skjer overganger fra vakuumfasen til kondenserte faser. Videre beregner vi pionkondensatets tilstandsligning til første og andre orden, samt inkludert effekten av elektromagnetiske vekselvirkninger. For å modellere et mer realistisk astrofysisk objekt, regner vi ut tilstandsligningen til et $\pi\ell\nu_\ell$ -system—et sammensatt system bestående av et pionkondensat, ladde leptoner, og neutrinoer.

Tilstandsligningene vi har kommet frem til brukes sammen med Tolman-Oppenheimer-Volkoffligningen for å regne ut trykk- og energiprofilen i pionstjerner, samt stjernenes masse og radius som funksjon av trykket i sentrum, kalt masseradiusrelasjonen. Vi sammenligner våre resultater for masseradiusrelasjonen med gitterberegninger av kvantekromodynamikk og finner god overenstemmelse. Analytiske resultater gjør det mulig å finne grenseverdier og gi fysiske tolkninger. Vi finner et uttrykk på lukket form for grenseverdien til radiusen for en pionstjerne bestående av et rent pionkondensat, og utforsker hvordan masseradiusrelasjonen til $\pi\ell\nu_\ell$ -systemet avhenger av overflatetrykket til stjernen.

Abstract

Recently, a new form of compact stars called pion stars has been proposed. These are massive, gravitationally bound, astrophysical objects composed of a pion condensate. In this thesis, we employ three-flavor chiral perturbation theory to calculate the thermodynamic properties of the pion condensate which we use to model pion stars. We survey the theoretical foundations of chiral perturbation and the construction of the effective Lagrangian of the pseudo-scalar mesons, which includes the pions. With this Lagrangian, we investigate its thermodynamics at zero temperature and non-zero isospin and strangeness chemical potential, μ_I and μ_S . We map out the phase diagram in the $\mu_I - \mu_S$ -plane, where the vacuum phase transitions into condensed phases. We furthermore calculate the equation of state of the pion condensate, parameterized by μ_I for a pure condensate to leading and next-to-leading order, and including the effects of electromagnetic interactions. To model more realistic astrophysical objects, we additionally calculate the equation of state of a $\pi\ell\nu_\ell$ -system—a composite system including charged leptons and neutrinos.

The equations of state we obtained are then used as inputs to the Tolman-Oppenheimer-Volkoff equation, which we use to calculate the pressure and energy distribution of pion stars, as well as the stellar mass and radius as a function of the central pressure—the mass-radius relation. We compare our results for the mass-radius relation to earlier results from lattice QCD calculations and find good agreement. Analytical results allow for discussion of their physical causes and derived various limits. We give a closed-form expression for the limiting radius of a pion star composed of a pure pion condensate and investigate how the mass-radius relation of the $\pi\ell\nu_\ell$ -system is determined by its surface pressure.

Contents

Preface	i
Sammendrag	ii
Abstract	iii
1 Introduction	1
1.1 Pion stars	1
1.2 The standard model, QCD, and effective theories	2
1.3 Thermodynamics and the physics of compact stars	4
1.4 The QCD phase diagram	4
1.5 Outline of theseis	6
I Theoretical background	9
2 Mathematics	11
2.1 Differential geometry	11
2.2 Lie theory and the mathematics of symmetry	19
3 Quantum field theory	23
3.1 *QFT via path integrals	23
3.2 *The 1PI effective action	25
3.3 *Symmetry and Goldstone's theorem	29
3.4 *CCWZ construction	34
3.5 Constructing an effective field theory	37
4 Gravity	43
4.1 Newtonian Gravity	43
4.2 General relativity	44
4.3 The TOV equation	47
4.4 A star of cold, non-interacting fermions	54
II χPT and the pion-condensed phase	63
5 Chiral perturbation theory	65
5.1 Quantum chromodynamics	65
5.2 Chiral perturbation theory	68
5.3 Three-flavor χ PT to leading order	72
5.4 Next-to-leading order Lagrangian	82
6 Thermodynamics	85
6.1 Free energy in a homogenous system	85
6.2 Leading order analysis	86
6.3 Phase transitions	90
6.4 Electric charge neutrality	94
6.5 Next-to-leading order results	100

III	Pion stars	109
7	Pion stars	111
7.1	Units and limiting radius	111
7.2	Leading order results	112
7.3	Next-to-leading order results	118
7.4	Key values and results	119
7.5	Comparison with lattice QCD results	121
8	Concluding remarks	125
8.1	Summary	125
8.2	Outlook and further research	126
	Appendices	131
A	Appendix A	131
A.1	Constants and units	131
A.2	Algebra bases	132
A.3	Functionals	133
A.4	*Consistent series expansion of observables	138
A.5	*Integrals in dimensional regularization	140
B	*Two flavor results	143
B.1	*Two-flavour χ PT to leading order	143
B.2	*Next-to-leading order Lagrangian	145
B.3	*Rewriting terms	147
B.4	*Rewriting NLO Lagrangian	149
C	*Thermal field theory	151
C.1	*Statistical mechanics	151
C.2	*Imaginary-time formalism	152
C.3	*Free scalar field	155
C.4	*Interacting scalar field	160
C.5	*Fermions	163
D	Code	165
D.1	Integrating the TOV equations	165
D.2	Symbolic calculations in χ PT	166
D.3	Spherically symmetric metric	166
	Bibliography	173

Sections with (*) are adapted from the specialization project with only minor changes as discussed in the preface.

Chapter 1

Introduction

This remark is based on a “theorem”, which as far as I know has never been proven, but which I cannot imagine could be wrong.

— Steven Weinberg, 1979 [1]

1.1 Pion stars

Stars and planets have long been one of the main driving engines behind the developments of physics. A lot of early mathematics was developed to navigate using the stars and to predict the seasons and the phases of the moon. One of the most important confirmations of Newton’s laws of motion and gravity was their prediction of Kepler’s laws from more basic assumptions. Kepler’s laws concern the orbits of planets around the sun. They are empirical observations made by Kepler after studying the data gathered by Tycho Brahe. Likewise, the successor to Newton’s law of gravitation, Einstein’s general relativity, was first shown to be more accurate than its predecessor by predicting the drift of the perihelion of the orbit of Mercury [2]. The radiation of the Sun has been part of the development of the theory of light and thermal radiation [3]. To understand the process that fuels the Sun, we had to develop special relativity, in which mass is described as just another form of energy, as well as quantum mechanics and the theory of nuclear fusion. Observations of the neutrinos resulting from these processes lead to the discovery of neutrino oscillations [4]. Today, this is one of the few empirical observations in physics that conflict with the standard model of particle physics. The Sun might therefore still be part of the development of new fundamental physics.

Even after a star has depleted its fusion fuel it can remain an object of great interest. Stars with less mass than around 10 times that of the sun, M_{\odot} , will towards the end of their active life shed most of their outer layers, leaving behind an inert white-hot mass only supported by the pressure from its electrons. These remnants are called *white dwarfs*. A characteristic property of fermions, such as electrons, is the Pauli exclusion principle, which states that two identical fermions may not occupy the same quantum state. This leads to *degeneracy pressure*, where tightly packed fermions exert pressure, not as a result of any interaction, but solely due to this exclusion principle. It is due to this effect that electrons can withstand the gravitational pull of white dwarfs. One cubic centimeter of the material that makes up white dwarfs weighs more than a ton. Sirius B, the fainter companion to Sirius, is a white dwarf. Type Ia supernovae happen as white dwarfs reach their upper mass limit, the Chandrasekhar limit, and are invaluable in mapping the distances of our universe [2]. White dwarfs, together with the even more dense *neutron stars*, are collectively known as *compact stars*. Neutron stars are left after the supernova explosions of massive stars [4]. They were first predicted solely on theoretical backgrounds and

later discovered in the form of pulsars, rotating neutron stars with frequencies below a tenth of a second, where strong magnetic fields act as particle accelerators [4]. Compact stars are some of the most extreme environments in our universe, and as such, they are excellent arenas for the study of exotic physics.

Recently, a new class of compact stars has been proposed, called pion stars [5–7]. These stars are composed of a pion condensate. As pions are bosons, they do not obey the Pauli exclusion principle, and pion stars cannot rely on degeneracy pressure to support themselves. Instead, the pions must have a repulsive interaction to exert such pressure. Pion stars are, as yet, only a theoretical proposal. However, if history is to be of any guidance, that does not mean there aren't valuable insights to be gained from researching them. Only with a model of how pion stars behave can we ever hope to detect them. To that end, we need a theory of the matter that makes up such a star.

1.2 The standard model, QCD, and effective theories

The Standard Model of particle physics is the totality of what particle physicists are confident they understand concerning the fundamental building blocks of our universe. It is arguably the most successful scientific theory of all time and makes fantastically accurate predictions of the behavior of fundamental particles. In combination with general relativity, it is our best framework for explaining how the world works. The Standard Model is a quantum field theory (QFT) and describes both the elementary matter particles and the forces between them as excitations in quantum fields permeating all space-time. These fields and their dynamics are captured in the *Lagrangian density*, or just Lagrangian, of the model. In deceptively compact notation, this can be written

$$\mathcal{L}_{\text{SM}} = \bar{\psi}_i \not{D}_{ij} \psi_j - \frac{1}{4} F_{\alpha}^{\mu\nu} F_{\mu\nu}^{\alpha} - (\bar{\psi}_{L,i} \Phi Y_{ij} \psi_{R,j} + \text{h.c.}) + |D_{\mu} \Phi|^2 + \mathcal{V}(\Phi). \quad (1.1)$$

Here, the ψ_i 's are the fermionic fields, of which atoms are made. The forces are encoded in D and F , and their form are determined by the *gauge group* of the Standard Model, $\text{SU}(3)_c \times \text{SU}(2)_L \times \text{U}(1)_Y$. This is the set of all gauge symmetries. More generally, symmetries such as gauge symmetries or the Lorentz symmetry of special relativity greatly constrain the form of \mathcal{L}_{SM} . Lastly, Φ is the Higgs-field, whose interaction with other fields are responsible for the mass of particles [8, 9]. The fundamental particles of the Standard Model, as well as composite particles such as atoms or molecules, are excitations in the fields of Eq. (1.1). The fundamental particles are illustrated in Figure 1.1 [9, 10]. If we include the masses of neutrinos in the Standard Model, it has 26 free parameters [11]. We should, in principle, be able to derive all of particle physics from the Standard Model together with these parameters, and from that subsequently chemistry and all other physical sciences. In practice, however, we must often resort to domain-specific models, which might be guided by the Standard Model, but ultimately are independent. However, unless you hope to supplant the Standard Model, no such model should violate it. The Standard Model obeys general constraints such as the conservation of energy and the speed of light as the ultimate speed limit. These constraints are powerful guiding lights as we seek to explore physics.

The part of the Standard Model that describes the interaction of quarks via the strong force, mediated by the gluons, is called *quantum chromodynamics* (QCD). Quarks are the building blocks of the nuclear particles, protons and neutrons, and the nuclear force that binds together atoms is a result of QCD. A complete understanding of this theory is of great interest. However, the fact that the force mediated by gluons is so strong greatly limits our understanding. This is because our main technique for handling quantum field theories, perturbation theory, fails. In perturbation theory, we rely on interactions being weak. This is quantified by an expansion parameter, α , to which the strength of each interaction is proportional. If $\alpha < 1$, then each

	Fermions		Bosons
gen.	leptons	quarks	
1	e ν_e	u_{up} d_{down}	Z g W^{\pm} γ
2	μ ν_{μ}	c_{charm} s_{strange}	
3	τ ν_{τ}	t_{top} b_{bottom}	H

Figure 1.1: The particles of the standard model come in two main groups. The bosons include the force-carrying gauge particles and the Higgs boson (H). The fermions make up matter, and come in three “generations”.

such interaction in a process will suppress it by a factor α . The scattering of two particles is then calculated as a sum of all possible processes—combinations of interactions between the fields—that could lead to that event. Processes with more interactions will contribute less to the total sum, as each interaction suppresses by α . Each process is illustrated by a Feynman diagram, in which particles come in from the left, interact via *virtual particles*, then leave to the right. The process of electron-muon scattering in quantum electrodynamics (QED) is given by

In QED, the expansion parameter is the fine structure constant, $\alpha = e^2/(4\pi)$ where e is the elementary electrical charge. In renormalized theories, such as QED, this parameter is dependent on the energy scale Q the processes happen at. This is called the *running* of the coupling. At $Q = 0$, $\alpha \approx 7 \times 10^{-3}$, and only a few orders in perturbation theory will therefore give highly precise and accurate results.¹

In QCD, we have no such luck. The equivalent of the fine-structure constant in QCD, α_s , increases as the energy scale decreases, in contrast to α . As a consequence, perturbation theory breaks down for Q below around 1 GeV. This includes everything but the most extreme situations in the universe. At such energy scales, quarks and gluons are bound together as *hadrons*. Hadrons are divided into two classes, *baryons* and *mesons*. The nucleons making up the core of atoms—the neutron and the proton—are among the baryons. Baryons are made up of three quarks, while mesons are made of two. The lightest meson, the pion, was predicted theoretically by Hideki Yukawa as the carrier of the nuclear force and later discovered by Cecil Powell *et al.* [10].

We are unable to directly and analytically describe QCD at low energies due to this breakdown of perturbation theory. There are numerical schemes, namely lattice QCD, which allow for calculations of low-energy QCD. These methods rely on large amounts of computing power, and as we will detail further, have problems with important cases of interest due to the so-called sign problem. We will tackle the problem by using an *effective field theory*. When constructing an effective field theory, we come to terms with the fact that we do not know all

¹The series expansion in terms of coupling constants is, strictly speaking, not a converging series, but rather an asymptotic series. We can see this by considering the consequences of exchanging α for $-\alpha$. Such a theory would be unstable as like charges would attract. This implies any expansion in α has a zero radius of converge [12]. We must therefore consider the sum of Feynman-diagrams as an asymptotic series, which yields a good approximation *if terminated soon enough* [13].

physics. Instead, we settle for a description of the most important parts. In modern physics, effective field theories have become a ubiquitous tool and are employed in both condensed matter physics and high-energy physics. In fact, it is now believed that the Standard model itself is an effective field theory, a low energy description of a more complete theory [14, 15]. The “theorem” Weinberg discusses in the opening quote of this chapter describes why effective field theories are such powerful tools. In short, it states that quantum field theories alone contain very little information, and thus can model almost everything. If we write down the most general Lagrangian, we have not made more than very basic assumptions [1]. This will be our guiding philosophy when constructing *chiral perturbation theory* (χ PT), the effective theory of mesons.

1.3 Thermodynamics and the physics of compact stars

In the same way that we are lucky nature allows us to ignore high-energy effects and instead use an effective theory of low-energy interactions, statistical mechanics and thermodynamics allow us to describe composite systems containing a large number of degrees of freedom with only a few variables. Instead of perfectly describing all degrees of freedom and their interactions, we consider what the average system would look like. As long as the system is large enough and is in thermal equilibrium, which means that the system is in a stable state where the thermodynamic variables are well-defined and without internal flows of matter or energy, then this gives an astonishingly effective and economical description of the system. There are several choices for free variables when describing a thermodynamic system. The temperature of a system, T , determines whether energy would flow to or from that system to a different system with a different temperature T' . In our description of pion stars, we will assume $T = 0$, as they are much denser than they are hot and thermal effects thus can be neglected to a first approximation. We work in the *grand canonical ensemble*, in which we consider the system coupled to a source of *conserved charges*, such as electrical charge, or particle number in non-relativistic physics. By adjusting the chemical potential, μ , corresponding to a conserved charge, Q , we set how energetically favorable it is to add a new charge to the system, and thus the charge density of a typical system.

In our case, all relevant thermodynamic variables are independent of the volume of the system, and chemical potential is thus the only free variable. Therefore, it determines all other variables, such as energy density u and pressure p . This relationship, which can be stated implicitly on the form $f(p, u, \mu) = 0$, is called the *equation of state* of the system. We will use the Tolman-Oppenheimer-Volkoff (TOV) equation to model pion stars. This is based on general relativity and describes a static sphere of matter and energy in which the outward push of its internal pressure is balanced by gravity. The TOV equation needs the equation of the state of the substance it describes as an input. To model pion stars, then, we must calculate the equation of state of the pion condensed-phase of QCD.

1.4 The QCD phase diagram

A phase diagram illustrates the properties of a medium under different circumstances. The pion condensed phase is only one part of the rich phase diagram of QCD, an active area of research. Our understanding of it is far from complete due to the difficulties of working with the strong force. Figure 1.2 shows a rough sketch of our current understanding of the QCD phase diagram. The axes are temperature T , baryon chemical potential μ_B , and isospin chemical potential μ_I . The baryon and isospin chemical potentials quantify the abundance of quarks compared to antiquarks and up quarks compared to down quarks, respectively.

Close to $T = \mu_B = \mu_I = 0$, QCD is in the vacuum phase, where hadrons form a gas whose

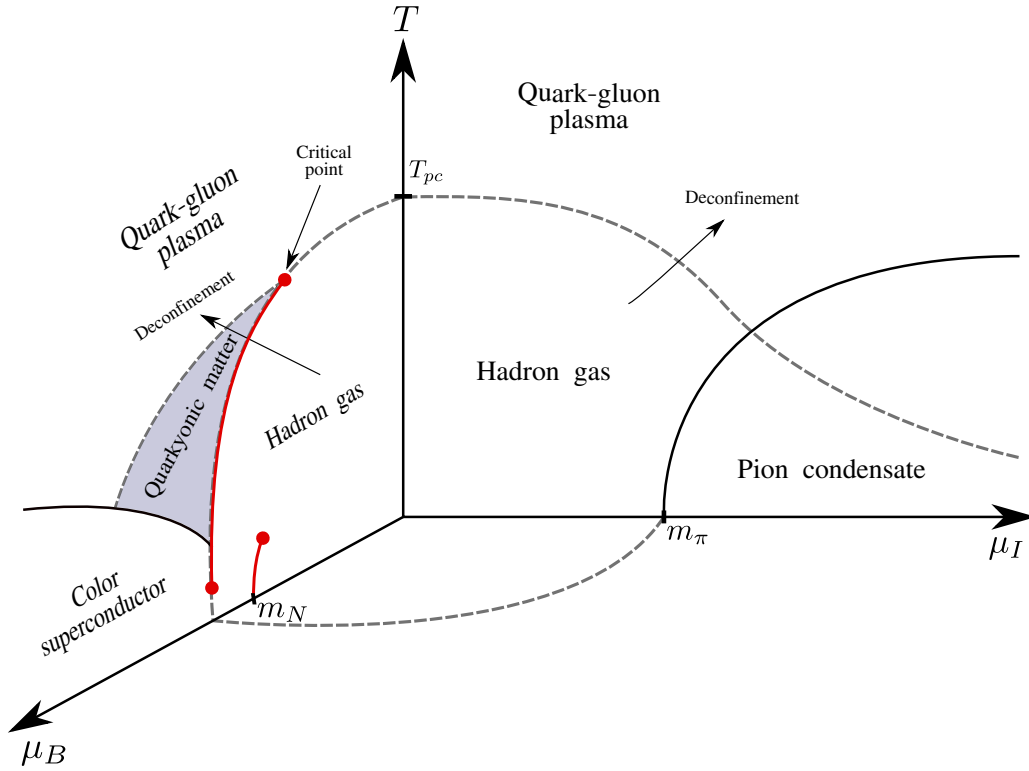


Figure 1.2: A sketch of the QCD phase diagram based on [16–18]. See main text for a detailed description.

density and composition depend on the temperature and chemical potentials. The first explorations of the phase transitions were done when it was noticed at CERN that hadrons seem to have a maximum temperature, the Hagedorn temperature of around 160 MeV or $1.9 \times 10^{12} \text{ K}$. A more modern understanding of this temperature is as a point of phase transition, in which the quarks cease to be bound together as hadrons and instead form a soup of nearly free particles called quark-gluon plasma. This process is called deconfinement and is a consequence of the weakening of the strong force at higher energies, called *asymptotic freedom* [19, 20]. At zero isospin and baryon chemical potential, this transition called a crossover, is smooth and characterized by a pseudo-critical temperature T_{pc} [16]. Recent lattice QCD results indicate T_{pc} is around 160 MeV [21]. Experimental observation of quark-gluon plasma was first reported by the Relativistic Heavy Ion Collider at Brookhaven National Laboratories in 2006 [22, 23].

As the baryon chemical momentum increases, nucleons undergo a gas-liquid transition at low temperatures. This happens approximately at the nuclear mass, $\mu_I \approx m_N \approx 0.9 \text{ GeV}$. When increasing μ_B further, asymptotic freedom means that perturbative treatments again become available. Under such conditions, QCD enters a phase analogous to that of an electrical superconductor and forms a *color superconductor*. Here, quarks form Cooper pairs as electrons do in the Bardeen-Cooper-Schrieffer (BCS) theory of electromagnetic superconductors. Furthermore, there is a color Meissner effect, in which gluons gain mass due to the Higgs mechanism, as the photon does in electromagnetic superconductors. The transition from the vacuum phase to the color superconducting phase is not well understood. Here, the density is still too low for perturbative treatment and numerical lattice calculations are haunted by the *sign problem*. Lattice methods discretize quantum fields on a finite lattice, representing space-time, then randomly sample configurations using the Metropolis-Hastings algorithm. This, however, relies on each configuration having a real, positive weight which allows for the inclusion of a minority of important configurations. For non-zero baryon chemical potential, this is not the case, and lattice methods, therefore, fail [24].

This problem does not arise in the case of zero baryon chemical potential, but a non-zero isospin

chemical potential. QCD lattice results, therefore, allow for an exploration of the behavior of QCD under non-zero μ_I . χ PT predicts a second order phase transition from the vacuum phase to a pion-condensed phase at $\mu_I = m_\pi$ [25]. Early lattice calculations agree with these results [26–29], which have been further confirmed by subsequent studies [6, 30–33]. The pion condensate is characterized by a non-zero condensate with an isospin charge. This phase is a Bose-Einstein condensed (BEC) phase, in which a zero-momentum state is highly occupied by identical bosons. At asymptotically large μ_I , it is conjectured that the BEC phase continuously transitions into a deconfined BCS state [25, 34].

Mapping out the full phase diagram and nature of the critical points and the phase transitions of QCD is one of the most basic questions in physics—what happens to the fundamental building blocks of matter if they are heated up or compressed? As such, it is an imperative in basic science to extend our knowledge on this subject and to develop a wide array of methods of investigation to check our assumptions. As stated earlier, the dynamics of stars have always been a great inspiration and guidance for the development of physics. As the most extreme furnaces in the universe, they serve as an excellent, real-world test for our theoretical understanding of exotic states of matter. It is believed that the core of neutron stars consists of deconfined quark matter, which could be in a color superconducting phase [18, 35]. They may thus play an important part in developing our understanding of the extreme forms of QCD. The early universe is another place of extreme conditions. Although the exact conditions are still unclear, it has been shown that the conditions there might have caused pion condensation. If so, this would leave possibly observable traces in the form of gravitational waves [36–38]. Furthering our understanding of the pion-condensed phase and the properties of the stars it might form, then, is an important part of a project to map out the behavior of the most fundamental building blocks in the universe and the traces they might have left for us to find.

1.5 Outline of theseis

To make this thesis as self-contained as possible, we have included some parts from the earlier specialization project with only minor modifications. These parts are therefore marked with an asterisk (*) in the headers and the table of contents. The parts are Appendix B and Appendix C; section A.4 and section A.5; from section 3.1 to and including section 3.4; subsection A.3.2, subsection A.3.2, subsection 5.2.2, subsection 5.2.1 and subsection A.3.2. We aim for this to be readable for someone who has the background equivalent of a master’s degree in physics and some familiarity with particle physics, quantum field theory, and general relativity, but not necessarily any specific knowledge of chiral perturbation theory or the modeling of compact stars. This thesis, therefore, contains an extensive introduction to the requisite theory as well as appendices with additional material.

Part I of this thesis surveys the theoretical foundations of χ PT and the modeling of pion stars. In Chapter 2, we summarize the mathematical prerequisites, specifically differential geometry and Lie theory. We introduce the notion of smooth manifolds and tensor fields. By introducing the metric, we develop a generalization of calculus to manifolds. This is then applied to study Lie groups and Lie algebras. Chapter 3 develops the necessary background in quantum field theory. We outline the path integral formulation of QFT and apply this to introduce the 1PI effective action, the role of symmetry and the CCWZ construction. We then discuss the notion of effective field theories, and how to construct one. In Chapter 4 we survey the physics of gravity. We discuss the Newtonian theory and its successor, general relativity, and apply this to derive the TOV equation of hydrostatic equilibrium. This is used to study a simple model of neutron stars.

In Part II, we apply the theory to develop and study χ PT. We start in Chapter 5 by summarizing QCD, which allows us to construct the effective Lagrangian of χ PT to leading and

next-to-leading order. We study the spectrum of the resulting particles, and how it is affected by electromagnetic interactions and a non-zero isospin and strangeness chemical potential. In Chapter 6, we investigate the thermodynamic properties of the condensed phases of χ PT. We draw the phase diagram in the $\mu_I - \mu_S$ plane and discuss the effect of EM interactions. The nature of the phase transitions is discussed. Furthermore, we calculate the equation of state of the pion-condensed phase to leading and next-to-leading order, and in a charge-neutral system including charged leptons and neutrons.

Finally, our results are applied to model pion stars in Part III. In Chapter 7, we use the equations of state we found together with the TOV equation to calculate the pressure and mass profile of pion stars, as well as the mass-radius relation. We discuss how the different compositions and orders in perturbation theory affect the resulting stars and compare our results to earlier numerical calculations. In Chapter 8, we summarize our results and discuss ways to improve them and avenues for further research.

The appendices include definitions, derivations, and background theory left out of the main text. They are referenced in the main text when relevant. Appendix A include the numerical values of physical constants, the properties and explicit forms of algebras used in the text as well as additional derivations. Appendix B and Appendix C are parts of the specialization project included as supplemental material. Appendix B details theory and results for the two-flavor case of χ PT, while Appendix C summarizes thermal field theory. The code used to derive the results of this thesis is discussed in Appendix D, where we also link to an online open source repository where it is available in full.

Part I

Theoretical background

Chapter 2

Mathematics

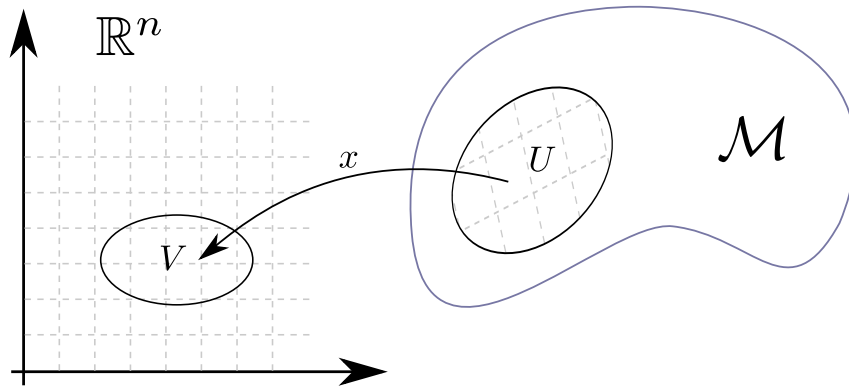


Figure 2.1: The coordinate function x maps a neighborhood U in the manifold \mathcal{M} to a neighborhood V in \mathbb{R}^n .

2.1 Differential geometry

This section is based on [2, 39].

General relativity, and a lot of quantum field theory, are formulated in the language of *differential geometry*. Differential geometry generalizes n -dimensional calculus to more general spaces than the usual \mathbb{R}^n , such as curved spacetime or the more abstract space of symmetries of a quantum field theory. The most important objects in differential geometry are *smooth manifolds*. An n -dimensional manifold, \mathcal{M} , is a set of points, locally homeomorphic to \mathbb{R}^n . That is, for all points $p \in \mathcal{M}$, there exists a neighborhood U around p , together with a corresponding set of continuous, bijective functions that map U to a neighborhood V in \mathbb{R}^n ,

$$x : U \subseteq \mathcal{M} \mapsto V \subseteq \mathbb{R}^n, \quad (2.1)$$

$$p \mapsto x^\mu(p), \quad \mu \in \{0, \dots, n-1\}. \quad (2.2)$$

This is illustrated in Figure 2.1. We call $x(p) = (x^0(p), \dots, x^{n-1}(p))$ a coordinate function of \mathcal{M} . The inverse of x , x^{-1} , obeys $x^{-1}(x(p)) = p$, for all $p \in U$. A smooth manifold is one in which the coordinate functions are infinitely differentiable. To define differentiability on manifolds, consider two coordinate functions, x , and x' . The corresponding domains U and U' may or may not overlap. We then define the transition function, a function between subsets of \mathbb{R}^n by mapping via \mathcal{M} , as

$$f_{x' \rightarrow x} = x \circ x'^{-1} : \mathbb{R}^n \mapsto \mathbb{R}^n. \quad (2.3)$$

This map is illustrated in Figure 2.2.¹ A set of coordinate functions $\mathcal{A} = \{x_i\}$ whose domain cover \mathcal{M} is called an *atlas* of \mathcal{M} . If the transition function between all pairings of coordinate functions in the atlas is smooth—that is, infinitely differentiable—we call the atlas smooth. We then define a smooth manifold as the topological manifold \mathcal{M} together with a *maximal* smooth atlas \mathcal{A} . A smooth atlas is maximal if no coordinate function can be added while the atlas remains smooth.²

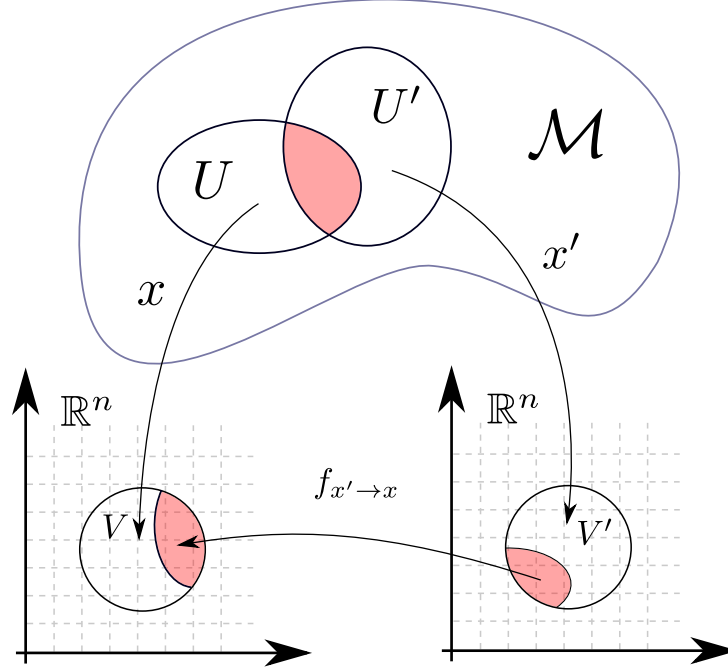


Figure 2.2: The transition map $f_{x' \rightarrow x}$ between two coordinate functions, x' and x , maps between the images of these function, via the manifold \mathcal{M} . The function's domain and image are restricted to a (possibly empty) subset of the images of x' and x . This is illustrated by the shaded regions in V' and V .

Consider two m - and n -dimensional smooth manifolds \mathcal{M} and \mathcal{N} . Let x denote the coordinates on \mathcal{M} , while y denotes the coordinates on \mathcal{N} . We can define smooth functions between these manifolds similarly to how we define smooth coordinates. Consider the function

$$F : \mathcal{M} \mapsto \mathcal{N}. \quad (2.4)$$

It is said to be smooth if, for all points $p \in \mathcal{M}$, there is a set of local coordinates x around p and y around $F(p)$ such that the map $\tilde{F} = y \circ F \circ x^{-1}$ is smooth. This map may be illustrated by a diagram,

$$\begin{array}{ccc} \mathcal{M} & \xrightarrow{F} & \mathcal{N} \\ \downarrow x & & \downarrow y \\ \mathbb{R}^m & \xrightarrow{\tilde{F}} & \mathbb{R}^n \end{array} \quad (2.5)$$

We will not be careful with the distinction between F , the function between the abstract manifolds, and \tilde{F} , the function of their coordinates, but rather denote both by $F(x)$. We may take the partial derivative of such a function with respect to the coordinates x , $\partial F / \partial x^\mu$. However, this is dependent on our choice of coordinates, as a set of local coordinates can always be scaled arbitrarily. Any physical theory must be independent of our choice of coordinates, so our next task is to define the properties of a smooth manifold in a coordinate-independent way.

¹To be rigorous, one has to restrict the domains and image of the coordinate function when combining them. This is illustrated in Figure 2.2.

²The maximal condition ensures that two equivalent atlases correspond to the same differentiable manifold. A single manifold can be combined with different maximal atlases of smooth coordinates or differentiable structures. A set of examples are *exotic spheres*, smooth manifolds *homeomorphic* to S^n , but not *diffeomorphic*.

2.1.1 Vectors and tensors

A curve γ through \mathcal{M} is a function from \mathbb{R} to \mathcal{M} ,

$$\gamma : \mathbb{R} \mapsto \mathcal{M}, \quad (2.6)$$

$$\lambda \mapsto \gamma(\lambda). \quad (2.7)$$

Such curves are often denoted only by their coordinates and the parameter λ , $x^\mu(\lambda) = (x^\mu \circ \gamma)(\lambda)$. With this curve, we can take the directional derivative of a real-valued function on the manifold, $f : \mathcal{M} \mapsto \mathbb{R}$. Assume $\gamma(\lambda = 0) = p$. As we are always taking the derivative of functions between \mathbb{R}^n , for different n , we can use the chain rule. The directional derivative of f at p , given by this curve γ , is then

$$\left. \frac{d}{d\lambda} f(x(\lambda)) \right|_p = \left. \frac{dx^\mu}{d\lambda} \right|_{\lambda=0} \left. \frac{\partial}{\partial x^\mu} f(x) \right|_p. \quad (2.8)$$

The set of all such directional derivatives, $d/d\lambda$ at p , form a vector space, $T_p\mathcal{M}$, called the *tangent space*. The tangent space is illustrated in Figure 2.3.

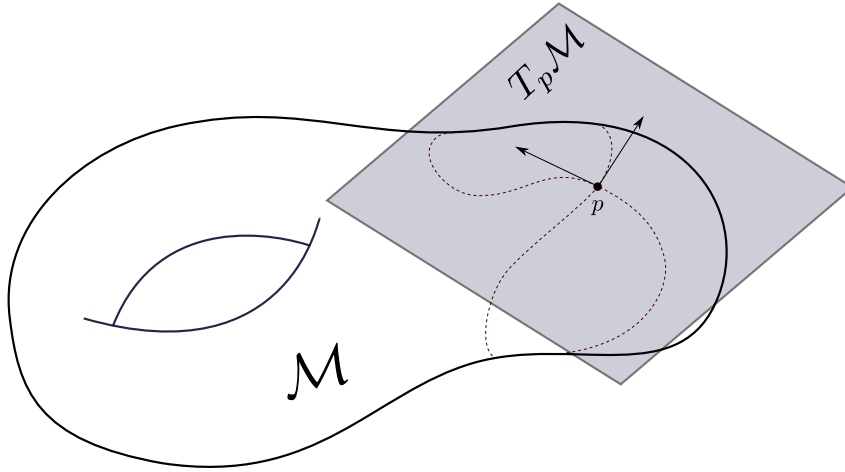


Figure 2.3: The tangent space $T_p\mathcal{M}$, the shaded rectangle, is the set of all directional derivatives at $p \in \mathcal{M}$. A directional derivative is defined in terms of a curve that passes through p .

The coordinates x^μ induce a basis of this vector space, namely partial derivatives with respect to the coordinate functions at p ,

$$e_\mu = \left. \frac{\partial}{\partial x^\mu} \right|_p = \partial_\mu|_p, \quad \mu \in \{0, \dots, n-1\}. \quad (2.9)$$

Any element $v \in T_p\mathcal{M}$ can therefore be written

$$v = v^\mu \partial_\mu|_p = \left. \frac{dx^\mu}{d\lambda} \right|_{\lambda=0} \left. \frac{\partial}{\partial x^\mu} \right|_p. \quad (2.10)$$

Here, λ is the parameter of the curve corresponding to the directional derivative v .³ The evaluation at $\lambda = 0$ and p will often be implicit for ease of notation. This directional derivative acts on functions $f : \mathcal{M} \mapsto \mathbb{R}$ as

$$v(f) = v^\mu \partial_\mu f. \quad (2.11)$$

³There is not only one curve corresponding to any directional derivative but rather an equivalence class. We will gloss over this technicality, as it does not affect our work.

A map F between two manifolds \mathcal{M} and \mathcal{N} also induces a map between the tangent spaces of these manifolds. This is the *differential* of F at p ,

$$dF_p : T_p\mathcal{M} \longrightarrow T_p\mathcal{N}, \quad (2.12)$$

$$v \longmapsto dF_p(v). \quad (2.13)$$

$dF_p(v)$ is an element of $T_p\mathcal{N}$, i.e., it is a directional derivative on \mathcal{N} . It is defined by how it acts on functions $g : \mathcal{N} \mapsto \mathbb{R}$,

$$dF_p(v)(g) = v(g \circ F), \quad (2.14)$$

It thus acts on functions on \mathcal{N} by “extending” the derivative v . This is a linear map between vector spaces and may be written in component form by considering the differentials of the coordinate functions. Denote the coordinates of \mathcal{N} by y^μ , and $y^\mu \circ F = F^\mu$. Then,

$$dF_p(\partial_\mu)(g) = \partial_\mu(g \circ F)|_p = \left. \frac{\partial F^\nu}{\partial x^\mu} \right|_p \left. \frac{\partial g}{\partial y^\nu} \right|_{F(p)}, \quad (2.15)$$

or more suggestively

$$dF \left(\frac{\partial}{\partial x^\mu} \right) = \frac{\partial F^\nu}{\partial x^\mu} \frac{\partial}{\partial y^\nu}. \quad (2.16)$$

This is a linear map of vectors between two vectors by the matrix $A_\mu{}^\nu = \partial_\mu F^\nu$. The differential is thus a generalization of the Jacobian. In the case of a real valued function, $f : \mathcal{M} \mapsto \mathbb{R}$, and $g : \mathbb{R} \mapsto \mathbb{R}$, we get

$$df(v)(g) = v(g \circ f) = (v^\mu \partial_\mu f) \frac{dg}{dy}. \quad (2.17)$$

df is thus a map from $T_p\mathcal{M}$ to $T_{f(p)}\mathbb{R}$, which is isomorphic to \mathbb{R} . Let g be the identity function, so that $dg/dy = 1$. Then, the differential of a scalar function, also called a 1-form, is a map from vectors v to real numbers,

$$df(v) := v^\mu \partial_\mu f. \quad (2.18)$$

The set of all linear maps from a vector space V to the real numbers is called the *dual space* of V , denoted V^* . This is a new vector space with the same dimensionality as V . We denote the dual of $T_p\mathcal{M}$ as $T_p^*\mathcal{M}$. We can regard each coordinate function as a real-valued function with a corresponding differential. This differential obeys

$$dx^\mu(\partial_\nu) = \frac{\partial x^\mu}{\partial x^\nu} = \delta_\nu^\mu. \quad (2.19)$$

The differentials of the coordinate functions thus form a basis for $T_p^*\mathcal{M}$, called the dual basis. Any differential df can thus be written as $df = \omega_\mu dx^\mu$ for some components ω_μ . We find the components by applying the differential to the coordinate basis, $df(\partial_\mu) = \partial_\mu f = \omega_\mu$. In other words, we recover the classical expression

$$df = \frac{\partial f}{\partial x^\mu} dx^\mu, \quad (2.20)$$

however we now interpret it as a covector-field instead of an “infinitesimal displacement”.

Linear maps from vectors to real numbers is generalized by *tensors*. Given a vector space V , a general (n, m) tensor T is a multilinear map, which associates n elements from V and m from its dual V^* to the real numbers, i.e.,

$$T : V \times V \times \cdots \times V^* \times \cdots \longmapsto \mathbb{R}, \quad (2.21)$$

$$(v, u, \dots; \omega, \dots) \longmapsto T(v, u, \dots; \omega, \dots). \quad (2.22)$$

Multilinear means that T is linear in each argument. The set of all such maps is the tensor product space $V \otimes V \otimes \cdots \otimes V^* \otimes \cdots$, a $\dim(V)^{n+m}$ -dimensional vector space. If $\{e_\mu\}$ and $\{e^\mu\}$

are the basis for V and V^* , then we can write the basis of this of the tensor product space as $\{e_\mu \otimes \cdots \otimes e^\nu \otimes \cdots\}$. The tensor can thus be written

$$T = T^{\mu\nu\cdots}_{\rho\cdots} e_\mu \otimes e_\nu \otimes \cdots e^\rho \otimes \cdots, \quad T^{\mu\nu\cdots}_{\rho\cdots} = T(e^\mu, e^\nu, \dots; e_\rho, \dots). \quad (2.23)$$

We often want to decompose a tensor down into its symmetric and antisymmetric parts. To do this, we introduce the symmetrization of a tensor T ,

$$T_{(\mu_1 \dots \mu_n)} = \frac{1}{n!} \sum_{\sigma \in S_n} T_{\mu_{\sigma(1)} \dots \mu_{\sigma(n)}}, \quad (2.24)$$

where S_n is the set of all permutations of n objects. The antisymmetrization of a tensor is defined as

$$T_{[\mu_1 \dots \mu_n]} = \frac{1}{n!} \sum_{\sigma \in S_n} \text{sgn}(\sigma) T_{\mu_{\sigma(1)} \dots \mu_{\sigma(n)}}. \quad (2.25)$$

The function $\sigma = \pm 1$, depending on if σ is a even or odd permutation. We may now write

$$T_{\mu\nu} = T_{(\mu\nu)} + T_{[\mu\nu]}. \quad (2.26)$$

2.1.2 Geometry and the metric

The metric is a symmetric, non-degenerate $(0, 2)$ tensor

$$ds^2 = g_{\mu\nu} dx^\mu \otimes dx^\nu. \quad (2.27)$$

It defines the geometry of the manifold \mathcal{M} and is the main object of study in general relativity. As it is invertible, we can define $g^{\mu\nu} = (g^{-1})_{\mu\nu}$, which is the components of a $(2, 0)$ tensor. We use this to raise and lower indices, as is done with the Minkowski metric $\eta_{\mu\nu}$ in special relativity.

Up until now, we have only considered the tangent space $T_p\mathcal{M}$ at a point p and the corresponding tensor-product spaces. We are, however, more interested in *fields* of vectors, covectors, or tensors. For each point $p \in \mathcal{M}$, a tensor field T “picks out” a tensor $T(p)$ from each tensor product space corresponding to the tangent space at p , $T_p\mathcal{M}$. A vector field can be written as

$$v(p) = v^\mu(p) \partial_\mu|_p. \quad (2.28)$$

We will mostly be working with the components v^μ , which are functions of \mathcal{M} . For ease of notation, we write the vector as a function of the coordinates x . The vector field $v(x)$ is unchanged by a coordinate-transformation $x^\mu \rightarrow x'^\mu$; the coordinates are only a tool for our convenience. However, with a new set of coordinates, we get a new set of basis vectors, ∂'_μ :

$$v = v^\mu \partial_\mu = v^\mu \frac{\partial x'^\nu}{\partial x^\mu} \partial'_\nu = v'^\mu \partial'_\mu, \quad (2.29)$$

This gives us the transformation rules for the components of vectors,

$$v'^\mu = \frac{\partial x'^\mu}{\partial x^\nu} v^\nu. \quad (2.30)$$

Tangent vectors are also called *contravariant* vectors, as their components transform contra to the basis vectors. For covectors, it is

$$\omega'_\mu = \omega_\nu \frac{\partial x^\nu}{\partial x'^\mu}, \quad (2.31)$$

which is why covectors also are called *covariant* vectors.

The gradient of a scalar function f , $df = \partial_\mu f dx^\mu$, is a coordinate-independent derivative, as $\partial_\mu f$ follows the transformation law for covectors. To generalize this, we define the covariant derivative, ∇ , as a map from (n, m) tensor fields to $(n, m + 1)$ tensor fields, as $f \rightarrow df$ maps a $(0, 0)$ tensor, a scalar, to a $(0, 1)$ -tensor. The components of a covariant derivative, $\nabla_\rho T^{\mu_1 \dots \mu_n}_{\nu_1 \dots \nu_m}$, must follow the tensor transformation law. However, this is not strong enough to uniquely define ∇ . In addition to $\nabla f = \partial f$, we further assume the derivative is linear, $\nabla(T + S) = \nabla T + \nabla S$, and follow the product rule: $\nabla(T \otimes S) = (\nabla T) \otimes S + T \otimes (\nabla S)$. Lastly, we assume the derivative of the Kronecker delta gives zero, $\nabla_\mu \delta^\rho_\nu = 0$. With this, we can, in general, write the covariant derivative for vectors and covectors as [2]

$$\nabla_\mu v^\nu = \partial_\mu v^\nu + \Gamma^\nu_{\mu\rho} v^\rho, \quad (2.32)$$

$$\nabla_\mu \omega_\nu = \partial_\mu \omega_\nu - \Gamma^\rho_{\mu\nu} \omega_\rho. \quad (2.33)$$

$\Gamma^\mu_{\nu\rho}$ are called *Christoffel symbols*. The generalization for higher-order tensors is straightforward,

$$\nabla_\mu T^{\nu \dots \rho \dots} = \partial_\mu T^{\nu \dots \rho \dots} + \Gamma^\mu_{\nu\lambda} T^{\lambda \dots \rho \dots} + \dots - \Gamma^\lambda_{\mu\rho} T^{\mu \dots \lambda \dots} - \dots \quad (2.34)$$

This is still not enough to uniquely determine the covariant derivative. We will furthermore assume $\Gamma^\lambda_{\mu\nu} = \Gamma^\lambda_{\nu\mu}$ and $\nabla_\mu g_{\nu\rho} = 0$. With these assumptions, we find an explicit formula of the Christoffel symbols in terms of the metric,

$$\Gamma^\rho_{\mu\nu} = \frac{1}{2} g^{\rho\sigma} (\partial_\mu g_{\nu\sigma} + \partial_\nu g_{\mu\sigma} - \partial_\sigma g_{\mu\nu}). \quad (2.35)$$

Using the notion of a covariant derivative, we may also generalize *parallel transport* to curved spaces. The notion of parallel transport of a vector in flat \mathbb{R}^n is intuitive—given a line $x^\mu(\lambda)$, a vector v^μ at $x^\mu(\lambda_0)$ is parallel transported to v^μ at $x^\mu(\lambda_1)$ if you carry it along the line without “turning it”. To make this more precise, a vector field v^μ is parallel transported along $x^\mu(\lambda)$ if $\frac{d}{d\lambda} v^\mu = \frac{dx^\nu}{d\lambda} \partial_\nu v^\mu = 0$. We generalize this to curved spaces by replacing the partial derivative with a covariant derivative, and so the criterion for parallel transport is

$$\frac{dx^\mu}{d\lambda} \nabla_\mu v^\nu = 0. \quad (2.36)$$

With this, we can imagine creating a special class of paths, called *geodesics*, namely those which parallel transport their tangent vectors $\frac{dx^\mu}{d\lambda}$. We imagine following an arrow we are holding without turning it as we walk. Using the definition of parallel transport Eq. (2.36), together with the covariant derivative Eq. (2.32), we get the geodesic equation,

$$\frac{d^2 x^\mu}{d\lambda^2} + \Gamma^\mu_{\rho\sigma} \frac{dx^\rho}{d\lambda} \frac{dx^\sigma}{d\lambda} = 0. \quad (2.37)$$

In a flat space, where the Christoffel symbols vanish, this reduces to the familiar criterion for straight lines, $\frac{d^2 x^\mu}{d\lambda^2} = 0$.

The curvature of a manifold \mathcal{M} , with the metric $g_{\mu\nu}$, is encoded in the Riemann tensor. It is defined by

$$[\nabla_\mu, \nabla_\nu] v^\rho = R^\rho_{\sigma\mu\nu} v^\sigma, \quad (2.38)$$

which, in our case, gives the explicit formula

$$R^\rho_{\sigma\mu\nu} = \partial_\mu \Gamma^\rho_{\nu\sigma} - \partial_\nu \Gamma^\rho_{\mu\sigma} + \Gamma^\rho_{\mu\lambda} \Gamma^\lambda_{\nu\sigma} - \Gamma^\rho_{\nu\lambda} \Gamma^\lambda_{\mu\sigma}. \quad (2.39)$$

This form of the Riemann tensor allows us to derive several useful identities, such as

$$R_{\rho\sigma\mu\nu} = R_{[\rho\sigma]\mu\nu} = R_{\rho\sigma[\mu\nu]} = R_{\mu\nu\rho\sigma}. \quad (2.40)$$

In addition, the properties of the commutator imply the Jacobi identity,

$$[\nabla_\mu, [\nabla_\nu, \nabla_\sigma]] + [\nabla_\sigma, [\nabla_\mu, \nabla_\nu]] + [\nabla_\nu, [\nabla_\sigma, \nabla_\mu]] = 0. \quad (2.41)$$

If we apply this on δ^μ_ν , we get the differential Bianchi identity, compactly written

$$\nabla_{[\mu} R_{\nu\rho]\sigma\eta} = 0. \quad (2.42)$$

Although the Christoffel symbols are not tensors, the Riemann tensor is, due to its definition using covariant derivatives. We can therefore contract some of its indices to get other tensorial quantities. We define the Ricci tensor and Ricci scalar as

$$R_{\mu\nu} = R^\rho{}_{\mu\rho\nu}, \quad (2.43)$$

$$R = R^\mu{}_\mu = g^{\mu\nu} R_{\mu\nu}. \quad (2.44)$$

To interpret the Riemann tensor, we define the parallel propagator P . We want this object to take a vector at one point and parallel transport it to another point. A vector that is transported along a curve parametrized by λ should then obey

$$v^\mu(\lambda) = P^\mu{}_\nu(\lambda) v^\nu. \quad (2.45)$$

Inserting this into the equation for parallel transport, Eq. (2.36), this operator must obey

$$\frac{d}{d\lambda} P^\mu{}_\nu = -\Gamma^\mu_{\rho\sigma} \frac{dx^\rho}{d\lambda} P^\sigma{}_\nu. \quad (2.46)$$

This has the same form as the definition of the unitary time-evolution operator in quantum mechanics, and we could therefore write down a solution involving an exponential and a path ordering operator, \mathcal{P} , analogous to the time ordering operator from quantum mechanics. We may rewrite the equation on an integral form,

$$P^\mu{}_\nu(\lambda) = \delta^\mu_\nu - \int_0^\lambda d\lambda' \Gamma^\mu_{\rho\sigma} V^\rho P^\sigma{}_\nu, \quad (2.47)$$

where we denote $\frac{dx^\mu}{d\lambda} = V^\mu$. This allows us to solve the equation iteratively. If $\lambda \leq \epsilon \ll 1$, we expect this to converge as long as the g is well-behaved. Starting with the zeroth-order solution $P^\mu{}_\nu = \delta^\mu_\nu$ and iterating twice gives us

$$P^\mu{}_\nu(\lambda) = \delta^\mu_\nu - \int_0^\lambda d\lambda' \Gamma^\mu_{\rho\nu} V^\rho + \int_0^\lambda d\lambda' \int_0^{\lambda'} d\lambda'' \Gamma^\mu_{\rho\sigma} \Gamma^\sigma_{\eta\nu} V^\rho V^\eta + \mathcal{O}(\epsilon^3). \quad (2.48)$$

With this, we will investigate how much a vector v^μ is changed by being parallel transported around in a small loop, as illustrated in Figure 2.4.

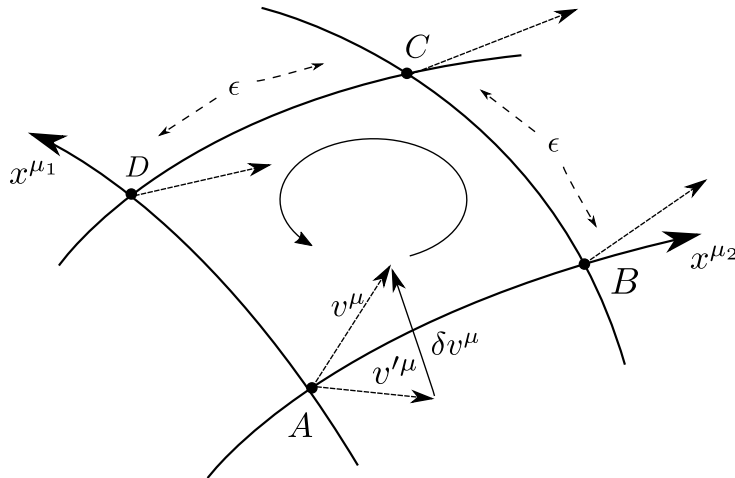


Figure 2.4: A vector v^μ is parallel transported in a small, closed loop, defined by the coordinate functions x^{μ_1} and x^{μ_2} . As a consequence of the curvature, it has changed by δv^μ by the time it arrives back at A .

We transport v^μ along the coordinate lines. These are lines where either of the coordinate functions x^{μ_1} or x^{μ_2} are equal to 0 or ϵ . Here, the indices μ_1 and μ_2 are not free but identify the two coordinate functions which define this loop. They will therefore break summation rules; such indices may appear only on one side of an equation. The line from A to B , defined by $x^{\mu_1} = 0$, is parametrized by $x^\mu(\lambda) = \lambda \delta_{\mu_2}^\mu$, so $V^\mu = \delta_{\mu_2}^\mu$. The Christoffel symbol along this line is

$$\Gamma_{\nu\rho}^\mu(\lambda) = \Gamma_{\nu\rho}^\mu|_A + \lambda \partial_{\mu_2} \Gamma_{\nu\rho}^\mu|_A + \mathcal{O}(\epsilon^2). \quad (2.49)$$

Inserting this into Eq. (2.48), we get

$$P^\mu{}_\nu(\epsilon) = \delta_\nu^\mu - \epsilon \Gamma_{\nu\mu_2}^\mu|_A + \frac{1}{2} \epsilon^2 (\Gamma_{\mu_2\sigma}^\mu \Gamma_{\mu_2\nu}^\sigma|_A - \partial_{\mu_2} \Gamma_{\nu\mu_2}^\mu|_A) + \mathcal{O}(\epsilon^3). \quad (2.50)$$

Next, from B to C , the line is $x^\mu(\lambda) = \epsilon \delta_{\mu_2}^\mu + \lambda \delta_{\mu_1}^\mu$, so $V^\mu = \delta_{\mu_1}^\mu$, and the Christoffel symbols are $\Gamma_{\nu\rho}^\mu = \Gamma_{\nu\rho}^\mu|_B + \lambda \partial_{\mu_1} \Gamma_{\nu\rho}^\mu|_B$ to first order in λ . Here, we have to expand once more to evaluate the symbols at A . Then, we get

$$\Gamma_{\nu\rho}^\mu = \Gamma_{\nu\rho}^\mu|_A + \epsilon \partial_{\mu_2} \Gamma_{\nu\rho}^\mu|_A + \lambda \partial_{\mu_1} \Gamma_{\nu\rho}^\mu|_A + \mathcal{O}(\epsilon^2), \quad (2.51)$$

The parallel propagator from B to C is then

$$P^\mu{}_\nu(\epsilon) = \delta_\nu^\mu - \epsilon \Gamma_{\nu\mu_1}^\mu|_A + \frac{1}{2} \epsilon^2 (\Gamma_{\sigma\mu_1}^\mu \Gamma_{\nu\mu_1}^\sigma|_A - \partial_{\mu_1} \Gamma_{\nu\mu_1}^\mu|_A - 2\partial_{\mu_2} \Gamma_{\nu\mu_1}^\mu|_A) + \mathcal{O}(\epsilon^3), \quad (2.52)$$

Which gives the combined propagator from A to C , to and including second order in ϵ , as

$$\begin{aligned} P_{AC}{}^\mu{}_\nu &= \left[\delta_\nu^\mu - \epsilon \Gamma_{\sigma\mu_1}^\mu + \frac{1}{2} \epsilon^2 (\Gamma_{\eta\mu_1}^\mu \Gamma_{\sigma\mu_1}^\eta - \partial_{\mu_2} \Gamma_{\sigma\mu_2}^\mu - 2\partial_{\mu_2} \Gamma_{\sigma\mu_1}^\mu) \right] \\ &\quad \times \left[\delta_\nu^\sigma - \epsilon \Gamma_{\nu\mu_2}^\sigma + \frac{1}{2} \epsilon^2 (\Gamma_{\eta\mu_2}^\sigma \Gamma_{\nu\mu_2}^\eta - \partial_{\mu_2} \Gamma_{\nu\mu_2}^\sigma) \right] \\ &= \delta_\nu^\mu - \epsilon (\Gamma_{\nu\mu_1}^\mu + \Gamma_{\nu\mu_2}^\mu) \\ &\quad + \epsilon^2 \frac{1}{2} (2\Gamma_{\sigma\mu_1}^\mu \Gamma_{\nu\mu_2}^\sigma + \Gamma_{\sigma\mu_1}^\mu \Gamma_{\nu\mu_1}^\sigma + \Gamma_{\sigma\mu_2}^\mu \Gamma_{\nu\mu_2}^\sigma - 2\partial_{\mu_2} \Gamma_{\nu\mu_1}^\mu - \partial_{\mu_1} \Gamma_{\nu\mu_1}^\mu - \partial_{\mu_2} \Gamma_{\nu\mu_2}^\mu). \end{aligned} \quad (2.53)$$

The parallel propagator for CDA is the propagator for ADC with its signs flipped. The ADC propagator is the same as ABC , only with the μ_1 and μ_2 indices switched. It is thus

$$\begin{aligned} P_{CA}{}^\mu{}_\nu &= \delta_\nu^\mu + \epsilon (\Gamma_{\nu\mu_2}^\mu + \Gamma_{\nu\mu_1}^\mu) \\ &\quad + \epsilon^2 \frac{1}{2} (2\Gamma_{\sigma\mu_2}^\mu \Gamma_{\nu\mu_1}^\sigma + \Gamma_{\sigma\mu_2}^\mu \Gamma_{\nu\mu_2}^\sigma + \Gamma_{\sigma\mu_1}^\mu \Gamma_{\nu\mu_1}^\sigma + 2\partial_{\mu_1} \Gamma_{\nu\mu_2}^\mu + \partial_{\mu_2} \Gamma_{\nu\mu_2}^\mu + \partial_{\mu_1} \Gamma_{\nu\mu_1}^\mu). \end{aligned} \quad (2.54)$$

The full propagator, from A to A , is $P^\mu{}_\nu = P_{CA}{}^\mu{}_\rho P_{AC}{}^\rho{}_\nu$. The terms linear in ϵ vanish, and the same with the terms with two equal μ_i -indices. The change in the vector as it is rotated around the loop is therefore, to second order in ϵ ,

$$\delta v^\mu = P^\mu{}_\nu v^\nu - v^\mu = \epsilon^2 (\Gamma_{\sigma\mu_1}^\mu \Gamma_{\nu\mu_2}^\sigma - \Gamma_{\sigma\mu_2}^\mu \Gamma_{\nu\mu_1}^\sigma + \partial_{\mu_1} \Gamma_{\nu\mu_2}^\mu - \partial_{\mu_2} \Gamma_{\nu\mu_1}^\mu) v^\nu. \quad (2.55)$$

Comparing with Eq. (2.39), we see that this is the Riemann curvature tensor. In other words, the Riemann tensor encodes how a vector is transformed when parallel transported in a small, closed loop.

2.1.3 Integration on manifolds

The integral of a scalar function on a manifold is not a coordinate-independent notion. To obtain this, we must introduce n -forms. A n -form ω is an antisymmetric $(0, n)$ tensor. This means that it has coordinates which obey $\omega_{\mu_1 \dots \mu_n} = \omega_{[\mu_1 \dots \mu_n]}$. The n -forms are ubiquitous objects in mathematics and physics, one example is the electromagnetic field-strength tensor $F_{\mu\nu}$, and they

allow for the definitions of coordinate independent integration and derivation. We will define two important maps between n -forms. The wedge product, \wedge , is a product that maps two n - and m -forms to an $n + m$ -form, and is defined as

$$(A \wedge B)_{\mu_1 \dots \mu_{n+m}} = \frac{(n+m)!}{n!m!} A_{[\mu_1 \dots \mu_n} B_{\mu_{n+1} \dots \mu_{n+m}]} \quad (2.56)$$

Furthermore, we define the exterior derivative, a map from n -forms to $n + 1$ -forms, defined by

$$(dT)_{\mu_1 \dots \mu_{n+1}} = (n+1) \partial_{[\mu_1} T_{\mu_2 \dots \mu_{n+1}]} \quad (2.57)$$

We are interested in a coordinated independent quantity that we can integrate over. To that end, we define

$$d^n x := dx^0 \wedge \dots \wedge dx^{n-1} = \varepsilon_{\mu_1 \dots \mu_n} dx^{\mu_1} \otimes \dots \otimes dx^{\mu_n}, \quad (2.58)$$

where $\varepsilon_{\mu_1 \dots \mu_n}$ is the Levi-Civita symbol. Given a new set of coordinates, x'^μ , we may similarly define a new n -form, $d^n x'$. These two n -forms are related by

$$d^n x = \det \left(\frac{\partial x}{\partial x'} \right) d^n x', \quad (2.59)$$

where we have used the relation $\varepsilon_{\mu_1 \dots \mu_n} \det(A) = \varepsilon_{\nu_1 \dots \nu_n} A^{\nu_1}_{\mu_1} \dots A^{\nu_n}_{\mu_n}$. We define $|g| = |\det(g_{\mu\nu})|$, where $|\cdot|$ denote the absolute value. By the transformation properties of tensors, this transforms as

$$\sqrt{|g'|} = \left| \det \left(\frac{\partial x'}{\partial x} \right) \right| \sqrt{|g|}, \quad (2.60)$$

This means we can use $|g|$ to compensate for the transformation of $d^n x$, and get a volume form with a coordinate independent definition,

$$dV = \sqrt{|g|} d^n x = \sqrt{|g'|} d^n x'. \quad (2.61)$$

With this, we can integrate scalars in a well-defined way by mapping them to a corresponding n -form, $f \rightarrow f dV$. We define the integral of a scalar function f on a manifold \mathcal{M} with a metric g as

$$I[f] = \int_{\mathcal{M}} dV f = \int_{\mathcal{M}} d^n x \sqrt{|g(x)|} f(x). \quad (2.62)$$

Stoke's theorem generalizes the fundamental theorem of calculus and the divergence theorem to manifolds. Let \mathcal{M} be a differential manifold of dimension n , with the boundary $\partial\mathcal{M}$. Stoke's theorem says that an $n - 1$ -form ω and its exterior derivative $d\omega$ are related by

$$\int_{\mathcal{M}} d\omega = \int_{\partial\mathcal{M}} \omega. \quad (2.63)$$

This theorem implies a generalized divergence theorem. The boundary of \mathcal{M} is a $n - 1$ manifold dimensional, and a metric g on \mathcal{M} will induce a new metric γ on $\partial\mathcal{M}$. This metric corresponds to the restriction of g to $\partial\mathcal{M}$. Furthermore, there will be a vector field n^μ of normalized vectors orthogonal to all elements of $T\partial\mathcal{M}$. This theorem states that for a vector field V^μ on \mathcal{M} ,

$$\int_{\mathcal{M}} d^n x \sqrt{|g|} \nabla_\mu V^\mu = \int_{\partial\mathcal{M}} d^{n-1} y \sqrt{|\gamma|} n_\mu V^\mu. \quad (2.64)$$

2.2 Lie theory and the mathematics of symmetry

This section is based on [9, 39–42].

One application of differential geometry is in the theory of Lie groups. The primary use case of these groups is to study the symmetries of manifolds, particularly those that represent physical systems. Symmetries are a vital part of modern physics and will be used throughout this text. In this section, we will develop the tools that we need for this study.

2.2.1 Lie groups

Inspired by Èvariste Galois' use of finite groups to study the finite solution set of algebraic equations, Sophus Lie introduced Lie groups, *topological groups*, to study the solutions of differential equations. Groups are natural structures to capture symmetries, as they can be defined as actions on an object which leave it unchanged. A group is a set, G , together with a map

$$(\cdot, \cdot) : G \times G \longrightarrow G, \quad (2.65)$$

$$(g_1, g_2) \longmapsto g_3 = g_1 g_2, \quad (2.66)$$

called group multiplication. This map obeys the group axioms, which are the existence of an identity element $\mathbb{1}$, associativity, and the existence of an inverse element g^{-1} for all $g \in G$. These can be written as

$$\begin{aligned} \exists \mathbb{1} \in G, \text{ s.t.}, \forall g \in G, \quad & g\mathbb{1} = g, \\ \forall g_1, g_2, g_3 \in G, \quad & g_1(g_2 g_3) = (g_1 g_2)g_3, \\ \forall g \in G, \exists g^{-1} \in G, \text{ s.t.}, \quad & gg^{-1} = \mathbb{1}. \end{aligned} \quad (2.67)$$

A Lie group is a manifold G with a group structure. Elements $g_1, g_2 \in G$ can thus be combined by group multiplication and mapped to their inverses. We additionally require these maps to be smooth, which is equivalent to $(g_1, g_2) \rightarrow g_1 g_2^{-1}$ being smooth.

As we will discuss in more detail in the next chapter, a symmetry transformation is a map between physical states which leaves the equations governing that system unchanged. Assume the field, or set of fields, φ is governed by the equation $f(\varphi) = 0$. A symmetry transformation $\varphi \mapsto g\varphi$, where $g\varphi$ represents the action g acting on φ , will then obey $f(g\varphi) = 0$. This is what makes groups the natural structures to describe symmetries. Assume G is the set of all symmetries of a system, or a subset of them closed under compositions

$$G = \{ g \mid f(g\varphi) = 0 \}. \quad (2.68)$$

The group G might act on φ linearly, so $(g\varphi)_i = g_{ij}\varphi_j$, or in a more complicated manner. A linear realization of a Lie group is called a *representation*. In any case, the group multiplication is composition, i.e., performing transformations in succession. This map is closed, as the composite of two symmetry transformations is another symmetry transformation. The identity map is a symmetry transformation, and composition is associative. This means that invertible symmetry transformations form a group, and for continuous sets, this group is a Lie group.

We will focus on connected Lie groups, in which all elements $g \in G$ are in the same connected piece as the identity map $\mathbb{1}\varphi = \varphi$. This means that for each $g \in G$, one can find a continuous path $\gamma(t)$ in the manifold, such that $\gamma(0) = \mathbb{1}$ and $\gamma(1) = g$. Given such a path, we can study transformations close to the identity element. As the Lie group is a smooth manifold, we can write⁴

$$\gamma(\epsilon) = \mathbb{1} + i\epsilon V + \mathcal{O}(\epsilon^2). \quad (2.69)$$

V is a generator, and is defined as

$$iV = \left. \frac{d\gamma}{dt} \right|_{t=0}. \quad (2.70)$$

The generator is thus a member of the tangent space of the identity element, $T_{\mathbb{1}}G$. We denote the coordinates of G by $\eta_\alpha \in \mathbb{R}^n$. As before, we can denote a path γ in a manifold G by its path through \mathbb{R}^n , $\gamma(t) = g(\eta(t))$. We will assume, without loss of generality, that $\eta_\alpha(0) = 0$ and $g(0) = \mathbb{1}$. We can then write the generator as

$$V = \left. \frac{d\gamma}{dt} \right|_{t=0} = \left. \frac{d\eta_\alpha}{dt} \right|_{t=0} \left. \frac{\partial g}{\partial \eta_\alpha} \right|_{\eta=0} = v_\alpha T_\alpha, \quad T_\alpha = \left. \frac{\partial g}{\partial \eta_\alpha} \right|_{\eta=0}, \quad v_\alpha = \left. \frac{d\eta_\alpha}{dt} \right|_{t=0}. \quad (2.71)$$

⁴The factor i is a physics convention and differs from how mathematicians define generators of a Lie group.

Infinitesimal transformations can therefore be written as

$$\gamma(\epsilon) = \mathbb{1} + i\epsilon v_\alpha T_\alpha + \mathcal{O}(\epsilon^2). \quad (2.72)$$

The generators form a new algebraic structure, the Lie algebra. This is the linearization of the Lie group, but it encodes information about the whole group. We will, in fact, mostly focus on the generators rather than the full transformations, which makes the Lie algebra an important structure.

2.2.2 Lie algebras

An abstract Lie algebra \mathfrak{g} is a vector space V , together with a binary operation,

$$[\cdot, \cdot] : \mathfrak{g} \times \mathfrak{g} \longrightarrow \mathfrak{g}, \quad (2.73)$$

$$(V_1, V_2) \longmapsto V_3 = [V_1, V_2]. \quad (2.74)$$

This map is linear in both arguments, antisymmetric, and obeys the *Jacobi identity*,

$$[V_1, [V_2, V_3]] + [V_2, [V_3, V_1]] + [V_3, [V_1, V_2]] = 0, \quad \forall V_1, V_2, V_3 \in \mathfrak{g}. \quad (2.75)$$

In our case, we will work with concrete Lie algebras \mathfrak{g} , corresponding to Lie groups G . As long as G is simply connected, i.e., connected to the identity and without holes, then this is a one-to-one correspondence. This was Sophus Lie's main result. The space V is then $T_1 G$ with the basis T_α , and we can define the Lie bracket by

$$[T_\alpha, T_\beta] = i f_{\alpha\beta}^\gamma T_\gamma, \quad (2.76)$$

where $f_{\alpha\beta}^\gamma$ are the structure constants of the algebra. These obey $f_{\alpha\beta}^\gamma = -f_{\beta\alpha}^\gamma$ and they follow their own version of the Jacobi identity,

$$f_{\alpha\beta}^\mu f_{\gamma\mu}^\nu + f_{\beta\gamma}^\mu f_{\alpha\mu}^\nu + f_{\gamma\alpha}^\mu f_{\beta\mu}^\nu = 0. \quad (2.77)$$

An algebra is called *abelian* if $f_{\beta\gamma}^\alpha = 0$. Any abelian algebra is just a direct sum of N of the Lie algebras of $U(1)$, $\mathfrak{u}(1)$. A simple Lie algebra is a non-abelian algebra that does not contain any non-trivial *ideals*, also called invariant sub-algebras.⁵ An ideal $\mathfrak{i} \subset \mathfrak{g}$ is a set such that $[\mathfrak{i}, \mathfrak{g}] \subset \mathfrak{i}$. A semi-simple Lie algebra can be written as a direct sum of simple algebras. The total classification of simple Lie algebras was done by Cartan and Killing and involved four infinite families, the classical algebras such as $\mathfrak{su}(N)$, and five exceptional algebras which do not fit into these families. There is a natural metric on Lie groups, called the Killing form, $B_{\alpha\beta} = -f_{\alpha\eta}^\gamma f_{\beta\gamma}^\eta$. This is non-degenerate if the corresponding Lie algebra is semi-simple. Additionally, if the Lie group is compact, it is positive definite. In that case, one can choose a basis of the algebras so that the structure constants are *totally antisymmetric*. This is trivially true for abelian groups, and as a consequence, the structure constants of a direct sum of compact, simple algebras and abelian algebras are totally antisymmetric, and we write $f_{\beta\gamma}^\alpha = f_{\alpha\beta\gamma}$ [42].

As with Lie groups, Lie algebras have representations. A representation of a Lie algebra \mathfrak{g} is a homomorphism, i.e., a map that preserves the Lie bracket, from \mathfrak{g} to the Lie algebra of linear maps on a vector space V , i.e., matrices, called $\mathfrak{gl}(V)$. In $\mathfrak{gl}(V)$, the Lie bracket is the matrix commutator. A representation is faithful if the homomorphism is injective. The most important representations are the fundamental and the adjoint. The fundamental representation is the smallest faithful representation, and in the case of the familiar groups such as $\mathfrak{so}(N)$ and $\mathfrak{su}(N)$, the fundamental representation is the defining one. In the adjoint representation, the generators T_α^A are the structure constants, $(T_\alpha^A)^\beta_\gamma = -i f_{\alpha\gamma}^\beta$. For compact Lie algebras, i.e., the algebras of compact Lie groups, the representations are Hermitian.

⁵Some authors do not have the non-abelian criterion and includes $\mathfrak{u}(1)$ as simple.

A subset of the original Lie group, $H \subset G$, closed under the group action, is called a subgroup. H then has its own Lie algebra \mathfrak{h} , with a set of $m = \dim H$ generators, t_a , which is a subset of the original generators T_α . We denote the remaining set of generators x_i , such that t_a and x_i together span \mathfrak{g} . Assume G is compact and its Lie algebra semi-simple. The commutators of t_a must be closed, which means that we can write

$$[t_a, t_b] = if_{abc}t_c, \quad (2.78)$$

$$[t_a, x_i] = if_{aik}x_k, \quad (2.79)$$

$$[x_i, x_j] = if_{ijk}x_k + if_{ijc}t_c, \quad (2.80)$$

where abc runs over the generators of \mathfrak{h} , and ijk runs over the rest. The second formula can be derived using the total anti-symmetry of the structure constants, which implies that $f_{abk} = 0 = -f_{akb}$. This is called a Cartan decomposition. One parameter subgroups are one special case of Lie subgroups. If a curve $\gamma(t)$ through G obey

$$\gamma(t)\gamma(s) = \gamma(t+s), \quad \gamma(0) = \mathbb{1}, \quad (2.81)$$

then all the points on this curve form a one parameter subgroup of G . This path is associated with a generator,

$$\left. \frac{d\gamma}{dt} \right|_{t=0} = i\eta_\alpha T_\alpha. \quad (2.82)$$

This association is one-to-one, and allows us to define the exponential map,

$$\exp \{i\eta_\alpha T_\alpha\} := \gamma(1). \quad (2.83)$$

For connected and compact Lie groups, all elements of the Lie group $g \in G$ can be written as an exponential of elements in the corresponding Lie algebra $\eta_\alpha T_\alpha \in \mathfrak{g}$. For matrix groups, the exponential equals the familiar series expansion

$$\exp \{X\} = \sum_n \frac{1}{n!} X^n. \quad (2.84)$$

Chapter 3

Quantum field theory

In this Chapter, we survey some general properties of quantum field theory that are necessary for chiral perturbation theory. First, we introduce the path integral, the 1-particle irreducible effective action, and the effective potential. We will derive Goldstone's theorem and present the CCWZ construction, which is the basis for χ PT, and discuss how to construct effective field theories.

3.1 *QFT via path integrals

This section is based on [9, 40–42]

In the path integral formalism, one evaluates quantum observable by integrating the contributions of all possible configurations. If the system has specified initial and final states, this amounts to all possible paths the system might evolve between these, hence the name. We assume the reader has some familiarity with this formalism. However, if a refresher is needed, section C.2 contains a derivation of the closely related imaginary-time formalism and compares it with the path integral approach. A summary of functional calculus is given in section A.3.

In the path integral formalism, the vacuum-to-vacuum transition amplitude, i.e., overlap between the vacuum at $t = -\infty$ and the vacuum at time $t = \infty$, is given by

$$\begin{aligned} Z &= \lim_{T \rightarrow \infty} \langle \Omega, T/2 | -T/2, \Omega \rangle \\ &= \lim_{T \rightarrow \infty} \langle \Omega | e^{-iHT} | \Omega \rangle \\ &= \int \mathcal{D}\pi \mathcal{D}\varphi \exp \left\{ i \int d^4x (\pi \dot{\varphi} - \mathcal{H}[\pi, \varphi]) \right\}, \end{aligned}$$

where $|\Omega\rangle$ is the vacuum state. The φ are the fields of the theory, and π their canonical momenta. We will work as if φ are a bosonic field. However, this can be readily generalized to fermions. By introducing a source term into the Hamiltonian density, $\mathcal{H} \rightarrow \mathcal{H} - J(x)\varphi(x)$, we get the generating functional

$$Z[J] = \int \mathcal{D}\pi \mathcal{D}\varphi \exp \left\{ i \int d^4x (\pi \dot{\varphi} - \mathcal{H}[\pi, \varphi] + J\varphi) \right\}. \quad (3.1)$$

If \mathcal{H} is quadratic in π , we can complete the square and integrate out π to obtain

$$Z[J] = C \int \mathcal{D}\varphi \exp \left\{ i \int d^4x (\mathcal{L}[\varphi] + J\varphi) \right\}. \quad (3.2)$$

C is infinite, but constant, and will drop out of physical quantities. In scattering theory, the main objects of study are correlation functions $\langle \varphi(x_1)\varphi(x_2)\dots \rangle = \langle \Omega | T \{ \varphi(x_1)\varphi(x_2)\dots \} | \Omega \rangle$, where T is the time ordering operator. These are given by functional derivatives of $Z[J]$,

$$\langle \varphi(x_1)\varphi(x_2)\dots \rangle = \frac{\int \mathcal{D}\varphi(x) [\varphi(x_1)\varphi(x_2)\dots] e^{iS[\varphi]}}{\int \mathcal{D}\varphi(x) e^{iS[\varphi]}} = \frac{1}{Z[0]} \prod_i \left(-i \frac{\delta}{\delta J(x_i)} \right) Z[J] \Big|_{J=0}, \quad (3.3)$$

where $S[\varphi] = \int d^4x \mathcal{L}[\varphi]$ is the action of the theory. The functional derivative is described in section A.3. In a free theory, we are able to write

$$Z_0[J] = Z_0[0] \exp \{ iW_0[J] \}, \quad iW_0[J] = -\frac{1}{2} \int d^4x d^4y J(x) D_0(x-y) J(y), \quad (3.4)$$

where D_0 is the propagator of the free theory. Using this form of the generating functional, Eq. (3.3) becomes

$$\begin{aligned} & \frac{1}{Z[0]} (-i)^n \frac{\delta}{\delta J(x_1)} \dots \frac{\delta}{\delta J(x_n)} Z_0[J] \Big|_{J=0} = (-i)^n \frac{\delta}{\delta J(x_1)} \dots \frac{\delta}{\delta J(x_n)} e^{iW_0[J]} \Big|_{J=0} \\ & = (-i)^n \frac{\delta}{\delta J(x_1)} \dots \frac{\delta}{\delta J(x_{n-1})} \left(i \frac{\delta W_0[J]}{\delta J(x_n)} \right) e^{iW_0[J]} \Big|_{J=0} \\ & = (-i)^n \frac{\delta}{\delta J(x_1)} \dots \frac{\delta}{\delta J(x_{n-2})} \left(i \frac{\delta^2 W_0[J]}{\delta J(x_{n-1}) \delta J(x_n)} + i^2 \frac{\delta W_0[J]}{\delta J(x_{n-1})} \frac{\delta W_0[J]}{\delta J(x_n)} \right) e^{iW_0[J]} \Big|_{J=0} \\ & = \dots \\ & = (-i)^{\lfloor n/2 \rfloor} \sum_{(a,b)} \prod_{i=1}^{\lfloor n/2 \rfloor} \frac{\delta^2 W_0[J]}{\delta J(x_{a(i)}) \delta J(x_{b(i)})} \Big|_{J=0}. \end{aligned}$$

In the last line, we have introduced the functions a, b , which define a way to pair n elements. $\lfloor \cdot \rfloor$ is the floor function. The domain of these functions are the integers between 1 and $\lfloor n/2 \rfloor$, the image a subset of the integers between 1 and n of size $\lfloor n/2 \rfloor$. A valid pairing is a set $\{(a(1), b(1)), \dots, (a(\lfloor n/2 \rfloor), b(\lfloor n/2 \rfloor))\}$, where all elements $a(i)$ and $b(j)$ are different, such that all integers up to and including n are featured. A pair is not directed, so $(a(i), b(i))$ is the same pair as $(b(i), a(i))$. The sum is over the set $\{(a, b)\}$ of all possible, unique pairings. If n is odd, the expression is equal to 0. This is Wick's theorem, and it can more simply be stated as *a correlation function is the sum of all possible pairings of 2-point functions*,

$$\left\langle \prod_{i=1}^n \varphi(x_i) \right\rangle_0 = \sum_{\{(a,b)\}} \prod_{i=1}^{\lfloor n/2 \rfloor} \langle \varphi(x_{a(i)}) \varphi(x_{b(i)}) \rangle_0. \quad (3.5)$$

The subscript on the expectation value indicates that it is evaluated in the free theory.

If we have an interacting theory, that is, a theory with an action $S = S_0 + S_I$, where S_0 is a free theory, the generating functional can be written

$$Z[J] = Z_0[0] \left\langle \exp \left\{ iS_I + i \int d^4x J(x) \varphi(x) \right\} \right\rangle_0. \quad (3.6)$$

We can expand the exponential in power series, which means the expectation value in Eq. (3.6) becomes

$$\sum_{n,m} \frac{1}{n!m!} \left\langle (iS_I)^n \left(i \int d^4x J(x) \varphi(x) \right)^m \right\rangle_0. \quad (3.7)$$

The terms in this series are represented by Feynman diagrams, constructed using the Feynman rules, and can be read from the action. We will not further detail how the Feynman rules are derived. The Feynman rules for a free scalar field in thermal field theory are derived in

section C.4, and the general procedure is found in any of the main sources for this section [9, 40–42] The source terms give rise to an additional vertex

$$\longrightarrow \bullet J(x). \quad (3.8)$$

The generating functional $Z[J]$ thus equals $Z_0[0]$ times *the sum of all diagrams with external sources $J(x)$* .

Consider a general diagram without external legs, built up of N different connected subdiagrams, where subdiagram i appears n_i times. As an illustration, a generic vacuum diagram in φ^4 -theory has the form

$$\mathcal{M} = \text{diagram 1} \times \text{diagram 2} \times \text{diagram 3} \times \text{diagram 4} \times \dots \quad (3.9)$$

If sub-diagram i as a stand-alone diagram equals \mathcal{M}_i , each copy of that subdiagram contributes a factor \mathcal{M}_i to the total diagram. However, due to the symmetry of permuting identical subdiagrams, one must divide by the extra symmetry factor $s = n_i!$, the total number of permutations of all the copies of diagram i . The full diagram therefore equals

$$\mathcal{M} = \prod_{i=1}^N \frac{1}{n_i!} \mathcal{M}_i^{n_i}. \quad (3.10)$$

\mathcal{M} is uniquely defined by a finite sequence of integers, $(n_1, n_2, \dots, n_N, 0, 0, \dots)$, so the sum of all diagrams is the sum over the set S of all finite sequences of integers. This allows us to write the sum of all diagrams as

$$\sum_{(n_1, \dots) \in S} \prod_i \frac{1}{n_i!} \mathcal{M}_i^{n_i} = \prod_{i=1}^{\infty} \sum_{n_i=1}^{\infty} \frac{1}{n_i!} \mathcal{M}_i^{n_i} = \exp \left\{ \sum_i \mathcal{M}_i \right\}. \quad (3.11)$$

We showed that the generating functional $Z[J]$ were the $Z_0[0]$ times the sum of all diagrams due to external sources. From Eq. (3.11), if we define

$$Z[J] = Z_0[0] \exp \{iW[J]\}, \quad (3.12)$$

then $W[J]$ is the sum of all connected diagrams. This is trivially true for the free theory, where the only connected diagram is

$$W_0[J] = J(x) \bullet \longrightarrow \bullet J(y). \quad (3.13)$$

The two-point function in the full, interacting theory can thus be written

$$-i \frac{\delta^2 W[J]}{\delta J(x) \delta J(y)} = D(x - y). \quad (3.14)$$

3.2 *The 1PI effective action

This section is based on [9, 40–42].

The generating functional for connected diagrams, $W[J]$, is dependent on the external source current J . We can define a new quantity with a different independent variable, using the Legendre transformation analogously to what is done in thermodynamics and Lagrangian mechanics. The new independent variable is

$$\varphi_J(x) := \frac{\delta W[J]}{\delta J(x)} = \langle \varphi(x) \rangle_J. \quad (3.15)$$

The subscript J on the expectation value indicate that it is evaluated in the presence of a source. The Legendre transformation of W is then

$$\Gamma[\varphi_J] := W[J] - \int d^4x J(x)\varphi_J(x). \quad (3.16)$$

Using the definition of φ_J , we have that

$$\frac{\delta\Gamma[\varphi_J]}{\delta\varphi_J(x)} = \int d^4y \frac{\delta J(y)}{\delta\varphi_J(x)} \frac{\delta W[J]}{\delta J(y)} - \int d^4y \frac{\delta J(y)}{\delta\varphi_J(x)} \varphi_J(y) - J(x) = -J(x). \quad (3.17)$$

If we compare this to the classical equations of motion of a field φ with the action S ,

$$\frac{\delta S[\varphi]}{\delta\varphi(x)} = -J(x), \quad (3.18)$$

we see that Γ is an action that gives the equation of motion for the expectation value of the field, given a source current $J(x)$.

To interpret Γ further, we observe what happens if we treat $\Gamma[\varphi]$ as a classical action with a coupling g . The generating functional in this new theory is

$$Z[J, g] = \int \mathcal{D}\varphi \exp \left\{ ig^{-1} \left(\Gamma[\varphi] + \int d^4x \varphi(x)J(x) \right) \right\}. \quad (3.19)$$

The free propagator in this theory will be proportional to g , as it is given by the inverse of the equation of motion for the free theory. All vertices in this theory, on the other hand, will be proportional to g^{-1} , as they are given by the higher-order terms in the action $g^{-1}\Gamma$. This means that a diagram with V vertices and I internal lines is proportional to g^{I-V} . Regardless of what the Feynman-diagrams in this theory are, the number of loops of a connected diagram is¹

$$L = I - V + 1. \quad (3.20)$$

To see this, we first observe that diagrams with one single loop must have equally many internal lines as vertices, so the formula holds for $L = 1$. The formula still holds if we add a new loop to a diagram with n loops by joining two vertices. If we attach a new vertex with one line, the formula still holds, and as the diagram is connected, any more lines connecting the new vertex to the diagram will create additional loops. This ensures that the formula holds by induction. As a consequence of this, any diagram is proportional to g^{L-1} . This means that in the limit $g \rightarrow 0$, the theory is fully described at the tree-level, i.e., by only considering diagrams without loops. In this limit, we may use the stationary phase approximation, as described in section A.3, which gives

$$Z[J, g \rightarrow 0] \sim C \det \left(-g \frac{\delta^2 \Gamma[\varphi_J]}{\delta\varphi(x)\delta\varphi(y)} \right)^{-1/2} \exp \left\{ ig^{-1} \left(\Gamma[\varphi_J] + \int d^4x J(x)\varphi_J(x) \right) \right\}. \quad (3.21)$$

This means that

$$-ig \ln(Z[J, g]) = gW[J, g] = \Gamma[\varphi_J] + \int d^4x J(x)\varphi_J(x) + \mathcal{O}(g), \quad (3.22)$$

which is exactly the Legendre transformation we started out with, modulo the factor g . Γ is, therefore, the action that describes the full theory at the tree level. For a free theory, the classical action S equals the effective action.

As we found in the last section, the propagator $D(x, y) = \langle \varphi(x)\varphi(y) \rangle_J$ is given by $-i$ times the second functional derivative of $W[J]$. Using the chain rule, together with Eq. (3.17), we get

$$\begin{aligned} (-i) \int d^4z \frac{\delta^2 W[J]}{\delta J(x)\delta J(z)} \frac{\delta^2 \Gamma[\varphi_J]}{\delta\varphi_J(z)\delta\varphi_J(y)} \\ = (-i) \int d^4z \frac{\delta\varphi_J[z]}{\delta J(x)} \frac{\delta^2 \Gamma[\varphi_J]}{\delta\varphi_J(z)\delta\varphi_J(y)} = (-i) \frac{\delta}{\delta J(x)} \frac{\delta\Gamma[\varphi_J]}{\delta\varphi_J(y)} = i\delta(x-y). \end{aligned}$$

¹This is a consequence of the Euler characteristic $\chi = V - E + F$, a topological invariant of graphs.

This is exactly the definition of the inverse propagator, which means

$$\frac{\delta^2 \Gamma[\varphi_J]}{\delta \varphi_J(x) \delta \varphi_J(y)} = D^{-1}(x, y). \quad (3.23)$$

The inverse propagator is the sum of all one-particle-irreducible (1PI) diagrams, with two external vertices. More generally, Γ is the generating functional for 1PI diagrams, which is why it is called the 1PI effective action.

We define η as the fluctuations around the expectation value of the field, $\varphi(x) = \varphi_J(x) + \eta(x)$, and use this to change variables of integration in the path integral. The expectation value φ_J is constant with respect to the integral, so

$$\int \mathcal{D}\varphi \exp \{iS[\varphi]\} = \int \mathcal{D}\eta \exp \{iS[\varphi_J + \eta]\}. \quad (3.24)$$

By assumption, $\langle \eta \rangle_J = 0$, which means this path integral is described by only 1PI diagrams, connected or not. We can therefore write

$$\exp \{i\Gamma[\varphi_J]\} = \int \mathcal{D}\eta \exp \{iS[\varphi_J + \eta]\}. \quad (3.25)$$

As we will discuss later, we interpret this form as *integrating out* the η degrees of freedom, leaving us with an effective description of the physics dependent only on the ground state solution φ_J . The disadvantage of this is that there is no bound on how complicated Γ might be—it is not restricted by the usual assumptions of the form of the action, such as locality [9]. With some simplifying assumptions, though, we can still make use of the 1PI effective action, as we will see in the next subsection.

3.2.1 Effective potential

For a constant field configuration $\varphi(x) = \varphi_0$, the effective action, a functional, becomes a regular function. We define the effective potential \mathcal{V}_{eff} by

$$\Gamma[\varphi_0] = -VT \mathcal{V}_{\text{eff}}(\varphi_0), \quad (3.26)$$

where VT is the volume of space-time. For a constant ground state, the effective potential will equal the energy of this state. To calculate the effective potential, we can expand the action around this state to calculate the effective action, by changing variables to $\varphi(x) = \varphi_0 + \eta(x)$. $\eta(x)$ now parametrizes fluctuations around the ground state and has by assumption a vanishing expectation value. The generating functional becomes

$$Z[J] = \int \mathcal{D}(\varphi_0 + \eta) \exp \left\{ iS[\varphi_0 + \eta] + i \int d^4x [\varphi_0 + \eta(x)] J(x) \right\}. \quad (3.27)$$

The functional version of a Taylor expansion, as described in section A.3, is

$$S[\varphi_0 + \eta] = S[\varphi_0] + \int dx \eta(x) \frac{\delta S[\varphi_0]}{\delta \varphi(x)} + \frac{1}{2} \int dx dy \eta(x) \eta(y) \frac{\delta^2 S[\varphi_0]}{\delta \varphi(x) \delta \varphi(y)} + \dots \quad (3.28)$$

The notation

$$\frac{\delta S[\varphi_0]}{\delta \varphi(x)} \quad (3.29)$$

indicates that the functional $S[\varphi]$ is differentiated with respect to $\varphi(x)$, then evaluated at $\varphi(x) = \varphi_0$. We define

$$S_0[\eta] := \frac{1}{2} \int d^4x d^4y \eta(x) \eta(y) \frac{\delta^2 S[\varphi_0]}{\delta \varphi(x) \delta \varphi(y)}, \quad (3.30)$$

$$S_I[\eta] := \frac{1}{6} \int d^4x d^4y d^4z \eta(x) \eta(y) \eta(z) \frac{\delta^3 S[\varphi_0]}{\delta \varphi(x) \delta \varphi(y) \delta \varphi(z)} + \dots, \quad (3.31)$$

where the dots indicate higher derivatives. When we insert this expansion into the generating functional $Z[J]$ we get

$$Z[J] = \int \mathcal{D}\eta \exp \left\{ i \int d^4x (\mathcal{L}[\varphi_0] + J\varphi_0) + i \int d^4x \eta(x) \left(\frac{\delta S[\varphi_0]}{\delta \varphi(x)} + J(x) \right) + iS_0[\eta] + iS_I[\eta] \right\}. \quad (3.32)$$

The first term is constant with respect to η and may be taken outside the path integral. The second term gives rise to tadpole diagrams, which alter the expectation value of $\eta(x)$. For $J = 0$, this expectation value should vanish, and this term can be ignored. Furthermore, this means that the ground state must minimize the classical potential,

$$\frac{\partial \mathcal{V}(\varphi_0)}{\partial \varphi} = 0. \quad (3.33)$$

This leaves us with

$$-i \ln Z[J] = W[J] = \int d^4x (\mathcal{L}[\varphi_0] + J\varphi_0) - i \ln \left(\int \mathcal{D}\eta \exp \{ iS_0[\eta] + iS_I[\eta] \} \right). \quad (3.34)$$

We can now use the definition of the 1PI effective action to obtain a formula for the effective potential,

$$\mathcal{V}_{\text{eff}}(\varphi_0) = -\frac{1}{VT} \left(W[J] - \int d^4x J(x)\varphi_0 \right) = \mathcal{V}(\varphi_0) - i \ln \left(\int \mathcal{D}\eta \exp \{ iS_0[\eta] + iS_I[\eta] \} \right). \quad (3.35)$$

We showed that the 1PI effective action describes the whole quantum theory of the original action at the tree level. This was done by inspecting a theory with an action proportional to g^{-1} . In this theory, Feynman diagrams with L loops are proportional to g^{L-1} . We can use the same argument to expand the effective potential in loops. This is done by modifying the action $S[\varphi] \rightarrow g^{-1}S[\varphi]$, and then expand in power of g . The first term in the effective potential is modified by $\mathcal{V} \rightarrow g^{-1}\mathcal{V}$, which means that it is made up of tree-level terms. This is as expected since the tree-level result corresponds to the classical result without any quantum corrections. The second term becomes

$$\begin{aligned} \ln \left(\int \mathcal{D}\eta e^{iS_0+iS_I} \right) &\longrightarrow \ln \left(\int \mathcal{D}\eta e^{ig^{-1}S_0+ig^{-1}S_I} \right) \\ &= \ln \left(\int \mathcal{D}\eta e^{ig^{-1}S_0} \right) + \ln \left(\frac{\int \mathcal{D}\eta e^{ig^{-1}S_I} e^{ig^{-1}S_0}}{\int \mathcal{D}\eta e^{ig^{-1}S_0}} \right) \end{aligned}$$

The first term is quadratic in η , and can therefore be evaluated as a generalized Gaussian integral, as described in section A.3,

$$\begin{aligned} &\ln \left[\int \mathcal{D}\eta \exp \left\{ ig^{-1} \frac{1}{2} \int d^4x d^4y \eta(x)\eta(y) \frac{\delta^2 S[\varphi_0]}{\delta \varphi(x) \delta \varphi(y)} \right\} \right] \\ &= \ln \left[\det \left(-g^{-1} \frac{\delta^2 S[\varphi_0]}{\delta \varphi(x) \delta \varphi(y)} \right)^{-1/2} \right] = -\frac{1}{2} \text{Tr} \left\{ \ln \left[-\frac{\delta^2 S[\varphi_0]}{\delta \varphi(x) \delta \varphi(y)} \right] \right\} + \text{const.} \end{aligned}$$

We used the identity $\ln\{\det(M)\} = \text{Tr}\{\ln(M)\}$. After we remove the constant, this term is proportional to g^0 , i.e., it is made up of one-loop terms.

The last term can be evaluated by first expanding the exponential containing the S_I term, then using $\ln(1+x) = \sum_n \frac{1}{n} x^n$. Using

$$\langle A \rangle_0 = \frac{\int \mathcal{D}\varphi A e^{ig^{-1}S_0}}{\int \mathcal{D}\varphi e^{ig^{-1}S_0}}, \quad (3.36)$$

we can write

$$\frac{\int \mathcal{D}\eta e^{ig^{-1}S_I} e^{ig^{-1}S_0}}{\int \mathcal{D}\eta e^{ig^{-1}S_0}} = \sum_{n=0}^{\infty} \frac{1}{n!} \langle (ig^{-1}S_I)^n \rangle_0. \quad (3.37)$$

We recognize this as the sum of all Feynman diagrams, with Feynman rules from the interaction term S_I . The logarithm of this is then the sum of all connected Feynman diagrams. We know that S_I is made up of terms that are third power or higher in the fields. Each internal line is connected to two vertices, and each vertex is connected to at least three internal lines, i.e., $I \geq 3/2V$. The number of loops is therefore $L = I - V + 1 \geq (3/2 - 1)V + 1$. There is at least one vertex, i.e. $L \geq 3/2$. This shows that the first logarithm contains *all* one-loop contributions. The effective potential at one-loop order is therefore

$$\mathcal{V}_{\text{eff}}(\varphi_0) = \mathcal{V}(\varphi_0) - \frac{i}{VT} \frac{1}{2} \text{Tr} \left\{ \ln \left(-\frac{\delta^2 S[\varphi_0]}{\delta\varphi(x)\delta\varphi(y)} \right) \right\}. \quad (3.38)$$

3.3 *Symmetry and Goldstone's theorem

This section is based on [9, 39–42].

Symmetry plays a prominent role in modern physics. If we can transform a physical state in such a way that the governing equations of this system are unchanged, we call that transformation a *symmetry transformation*. All such transformations are known as the symmetries of that theory. The symmetries of a theory encode a lot of physics, such as the presence of conserved quantities and the system's low energy behavior. We distinguish between internal and external symmetries. An external symmetry is an active coordinate transformation, such as rotations or translations. They relate degrees of freedom at different space-time points, while internal symmetries transform degrees of freedom at each space-time point independently. A further distinction is between global and local symmetry transformations. Global transformations have one rule for transforming degrees of freedom at each point, which is applied everywhere, while local transformations are functions of space-time.

In classical field theory, symmetries are encoded in the behavior of the Lagrangian when the fields are transformed. We will consider continuous transformations, which can in general be written as

$$\varphi(x) \longrightarrow \varphi'(x) = f_t[\varphi](x), \quad t \in [0, 1]. \quad (3.39)$$

Here, $f_t[\varphi]$ is a functional in φ , and a smooth function of t , with the constraint that $f_0[\varphi] = \varphi$. This allows us to look at “infinitesimal” transformations,

$$\varphi'(x) = f_\epsilon[\varphi] = \varphi(x) + \epsilon \left. \frac{df_t[\varphi]}{dt} \right|_{t=0} + \mathcal{O}(\epsilon). \quad (3.40)$$

When considering infinitesimal transformations, we will not always write $+\mathcal{O}(\epsilon)$, but rather consider it implicit. We will consider internal, global transformations which act linearly on φ . For N fields, φ_i , this can be written

$$\varphi'_i(x) = \varphi_i(x) + i\epsilon V_{ij} \varphi_j(x). \quad (3.41)$$

V_{ij} is called the generator of the transformation. A symmetry transformation of the system is then a transformation in which the Lagrangian left is unchanged, or at most differs by a 4-divergence term. That is, a transformation $\varphi \rightarrow \varphi'$ is a symmetry if

$$\mathcal{L}[\varphi'] = \mathcal{L}[\varphi] + \partial_\mu K^\mu[\varphi], \quad (3.42)$$

where $K^\mu[\varphi]$ is a functional of φ .² This is a requirement for symmetry in quantum field theory too. However, as physical quantities in quantum field theory are given not just by the action of a single state but the path integral, the integration measure $\mathcal{D}\varphi$ has to be invariant as well. If a classical symmetry fails due to the non-invariance of the integration measure, it is called an *anomaly*.

To investigate the symmetry properties of a quantum theory, we explore what constraints a symmetry imposes on the effective action. To that end, assume

$$\mathcal{D}\varphi'(x) = \mathcal{D}\varphi(x), \quad S[\varphi'] = S[\varphi]. \quad (3.43)$$

In the generating functional, such a transformation corresponds to a change of integration variable. Using the infinitesimal version of the transformation, we may write

$$\begin{aligned} Z[J] &= \int \mathcal{D}\varphi \exp \left\{ iS[\varphi] + i \int d^4x J_i(x) \varphi_i(x) \right\} \\ &= \int \mathcal{D}\varphi' \exp \left\{ iS[\varphi'] + i \int d^4x J_i(x) \varphi'_i(x) \right\} \\ &= Z[J] + i\epsilon \int d^4x J_i(x) \int \mathcal{D}\varphi [V_{ij} \varphi_j(x)] e^{iS[\varphi]}. \end{aligned} \quad (3.44)$$

Using Eq. (3.17), we can write this as

$$\int d^4x \frac{\delta \Gamma[\varphi_J]}{\delta \varphi_i(x)} V_{ij} \langle \varphi_j(x) \rangle_J = 0. \quad (3.45)$$

This constraint will allow us to deduce the properties of a theory close to the ground state, only using information about the symmetries of the theory.

The archetypical example of an internal, global, and continuous symmetry is the linear sigma model, which we will use as an example throughout this section. The linear sigma model is made up of N real scalar fields φ_i , whose Lagrangian is

$$\mathcal{L}[\varphi] = \frac{1}{2} \partial_\mu \varphi_i(x) \partial^\mu \varphi_i(x) - \mathcal{V}(\varphi), \quad \mathcal{V}(\varphi) = -\frac{1}{2} \mu^2 \varphi_i(x) \varphi_i(x) + \frac{1}{4} \lambda [\varphi_i(x) \varphi_i(x)]^2. \quad (3.46)$$

This system is invariant under the rotation of the N fields into each other,

$$\varphi_i \longrightarrow \varphi'_i = M_{ij} \varphi_j, \quad M^{-1} = M^T. \quad (3.47)$$

The set of all such transformations forms the Lie group $O(N)$. For $N = 2$, and $\mu^2, \lambda > 0$ we get the ubiquitous Mexican hat potential, as illustrated in Figure 3.1.

3.3.1 Nöther's theorem

One of the most profound consequences of symmetry in physics is the appearance of conserved quantities. Assume we have a set of fields φ_i . Nöther's theorem tells us that if the Lagrangian $\mathcal{L}[\varphi_i]$ has a continuous symmetry, then there is a corresponding conserved current [2, 40]. Consider an infinitesimal transformation,

$$\varphi_i(x) \longrightarrow \varphi'_i(x) = \varphi_i(x) + \delta \varphi_i(x). \quad (3.48)$$

Applying this transformation to the Lagrangian will in general change its form,

$$\mathcal{L}[\varphi] \rightarrow \mathcal{L}[\varphi'] = \mathcal{L}[\varphi] + \delta \mathcal{L}. \quad (3.49)$$

²Terms of the form $\partial_\mu K^\mu$ do not affect the physics, as the variational principle $\delta S = 0$ does not vary the fields at infinity. Together with the divergence theorem, this means that such terms do not influence the equations of motion.

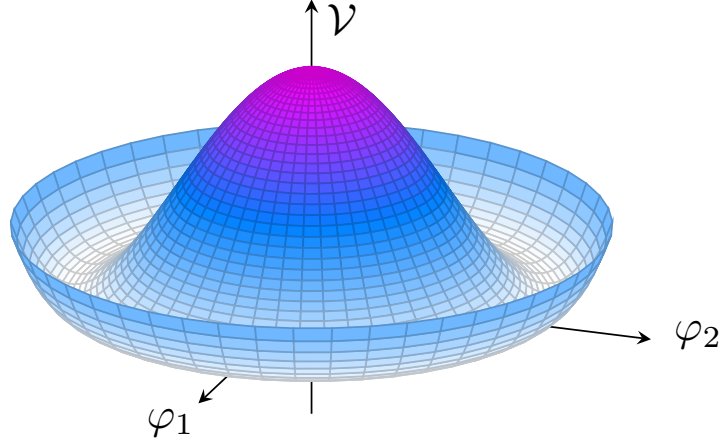


Figure 3.1: The Mexican hat potential is the classical potential \mathcal{V} for the $N = 2$ linear sigma model.

We assume this transformation is a symmetry, i.e.,

$$\delta\mathcal{L} = \partial_\mu K^\mu. \quad (3.50)$$

By considering the Lagrangian as a function of the field and its derivatives, $\mathcal{L} = \mathcal{L}(\varphi_i, \partial_\mu \varphi_i)$, we can write the difference term as a Taylor expansion around $(\varphi_i, \partial_\mu \varphi_i)$,

$$\delta\mathcal{L} = \frac{\partial\mathcal{L}}{\partial\varphi_i} \delta\varphi_i + \frac{\partial\mathcal{L}}{\partial(\partial_\mu \varphi_i)} \delta(\partial_\mu \varphi_i), \quad (3.51)$$

where $\delta(\partial_\mu \varphi_i) = \partial_\mu \varphi'_i - \partial_\mu \varphi_i$. By the linearity of the derivative,

$$\delta(\partial_\mu \varphi_i) = \partial_\mu \varphi'_i - \partial_\mu \varphi_i = \partial_\mu (\varphi'_i - \varphi_i) = \partial_\mu \delta\varphi_i. \quad (3.52)$$

With this, and the Euler-Lagrange equations

$$\partial_\mu \frac{\partial\mathcal{L}}{\partial(\partial_\mu \varphi_i)} - \frac{\partial\mathcal{L}}{\partial\varphi_i} = 0, \quad (3.53)$$

we can rewrite

$$\delta\mathcal{L} = \left(\partial_\mu \frac{\partial\mathcal{L}}{\partial(\partial_\mu \varphi_i)} \right) \delta\varphi_i + \frac{\partial\mathcal{L}}{\partial(\partial_\mu \varphi_i)} (\partial_\mu \delta\varphi_i) = \partial_\mu \left(\frac{\partial\mathcal{L}}{\partial(\partial_\mu \varphi_i)} \delta\varphi_i \right). \quad (3.54)$$

If we define the current

$$J^\mu = \frac{\partial\mathcal{L}}{\partial(\partial_\mu \varphi_i)} \delta\varphi_i(x) - K^\mu, \quad (3.55)$$

then combining Eq. (3.50) and Eq. (3.54) gives

$$\partial_\mu J^\mu = 0. \quad (3.56)$$

This is Nöther's theorem; a continuous symmetry implies the existence of a conserved current.

The current flux through some spacelike surface V defines a conserved charge. The surface of constant time in some reference frame has the normal vector $n_\mu = (1, 0, 0, 0)$, so the charge is

$$Q = \int_V d^4x n_\mu J^\mu = \int_V d^3x J^0. \quad (3.57)$$

We can then use the divergence theorem. Assume ∂V is the boundary of V , which has the space-like normal vector k_i , and that the current falls quickly towards infinity. Then, using $\partial_\mu J^\mu = 0$,

$$\frac{dQ}{dt} = \int_V d^3x \partial_0 J^0 = - \int_V d^3x \partial_i J^i = - \int_{\partial V} d^2x k_i J^i = 0, \quad (3.58)$$

proving that the charge is conserved over time. These results, however, rely on the equations of motion. This is generally valid in classical mechanics. However, in quantum mechanics, the path integral is over *all* paths, not just those that are on-shell, and we can therefore not assume the equations of motion vanish. We will later derive the quantum version of the conservation law Eq. (3.56).

3.3.2 Goldstone's theorem

A symmetry transformation will leave the governing equation of a theory unchanged. This, however, does not imply that physical states, such as the ground state, are invariant under this transformation. The $N = 2$ linear sigma model illustrates this. If we assume the ground state φ_0 is translationally invariant, then it is given by minimizing the effective potential, of which the classical potential, \mathcal{V} , is the leading order approximation. This potential is illustrated in Figure 3.1. The ground state is therefore given by any of the values along the brim of the potential. If we, without loss of generality, choose $\varphi_0 = (0, v)$ as the ground state, then any rotation will change this state. We say that the symmetry has been *spontaneously broken*.

To explore this in a general context, assume a theory of N real scalar fields φ_i are invariant under the actions of some Lie group, G . A symmetry $g \in G$ is broken if the vacuum expectation value of the original fields and the transformed fields differ. That is, if

$$\langle \varphi \rangle_0 \neq \langle \varphi' \rangle_0 = \langle g\varphi \rangle_0. \quad (3.59)$$

We can now exploit what we learned about Lie groups to write the infinitesimal transformation as

$$\langle \varphi' \rangle_0 = \langle \varphi \rangle_0 + i\epsilon\eta_\alpha T_\alpha \langle \varphi \rangle_0. \quad (3.60)$$

Let x_ℓ be the set of generators corresponding to broken symmetries, i.e.,

$$x_\ell \langle \varphi \rangle_0 \neq 0. \quad (3.61)$$

These are called the *broken generators*. The remaining set of generators t_a , which obey

$$t_a \langle \varphi \rangle_0 = 0, \quad (3.62)$$

are called unbroken, and generate a subgroup $H \subset G$ as the set of symmetry transformations of the vacuum is a group.

In Eq. (3.45) we found that, if V is the generator of some symmetry, then the effective action obeys

$$\int d^4x \frac{\delta \Gamma[\varphi_J]}{\delta \varphi_i} V_{ij} \langle \varphi_j \rangle_0 = 0. \quad (3.63)$$

We now differentiate this expression with respect to $\varphi_k(y)$, which gives

$$\int d^4x \frac{\delta^2 \Gamma[\varphi_0]}{\delta \varphi_k(y) \delta \varphi_i(x)} V_{ij} \langle \varphi_j \rangle_0 = 0. \quad (3.64)$$

With the assumption that the ground state is constant, we get

$$\frac{\partial^2 \mathcal{V}_{\text{eff}}}{\partial \varphi_k \partial \varphi_i} V_{ij} \langle \varphi_j \rangle_0 = 0. \quad (3.65)$$

This is trivial for unbroken symmetries, as $t_{ij}^a \langle \varphi_j \rangle_0 = 0$ by definition. However, in the case of broken symmetries, the second derivative of the effective potential must have an eigenvector $x_{ij}^\ell \langle \varphi_j \rangle_0$ with a zero eigenvalue for each broken generator. Here, ℓ labels the set of generators,

while (ij) are the indices corresponding to field-components φ_i . We found that the second derivative of the effective action is the inverse propagator,

$$D_{ij}^{-1}(x, y) = \frac{\delta^2 \Gamma[\varphi_0]}{\delta \varphi_i(y) \delta \varphi_j(x)} = \int \frac{d^4 p}{(2\pi)^4} e^{-ip(x-y)} \tilde{D}_{ij}^{-1}(p). \quad (3.66)$$

Using this, we can write

$$\tilde{D}_{ij}^{-1}(p=0) x_{jk}^\ell \langle \varphi_k \rangle_0 = 0. \quad (3.67)$$

Zeros of the inverse propagator correspond to the physical mass of particles. In Lorentz-invariant systems, each zero-eigenvalue vector corresponds to a massless particle, called a Goldstone boson.³ This means there are $n_G = \dim G - \dim H$ zero-mass modes. In general, the counting of massless modes is complicated and depends on the dispersion relation of the particles at low momenta. Systems with Goldstone bosons with quadratic dispersion relation, that is $E \propto |\vec{p}|^2$ when $\vec{p} \rightarrow 0$, often exhibit a lower number of massless modes. An example is ferromagnetic, where the $SU(2)$ rotational symmetry is broken down to $U(1)$ when they align along one axis. This corresponds to two broken generators, yet the system exhibits only one massless mode [43].

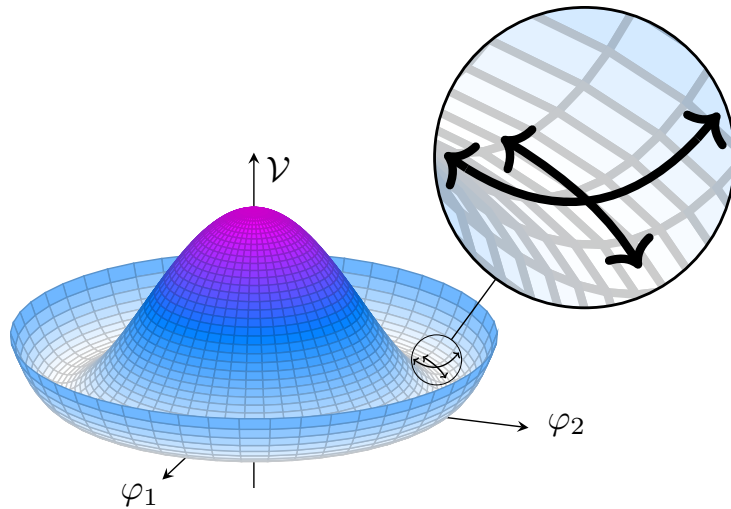


Figure 3.2: Excitations along the brim does not cost any energy, as the potential is flat, unlike excitations in the radial direction.

The linear sigma model gives an intuition for the Goldstone mode. In the case of $N = 2$, the symmetry of the Lagrangian are rotations in the plane. As the ground state is a point along the “brim” of the hat, this rotational symmetry is broken. However, any excitations in the angular direction do not cost any energy, which is indicative of a massless mode. This is illustrated in Figure 3.2. In this example, the original symmetry group is one-dimensional, so there are no unbroken symmetries. Consider instead the $N = 3$ linear sigma model, which has the three-dimensional symmetry group $SO(3)$, rotations of the sphere. We see that the ground state is left invariant under a subgroup of the original symmetry transformations. The ground state manifold of this system, the set of all states that minimizes the effective potential, is then a sphere. When the system chooses one single ground state, this symmetry is broken, but only for two of the generators. The generator for rotations around the ground state leaves that point unchanged and is thus an unbroken symmetry. Any excitations in the direction of the broken symmetries do not cost energy, as it is in the ground state manifold. On the other hand, the unbroken symmetry does not correspond to an excitation. This is illustrated in Figure 3.3.

³The particles are bosons due to the bosonic nature of the transformations, g . If the generators are Grassmann numbers, the resulting particles, called goldstinos, are fermions.

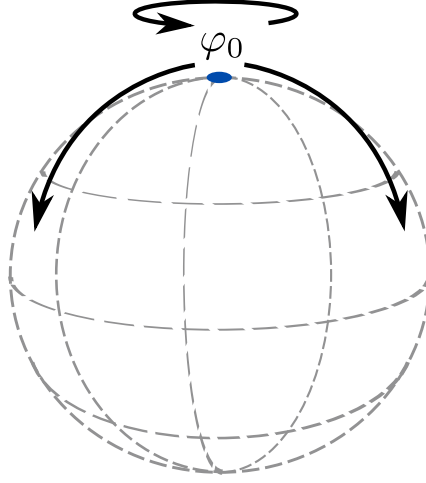


Figure 3.3: Excitations for the $N = 3$ sigma model. Two of the symmetries are broken, while rotations around the ground state leaves the system unchanged.

3.4 *CCWZ construction

This section is based on [42, 44–48].

As Goldstone bosons are massless, they play a crucial role in low-energy dynamics. To best describe this limit, we seek a parametrization of the theory in which they are the degrees of freedom. This can be done using the CCWZ construction, named after Callan, Coleman, Wess, and Zumino.

3.4.1 Parametrizing the Goldstone manifold

We saw that the Goldstone bosons correspond to excitations within the vacuum manifold. The vacuum manifold corresponds to points in field space φ that can be reached from the vacuum φ_0 with a transformation $g \in G$. Assume this group acts linearly on the fields. This means that we can write such excitations as

$$\varphi_i = (\tilde{\Sigma}\varphi_0)_i = \tilde{\Sigma}_{ij}(\varphi_0)_j, \quad \tilde{\Sigma} = \tilde{\Sigma}(\eta) = \exp\{i\eta_\alpha T_\alpha\}. \quad (3.68)$$

We will drop the indices (i, j) for the sake of compact notation. $\tilde{\Sigma}$ is thus a function from the parameter space, $\eta_\alpha \in \mathbb{R}^n$, to G ,

$$\tilde{\Sigma} : \mathbb{R}^n \mapsto G. \quad (3.69)$$

We then get field configurations by making the parameters dependent on space-time. We will for now assume η_α is constant. This parametrization is highly redundant. Two elements $\tilde{\Sigma}$ and $\tilde{\Sigma}'$, related by

$$\tilde{\Sigma}' = \tilde{\Sigma} e^{i\theta_a t_a} \quad (3.70)$$

results in the same φ . This is because $e^{i\theta_a t_a} = h \in H$, and $h\varphi_0 = \varphi_0$, by assumption. The set of all equivalent $\tilde{\Sigma}$'s is exactly the left coset, $gH = \{gh \mid h \in H\}$. The set of cosets forms a new manifold, G/H , called the Goldstone manifold. This is a manifold of dimension $\dim(G/H) = \dim(G) - \dim(H)$, which is the number of broken generators and thus also the number of Goldstone modes. Membership of a certain coset is an equivalence relation, $g \sim g'$ if $g' = gh$. This means that the cosets gH form a partition of G and that each element $g \in G$ belongs to one, and only one, coset. To remove the redundancy in the parametrization, we need to choose one representative element from each coset.

By the inverse function theorem, any mapping between manifolds $f : \mathcal{M} \mapsto \mathcal{N}$ that has a non-degenerate differential, that is an invertible Jacobian, at a point $p \in \mathcal{M}$, is invertible in a neighborhood of p . If we write

$$\tilde{\Sigma}(\xi, \theta) = \exp \{i\xi_i x_i\} \exp \{i\theta_a t_a\}, \quad (3.71)$$

then the map is invertible at $p = (\xi_i = 0, \theta_a = 0)$, as the Jacobian is the identity matrix. This point is mapped to the identity element of G . This means that, in a neighborhood $U \subset G$ of the identity, each element g has a unique representation $g = \tilde{\Sigma}$ [39]. Furthermore, two elements $\tilde{\Sigma}'$ and $\tilde{\Sigma}$ related by $\tilde{\Sigma}' = \tilde{\Sigma}h$, $h \in H$ have the same ξ -arguments. We see that ξ_i parametrize G/H , in the neighborhood of the identity. We therefore demand that $\tilde{\Sigma}$ always appear in the standard form

$$\Sigma(\xi) = \tilde{\Sigma}(\xi, 0) = \exp \{i\xi_i x_i\}. \quad (3.72)$$

The field $\varphi(x)$ can therefore be written as

$$\varphi(x) = \Sigma(x)\varphi_0 = \exp \{i\xi_i(x)x_i\} \varphi_0, \quad (3.73)$$

and $\xi_i(x)$ can be associated with the Goldstone bosons.

In the linear sigma model, the original $O(N)$ symmetry is broken down to $O(N-1)$, which transforms the remaining $N-1$ fields with vanishing expectation values into each other. However, $O(N)$ consists of two disconnected subsets, those matrices with determinant 1 and those with determinant -1. There is no continuous path that takes an element of $O(N)$ with determinant -1 to an element with determinant 1.⁴ The set of symmetries that are connected to the identity is

$$G = SO(N) = \{M \in O(N) \mid \det M = 1\}. \quad (3.74)$$

If we choose $\varphi_0 = (0, 0, \dots, v)$, then it is apparent that the ground state is invariant under the rotations of the $N-1$ first fields, so the unbroken symmetry is $H = SO(N-1)$. The Goldstone manifold is $G/H = SO(N)/SO(N-1)$.

Consider the case of $N = 3$, which is illustrated in Figure 3.3. G is the rotations of the sphere, while H is rotations around φ_0 , $SO(2)$. The Goldstone manifold consists of the rotations of φ_0 to other points of the sphere, i.e. $G/H = SO(3)/SO(2) = S^2$, the 2-sphere. This is not a Lie group, as translating φ in a closed path around the sphere may result in a rotation around the z-axis. This is illustrated in Figure 3.4

To check that ξ_i are the Goldstone modes, we study the way they appear in the Lagrangian. As they are massless, no mass term of the form $M_{ij}\xi_i\xi_j$ should appear. The original Lagrangian $\mathcal{L}[\varphi]$ was invariant under global transformations $\varphi(x) \mapsto g\varphi(x)$. However, any terms that only depend on $\varphi(x)$, and not its derivatives, will also be invariant under a *local* transformation, $\varphi(x) \mapsto g(x)\varphi(x)$. Our parametrization of the fields, $\varphi(x) = \Sigma(x)\varphi_0$ is exactly such a transformation, which means that any such terms are independent of the Goldstone bosons. We can therefore write

$$\mathcal{L}[\varphi] = \mathcal{L}_{\text{kin}}[\varphi] + \mathcal{V}(\varphi_0), \quad (3.75)$$

where all terms in \mathcal{L}_{kin} are proportional to at least one derivative term, $\partial_\mu \varphi(x)$, while \mathcal{V} is independent of $\Sigma(x)$. Inserting the parametrization into this derivative term, we get

$$\partial_\mu \varphi(x) = \partial_\mu [\Sigma(x)\varphi_0] = \Sigma(x)[\partial_\mu \Sigma(x)]\varphi_0. \quad (3.76)$$

The Lagrangian will therefore depend on ξ_i via terms of the form $\Sigma(x)^{-1}\partial_\mu \Sigma(x)$, which is called the Maurer-Cartan form. This is a \mathfrak{g} -valued function, which means that it can be written as

$$i\Sigma(x)^{-1}\partial_\mu \Sigma(x) = d_\mu(x) + e_\mu(x), \quad (3.77)$$

$$d_\mu = ix_i d_{ij}(\xi) \partial_\mu \xi_j, \quad (3.78)$$

$$e_\mu = it_a e_{ai}(\xi) \partial_\mu \xi_i, \quad (3.79)$$

⁴A simple proof of this is the fact that the determinant is a continuous function, while any path $\det M(t)$ such that $\det M(1) = -1$, $\det M(0) = 1$ must make a discontinuous jump.

where d_{ij} and e_{ai} are as-of-yet unknown real valued functions of ξ [42, 49].

3.4.2 Transformation properties of Goldstone bosons

We can deduce how the Goldstone bosons transform under G from how φ transforms. In general,

$$\varphi' = g\varphi = (g\Sigma(\xi))\varphi_0 = \Sigma(\xi')\varphi_0 \quad g \in G. \quad (3.80)$$

While $\Sigma(\xi')$ has the standard form by assumption,

$$\Sigma(\xi') = \exp \{i\xi'_i x_i\}, \quad (3.81)$$

$g\Sigma(\xi)$ does not, in general.

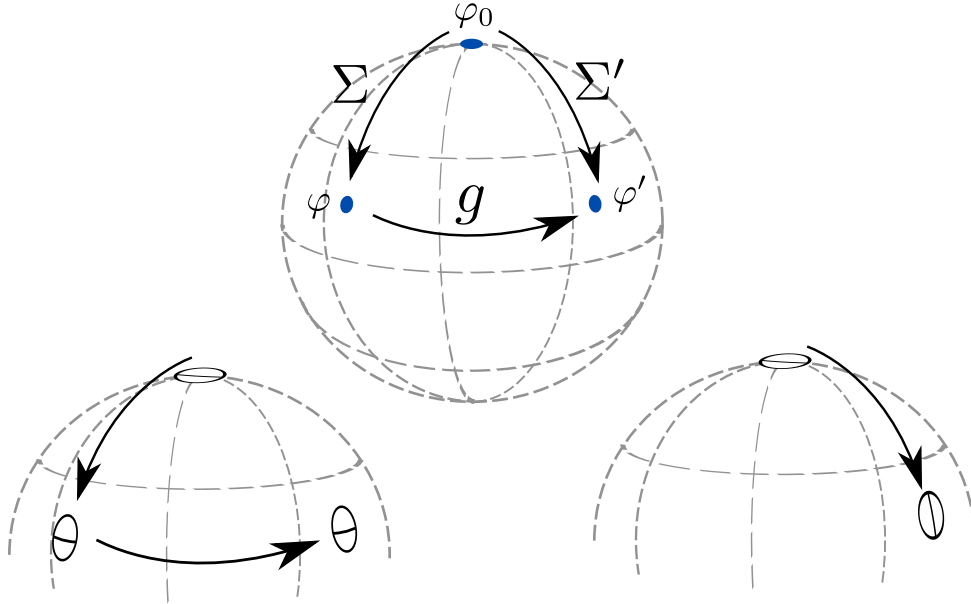


Figure 3.4: The top figure illustrates the transformation of φ_0 to φ and then φ' , and the alternative, direct transformation $\varphi_0 \rightarrow \varphi'$. The bottom figure illustrates how this can rotate a neighborhood of φ_0 differently.

Figure 3.4 illustrates this in the case of $G = \text{SO}(3)$. $\Sigma(\xi)$ transforms φ_0 to φ , then g transforms φ to $\varphi' = \Sigma(\xi')\varphi_0$. Assuming φ and φ' are close enough to φ_0 , we can write $\Sigma(\xi)$ and $\Sigma(\xi')$ on the standard form. However, if we follow a small neighborhood around φ_0 as it is acted on by $\Sigma(\xi)$, then g , it will be rotated by the time it arrives at φ' when compared to the same neighborhood if it was acted on by $\Sigma(\xi')$.

$g\Sigma(\xi)$ and $\Sigma(\xi')$ are in the same coset, as they by assumption corresponds to the same physical state. This means that we can write $g\Sigma(\xi) = \Sigma(\xi')h(g, \xi)$, where $h(g, \xi) \in H$. The transformation rule of ξ under G is therefore implicitly defined by

$$\Sigma(\xi') = g\Sigma(\xi)[h(g, \xi)]^{-1}. \quad (3.82)$$

This is, in general, not a linear representation, which is why this construction also is called a *non-linear realization*. Using the transformation rule, we can obtain the transformation rule of the Maurer-Cartan form. We use the shorthand $\Sigma = \Sigma(\xi)$, $\Sigma' = \Sigma(\xi')$, and $h = h(g, \xi)$. This

gives

$$\begin{aligned}
\Sigma^{-1}\partial_\mu\Sigma &\rightarrow \Sigma'^{-1}\partial_\mu\Sigma' \\
&= (g\Sigma h^{-1})^{-1}\partial_\mu(g\Sigma h^{-1}) \\
&= (h\Sigma^{-1}g^{-1})g[(\partial_\mu\Sigma)h^{-1} + \Sigma\partial_\mu h^{-1}] \\
&= h\Sigma^{-1}(\partial_\mu\Sigma)h^{-1} + h\partial_\mu h^{-1} \\
&= h(\Sigma^{-1}\partial_\mu\Sigma + \partial_\mu)h^{-1}.
\end{aligned}$$

In terms of d_μ and e_μ ,

$$d_\mu \rightarrow h d_\mu h^{-1}, \quad (3.83)$$

$$e_\mu \rightarrow h(e_\mu + i\partial_\mu)h^{-1}. \quad (3.84)$$

The transformation rule of e_μ is that of a gauge field, with the gauge group H . We will discuss gauge fields in more detail in Chapter 5. If we include massive degrees of freedom and not only the Goldstone modes, e_μ is used to create a covariant derivative of the massive modes. We are only interested in the Goldstone modes and will therefore be satisfied with d_μ . We have now greatly constrained the way the Goldstone modes may appear in the Lagrangian. However, this does not yet solve the problem of the strong force being non-perturbative. To do this, we need to create an effective field theory in which the strong force has been integrated out.

3.5 Constructing an effective field theory

This section is based on [9, 14, 15, 40, 50].

One of the most powerful concepts in quantum field theory is the notion of effective field theories. The methods we have laid out for quantum field theory involve, in general, calculations where we must integrate over all possible momenta and thus all possible energies. However, we do not profess to know how physics behaves at arbitrarily high energies, which at first glance seem to render our theories moot. The fact that the standard model allows for such precise predictions suggests that the physics that happens at energies that are accessible to us can be described without knowledge of physics at the highest energies. This is a familiar concept from our everyday life—we can describe billiard balls colliding or rocks falling with high precision without having an accurate microscopic description of these objects. An effective field theory is a description of the physics of some underlying theory, some degrees of freedom φ_a governed by a Lagrangian $\mathcal{L}[\varphi]$, in terms of a smaller set of degrees of freedom, π_i , governed by an effective Lagrangian $\mathcal{L}_{\text{eff}}[\pi]$. As they describe the same physics, these two descriptions are related by

$$Z = \int \mathcal{D}\varphi \exp \left\{ i \int d^4x \mathcal{L}[\varphi] \right\} = \int \mathcal{D}\pi \exp \left\{ i \int d^4x \mathcal{L}_{\text{eff}}[\pi] \right\}. \quad (3.85)$$

We say that the degrees of freedom not present in the effective description have been *integrated out*. An effective theory can come from integrating out all degrees of freedom above some energy cut off or integrating out a particle and describing the interactions it mediates as point-like. In section 3.2, we found that the 1PI effective action resulted from integrating out all fluctuations away from the ground state, leaving us with an effective field theory in which all interactions are described entirely at the tree level. Furthermore, the modern understanding of the Standard Model is that it is an effective field theory. This would mean some more complete theory of physics—perhaps string theory, quantum loop gravity or something we have yet to think of—acts as an effective theory at low energies. Low energies, in this context, include collisions at the LHC, which is why the Standard Model is so successful [14].

One of the pioneers of the philosophy of effective field theories was Steven Weinberg. He proposed that quantum field theories, in themselves, have almost no content beyond some basic

assumptions [15]. This means that if we try to model a system by writing down the most general possible Lagrangian, we cannot be wrong. This was formulated more precisely in—as Weinberg himself called it—a “theorem”:

“[I]f one writes down the most general possible Lagrangian, including all terms consistent with assumed symmetry principles, and then calculates matrix elements with this Lagrangian to any given order of perturbation theory, the result will simply be the most general possible S -matrix consistent with analyticity, perturbative unitarity, cluster decomposition and the assumed symmetry principles.” [1]

The properties of “analyticity, perturbative unitarity and cluster decomposition” are basic properties we expect of good, effective theories. Analyticity is an assumption about the poles of the S -matrix, and perturbative unitarity says that the theory should be unitary, as quantum theories should, for *any order in perturbation theory*. Cluster decomposition states that non-entangled processes far apart should be independent [41, 42]. Such a “most general possible Lagrangian” will have the form

$$\mathcal{L}_{\text{eff}}[\pi] = \sum_i \lambda_i \mathcal{O}_i[\pi], \quad (3.86)$$

where $\mathcal{O}_i[\pi]$ are local functionals of the effective fields and their derivatives, and λ_i are coupling constants. The coupling constants are free parameters, which parametrizes the most general S -matrix consistent with foundational assumptions and the underlying theory. A Lagrangian with an infinite amount of free parameters might seem useless. However, if we can find a consistent series expansion, then only a finite number of terms are needed to calculate quantities to any given order in perturbation theory. Furthermore, even though such a theory is called “non-renormalizable”—renormalizing an arbitrary order in perturbation theory requires an arbitrary number of parameters—only a finite number of parameters are needed to renormalize any *given* order. Non-renormalizable theories can thus perfectly well be renormalized [9].

In the last section, we showed that the Goldstone modes will always appear in the Lagrangian as the terms of the Maurer-Cartan form, d_μ , and e_μ . Thus, the approach to creating an effective theory of Goldstone bosons, such as chiral perturbation theory, is to write down the most general Lagrangian, consistent with the underlying symmetries, made up of these terms. Then, using Weinberg’s power counting scheme, as we discuss in subsection 5.2.1, we expand perturbatively in the Goldstone boson energies. This will give us a self-consistent description of the Goldstone bosons of the theory, the pseudoscalar mesons. The world is, of course, not only made up of only pseudoscalar mesons. We also need to describe how these fields interact with other fields or external sources. Furthermore, the global $\text{SU}(N_f) \times \text{SU}(N_f)$ symmetry of QCD with N_f quarks is only approximate, as we will explore further in Chapter 5. We must extend the CCWZ construction to incorporate these effects, which we will do by introducing some new QFT tools in the next subsection.

3.5.1 Schwinger-Dyson equations and Ward identities

Given a system of fields φ_a governed by some action $S[\varphi]$, the expectation value of a functional of the fields, $F[\varphi]$, is given by

$$\langle F[\varphi] \rangle = \int \mathcal{D}\varphi e^{iS[\varphi]} F[\varphi]. \quad (3.87)$$

If we perform a *local* transformation of the field on the form $\varphi(x) \rightarrow \varphi(x) + \epsilon \eta(x)$, the integral measure will remain unchanged. The expectation value, to first order in ϵ , then changes as

$$\langle F \rangle \rightarrow \int \mathcal{D}\varphi e^{i(S+\epsilon\delta S)} (F + \epsilon\delta F) = \langle F \rangle + \epsilon \langle i(\delta_\eta S) F \rangle + \epsilon \langle \delta_\eta F \rangle. \quad (3.88)$$

The variation δ_η is related to the functional derivative through $\delta_\eta S = \int d^n x \frac{\delta S[\varphi]}{\delta \varphi(x)} \eta(x)$, as defined in section A.3. As this amounts to a change of integration variable, the expectation value should remain unchanged. This gives us the important identity

$$\langle i(\delta_\eta S[\varphi])F[\varphi] \rangle + \langle \delta_\eta F[\varphi] \rangle = 0. \quad (3.89)$$

Inserting the integral form of the variation, and using the fact that η is independent of φ , we may write this identity as

$$\left\langle \frac{\delta S[\varphi]}{\delta \varphi(x)} F[\varphi] \right\rangle = i \left\langle \frac{\delta F[\varphi]}{\delta \varphi(x)} \right\rangle. \quad (3.90)$$

The Schwinger-Dyson equations are important special cases of this identity. They are the equations of motion of correlation functions. They thus incorporate the dynamics of a theory. We derive them by setting $F[\varphi] = \varphi(x_1) \dots \varphi(x_n)$. If we have a Lagrangian on the form $\mathcal{L} = -\frac{1}{2}\varphi(\partial^2 + m^2)\varphi - V[\varphi]$, then Eq. (3.90) becomes

$$\begin{aligned} (\partial_x^2 + m^2) \langle \varphi(x) \varphi(x_1) \dots \varphi(x_n) \rangle &= - \langle \mathcal{V}'[\varphi](x) \varphi(x_1) \dots \varphi(x_n) \rangle \\ &\quad - i \sum_i \delta(x - x_i) \langle \varphi(x_1) \dots \varphi(x_{i-1}) \varphi(x_{i+1}) \dots \varphi(x_n) \rangle. \end{aligned}$$

If $n = 1$ and $\mathcal{V} = 0$, we get the defining relation for the free Greens function,

$$(\partial_x^2 + m^2) \langle \varphi(x) \varphi(y) \rangle = -i\delta(x - y). \quad (3.91)$$

We may also consider slightly more general transformations of $\varphi(x)$, such as local phase-transformations $\varphi(x) \rightarrow e^{i\epsilon(x)}\varphi(x)$, as long as they do not affect the measure of the path integral. We will use this to derive identities related to the Schwinger-Dyson equations that incorporate the symmetries of a given theory. If $\varphi(x) \rightarrow \varphi(x) + \delta\varphi(x)$ is a global symmetry transformation, so that $\delta\mathcal{L} = \partial_\mu K^\mu$ and the integration measure is unchanged, then $\varphi(x) \rightarrow \varphi(x) + \eta(x)\delta\varphi(x)$ is a corresponding local transformation. We recover the global transformation for $\eta = 1$. The variation of the action from this transformation will be

$$\begin{aligned} \delta S &= \int d^4x \left(\frac{\partial \mathcal{L}}{\partial \varphi} \eta \delta\varphi + \frac{\partial \mathcal{L}}{\partial(\partial_\mu \varphi)} \partial_\mu(\eta \delta\varphi) \right) \\ &= \int d^4x \left(\frac{\partial \mathcal{L}}{\partial(\partial_\mu \varphi)} \delta\varphi \right) \partial_\mu \eta + \int d^4x \eta(x) \left(\frac{\partial \mathcal{L}}{\partial \varphi} \delta\varphi + \frac{\partial \mathcal{L}}{\partial(\partial_\mu \varphi)} \partial_\mu \delta\varphi \right) \\ &= - \int d^4x \eta(x) \partial_\mu \left(\frac{\partial \mathcal{L}}{\partial(\partial_\mu \varphi)} \delta\varphi - K^\mu \right). \end{aligned}$$

In the last line, we integrated by parts, and used $\delta\mathcal{L} = \partial_\mu K^\mu$. From subsection 3.3.1, we recognize the term within the parenthesis as precisely the Nöther current J^μ , so

$$\delta S = - \int d^4x \eta(x) \partial_\mu J^\mu. \quad (3.92)$$

As φ is an integration variable in the path integral, it is not necessarily on-shell. We can therefore not use Nöther's theorem, $\partial_\mu J^\mu = 0$, as this relies on the equation of motion. However, for $F = 1$ and thus $\delta F = 0$, we can insert Eq. (3.92) into Eq. (3.87) to obtain the quantum version of the current conservation equation of Nöther's theorem, Eq. (3.56),

$$\partial_\mu \langle J^\mu \rangle = 0. \quad (3.93)$$

With $F = \varphi(x_1)\varphi(x_2)$, we get [9, 40]

$$\partial_{x,\mu} \langle J^\mu(x) \varphi(x_1) \varphi(x_2) \rangle = -i\delta(x - x_1) \langle \delta\varphi(x_1) \varphi(x_2) \rangle - i\delta(x - x_2) \langle \varphi(x_1) \delta\varphi(x_2) \rangle. \quad (3.94)$$

Identities of this form are called Ward-Takashi identities, often just Ward-identities, and encode the symmetries of a theory. In case symmetry is only approximate, so $\delta\mathcal{L} = \partial_\mu K^\mu + \Delta$, where Δ

is some small symmetry breaking operator, or it is subject to an anomaly, so $\mathcal{D}\varphi \rightarrow \mathcal{D}\varphi(1 + \Delta)$, then the conservation equation is modified to

$$\partial_\mu \langle J^\mu \rangle = \langle \Delta \rangle. \quad (3.95)$$

To create the generating functional, we must add external currents j . However, these new terms in the Lagrangian might break the invariance under a symmetry transformation $\varphi \rightarrow \varphi'$. If we transform the external currents as $j \rightarrow j'$ to counteract the transformation of the fields, then the theory should remain invariant. As before, we make both these transformations local, making sure that they leave the measure invariant. We can then perform a change of variable in the path integral, which relates generating functionals with different external currents, $Z[j] = Z[j']$. This relation must not only be obeyed by the underlying theory but also by any effective theory, which significantly constrains the form of the effective Lagrangian. As an illustration, we consider an example of spinor fields adapted from [50], as this is closely related to the construction of chiral perturbation theory. Spinors and gauge theory, which are relevant for this example, are discussed in more depth in Chapter 5. Consider a massless spinor field with the Lagrangian,

$$\mathcal{L} = i\bar{\psi}\not{\partial}\psi - \mathcal{V}[\psi, \bar{\psi}]. \quad (3.96)$$

Assume this theory has a global $SU(N)$ symmetry, so the \mathcal{V} remains unchanged under the transformation $\psi \rightarrow U\psi$, $\bar{\psi} \rightarrow \bar{\psi}U^\dagger$. The system then has a corresponding conserved current,

$$J_\alpha^\mu = \bar{\psi}T_\alpha\gamma^\mu\psi, \quad (3.97)$$

where T_α are the generators of $SU(N)$. We then include spinor sources $\eta = \eta_\alpha T_\alpha$ and vector sources $v_\mu = v_\mu^\alpha T_\alpha$ by adding the terms $\bar{\eta}\psi$, $\bar{\psi}\eta$, and $v_\mu^\alpha J_\alpha^\mu$ to the Lagrangian. Under a local $SU(N)$ transformation, $\psi \rightarrow e^{i\theta_\alpha(x)T_\alpha}\psi$, the action changes as

$$S \rightarrow \int d^4x \left[i\bar{\psi}\not{\partial}\psi - \mathcal{V}[\psi, \bar{\psi}] + \bar{\eta}U\psi + \bar{\psi}U^\dagger\eta + \bar{\psi}\gamma^\mu(U^\dagger v_\mu U + iU^\dagger\partial_\mu U)\psi \right]. \quad (3.98)$$

The last term corresponds to the change in action without sources, which we found earlier Eq. (3.92). We then define transformations of the external fields to counteract the transformation of ψ . As these transformations are local, the sources now act as gauge fields. The gauge transformation of the external sources are

$$\eta \rightarrow U\eta, \quad \bar{\eta} \rightarrow \bar{\eta}U^\dagger, \quad v_\mu \rightarrow U(v_\mu + i\partial_\mu)U^\dagger. \quad (3.99)$$

This gives the relation $S[\psi', \bar{\psi}', \eta', \bar{\eta}', v'] = S[\psi, \bar{\psi}, \eta, \bar{\eta}, v]$, where the prime indicates gauge transformed fields. As we argued in the subsection on the Dyson-Schwinger equations, we can change the integration variables inside the path integral without changing the result. Considering an infinitesimal transformation, and expanding to first order in θ , we get

$$\begin{aligned} 0 &= Z[\eta', \bar{\eta}', v'] - Z[\eta, \bar{\eta}, v] \\ &= i \int d^4x \langle i\theta_\alpha(x)\bar{\psi}T_\alpha\eta - i\theta_\alpha(x)\bar{\eta}T_\alpha\psi + i\bar{\psi}\gamma^\mu(i\theta_\alpha(x)[T_\alpha, v_\mu] - i\partial_\mu\theta_\alpha(x)T_\alpha)\psi \rangle \end{aligned} \quad (3.100)$$

As the transformation, and thus θ_α , is arbitrary, the integrand must vanish. After partial integration, we are left with

$$\langle \bar{\psi}T_\alpha\eta - \bar{\eta}T_\alpha\psi + D_\mu^{\alpha\beta}J_\beta^\mu \rangle = 0. \quad (3.101)$$

Here, $D_\mu^{\alpha\beta}$ is the covariant derivative in the adjoint representation, $D_\mu^{\alpha\beta}J_\nu^\beta = (\delta_{\alpha\beta}\partial_\mu + iv_\mu^\gamma f^{\alpha\gamma\beta})J_\nu^\beta$, and $f^{\alpha\beta\gamma}$ are the structure constants of $\mathfrak{su}(N)$. We can get a more general expression by writing this using the generating functional W ,

$$\left(\frac{\delta}{\delta\eta_\alpha(x)}\eta - \bar{\eta}\frac{\delta}{\delta\bar{\eta}_\alpha(x)} + D_\mu^{\alpha\beta}\frac{\delta}{\delta v_\mu^\beta(x)} \right) W[\eta, \bar{\eta}, v] = 0. \quad (3.102)$$

If we evaluate this at $\eta = \bar{\eta} = v_\mu = 0$, we get the quantum conservation equation $\partial_\mu \langle J_\alpha^\mu \rangle = 0$. From Eq. (3.102), we can also get more general Ward identities by taking functional derivatives with respect to the external sources.

We have now seen how the Ward identities encode the global symmetries of the theory, and that they may be derived by transforming external source fields as gauge fields to ensure the invariance of the action under the corresponding *local* transformations. This is the key insight behind the systematic development of chiral perturbation theory [51–53]. With the CCWZ construction, we can create the Lagrangian of Goldstone bosons alone, given only the symmetry breaking pattern $G \rightarrow H$. However, it does not tell us how they are coupled to external fields. With the constraint Eq. (3.100), we know that the new action must be invariant under *local* G transformations, given that we transform the external fields as gauge fields. When including external fields, the new effective Lagrangian \mathcal{L}_{eff} must therefore not only be invariant under global G transformations but rather local G transformations. If we modify the Mauer-Cartan form Eq. (3.77) by introducing a covariant derivative,

$$i\Sigma(x)^{-1}\partial_\mu\Sigma(x) \rightarrow i\Sigma(x)^{-1}\nabla_\mu\Sigma(x), \quad (3.103)$$

then all terms that were invariant under global G become locally so. This is because, as in the case of covariant derivative in subsection 2.1.2, the covariant derivative transforms as the object it acts on. In addition to new and modified terms due to the covariant derivative, we can now also combine the external currents and Σ into G -invariant terms. This will allow us to take into account approximate symmetries as well. By treating the symmetry-breaking parameter in the underlying Lagrangian, such as the mass of quarks in the case of chiral perturbation theory, as an external current, we can still apply this procedure. Such fields are called *spurion fields*. We will apply this to derive chiral perturbation theory in Chapter 5.

Chapter 4

Gravity

General relativity describes how matter and energy curve the fabric of space and time. Einstein first wrote down the theory more than a century ago, and it is still our most accurate theory of gravitational effects. It makes precise and counterintuitive predictions, which experiments have borne out. This chapter surveys the basics of general relativity. We will then use this to derive the Tolman-Oppenheimer-Volkoff (TOV) equation, a differential equation used to model stars. We start by summarizing the theory it succeeded.

4.1 Newtonian Gravity

This section is based on [2].

Newton's famous law of gravity states that the force of gravity from an object of mass M acting on another object of mass m is proportional to both objects' masses and is inversely proportional to the distance between them squared. This force is directed radially inwards. Formulating this as an equation, with \vec{r} as the vector from the object with mass M to that with mass m with length $|\vec{r}| = r$, gives

$$\vec{F}_g = -\frac{GMm}{r^2}\hat{r}. \quad (4.1)$$

Here, G is Newton's gravitation constant, and $\hat{r} = \vec{r}/r$. The vector \vec{r} is a purely spatial three-vector, as space is separated from time in the Newtonian picture. The law of gravitation, together with Newton's second law of motion

$$\sum_i \vec{F}_i = m\vec{a}, \quad (4.2)$$

where \vec{a} is the acceleration of an object and \vec{F}_i the forces acting upon it, can account for the motion of stellar objects. These laws work well in all but the most extreme circumstances, involving very massive objects or very short distances. As we will see, such extreme circumstances can be quantified by $2GM \approx r$. Newtonian gravity works well as an approximation because G is small in everyday units. Highly precise measurements of the orbit of Mercury were needed before any deviation from it was noticed.

We restate Newtonian gravity in a field-theoretic language to better compare Newtonian gravity to its successor theory. The gravitational potential from a mass M , which gives rise to Newton's force law, obeys the equation

$$\nabla^2\Phi_g = -4\pi G\rho. \quad (4.3)$$

Here, ρ is the mass density. For a single point mass, $\rho(\vec{r}) = M\delta(\vec{r})$, this has the solution

$\Phi_g = -GM/r$. The acceleration due to gravity is then

$$\vec{a} = -\vec{\nabla}\Phi_g. \quad (4.4)$$

We see that mass acts as a gravitational charge. Due to the success of Newtonian gravity, we expect it to be a limit of any theory that succeeds it. This gives us the ability to theoretically test any new theory of gravity, as well as to connect parameters in the new theory to old, known quantities.

4.2 General relativity

This section is based on [2, 54].

The derivation of the spherically symmetric metric is done using computer code, as described in Appendix D.

4.2.1 Einstein's field equations

General relativity describes spacetime as a smooth manifold \mathcal{M} , with a (pseudo-Riemannian) metric, $g_{\mu\nu}$. This metric is treated as a dynamical field, which is affected by the presence of matter and energy. The matter and energy contents of spacetime are encoded in the stress-energy tensor $T_{\mu\nu}$, while the behavior of $g^{\mu\nu}$ is encoded in a scalar Lagrangian density. We employ the minimal-coupling rule to reformulate laws from special relativity to curved spacetime. This rule states that laws written in an inertial frame in a coordinate-independent way remain true in curved spacetime. In an inertial frame, the Christoffel-symbols vanish, so $\nabla_\mu = \partial_\mu$. We can thus write any laws containing partial derivatives in a coordinate independent way by exchanging them for covariant derivatives. To generalize Newton's second law Eq. (4.2), we must first make it relativistic by introducing a 4-force, $F^\mu = \frac{d}{d\tau}p^\mu$, where p^μ is the 4-momentum. When applying the minimal coupling rule, Newton's second law then becomes Eq. (2.37), [55]

$$\sum_i F_i^\mu = m \left(\frac{d^2 x^\mu}{d\tau^2} + \Gamma_{\nu\rho}^\mu \frac{dx^\nu}{d\tau} \frac{dx^\rho}{d\tau} \right). \quad (4.5)$$

In the absence of any external forces, objects will follow geodesics in spacetime. With this, we must now find the law governing $g^{\mu\nu}$. As this is a field, we will do this by assigning it a Lagrangian density. The most obvious—and correct—choice as the Lagrangian is the Ricci scalar, which results in the Einstein-Hilbert action,

$$S_{\text{EH}} = \frac{1}{2\kappa} \int_{\mathcal{M}} d^n x \sqrt{|g|} R. \quad (4.6)$$

The $\sqrt{|g|}$ -factor is included for the integral to be coordinate-independent, as discussed in subsection 2.1.3.¹ The κ is a constant and decides how strong the coupling of gravity to matter and energy is. This constant can then be related to Newton's constant of gravitation G by $\kappa = 8\pi G$. When including the contributions from other fields with an action S_m , the total action becomes

$$S = S_{\text{EH}} + S_m. \quad (4.7)$$

The equations of motion of the dynamical field, which in this case is the metric, are given by Hamilton's principle of stationary action. Using functional derivatives, as defined in subsection A.3.4, this is stated as

$$\frac{\delta S}{\delta g^{\mu\nu}} = 0. \quad (4.8)$$

¹The gravitational action can also include a cosmological constant, modifying the Lagrangian to $R + 2\Lambda$. This constant does not affect the subject of this thesis and is therefore not included here.

We define the stress-energy tensor as

$$T_{\mu\nu} = -2 \frac{\delta S_m}{\delta g^{\mu\nu}}. \quad (4.9)$$

The functional derivative of the Einstein-Hilbert action is evaluated in subsection A.3.5, and with the result, Eq. (A.84), we get the Einstein field equations

$$R_{\mu\nu} - \frac{1}{2} R g_{\mu\nu} = \kappa T_{\mu\nu}. \quad (4.10)$$

The left-hand side of the Einstein field equations is called the Einstein tensor, $G_{\mu\nu} = R_{\mu\nu} - \frac{1}{2} R g_{\mu\nu}$. This tensor obeys the identity

$$\nabla^\mu G_{\mu\nu} = 0, \quad (4.11)$$

as a consequence of the more general Bianchi identity, Eq. (2.42).

4.2.2 Spherically symmetric spacetime

To model stars, we will assume that the metric is spherically symmetric and time-independent. In this case, the most general metric can be written, at least locally, as [2]

$$ds^2 = e^{2\alpha(r)} dt^2 - e^{2\beta(r)} dr^2 - r^2 (d\theta^2 + \sin^2 \theta d\varphi^2), \quad (4.12)$$

where α and β are general functions of the radial coordinate r . In matrix form, this corresponds to

$$g_{\mu\nu} = \begin{pmatrix} e^{2\alpha(r)} & 0 & 0 & 0 \\ 0 & -e^{2\beta(r)} & 0 & 0 \\ 0 & 0 & -r^2 & 0 \\ 0 & 0 & 0 & -r^2 \sin^2(\theta) \end{pmatrix}. \quad (4.13)$$

Using Eq. (2.35), we can now compute the Christoffel symbols in terms of the unknown functions. These computations in this subsection are done using computer code, which is shown in Appendix D. The results are

$$\Gamma_{\mu\nu}^t = \begin{pmatrix} 0 & \frac{d}{dr}\alpha(r) & 0 & 0 \\ \frac{d}{dr}\alpha(r) & 0 & 0 & 0 \\ 0 & 0 & 0 & 0 \\ 0 & 0 & 0 & 0 \end{pmatrix}, \quad (4.14)$$

$$\Gamma_{\mu\nu}^r = \begin{pmatrix} e^{2\alpha(r)} e^{-2\beta(r)} \frac{d}{dr}\alpha(r) & 0 & 0 & 0 \\ 0 & \frac{d}{dr}\beta(r) & 0 & 0 \\ 0 & 0 & -r e^{-2\beta(r)} & 0 \\ 0 & 0 & 0 & -r e^{-2\beta(r)} \sin^2(\theta) \end{pmatrix}, \quad (4.15)$$

$$\Gamma_{\mu\nu}^\theta = \begin{pmatrix} 0 & 0 & 0 & 0 \\ 0 & 0 & \frac{1}{r} & 0 \\ 0 & \frac{1}{r} & 0 & 0 \\ 0 & 0 & 0 & -\sin(\theta) \cos(\theta) \end{pmatrix}, \quad (4.16)$$

$$\Gamma_{\mu\nu}^\phi = \begin{pmatrix} 0 & 0 & 0 & 0 \\ 0 & 0 & 0 & \frac{1}{r} \\ 0 & 0 & 0 & \frac{\cos(\theta)}{\sin(\theta)} \\ 0 & \frac{1}{r} & \frac{\cos(\theta)}{\sin(\theta)} & 0 \end{pmatrix}. \quad (4.17)$$

The symbols not included are zero. Substituting these results into Eq. (2.39) gives the Riemann curvature tensor. We can then obtain the Ricci tensor by taking the trace, as shown in Eq. (2.43).

The results are

$$R_{tt} = \left[r \left(\frac{d}{dr} \alpha(r) \right)^2 - r \frac{d}{dr} \alpha(r) \frac{d}{dr} \beta(r) + r \frac{d^2}{dr^2} \alpha(r) + 2 \frac{d}{dr} \alpha(r) \right] \frac{e^{2\alpha(r)} e^{-2\beta(r)}}{r}, \quad (4.18)$$

$$R_{rr} = -\frac{1}{r} \left[r \left(\frac{d}{dr} \alpha(r) \right)^2 - r \frac{d}{dr} \alpha(r) \frac{d}{dr} \beta(r) + r \frac{d^2}{dr^2} \alpha(r) - 2 \frac{d}{dr} \beta(r) \right], \quad (4.19)$$

$$R_{\theta\theta} = - \left[r \frac{d}{dr} \alpha(r) - r \frac{d}{dr} \beta(r) - e^{2\beta(r)} + 1 \right] e^{-2\beta(r)}, \quad (4.20)$$

$$R_{\varphi\varphi} = R_{\theta\theta} \sin^2(\theta). \quad (4.21)$$

All other components are zero. Finally, the trace of the Ricci tensor gives the Ricci scalar,

$$R = \frac{2e^{-2\beta(r)}}{r^2} \left[r^2 \left(\frac{d}{dr} \alpha(r) \right)^2 - r^2 \frac{d}{dr} \alpha(r) \frac{d}{dr} \beta(r) + r^2 \frac{d^2}{dr^2} \alpha(r) + 2r \frac{d}{dr} \alpha(r) - 2r \frac{d}{dr} \beta(r) - e^{2\beta(r)} + 1 \right]. \quad (4.22)$$

The unknown functions α and β are now determined by the matter and energy content of the universe, which is encoded in $T_{\mu\nu}$, through Einstein's field equation, Eq. (4.10).

4.2.3 The Schwarzschild metric

The simplest case for a matter distribution in spacetime is $T_{\mu\nu} = 0$. Although this might only seem to be useful to model a non-empty universe, it can be combined with a central point particle and empty space elsewhere. In this case, the Einstein equations are simply $R_{\mu\nu} - \frac{1}{2} R g_{\mu\nu} = 0$. We can show that the trace of the Ricci tensor is zero by taking the trace of this equation, simplifying it to $R_{\mu\nu} = 0$. By combining Eq. (4.18) and Eq. (4.19), we find

$$R_{tt} + e^{2(\alpha-\beta)} R_{rr} = 2 \frac{d}{dr} (\alpha + \beta) = 0, \quad (4.23)$$

which implies $\alpha = -\beta + \text{const.}$ The constant corresponds to rescaling the coordinates, which allows us to set it to zero. From Eq. (4.20), we get

$$e^{2\beta} R_{\theta\theta} = -2r \frac{d}{dr} \alpha - e^{-2\alpha} + 1 = 0, \quad (4.24)$$

which may be restated as

$$\frac{d}{dr} (r e^{2\alpha}) = 1. \quad (4.25)$$

This equation has the solution

$$e^{2\alpha(r)} = e^{-2\beta(r)} = \left(1 - \frac{R_s}{r} \right), \quad (4.26)$$

where R_s , the Schwarzschild radius, is a constant. With this, we should obtain Newton's law of gravity with a small perturbation, $g_{\mu\nu} = \eta_{\mu\nu} + h_{\mu\nu}$, and at slow speeds, $\frac{d}{d\tau} x^i \ll \frac{d}{d\tau} t$. Inserting this into the geodesic equation Eq. (4.5) with $F_i = 0$, using $\partial_0 g_{\mu\nu} = 0$ and expanding to leading order, we get

$$\frac{d^2 x^i}{dt^2} = \frac{1}{2} \eta^{ij} \partial_j h_{00}. \quad (4.27)$$

We now obtain Newtonian gravity, as formulated in Eq. (4.4), if we identify $h_{00} = 1 - e^{2\alpha} = -2\Phi_g$. The Schwarzschild radius is thus $R_s = 2GM$, and we see that this solution corresponds to a point-mass M located at $\vec{r} = 0$. We will extend our discussion to finite densities in the next section. Inserting our results into the metric, we get the Schwarzschild metric

$$ds^2 = \left(1 - \frac{2GM}{r} \right) dt^2 - \left(1 - \frac{2GM}{r} \right)^{-1} dr^2 - r^2 (d\theta^2 + \sin^2 \theta d\varphi^2). \quad (4.28)$$

4.3 The TOV equation

This section is in part based on [2, 54, 56].

We will model a star as being made up of a *perfect fluid*. Fluids have a velocity field, v_μ , and perfect fluids have zero viscosity and thus no sheer stress. Therefore, in the rest frame of the fluid, the stress-energy tensor will be diagonal. A perfect fluid is furthermore *isotropic* in its rest frame, which means there are no preferred directions. The stress-energy tensor thus takes the form $\text{diag}(u, -p, -p, -p)$, where u is the energy density and p the pressure. We can then construct the stress-energy tensor in an arbitrary frame either by a Lorentz boost or by constructing a covariant tensor expression which gives us the correct equation in the rest frame. The result is

$$T_{\mu\nu} = (u + p)v_\mu v_\nu - pg_{\mu\nu}, \quad (4.29)$$

We now want an explicit expression for this tensor in our spherically symmetric spacetime. In the rest frame of the fluid, we may write

$$v_\mu = (v_0, 0, 0, 0). \quad (4.30)$$

This, together with the normalization condition of 4-velocities, $v_\mu v^\mu = 1$, allows us to calculate that

$$v_\mu v^\mu = g^{\mu\nu} v_\mu v_\nu = g^{00}(v_0)^2 = 1. \quad (4.31)$$

Using Eq. (4.13), we see that

$$v_0 = e^{\alpha(r)}. \quad (4.32)$$

This gives us the stress-energy tensor of the perfect fluid in its rest frame of our spacetime,

$$T_{\mu\nu} = \begin{pmatrix} u(r)e^{2\alpha(r)} & 0 & 0 & 0 \\ 0 & p(r)e^{2\beta(r)} & 0 & 0 \\ 0 & 0 & p(r)r^2 & 0 \\ 0 & 0 & 0 & p(r)r^2 \sin^2(\theta) \end{pmatrix}. \quad (4.33)$$

With the stress-energy tensor, we may now input it into the Einstein field equation. We will use the tt and rr components of the equations,

$$8\pi Gr^2 u(r) e^{2\beta(r)} = 2r \frac{d}{dr} \beta(r) + e^{2\beta(r)} - 1, \quad (4.34)$$

$$8\pi Gr^2 p(r) e^{2\beta(r)} = 2r \frac{d}{dr} \alpha(r) - e^{2\beta(r)} + 1. \quad (4.35)$$

In analogy with the Schwarzschild metric, we define the function $m(r)$ by

$$e^{2\beta(r)} = \left(1 - \frac{2Gm(r)}{r}\right)^{-1}. \quad (4.36)$$

Substituting this into Eq. (4.34) yields

$$\frac{dm(r)}{dr} = 4\pi r^2 u(r). \quad (4.37)$$

The solution is simply

$$m(r) = 4\pi \int_0^r dr' r'^2 u(r'). \quad (4.38)$$

In flat spacetime, we would have no qualms simply calling this the mass contained within a radius r . However, as discussed in section 2.1, the volume element of a curved geometry is $dV = \sqrt{|g|}d^n x$. In this case, we are interested in the mass contained in a 3-volume, and

the volume form is therefore given by the metric restricted by $dt = 0$. Using Eq. (4.13), $\sqrt{|g|} = e^\beta r^2 \sin \theta$, the total mass-energy contents of the star is

$$M' = 4\pi \int dr' r'^2 \left(1 - \frac{2Gm(r')}{r'}\right)^{-1/2} u(r'). \quad (4.39)$$

However, this does not take into account the gravitational potential energy. Gravitation is self-interacting, and we must therefore include the gravitational potential energy when calculating gravitational effects. It can be shown that the definition of *gravitational mass*, Eq. (4.38), does exactly this. Furthermore, as we will see later, it matches up with what we call mass in the Newtonian limit [57].

Using the Bianchi identity, Eq. (4.11), together with Einstein's equation, we find

$$\nabla^\mu G_{\mu\nu} = \nabla^\mu T_{\mu\nu} = 0. \quad (4.40)$$

The r -component of this equation is

$$\begin{aligned} \nabla_\mu T^{\mu r} &= \partial_r T^{rr} + \Gamma_{\mu\nu}^\mu T^{\nu r} + \Gamma_{\mu\nu}^r T^{\mu\nu} \\ &= \partial_r (pe^{-2\beta}) + (2\Gamma_{rr}^r + \Gamma_{tr}^t)T^{rr} + \Gamma_{tt}^r T^{tt} \\ &= e^{-2\beta} (\partial_r p + p\partial_r \alpha + u\partial_r \alpha) = 0. \end{aligned}$$

This allows us to relate α to p and u , via

$$\frac{d\alpha}{dr} = -\frac{1}{p+u} \frac{dp}{dr} \quad (4.41)$$

When we substitute this, together with the definition of $m(r)$, into Eq. (4.35), we obtain

$$\frac{dp}{dr} = -\frac{G}{r^2} (4\pi r^3 p + m) (p + u) \left(1 - \frac{2Gm}{r}\right)^{-1}, \quad (4.42)$$

the Tolman-Oppenheimer-Volkoff (TOV) equation. This equation was first obtained by Oppenheimer and Volkoff in 1939 [58] and was based on earlier work by Tolman [59]. In their paper, Oppenheimer and Volkoff studied the properties of a star made up of cold, degenerate fermions.

With $p(r)$, $u(r)$, and $m(r)$, we can construct the metric. We already have the rr -component of the metric from Eq. (4.36). If we combine Eq. (4.41), with Eq. (4.42), we get the solution

$$\alpha(r) = G \int^r dr \frac{1}{r^2} (4\pi r^3 p + m) \left(1 - \frac{2Gm}{r}\right)^{-1}. \quad (4.43)$$

Outside the star, we have $p(r) = 0$, and $m(r) = M$. This then reduces to

$$\alpha(r) = GM \int^r dr \frac{1}{r^2} \left(1 - \frac{2GM}{r}\right)^{-1}. \quad (4.44)$$

We can evaluate this integral by making the substitution $x = (1 - 2GM/r)$, $dx = -2GM/r^2 dr$,

$$\alpha(r) = \frac{1}{2} \int^{1-2GM/r} \frac{dx}{x} = \frac{1}{2} \ln \left(1 - \frac{2GM}{r}\right) + \text{const.} \quad (4.45)$$

We then impose the boundary condition $\alpha(\infty) = 0$, which means setting the constant to zero. Inserting this into Eq. (4.13) gives the metric for $r < R$,

$$ds^2 = \left(1 - \frac{2GM}{r}\right) dt^2 + \left(1 - \frac{2GM}{r}\right)^{-1} dr^2 + r^2 (d\theta^2 + \sin^2 \theta d\varphi^2). \quad (4.46)$$

We recognize this as the Schwarzschild metric, Eq. (4.28). This justifies our choice of $m(r)$ as gravitational mass. As discussed earlier, the quantity M in the Schwarzschild solution maps corresponds to Newtonian gravitational mass in the weak-field limit.

In addition to the dynamics of spacetime, we need to know the thermodynamic properties of the matter that make up our star. The relationship between the pressure and energy density of a substance is called the *equation of state*, or EOS, and has the form

$$f(p, u, \{\xi_i\}) = 0, \quad (4.47)$$

where $\{\xi_i\}$ are possible other thermodynamic variables. This allows us to, at least locally, express the energy density as a function of the pressure, $u = u(p, \{\xi_i\})$, which is what we in this text will call the “equation of state”. Our fluid is by assumption in thermodynamic equilibrium and is therefore bound by the first law of thermodynamics,

$$dU = TdS - pdV, \quad (4.48)$$

where $U = uV$ is the internal energy, $T = 1/\beta$ the temperature, S the entropy, and V the volume. Given a conserved charge $Q = nV$, which in our case will be particle number and thus n particle number density. We will in be concerned with stars at $T = 0$. Inserting this into Eq. (4.48), we get

$$\frac{du}{p + u} = \frac{dn}{n}. \quad (4.49)$$

To summarize, we have three unknown functions, $u(r)$, $p(r)$, and $m(r)$. The equation of state, Eq. (4.47), determines $u = u(p)$, eliminating one unknown. The two differential equations Eq. (4.38) and Eq. (4.42), together with the boundary conditions $p(0) = p_c$ and $m(0) = 0$, then yield $p(r)$ and $m(r)$ when integrated. As long as both the pressure and the energy density are positive, and we always are outside the Schwarzschild radius, i.e., $r < 2Gm(r)$, then $dp/dr \leq 0$ and the pressure is strictly decreasing. We define the point where the pressure vanishes as the stellar radius R , i.e., $p(R) = 0$. Given this, we can solve for all the unknown functions, either analytically or numerically.

We can gain some insight into the system without solving these equations by expressing the problem in terms of dimensionless variables. We define

$$u = u_0 \tilde{u}, \quad p = p_0 \tilde{p}, \quad m = m_0 \tilde{m}, \quad r = r_0 \tilde{r}. \quad (4.50)$$

Here, quantities with subscript 0 are dimensionful constants, which may be chosen as the characteristic quantities of the problem, while the tilde indicates a dimensionless variable. By substituting this into Eq. (4.37) and Eq. (4.42), we can collect the dimensionful constants into a smaller number of dimensionless constants, k_i . These constants will decide the nature of the solution. Any change in the dimensionful constants that leave the k_i ’s invariant is a scaling of the problem — it corresponds to the same solution in different units. The new differential equations are

$$\frac{d\tilde{m}}{d\tilde{r}} = 3k_2 \tilde{r}^2 \tilde{u} \quad (4.51)$$

$$\frac{d\tilde{p}}{d\tilde{r}} = -\frac{k_1}{k_3} \frac{1}{\tilde{r}^2} (k_3 \tilde{p} + \tilde{u}) (3k_2 k_3 \tilde{r}^3 \tilde{p} + \tilde{m}) \left(1 - \frac{2k_1 \tilde{m}}{\tilde{r}}\right)^{-1}, \quad (4.52)$$

where the dimensionless constants are defined as

$$k_1 = G \frac{m_0}{r_0}, \quad k_2 = \frac{4\pi}{3} \frac{r_0^3 u_0}{m_0}, \quad k_3 = \frac{p_0}{u_0}. \quad (4.53)$$

The energy density and pressure are of comparable magnitude in the relativistic regime. We will therefore often choose $k_3 = 1$, defining $p_0 = u_0$. If we have a non-complete set of characteristic

quantities, the dimensionless constants k_i tell us something about the magnitude we should expect the solution to have. After defining the remaining dimensionful constants by setting $k_i = 1$, we expect that the dimensionless sizes of a typical solution will be of order 1. In other words, the dimensionful constants defined by $k_i = 1$ are new, characteristic quantities given to us by the form of the governing equation only.

4.3.1 Newtonian limit and polytropes

In the Newtonian limit, the rest energy, i.e., mass, gives the dominant contribution to the gravitational field, while the contribution from pressure is negligible. In other words, the characteristic pressure, p_0 , is far smaller than the characteristic energy density u_0 , and we can use the approximation $k_3 \ll 1$. Furthermore, the star's radius should be much larger than the Schwarzschild radius, $R_s = 2GM$. If we choose $r_0 = R$, then $k_1 \ll 1$. In this limit, the lowest-order contribution to the TOV equation is

$$\frac{d\tilde{p}}{d\tilde{r}} = -\frac{k}{\tilde{r}^2} \tilde{u} \tilde{m}, \quad k = \frac{k_1}{k_3} = G \frac{u_0 m_0}{p_0 r_0}. \quad (4.54)$$

Using the mass equation Eq. (4.51), we can write this as

$$4\pi \tilde{r}^2 \frac{d\tilde{p}}{d\tilde{m}} = -k' \frac{\tilde{m}}{\tilde{r}^2}, \quad k' = \frac{4\pi}{3} \frac{k_1}{k_2 k_3} = G \frac{m_0^2}{r_0^4 p_0}. \quad (4.55)$$

It is illuminating to derive this equation directly from Newtonian gravity. Assume we have a static, gravitationally bound ball of matter, as illustrated in Figure 4.1. The force due to the pressure gradient over a thin, spherical shell, $F_p = 4\pi r^2 dp$, must be counteracted by the gravitational force on the same shell, $F_g = -Gmdm/r^2$. Setting $F_g = F_p$, we obtain Eq. (4.55)

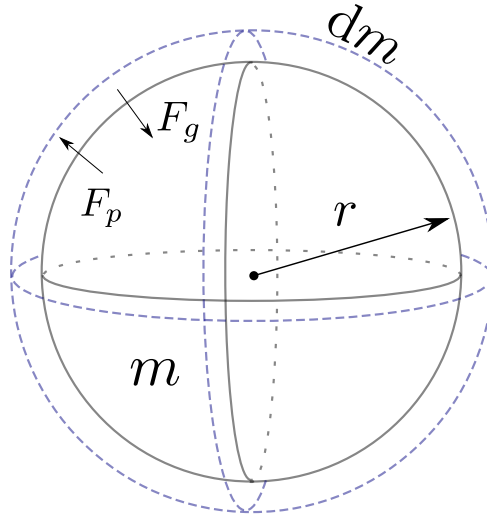


Figure 4.1: The forces acting on a thin shell with mass dm at a distance r from the center.

Both the Newtonian limit and the TOV equation are equations of *hydrostatic equilibrium*, where the forces on a small volume of the fluid cancel out. In the case of the TOV equation, we tacitly assumed hydrostatic equilibrium when we gave the fluid a rest frame where we could write $v_\mu = (v_0, 0, 0, 0)$ globally. We can eliminate the equation for mass by differentiating Eq. (4.54) with respect to \tilde{r} . This gives us a single equation for hydrostatic equilibrium in the Newtonian limit,

$$\frac{d}{d\tilde{r}} \left(\frac{\tilde{r}^2}{\tilde{u}} \frac{d\tilde{p}}{d\tilde{r}} \right) = -k'' \tilde{r}^2 \tilde{u}, \quad k'' = 3 \frac{k_2 k_1}{k_3} = 4\pi G \frac{u_0^2 r_0^2}{p_0}. \quad (4.56)$$

This is a second order differential equation, so we need an new boundary condition in addition to $p(0) = p_c$. Close to the center, we can see from Eq. (4.54) that for a finite energy density, we must have $p'(0) = 0$, our second boundary condition.

One important model for stars is the *polytrope*, which has an equation of state of the form $p = Ku^\gamma$ for some constant K . As we will see, this fits well as the Newtonian limit of many equations of state and can be used to make predictions such as the Chandrasekhar limit, which sets the upper limit of the mass of white dwarf stars to $M \approx 1.5 M_\odot$ [54, 60]. To write Eq. (4.56) on the standard form, we assume $\gamma \neq 1$ and introduce

$$\tilde{u} = a\theta^n, \quad n = \frac{1}{\gamma - 1}, \quad a = \frac{u(p_c)}{u_0}, \quad a^{\frac{\gamma-2}{2}} C \xi = r, \quad C = \sqrt{\frac{K}{k''} \frac{\gamma}{\gamma - 1}}. \quad (4.57)$$

n is called the *polytropic index* of the star. Inserting these new variables into the equation of hydrostatic equilibrium gives

$$\frac{1}{\xi^2} \frac{d}{d\xi} \left(\xi^2 \frac{d\theta}{d\xi} \right) + \theta^n = 0. \quad (4.58)$$

This is called the Lane-Emden equation and was first used to model stars as early as 1870 [61]. The boundary conditions $p(0) = p_c$ and $p'(0) = 0$ now read $\theta(0) = 1$ and $\theta'(0) = 0$. The stellar radius is defined by the first zero of the Lane-Emden function above $\xi = 0$, $\theta(\xi_1) = 0$, so that

$$R = C\xi_1 a^{\frac{\gamma-2}{2}}. \quad (4.59)$$

The total mass of the star can be integrated using Eq. (4.51) and Eq. (4.58),

$$M = \frac{3k_2 C^3}{r_0^3} a^{\frac{3\gamma-4}{2}} \int_0^{\xi_1} d\xi \xi^2 \theta^n = -\frac{3k_2 C^3}{r_0^3} \xi_1^2 \theta'(\xi_1) a^{\frac{3\gamma-4}{2}}. \quad (4.60)$$

Thus, given a specific equation of state, and thus γ , the mass-radius relationship is given by

$$R \propto M^\beta, \quad \beta = \frac{\gamma - 2}{3\gamma - 4}. \quad (4.61)$$

Figure 4.2 illustrates this relationship, in arbitrary units, for a series of different values of γ , as well as the dependence of β on γ . For most values of γ , the stellar radius will increase as the mass increases. The only range within which the radius decrease as the mass increase is $\gamma \in (\frac{4}{3}, 2)$. At $\gamma = \frac{4}{3}$ and $\gamma = 2$, respectively the mass and radius become independent of the central density. If included in our figure, these polytropes would correspond to a horizontal and a vertical line.

The case of $\gamma = \frac{4}{3}$ was used by Chandrasekhar to find his eponymous upper mass limit for white dwarfs. In white dwarfs, most of the energy density is due to the rest mass of nucleons, while the pressure is provided by electron degeneracy. In the ultrarelativistic limit, where the Fermi energy of the electrons is much larger than their mass, this results in a polytrope with $\gamma = \frac{4}{3}$. As we will see, a pion condensate has a non-relativistic limit with $\gamma = 2$. In Chapter 7, we will use this to derive an upper limit for the radius of pion stars.

In the case of $\gamma = 1$, we can integrate Eq. (4.48), and obtain

$$u \propto n^{K+1}, \quad (4.62)$$

The non-relativistic limit of massive matter, on the other hand, is $u = mn$, where m is the rest mass of the particles. $\gamma = 1$ is thus not a realistic model of low energy matter. Rather, it corresponds to radiation, in which case $p = \frac{1}{3}u$, or the ultrarelativistic limit of matter, as we will find later in this text.

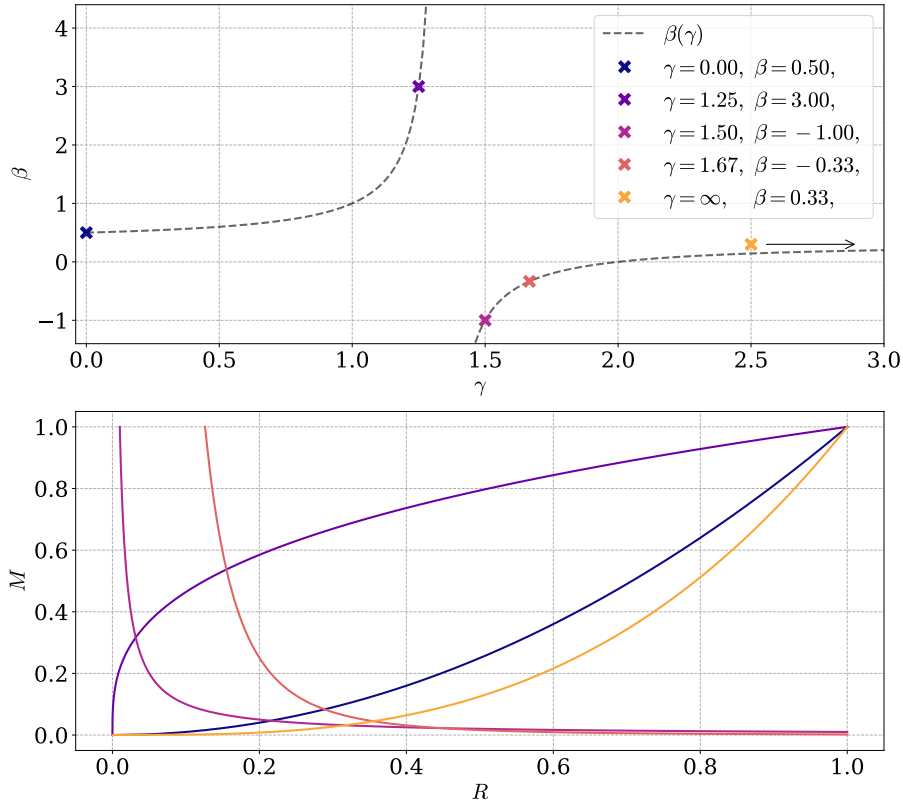


Figure 4.2: Left: The dependence of β on γ , together with a selection of points. Right: The mass-radius relation, in arbitrary units, for polytropes corresponding to the selected points on the left side. The color of the lines indicates to which point it corresponds.

4.3.2 Incompressible fluid

The simplest model for a star is one made up of an incompressible fluid, where the energy density is independent of the pressure. This corresponds to a polytrope with $\gamma = \infty$. In this case, the energy density of the star will be constant for a radius $r < R$, before it drops to zero,

$$u(r) = u_0 \theta(R - r), \quad (4.63)$$

where u_0 is a constant and $\theta(x)$ the Heaviside step function. We choose $r_0 = R$. Inserting this into the differential equation of the mass function, Eq. (4.51), together with the boundary condition $m(0) = 0$, yields

$$\tilde{m}(\tilde{r}) = k_2 \tilde{r}^3, \quad (4.64)$$

when $r < R$. For $r \geq R$, or $\tilde{r} \geq 1$, this relationship is simply constant $\tilde{m}(\tilde{r}) = \tilde{m}(1) = k_2$. We choose m_0 to be the gravitational mass of the star, $M = \frac{4\pi}{3} R^3 u_0$, which is equivalent to setting $k_2 = 1$. Lastly, we choose $u_0 = p_0$, so that $k_3 = 1$. With this the TOV equation, Eq. (4.52), becomes

$$\frac{d\tilde{p}}{d\tilde{r}} = -k_1 \tilde{r} \frac{(1 + \tilde{p})(1 + 3\tilde{p})}{(1 - 2k_1 \tilde{r}^2)}. \quad (4.65)$$

This is a separable ODE, and each variable may be integrated separately. Using

$$\int \frac{dx}{(1+x)(1+3x)} = \frac{1}{2} \ln \frac{3x+1}{x+1} + \text{const.}, \quad \int dx \frac{x}{1-2x^2} = \frac{1}{4} \ln(1-2x^2) + \text{const.}, \quad (4.66)$$

together with the boundary condition $p(r = R) = 0$, we get

$$\tilde{p}(\tilde{r}) = -\frac{\sqrt{1-2k_1} - \sqrt{1-2k_1 \tilde{r}^2}}{3\sqrt{1-2k_1} - \sqrt{1-2k_1 \tilde{r}^2}}. \quad (4.67)$$

We see that the star is entirely characterized by k_1 . In Figure 4.3, we have plotted the pressure as a function of radius for some values of k_1 . As k_1 approaches $0.4 = 4/9$, the pressure at the center of the star increases rapidly. From the denominator of Eq. (4.67) at $r \rightarrow 0$, we find the limit

$$k_1 = G \frac{M}{R} < \frac{4}{9} \quad (4.68)$$

for the pressure to remain finite. This is an absolute limit of the mass of an object given its radius or vice versa. Although this limit is derived for a particular, unrealistic case, the more general statement can be shown to hold. General relativity does not allow for a static solution with energy densities greater than this limit; any such configuration would collapse [2]. If we expand the solution Eq. (4.67) in powers of k_1 , then the leading order contribution is

$$\tilde{p}(r) = \frac{1}{2}k_1(1 - \tilde{r}^2). \quad (4.69)$$

This is the Newtonian limit. As a cross-check, we see that this solution obeys the equation of hydrostatic equilibrium in this limit, Eq. (4.54), as $\tilde{u} = 1$ and $k_2 = k_3 = 1$. This is the general solution for an incompressible fluid in Newtonian gravity. This solution does not have any upper limit for k_1 ; the limit $M/R < 4/9$ is a purely relativistic phenomenon. In the lower plot of Figure 4.3, the Newtonian approximation is compared to the full, relativistic solution. We see that the Newtonian approximation is highly accurate for k_1 less than around 0.01.

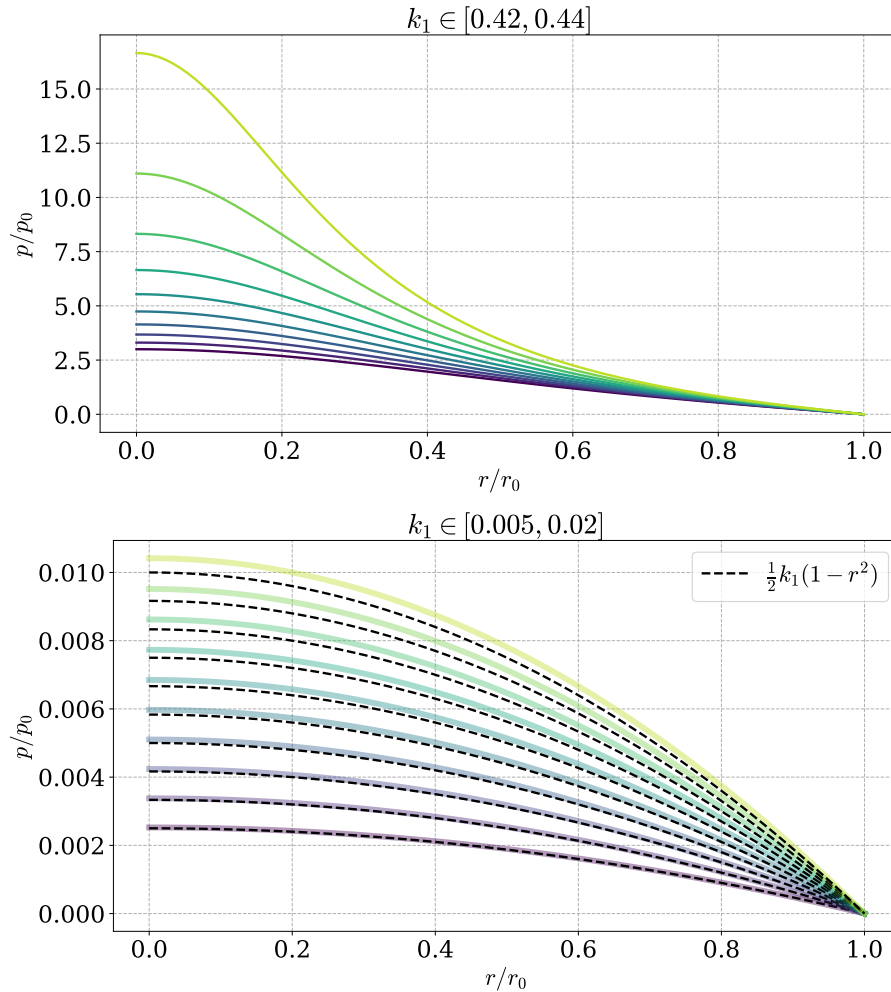


Figure 4.3: The pressure as a function of the radius, in units of p_0 and r_0 . The graphs with lighter color and higher pressure at $r = 0$ corresponds to higher values of k_1 . Values of k_1 are linearly spaced. The dashed lines in the bottom plot correspond to the Newtonian solution.

4.4 A star of cold, non-interacting fermions

This section is based on [54, 62, 63].

In this section, we will study a simple model of a star made up of non-interacting, cold neutrons. This is one of the earliest models used to study neutron stars, the remnants of massive stars [54]. For this model, we use results derived in section C.5.

4.4.1 Thermodynamics and the equation of state

The total energy U is related to the grand canonical free energy F by a Legendre transformation,

$$F(T, V, \mu) = U - TS - \mu Q, \quad dF = -SdT - pdV - Qd\mu. \quad (4.70)$$

Here $T = 1/\beta$ is temperature, and S entropy, p pressure, and V volume. Q is some conserved charge, in our case the number of particles minus antiparticles, and μ is the corresponding chemical potential. These thermodynamic variables are related to the free energy by

$$S = -\frac{\partial F}{\partial T} = \beta^2 \frac{\partial F}{\partial \beta}, \quad Q = -\frac{\partial F}{\partial \mu}, \quad p = -\frac{\partial F}{\partial V}. \quad (4.71)$$

When the free energy can be written as $F = V\mathcal{F}$, where the free energy density \mathcal{F} is independent of the volume V , then $\mathcal{F} = -p$ and

$$d(V\mathcal{F}) = Vd\mathcal{F} - pdV, \quad (4.72)$$

allowing us to write

$$\mathcal{F}(T, \mu) = u - Ts - \mu n, \quad d\mathcal{F} = -sdT - nd\mu, \quad (4.73)$$

where s and n are entropy and charge density, defined by

$$s = -\frac{\partial \mathcal{F}}{\partial T} = \beta^2 \frac{\partial \mathcal{F}}{\partial \beta}, \quad n = -\frac{\partial \mathcal{F}}{\partial \mu}. \quad (4.74)$$

With this, we can write the energy density as [62]

$$u = \frac{\partial}{\partial \beta} (\beta \mathcal{F}) + \mu n. \quad (4.75)$$

We calculate the free energy density of non-interacting fermions in section C.5, with the result Eq. (C.102),

$$\mathcal{F} = -\frac{2}{\beta} \int \frac{d^3 p}{(2\pi)^3} \left[\beta \omega + \ln \left(1 + e^{-\beta(\omega - \mu)} \right) + \ln \left(1 + e^{-\beta(\omega + \mu)} \right) \right], \quad (4.76)$$

where $\omega = \sqrt{p^2 + m^2}$. The first term in the integral is the divergent vacuum energy, which must be renormalized. We can drop this term; it does not have any observable effects on our results, as we are interested in relative pressure and energy density. With this, we find the charge density

$$n = \frac{1}{\pi^2} \int \frac{d^3 p}{(2\pi)^3} [n_f(\omega - \mu) - n_f(\omega + \mu)], \quad (4.77)$$

where

$$n_f(\omega) = \frac{1}{e^{\beta\omega} + 1}. \quad (4.78)$$

is the Fermi-Dirac distribution. Using this, we find that the energy density is

$$u = \frac{1}{\pi^2} \int_0^\infty dp p^2 \omega [n_f(\omega - \mu) + n_f(\omega + \mu)]. \quad (4.79)$$

As expected, this is the energy per mode times the density of states, integrated over all modes. To write the pressure, $p = -\mathcal{F}$ in terms of an integral over the Fermi-Dirac distribution, we integrate by parts. We have

$$\int_0^\infty dp p^2 \ln [1 + e^{-\beta(\omega \pm m)}] = \frac{1}{3} p^3 \ln [1 + e^{-\beta(\omega \pm m)}] \Big|_0^\infty + \frac{1}{3} \int_0^\infty dp \frac{\beta p^4}{\omega} n_f(\omega \pm \mu), \quad (4.80)$$

where the boundary term vanishes. This allows us to write the pressure as

$$p = \frac{1}{3} \int_0^\infty dp \frac{p^4}{\omega} [n_f(\omega - \mu) + n_f(\omega + \mu)] \quad (4.81)$$

We are interested in the $T = 0$ limit. In this case, the Fermi distribution becomes a step function, $n_f(\omega) = \theta(-\omega)$. Without loss of generality, we assume that $\mu > 0$, i.e., we are dealing with an abundance of matter compared to anti-matter. The dispersion relation $\omega = \sqrt{p^2 + m^2}$ is always positive. This means that the contribution to thermodynamic quantities from anti-particles vanish, as the integral is multiplied with $n_f(\omega + \mu) = \theta(-\omega - \mu)$, where the argument $-\omega - \mu$ is strictly negative on the domain of integration. At zero temperature, the only dynamics are due to the degeneracy pressure of the fermions, that is, due to the Pauli exclusion principle. There are no thermal fluctuations that can create a particle-antiparticle pair. Thus, if the system has a positive chemical potential, it will contain no antiparticles. Furthermore, if $\mu < m$, then integrand multiplied with $n_f(\omega - \mu)$ is also zero in the whole domain of integration. It is only when $\mu \geq m$ that it is energetically favorable for the system to be in a state with particles. We define the Fermi momentum p_f by $\mu = \sqrt{p_f^2 + m^2}$. In the zero-temperature limit, we can then rewrite any integral over the Fermi distribution as

$$\int_0^\infty dp [f(p)n_f(\omega - \mu) + g(p)n_f(\omega + \mu)] = \int_0^{p_f} dp f(p). \quad (4.82)$$

The charge density is thus

$$n = \frac{1}{\pi^2} \int_0^{p_f} dp p^2 = \frac{p_f^3}{3\pi^2}. \quad (4.83)$$

At $T = 0$, this is the particle number density, as there are no antiparticles. This density is given by the chemical potential and vanishes when $\mu \leq m$, i.e. when the free energy cost of creating a particle is positive. We can write the energy density and pressure integrals, Eq. (4.79) and Eq. (4.81), as

$$u = \frac{1}{\pi^2} \int_0^{p_f} dp p^2 \sqrt{p^2 + m^2} = \frac{m^4}{\pi^2} \int_0^{x_f} dx x^2 \sqrt{x^2 + 1}, \quad (4.84)$$

$$p = \frac{1}{3\pi^2} \int_0^{p_f} dp \frac{p^4}{\sqrt{p^2 + m^2}} = \frac{m^4}{3\pi^2} \int_0^{x_f} \frac{dx x^4}{\sqrt{x^2 + 1}}. \quad (4.85)$$

We have defined $x = p/m$ and $x_f = p_f/m$. These integrals can be evaluated exactly as

$$\int_0^a dx x^2 \sqrt{x^2 + 1} = \frac{1}{8} [\sqrt{a^4 + 1}(2a^3 + a) - \operatorname{arcsinh}(a)], \quad (4.86)$$

$$\int_0^a dx \frac{x^4}{\sqrt{x^2 + 1}} = \frac{1}{8} [\sqrt{a^2 + 1}(2a^3 - 3a) + 3 \operatorname{arcsinh}(a)]. \quad (4.87)$$

We introduce the characteristic energy and number density,

$$u_0 = \frac{m^4}{8\pi^2}, \quad n_0 = \frac{u_0}{m}, \quad (4.88)$$

which allows us to write the thermodynamic variables as

$$n = \frac{8}{3} n_0 x_f^3 \quad (4.89)$$

$$u = u_0 \left[(2x_f^3 + x_f) \sqrt{1 + x_f^2} - \operatorname{arcsinh}(x_f) \right], \quad (4.90)$$

$$p = \frac{u_0}{3} \left[(2x_f^3 - 3x_f) \sqrt{1 + x_f^2} + 3 \operatorname{arcsinh}(x_f) \right]. \quad (4.91)$$

We have thus chosen $u_0 = p_0$, or equivalently set $k_3 = 1$. This is natural in the case of a relativistic fluid.

4.4.2 Limits

In the non-relativistic limit, as the chemical potential approaches m and thus $p_f \ll m$, the lowest order contributions to the energy density and pressure are given by the Taylor series around $x_f = 0$,

$$\tilde{u}(x_f) = \frac{8}{3} x_f^3 + \frac{4}{5} x_f^5 + \mathcal{O}(x_f^7), \quad (4.92)$$

$$\tilde{p}(x_f) = \frac{8}{15} x_f^5 + \mathcal{O}(x_f^7). \quad (4.93)$$

By neglecting terms of order x_f^7 and higher, we can write this as

$$\tilde{u} = \tilde{n} + \frac{4}{5} \left(\frac{8}{3} \tilde{n} \right)^{5/3}, \quad \tilde{p} = \frac{8}{15} \left(\frac{8}{3} \tilde{n} \right)^{5/3}. \quad (4.94)$$

The leading order contribution to the energy density is the rest mass of the particles. This term does not contribute to the pressure. As discussed earlier, the non-relativistic limit corresponds to $k_3 \ll 1$, if we chose units so that $\tilde{u} \approx \tilde{p}$, or $\tilde{u} \gg \tilde{p}$ if we demand that $k_3 = 1$. We see that $x_f \rightarrow 0$ corresponds to the latter case. By including only the leading order term, we can eliminate the Fermi momentum and write the equation of state in the non-relativistic limit as $u_{\text{nr}} = k p^{\frac{3}{5}}$ where $k = 8/3 \cdot (15/8)^{3/5}$. The non-relativistic approximation of the cold fermions is thus a polytrope with $\gamma = \frac{5}{3}$. As we see from Figure 4.2, this is within the range where the mass decreases with the size of the star.

In the ultrarelativistic limit, where $p_f \gg m$, the leading order contributions to the pressure and energy density are

$$\tilde{u} = 2x_f^4, \quad \tilde{p} = \frac{2}{3}x_f^4, \quad (4.95)$$

and we get the particularly simple equation of state for the ultrarelativistic limit, $u_{\text{ur}} = 3p$, which we recognize as the formula for radiation pressure. The equation of state $\tilde{u}(\tilde{p})$ in two different regimes are shown in Figure 4.4. The full equation of state is compared to the non-relativistic and ultrarelativistic approximations.

4.4.3 Units

The equation of state has given us the characteristic energy density and pressure, u_0 and p_0 . If we demand

$$G \frac{m_0}{r_0} = \frac{4\pi}{3} \frac{r_0^3 u_0}{m_0} = 1, \quad (4.96)$$

we have two equations and two unknowns, m_0 and r_0 . This thus defines a complete set of units. We are using the cold Fermi-gas as a model for a neutron star, and the mass of the fermion m

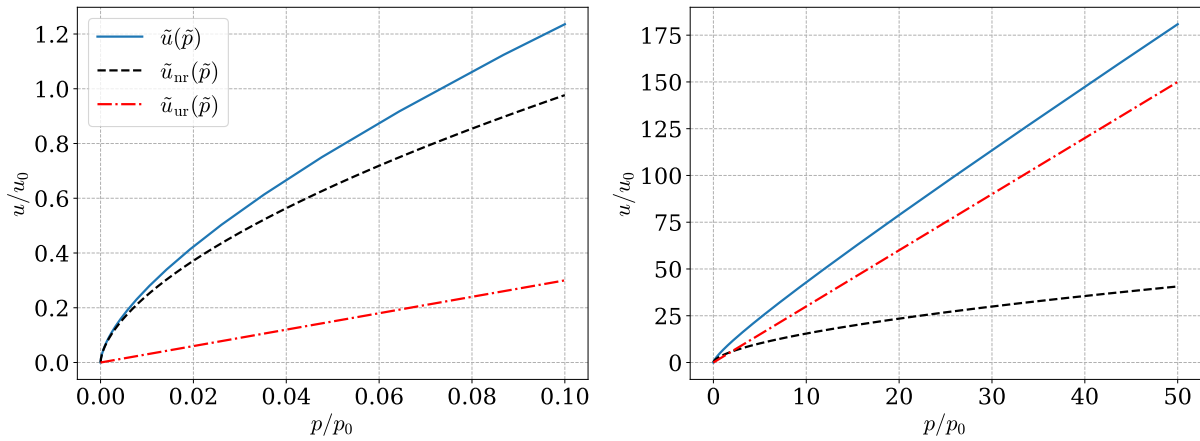


Figure 4.4: The equation of state of a cold Fermi gas. Both pressure and energy density is normalized to their characteristic quantities, p_0 and u_0 . The equation of state is compared to the non-relativistic approximation, \tilde{u}_{nr} as well as the ultrarelativistic approximation, \tilde{u}_{ur} , in two different regimes.

is therefore the neutron mass, Eq. (A.17), $m_N = 1.674 \cdot 10^{-27}$ kg. After reinstating \hbar and c in metric units, we get

$$u_0 = p_0 = \frac{m^4 c^5}{8\pi^2 \hbar^3} = 2.056 \cdot 10^{35} \text{ J m}^{-3}, \quad (4.97)$$

$$m_0 = \frac{c^4}{\sqrt{\frac{4\pi}{3} u_0 G^3}} = 1.598 \cdot 10^{31} \text{ kg} = 8.032 M_\odot, \quad (4.98)$$

$$r_0 = \frac{G m_0}{c^2} = 11.86 \text{ km}. \quad (4.99)$$

From this, we expect our star to have a mass of the order of a solar mass M_\odot and a radius of the order of kilometers, without solving the TOV equation.

4.4.4 Numerical results

With the energy density, Eq. (4.90), and pressure, Eq. (4.91), we can numerically solve the TOV equation given a central pressure p_c . This is done using an adaptive Runge-Kutta method, with the stop criterion $p(r) = 0$. Description of the code and where to find it is given in Appendix D. The top graph in Figure 4.5 shows the pressure, normalized to the central pressure p_c , as a function of radius, normalized to the corresponding stellar radius R . The boundary conditions are logarithmically spaced. The lower graph in Figure 4.5 shows the mass, normalized to the total mass $M = m(R)$, as a function of the radius, again normalized to the stellar radius. As in the case of an incompressible fluid, the pressure follows a half bell-shaped curve, with a peak that becomes narrower as the central pressure increases. The black dashed line corresponds to the solution with the maximum mass, which will discuss shortly. We see that the pressure and mass curves change most drastically when the central pressure is higher than that corresponding to the most massive star.

In Figure 4.6, we see the relationship between the mass and radius of the star. This line is parametrized by the base-10 logarithm of the central pressure, $p(0)$, normalized by $p_0 = u_0$. The cross marks the maximum mass, $M_{\text{max}} = 0.711 M_\odot$, which corresponds to a radius of $R = 9.27$ km. This matches the results obtained by Oppenheimer and Volkoff [58], $M_{\text{max}} = 0.71$. In their 1939 paper, Oppenheimer and Volkoff computed five data points in the mass-radius plane. The results are marked by blue circles in Figure 4.6. We find good agreement between the three points closest to the maximum value and our results. However, the two results of

Oppenheimer and Volkoff furthest away differ significantly from our results. The black dashed line is the absolute mass-radius constraint, Eq. (4.68), and any stable configuration must be on the right side of this line. As we predicted from looking at the non-relativistic equation of state, the mass decreases with the star's radius, at least for stars with low central pressure.

In Figure 4.7, we compare the mass-radius relationship obtained from the full theory with results from approximations. The lowest line is obtained by using both the full TOV equation and the exact equation of state. The next line above is obtained using the non-relativistic equation of state together with the full TOV equation. The second uppermost line is obtained from the exact equation of state and the Newtonian approximation for the TOV equation. The uppermost line uses both the Newtonian approximation to the TOV equation and the non-relativistic approximation for the equation of state. This last line corresponds to a polytrope in Newtonian gravity, as we studied in subsection 4.3.1. Unlike the other systems, it does not seem to have an upper limit for the mass.

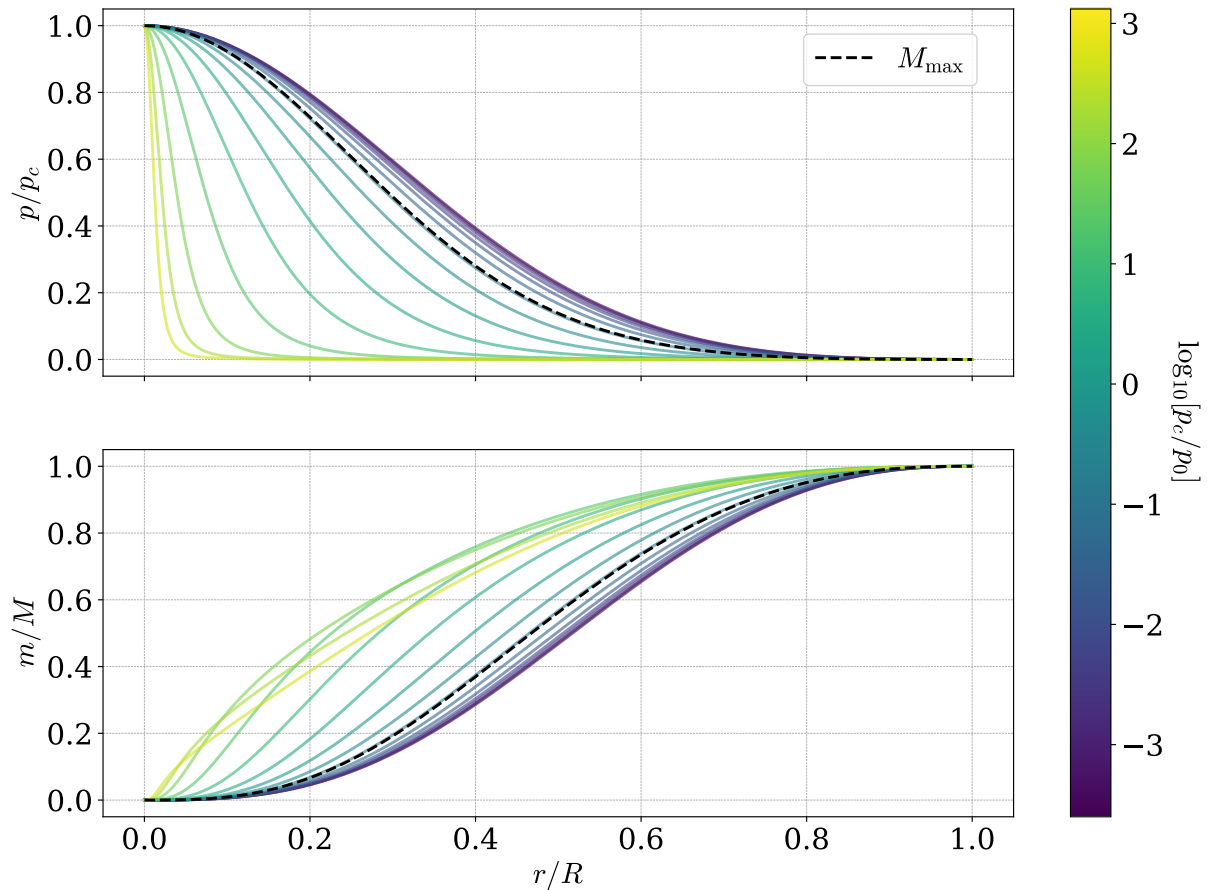


Figure 4.5: Top: The pressure normalized to central value, as a function of radius, normalized to the stellar radius. Bottom: The mass normalized to the total mass, as a function of radius, normalized to the stellar radius. This is plotted for several different values of central pressure, which is indicated by the color scheme.

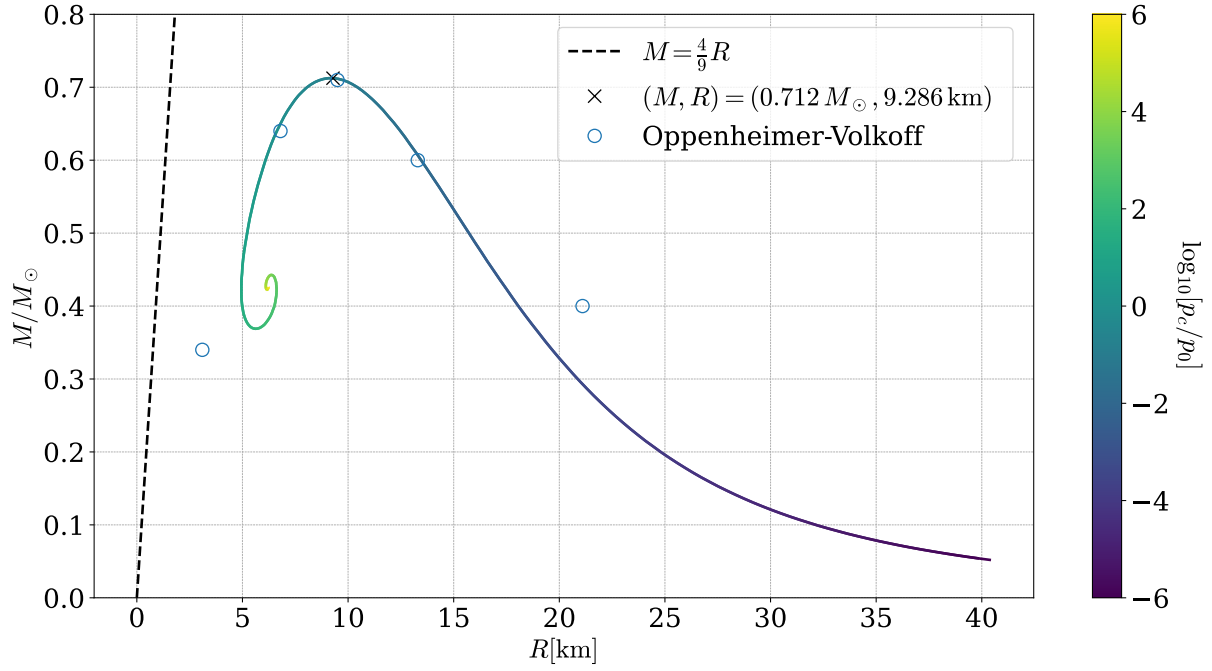


Figure 4.6: The mass-radius relationship of a star made of a cold gas of neutrons. The line is parametrized by the central pressure p_c . The cross indicates the maximum mass solution. The blue circles are results from the 1939 paper of Oppenheimer and Volkoff [58].

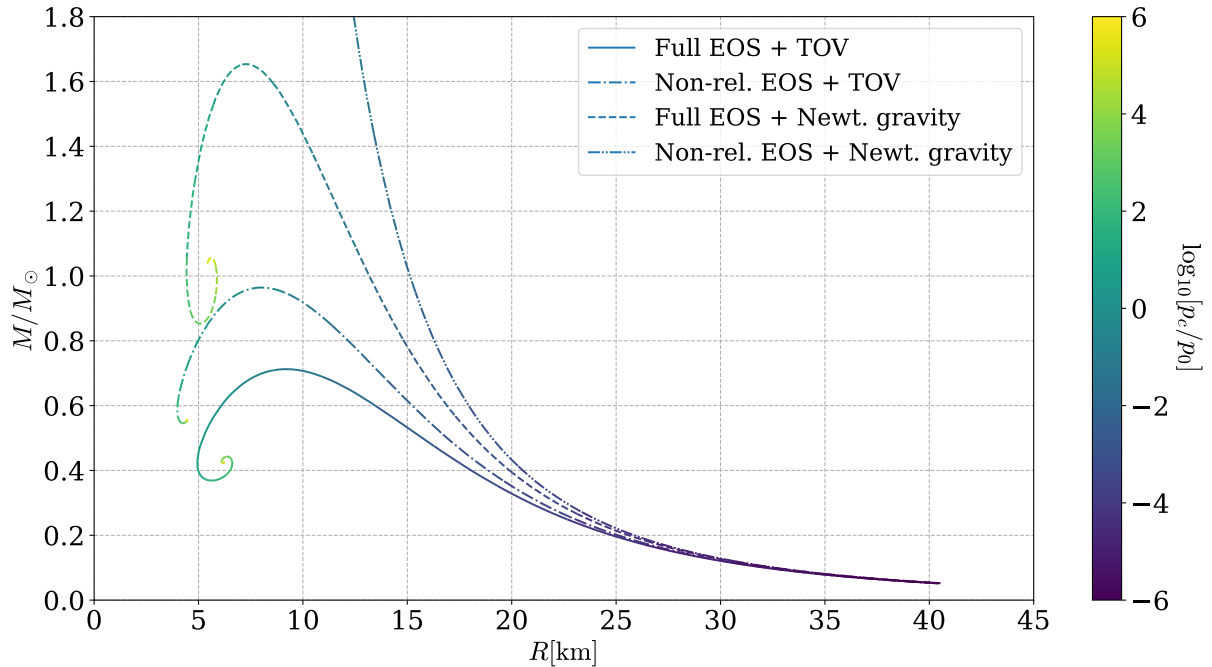


Figure 4.7: The mass-radius relationship of a cold gas of neutrons. The lowest line is obtained from the TOV equation and full equation of state. The middle line is from the TOV equation and the non-relativistic equation of state. The upper line is obtained from the Newtonian approximation of the TOV equation and the non-relativistic equation of state.

4.4.5 Upper bound and stability

For any equation of state, the TOV equation will give a one-parameter family of stars, parametrized by the central pressure p_c [57]. This leads to the possibility of an *absolute maximum* mass for a given equation of state. In the case of a non-interacting neutron, we found the limit to be $0.71 M_\odot$, in agreement with Oppenheimer and Volkoff [58]. To obtain a more general upper limit for the mass of neutron stars or other compact stars in, one has to account for more general equations of state. To constrain the equation of state, we assume firstly that $dp/du \geq 0$. To justify this, take the non-relativistic case, $u \propto n$, in which case the assumption is equivalent to $dp/dn \geq 0$. This says that an increase in particle density, for example, due to compression, will result in a rise in pressure. This is an instance of Le Chatelier's principle: nature will counteract any change forced upon it. If we perturb a perfect fluid, then in its stationary frame we have $n = n_0 + \delta n$, $v^\mu = (1, \delta v^i)$, $p = p_0 + \delta p$ and $u = u_0 + \delta u$. Combining the conservation of energy, $\partial_\mu T^{\mu\nu} = 0$, and conservation of matter, $\partial_\mu (nv^\mu) = 0$, with the first law of thermodynamics, Eq. (4.49), we can obtain a wave equation for the propagation of the perturbation,

$$(\partial_t^2 - v_s^2 \nabla^2) \delta n = 0, \quad (4.100)$$

where the speed of sound in the fluid, v_s , is given by [56]

$$v_s^2 = \frac{dp}{du}. \quad (4.101)$$

A realistic fluid should not have a speed of sound greater than the speed of light, leading to the constraint $dp/du < 1$. Using these general assumptions, Rhoades and Ruffini found an upper limit for neutron stars of $3.2 M_\odot$ [64].

An equation of state with a *high* speed of sound, i.e., with a flat curve in the $p - u$ -plane, is called *stiff*. From Figure 4.4, we see that the Newtonian equation of state is stiffer in the high-energy regime. The most extreme case is the incompressible model we saw earlier, which breaks causality. In general, a stiffer equation of state leads to a larger maximum mass. This is intuitive; the TOV equation describes the balancing of forces from pressure and gravity, and if the pressure raises fast as the density increases, then it can sustain a large total mass before it collapses [54].

Solutions to the TOV equation are systems in hydrostatic equilibrium. However, as a with pen perfectly balances on its edge, equilibrium does not imply stability. When perturbed, a stable system returns to its equilibrium position like a marble at the bottom of a bowl. On the other hand, an unstable system will amplify perturbations, leading to a collapse or an explosion. We can make an intuitive argument for which configurations for a given family of stars are stable. We will again assume that the equation of state, on a microscopic level, obeys Le Chatelier's principle in the form $dp/dn > 0$. We can see that this holds for all the cases we are considering. A star in equilibrium will find itself on the line parametrized by its central pressure, such as Figure 4.6. In this case, a perturbation reducing the radius of the star will increase the central pressure as the particle density increases. This is illustrated in Figure 4.8. A star in equilibrium at point A can be compressed to an out-of-equilibrium configuration, point B. This point has a central pressure corresponding to the equilibrium state at point C. As the equilibrium configuration at point C has a *lower* mass than the configuration at B, it has a weaker gravitational effect. Therefore, we would expect it to shrink further, as the central pressure of B is not enough to support its gravitational mass. This compression will lead to an even higher central pressure. We thus have a positive feedback loop, and the initial perturbation will continue to grow. We can make a similar argument in the case where the mass increases with an increase in the central pressure. Here, a compression will lead to a state in which central pressure corresponds to an equilibrium state with a *higher* mass. This state will thus tend to expand after a compression, counteracting the perturbation. This gives us the following criterion for stability,

$$\frac{dM}{dp_c} > 0. \quad (4.102)$$

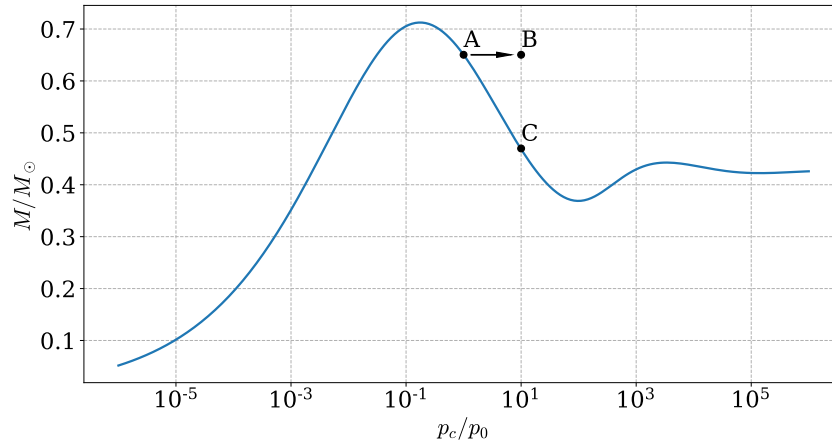


Figure 4.8: The plot shows the mass, in units of solar masses, of a star of a cold gas of neutrons, as a function of the central pressure, normalized to the characteristic pressure. Point A denotes a position of equilibrium, which can be compressed to an out-of-equilibrium point, B, which has a central pressure corresponding to an equilibrium configuration, point C.

As it turns out, this is a necessary but not sufficient requirement for stability [54]. To conduct a more rigorous study of stability, one must derive the equation of hydrostatic equilibrium with the addition of perturbations as time-dependent, radial oscillations. This is beyond the scope of this thesis, but we shortly recap the procedure. This is done by displacing a fluid element at a radius r and time t by $\delta r(r, t) = \sum_n A_n \xi_n(r) e^{i\omega_n t}$. Here, ξ_n are normal modes with frequencies ω_n , $n \in \{0, 1, \dots\}$. The equation for the eigenmodes was first obtained by Chandrasekhar [65], and can be written in the form of a Sturm-Liouville equation,

$$\left[\frac{d}{dr} \left(\Pi \frac{d}{dr} \right) + Q + \omega_n^2 W \right] \xi_n = 0, \quad (4.103)$$

where Π , Q , and W are functions of the pressure, energy density, particle density, α , and β . These quantities are thus given by a solution to the equilibrium problem [54]. Stability is encoded in the sign of the square of the frequencies. For $\omega_n^2 > 0$, the mode will remain oscillatory, while if $\omega_n^2 < 0$, it will grow exponentially. Thus, if the system has *any* modes such that $\omega_n^2 < 0$, it is unstable. One mode ω_n can change stability at a critical point on the $M - R$ curve, where

$$\frac{dM}{du_c} = 0, \quad (4.104)$$

and this will *only* happen at critical points [66]. Here, u_c is the central energy density corresponding to p_c . This is equivalent to the criterion $dM/dp_c = 0$ as long as dp/du is finite. Whether the change is from a stable mode to an unstable one is dependent on whether the curve turns clockwise (a mode becomes stable) or counterclockwise (a mode becomes unstable) [66]. We know that very low-pressure, cold fermions are stable, which means that configuration with a radius larger than the maximum has $0.71 M_\odot$ will be stable. As illustrated in Figure 4.6, the curve then turns counterclockwise, and a new mode is made unstable each half turn.

Part II

χ PT and the pion-condensed phase

Chapter 5

Chiral perturbation theory

In this chapter, we will take the theory in Chapter 3 and apply it to the specific case of quantum chromodynamics to derive *chiral perturbation theory* (χ PT). Chiral perturbation theory is an effective description in which the *pseudoscalar mesons*, such as the pions, are the degrees of freedom. They are pseudo-Goldstone bosons due to the spontaneous breaking of the QCD vacuum and allow for a perturbative description of the strong force even at low energies. We begin with a description of quantum chromodynamics.

5.1 Quantum chromodynamics

This section is based on [9, 40, 50].

Quantum chromodynamics, QCD, is the theory of quarks, q_{fc} , interacting via the strong force. Quarks are spin- $\frac{1}{2}$ spinors, and thus fermions. There are six *flavors* of quarks divided into three *generations*. The first generation is the up and down quarks, the second is the charm and strange quarks, and the third generation is the top and bottom quarks. The flavors are labeled by the index f . The second index, c , labels the quantum number associated with the strong force, called color. The strong force is mediated by gluons, denoted A_μ^c , and is an example of a Yang-Mills theory. We will give a short overview of Yang-Mills theory before we detail QCD further.

5.1.1 Yang-Mills theory and Gauge symmetry

In quantum electrodynamics, two systems are related by a gauge transform where the photon field transforms as $\mathcal{A}_\mu \rightarrow \mathcal{A}_\mu + \partial_\mu \alpha(x)$, are physically indistinguishable. This principle of gauge invariance dictates the form of interactions of the theory. Yang-Mills theory generalizes this approach. In our discussion on global symmetries, we considered the global transformation of fields by some group G . As we did in subsection 3.5.1, we now promote this to a local transformation. That is, the transformations are themselves functions of spacetime, $U = U(x)$, and take on some value in G for all points in space. With this, however, we encounter a problem with comparing the value of a field at different points. As the symmetry is local, a gauge transformation will generally affect the field at two points differently. We must find a way independent of gauge choice to compare fields at different points in space. This is similar to a problem we have encountered before. In differential geometry, as described in section 2.1, we needed a connection $\Gamma_{\mu\nu}^\rho$ to compare vectors in different tangent spaces in a coordinate independent way. In gauge theories, we generalize this by defining a connection, A_μ , to compare field values at different points in a gauge-independent way.

Consider a set of N fields ψ_c , which the symmetry group $\text{SU}(N)$ acts linearly on as $\psi_c \rightarrow U_{cc'}\psi_{c'}$. We can write $U = \exp\{i\eta_\alpha T_\alpha\}$, where T_α are the generators of $\mathfrak{su}(N)$. The transformation is then made local by letting the coordinates of $\text{SU}(N)$ be functions of spacetime, $\eta_\alpha = \eta_\alpha(x)$. As we did in section 2.1, we define the covariant derivative D_μ to transform as the thing on which it acts. Assume this covariant derivative has the form

$$D_\mu^{cc'}\psi_{c'} = (\delta_{cc'}\partial_\mu - igA_\mu^{cc'})\psi_{c'}, \quad (5.1)$$

where $A_\mu^{cc'}(x)$ is a new, dynamic field. This is similar to what we did in differential geometry, Eq. (2.32). We will suppress the c -indices for cleaner notation. By enforcing the transformation rule $D_\mu\psi \rightarrow UD_\mu\psi$, we can deduce the transformation properties of the gauge field,

$$A_\mu \rightarrow U \left(A_\mu + \frac{i}{g}\partial_\mu \right) U^\dagger \quad (5.2)$$

For an infinitesimal transformation, this becomes

$$A_\mu \rightarrow A_\mu + i\eta_\alpha[T_\alpha, A_\mu] + \frac{1}{g}\partial_\mu\eta_\alpha T_\alpha. \quad (5.3)$$

From subsection 2.2.2, we see that A_μ transform under the adjoint representation of global $\mathfrak{su}(N)$. We can therefore write $A_\mu = A_\mu^\alpha T_\alpha$. With the covariant derivative, we can create gauge-invariant terms, such as $\bar{\psi}D_\mu\psi$. In section 2.1, we introduced the Riemann tensor as the commutator of covariant derivatives, Eq. (2.38), which ensures that it transforms as a tensor. We found that this tensor measures how much a vector is rotated by the curvature of space when parallel transported around in a small loop. In analogy, we define the *field strength tensor*,

$$G_{\mu\nu} := \frac{i}{g}[D_\mu, D_\nu] = \partial_\mu A_\nu - \partial_\nu A_\mu - ig[A_\mu, A_\nu]. \quad (5.4)$$

A_μ is an element of a Lie algebra, so the commutator is given by the structure constants of that algebra, Eq. (2.76). The field strength tensor transforms as $G_{\mu\nu} \rightarrow UG_{\mu\nu}U^\dagger$. This allows us to create gauge-invariant terms of only this tensor, which, as with the Ricci scalar in general relativity, are the building blocks of the Lagrangian of the gauge field. The lowest order terms are

$$G_{\alpha}^{\mu\nu}G_{\mu\nu}^{\alpha}, \quad \epsilon^{\mu\nu\rho\sigma}G_{\mu\nu}^{\alpha}G_{\rho\sigma}^{\alpha}. \quad (5.5)$$

Here, α is the index in $\mathfrak{su}(N)$ -space.

5.1.2 The QCD Lagrangian

The Lagrangian of QCD, including only the strong force, is

$$\mathcal{L}_{\text{QCD}} = \bar{q}(i\not{D} - m)q - \frac{1}{4}G_{\mu\nu}^{\alpha}G_{\alpha}^{\mu\nu}. \quad (5.6)$$

We have suppressed color and flavor indices, which are summed over, and $\bar{q} = q^\dagger\gamma^0$. The gauge group of the strong force is $\text{SU}(3)_c$ with the coupling constant g , and the corresponding covariant derivative is

$$(D_\mu q)_{cf} = (\delta_{cc'}\partial_\mu - igA_\mu^{cc'})q_{c'f}, \quad (5.7)$$

We employ the Feynman slash-notation, where $\not{D} = \gamma^\mu D_\mu$, and γ^μ are the Dirac matrices, as described in section A.2. The quark mass matrix, m , acts on the flavor indexes as the flavor states are mass eigenstates. There are no known symmetries that forbid an $\epsilon^{\mu\nu\rho\sigma}G_{\mu\nu}^{\alpha}G_{\rho\sigma}^{\alpha}$ -term, however it is an empirical fact that it is either not present or highly suppressed. Its absence is dubbed the strong CP problem [9].

5.1.3 Chiral symmetry

If we consider the massless QCD Lagrangian, $m = 0$, it has an additional symmetry of rotation in its flavour indices. We can project the quarks down to their *chiral* components by introducing projection operators

$$P_R = \frac{1}{2} (1 + \gamma^5), \quad P_L = \frac{1}{2} (1 - \gamma^5). \quad (5.8)$$

Here, γ^5 is the “fifth gamma-matrix”, as described in section A.2. As good projection operators, they obey

$$P_R + P_L = 0, \quad P_R P_L = P_L P_R = 0, \quad P_I^2 = P_I, \quad I = R, L. \quad (5.9)$$

By the properties of γ^5 and $\bar{q} = q^\dagger \gamma^0$, these operators project out the opposite chirality of q and \bar{q} ,

$$P_I q = q_I, \quad \bar{q} P_I = \bar{q}_{\bar{I}}, \quad I = R, L, \quad \bar{I} = L, R. \quad (5.10)$$

With this, we can write the quark-sector of massless QCD as

$$i\bar{q}\not{D}q = i\bar{q}\not{D}(P_R + P_L)^2 q = i\bar{q}_L\not{D}q_L + i\bar{q}_R\not{D}q_R. \quad (5.11)$$

This operator is invariant under the transformations

$$q_R \rightarrow U_R q_R, \quad q_L \rightarrow U_L q_L, \quad (5.12)$$

where U_L and U_R are Hermitian matrices that act on the flavor indices. These transformations form the Lie group $U(N_f)_R \times U(N_f)_L = U(1)_R \times SU(N_f)_R \times U(1)_L \times SU(N_f)_L$. This transformation can also be described in terms of the diagonal subgroup. This subgroup is made up of transformations where $U_R = U_L$, called vector transformations, and the remaining subgroup of transformations where $U_L = U_R^\dagger$, called axial transformations. These together form $U(N_f)_A \times U(N_f)_V = U(1)_V \times SU(N_f)_V \times U(1)_A \times SU(N_f)_A$. The currents corresponding to these transformations are

$$J_V^\mu = \bar{q}\gamma^\mu q, \quad V_\alpha^\mu = \bar{q}T_\alpha\gamma^\mu q, \quad J_A^\mu = \bar{q}\gamma^\mu\gamma^5 q, \quad A_\alpha^\mu = \bar{q}T_\alpha\gamma^\mu\gamma^5 q. \quad (5.13)$$

Here, T_α and $T_\alpha\gamma^5$ are the generators of $SU(N_f)_V$ and $SU(N_f)_A$. This symmetry, though, is broken in several ways. Firstly, transformations of the form $e^{i\alpha\gamma^5} \in U(1)_A$ are subject to the *axial anomaly*. As mentioned in section 3.3, in a quantum theory not only the action has to be invariant but the integration measure as well, and $\mathcal{D}q\mathcal{D}\bar{q}$ is not. This is encoded in the Schwinger-Dyson equation [9]

$$\partial_\mu \langle J_A^\mu \rangle = -\frac{e^2}{(4\pi)^2} \langle \varepsilon^{\mu\nu\rho\sigma} F_{\mu\nu} F_{\rho\sigma} \rangle. \quad (5.14)$$

The remaining symmetry is $U(1)_V \times SU(N_f)_V \times SU(N_f)_A$. Next, the mass term explicitly breaks this symmetry. If we consider all quarks to have the same mass m_q , so that $m = m_q \mathbb{1}$, only $U(N_f)_A$ is broken. This is called the *chiral limit*. However, when we include the fact that the masses of the quarks are different, we break the symmetry further. Other external currents, chemical potentials, and electromagnetic interactions also break the symmetry.

Lastly, the symmetry is broken spontaneously by the ground state quark condensate, $\langle \bar{q}q \rangle \neq 0$. In the chiral limit, one can show that the scalar bilinear for all three quarks u , d , and s must be equal, and we define $\langle \bar{q}q \rangle = \langle \bar{u}u \rangle = \langle \bar{d}d \rangle = \langle \bar{s}s \rangle$ [50]. The scalar quark operator is not invariant under $SU(N_f)_A$, and as discussed in section 3.3, this leads to the spontaneous symmetry breaking pattern.

$$SU(N_f)_L \times SU(N_f)_R \longrightarrow SU(N_f)_L \times SU(N_f)_R / SU(N_f)_A = SU(N_f)_V. \quad (5.15)$$

This pattern enables us to construct an effective low energy theory for QCD physics. We will take this symmetry breaking as an axiom and use it to construct χ PT. The scalar quark condensate is quantified by the constant B_0 via the relation

$$\langle \bar{q}q \rangle = -f_\pi^2 B_0. \quad (5.16)$$

With the spontaneous symmetry breaking of the quark condensate, we get the resulting Goldstone bosons φ_α . The pion decay constant f_π is defined by the matrix element of current corresponding to the broken symmetry, A_α^μ between the vacuum $|0\rangle$ and Goldstone boson momentum states, $|\varphi_\alpha(p)\rangle$. One can show that this element, by Lorentz covariance, must have the form [9, 50]

$$\langle 0 | A_\alpha^\mu(x) | \varphi_\beta(p) \rangle = i f_\pi \delta_{\alpha\beta} p^\mu e^{ip_\mu x^\mu}. \quad (5.17)$$

We are now ready to construct χ PT.

5.2 Chiral perturbation theory

This section is based on [1, 50–52, 67, 68].

We now apply the theory we developed in Chapter 3. The systematics of chiral perturbation theory, or χ PT, was laid out by Gasser and Leutwyler [51, 52] and is based on Weinberg’s “theorem” stating that quantum field theories on their own do not contain more information than the bare minimum [1].

5.2.1 *Weinberg’s power counting scheme

Our plan is now to use the results from section 3.4 to construct the most general Lagrangian of the Goldstone bosons due to the breaking of the QCD vacuum. This, however, will result in a theory with an infinite number of free parameters, making it unwieldy. We need an expansion scheme in order to compute observable perturbatively. We are working in the low-energy limit, so it is natural to expand in pion momenta. As we saw in section 3.4, the terms in the Lagrangian will be made up of combinations of the terms e_μ and d_μ of the Maurer-Cartan form, $i\Sigma\partial_\mu\Sigma = e_\mu + d_\mu$. Therefore, all terms in the effective Lagrangian will be proportional to a certain number of derivatives of the Goldstone bosons, which Lorentz invariance demands to be even.

Consider the matrix element \mathcal{M} for a given Feynman diagram with external pion lines with momenta q , where both the energies and momenta are less than or equal to some energy scale Q . If we scale $Q \rightarrow tQ$, and consequently also the external momenta $q \rightarrow tq$, momentum conservation at each vertex ensures that each internal momentum p of the diagram scales as $p \rightarrow tp$. Assume this diagram is made up of V_i copies of the vertex i , which contain d_i derivatives. Each of these vertices scale as t^{d_i} . The propagators contribute a factor p^{-2} and will therefore scale as t^{-2} , and the integration measure d^4p scales as t^4 . This means that a matrix element with L loops and I internal lines scales as

$$\mathcal{M}(q) \rightarrow \mathcal{M}(tq) = t^D \mathcal{M}(q), \quad (5.18)$$

where

$$D = \sum_i V_i d_i - 2I + 4L. \quad (5.19)$$

D is called the *chiral dimension* of \mathcal{M} . Using the formula Eq. (3.20) for number of loops in a Feynman diagram, we get

$$D = \sum_i V_i (d_i - 2) + 2L + 2. \quad (5.20)$$

For low energy scales Q , the largest contribution will come from the matrix elements of the smallest chiral dimension D . A general process will consist of a sum of matrix elements of different chiral dimensions. We can expand this element in powers of the pion momenta by using t as the expansion parameter. The leading order term will be those where $L = 0$ and $d_i = 2$ so that $D = 2$. This means that all tree-level contributions of the lowest chiral dimension are from terms in the Lagrangian with exactly two derivatives. Next is $D = 4$, which contains both tree-level contributions from terms with $d_i = 4$ and a one-loop contribution from $d_i = 2$. We therefore expand the effective Lagrangian as

$$\mathcal{L}_{\text{eff}} = \mathcal{L}_2 + \mathcal{L}_4 + \dots, \quad (5.21)$$

where \mathcal{L}_D contains D derivatives. This is equivalent to scaling the space-time coordinates as $x^\mu \rightarrow tx^\mu$ and expanding the Lagrangian in powers of t .

We must also allow for the fact that pions have non-zero mass, interact in a symmetry-breaking way with the electromagnetic field, and the possibility of external currents. We showed in section 3.5 that this can be done using the technique of spurion fields, in which symmetry-breaking terms are treated as external fields with their own transformation rules. These fields, too, must be given chiral dimensions. Any external pions are on-shell, so the pion mass m_π must be less than the energy scale Q . As we will see, this corresponds to scaling the quark masses as $m_q \rightarrow t^2 m_q$. Similarly, μ_I must also be less than Q , which means that we scale it as $\mu_I \rightarrow t\mu_I$. We include electromagnetic interaction by scaling the fundamental electric charge e as $e \rightarrow te$ [69]. Following these rules, each term in the effective Lagrangian will have a well-defined chiral dimension D , ensuring a consistent series expansion. The term \mathcal{L}_D then contain all allowed terms that scale as t^D [1, 42, 50].

The chiral dimension gives a formal power series to expand the Lagrangian, and as we will show later, ensures that we can perform renormalization order-by-order. However, for perturbation theory to be of any use, we need the series to converge. For the series to converge, external momentum q or in our case chemical potential μ_I must be small *compared to some energy scale*. Couplings between the Goldstone bosons will be accompanied by a factor $1/f^2$, where f is the *bare* pion decay constant. To leading order, $f = f_\pi$. As will see, convergence is therefore dependent on if $\mu_I/4\pi f_\pi$ is smaller than one [42]. The 4π -factor shows up due to Fourier integrals over loop diagrams and will be important in giving chiral perturbation theory a larger domain of applicability, as it allows us to explore the phase outside the vacuum phase.

5.2.2 *Non-linear realization

To construct the Lagrangian of chiral perturbation theory, we start with the Lagrangian of massless QCD,

$$\mathcal{L}_{\text{QCD}}^0 = i\bar{q}\not{D}q - \frac{1}{4}G_{\mu\nu}^\alpha G_{\alpha}^{\mu\nu}. \quad (5.22)$$

As discussed in last section, this Lagrangian is invariant under the full symmetry group $G = \text{SU}(N_f)_R \times \text{SU}(N_f)_L$, but the system undergoes spontaneous symmetry breaking to the smaller group $H = \text{SU}(N_f)_V$. As we found in section 3.4, the low energy dynamics will therefore be described by a $G/H = \text{SU}(N_f)_A$ -valued field Σ . Let $g \in G$. We write $g = (U_L, U_R)$, where $U_R \in \text{SU}(N_f)_R$, $U_L \in \text{SU}(N_f)_L$. Elements in H are then of the form (U, U) , while elements in G are of the for (U, U^\dagger) . A general element g can be written as

$$g = (U_L, U_R) = (1, U_R U_L^\dagger)(U_L, U_L). \quad (5.23)$$

Since $(U_L, U_L) \in H$, this means that we can write the coset gH as $(1, U_R U_L^\dagger)H$, which gives a way to choose a representative element for each coset. We identify

$$\Sigma = U_R U_L^\dagger. \quad (5.24)$$

This is our standard form for elements in gH . As we saw in section 3.4, it therefore implicitly defines transformation properties of the Goldstone bosons, which is given by the function $h(g, \xi)$. For $\tilde{g} \in G$, we have

$$\tilde{g}(1, \Sigma) = (\tilde{U}_L, \tilde{U}_R)(1, U_R U_L^\dagger) = (1, \tilde{U}_R(U_R U_L^\dagger) \tilde{U}_L^\dagger)(\tilde{U}_L, \tilde{U}_L) = (1, \tilde{U}_R \Sigma \tilde{U}_L^\dagger) \tilde{h}. \quad (5.25)$$

This gives the transformation rule

$$\Sigma \rightarrow \Sigma' = U_R \Sigma U_L^\dagger. \quad (5.26)$$

This gives simple transformation rules for $(U, U) \in H$ and $(U, U^\dagger) \in G/H$,

$$H : \quad \Sigma \rightarrow \Sigma' = U \Sigma U^\dagger, \quad (5.27)$$

$$G/H : \quad \Sigma \rightarrow \Sigma' = U \Sigma U. \quad (5.28)$$

Due to how G factors into two Lie groups, the constituents of the Maurer-Cartan form are

$$d_\mu = i \Sigma(x)^\dagger \partial_\mu \Sigma(x), \quad e_\mu = 0. \quad (5.29)$$

We can now create G -invariant terms by taking traces of d_μ 's. As we will discuss in subsection 5.2.1, the order of a term in the Lagrangian will be dependent on the number of d_μ 's. As $d_\mu \in \mathfrak{su}(N_f)$, which we represent by the traceless matrices, the lowest order term is trivial,

$$\text{Tr} \{d_\mu\} = 0. \quad (5.30)$$

Using $\partial_\mu [\Sigma(x)^\dagger \Sigma(x)] = 0$, we can write

$$d_\mu d_\nu = -\Sigma(x)^\dagger [\partial_\mu \Sigma(x)] \Sigma(x)^\dagger [\partial_\nu \Sigma(x)] = \Sigma(x)^\dagger [\partial_\mu \Sigma(x)] [\partial_\nu \Sigma(x)^\dagger] \Sigma(x). \quad (5.31)$$

This leaves us with the single Lorentz invariant leading order term,

$$\text{Tr} \{d_\mu d^\mu\} = \text{Tr} \left\{ \partial_\mu \Sigma (\partial^\mu \Sigma)^\dagger \right\}, \quad (5.32)$$

Constructing the effective Lagrangian out of terms invariant under G is too restrictive to get the most general effective action, however. This only allows for an even number of d_μ 's, and observed processes such as the decay of the neutral pion through $\pi^0 \rightarrow \gamma\gamma$ would not be possible [50]. This is because we have not allowed for terms that change the Lagrangian with a divergence term, as discussed in section 3.3. Terms of this type are called Wess-Zumino-Witten (WZW) terms [42]. We will not consider these here, as they do not affect the thermodynamic quantities in question [70].

5.2.3 External currents

As discussed in section 3.5, we can incorporate external currents and symmetry breaking terms by promoting the symmetry G to a gauge symmetry, treating the external currents as gauge fields, and demanding gauge invariance of the effective Lagrangian. The external currents may couple to conserved currents, Eq. (5.13), or the other bilinears we can create out of quarks, $\bar{q}q$, $\bar{q}\gamma^5 q$, $\bar{q}T_\alpha q$, and $\bar{q}T_\alpha \gamma^5 q$. The Lagrangian of these external currents is

$$\mathcal{L}_{\text{ext}} = -\bar{q} (s - i\gamma^5 p) q + \bar{q} \gamma^\mu (v_\mu + \gamma^5 a_\mu) q. \quad (5.33)$$

Here, s , p , v_μ and a_μ are all $N_f \times N_f$ matrices acting on the flavor indices. They are, respectively, the scalar, pseudo-scalar, vector, and pseudo-vector currents. We denote these currents collectively as $j = (s, p, v^\mu, a^\mu)$. The masses of the quarks are accounted for by setting the scalar current $s = m + \tilde{s}$. Here, m is the mass matrix of the quarks, while \tilde{s} are possible other scalar currents. Other examples of external currents are chemical potentials, such as the isospin

chemical potential, which regulate conserved charges in the system. We now need to find the transformation properties of these currents under G . We define

$$r_\mu = v_\mu + a_\mu, \quad l_\mu = v_\mu - a_\mu, \quad \chi = 2B_0(s + ip), \quad \chi^\dagger = 2B_0(s - ip). \quad (5.34)$$

By making a local G -transformation and enforcing gauge invariance, we find that these transform as

$$r_\mu \rightarrow U_R(r_\mu + i\partial_\mu)U_R^\dagger, \quad (5.35)$$

$$l_\mu \rightarrow U_L(l_\mu + i\partial_\mu)U_L^\dagger, \quad (5.36)$$

$$\chi \rightarrow U_R\chi U_L^\dagger, \quad (5.37)$$

$$\chi^\dagger \rightarrow U_L\chi^\dagger U_R^\dagger. \quad (5.38)$$

As in Yang-Mills theory, we can now create field strength tensors of the gauge fields, to build more gauge-invariant terms. We define

$$f_{\mu\nu}^{(r)} = \partial_\mu r_\nu - \partial_\nu r_\mu - i[r_\mu, r_\nu], \quad f_{\mu\nu}^{(l)} = \partial_\mu l_\nu - \partial_\nu l_\mu - i[l_\mu, l_\nu], \quad (5.39)$$

which transform as

$$f_{\mu\nu}^{(r/l)} \rightarrow U_{R/L} f_{\mu\nu}^{(r/l)} U_{R/L}^\dagger. \quad (5.40)$$

Including dynamical fields, such as the photon field \mathcal{A}_μ , is slightly more complicated. Quantum electrodynamics, or QED, is a gauge theory with a $U(1)_{\text{EM}}$ gauge group, where the covariant derivative acting on quarks is

$$i\bar{q}\not{D}'q = i\bar{q}\gamma^\mu (1\partial_\mu - ieQ\mathcal{A}_\mu)q = i\bar{q}\not{\partial}q - e\mathcal{A}_\mu J^\mu, \quad (5.41)$$

Here, \mathcal{A}_μ is the photon field corresponding to the gauge group, $e = |e|$ is the elementary charge as given in Eq. (A.7), $J^\mu = -\bar{q}Q\gamma^\mu q$ is the electromagnetic charge current, and Q is the quark charge matrix. This matrix is the generator of $U(1)_{\text{EM}}$. In the case of $N_f = 3$, $Q = \text{diag}(\frac{2}{3}, -\frac{1}{3}, -\frac{1}{3})$. From Eq. (5.41), we see that $eQ\mathcal{A}_\mu$ is a vector current. Although the transformation of the quarks under the electromagnetic gauge group can be seen as a subgroup of G , we *do not* transform external currents to enforce gauge invariance, this is instead done by \mathcal{A}_μ . As \mathcal{A}_μ is a dynamical field, we can not use it to enforce G -gauge invariance. However, if we treat the charge matrix Q as an external field, then we can restore the invariance. This gives the transformation rule

$$Q_I \rightarrow U_I Q_I U_I^\dagger, \quad I = R, L. \quad (5.42)$$

Here, $Q_I = P_I Q$ are the chiral charge matrices. With these external fields, we must introduce a covariant derivative acting on Σ to enforce local G invariance. This is

$$\nabla_\mu \Sigma = \partial_\mu \Sigma - ir'_\mu \Sigma + i\Sigma l'_\mu, \quad (5.43)$$

where $r'_\mu = r_\mu + eQ\mathcal{A}_\mu$ and $l'_\mu = l_\mu + eQ\mathcal{A}_\mu$. We do not strictly *need* to include the electromagnetic field in the gauge derivative, we could just build G invariant terms of eQ , \mathcal{A}_μ and Σ , however, this is the most economical way to achieve this.

Lastly, we must include terms from quantum electrodynamics involving only the photon field, which are

$$\mathcal{L}_{\text{QED}}[\mathcal{A}] = -\frac{1}{4}F^{\mu\nu}F_{\mu\nu}, \quad F_{\mu\nu} = \partial_\mu \mathcal{A}_\nu - \partial_\nu \mathcal{A}_\mu. \quad (5.44)$$

Furthermore, the covariant derivative is extended to include the photon field in addition to the gluon field. The full Lagrangian is then

$$\mathcal{L}_{\text{QCD}}[q, \bar{q}, A, \mathcal{A}, j] = \mathcal{L}_{\text{QCD}}^0[q, \bar{q}, A, \mathcal{A}] + \mathcal{L}_{\text{QED}}[\mathcal{A}] + \mathcal{L}_{\text{ext}}[q, \bar{q}, j]. \quad (5.45)$$

We now define the effective Lagrangian of χ PT, \mathcal{L}_{eff} as

$$\begin{aligned} Z[j] &= \int \mathcal{D}q \mathcal{D}\bar{q} \mathcal{D}A \mathcal{D}\mathcal{A} \exp \left\{ i \int d^4x \mathcal{L}_{\text{QCD}}[q, \bar{q}, A, \mathcal{A}, j] \right\} \\ &= \int \mathcal{D}\varphi \mathcal{D}\mathcal{A} \exp \left\{ i \int d^4x \mathcal{L}_{\text{eff}}[\varphi, \mathcal{A}, j] \right\}. \end{aligned} \quad (5.46)$$

We know the symmetries of \mathcal{L}_{QCD} , and we have found constituent terms of \mathcal{L}_{eff} and their transformation properties under these symmetries. Weinberg's "theorem" now tells us that we can construct \mathcal{L}_{eff} by including all terms that obey the symmetry principles of \mathcal{L}_{QCD} . In addition, the Lagrangian must be a scalar. We have not listed the transformation properties of the constituent terms under C and P , however, these lay further restrictions on \mathcal{L}_{eff} . As all terms have a chiral dimension, we have a way of ordering them in a series expansion. This is all we need to start doing calculations.

5.3 Three-flavor χ PT to leading order

We will begin by considering the leading order Lagrangian, which chiral dimension $D = 2$. However, we will not include the QED Lagrangian, as we will not consider electromagnetic interaction beyond leading order. In this case, the dynamics of the photon will not contribute. With this, the leading order Lagrangian is [50–52, 71]

$$\mathcal{L}_2 = \frac{1}{4} f^2 \text{Tr} \left\{ \nabla_\mu \Sigma \nabla^\mu \Sigma^\dagger \right\} + \frac{1}{4} f^2 \text{Tr} \left\{ \chi \Sigma^\dagger + \Sigma \chi^\dagger \right\} + e^2 C \text{Tr} \left\{ \Sigma Q_L \Sigma^\dagger Q_R \right\}. \quad (5.47)$$

We will work with three flavors, i.e. $N_f = 3$, so the mass matrix is now

$$m = \begin{pmatrix} m_u & 0 & 0 \\ 0 & m_d & 0 \\ 0 & 0 & m_s \end{pmatrix}. \quad (5.48)$$

When we evaluate $s = m$ and $p = 0$, the scalar term then becomes

$$\chi = 2B_0 m = \begin{pmatrix} \bar{m}^2 - \Delta m^2 & 0 & 0 \\ 0 & \bar{m}^2 + \Delta m^2 & 0 \\ 0 & 0 & m_S^2 \end{pmatrix}, \quad (5.49)$$

where we have defined

$$\bar{m}^2 = B_0(m_u + m_d), \quad \Delta m^2 = B_0(m_d - m_u), \quad m_S^2 = 2B_0 m_s. \quad (5.50)$$

The charge matrix is

$$Q = \frac{1}{3} \begin{pmatrix} 2 & 0 & 0 \\ 0 & -1 & 0 \\ 0 & 0 & -1 \end{pmatrix} = \frac{1}{2} \left(\lambda_3 + \frac{1}{\sqrt{3}} \lambda_8 \right). \quad (5.51)$$

In the vacuum, when there are no external currents, we choose the standard, exponential parametrization of the Goldstone manifold,

$$\Sigma(x) = \exp \left\{ i \frac{\varphi_a \lambda_a}{f} \right\}. \quad (5.52)$$

Here, λ_a are the Gell-Mann matrices, as shown in section A.2. $T_a = \lambda_a/2$ are the generators of $\text{SU}(3)$, and f is the bare pion decay constant. There are eight Goldstone bosons, φ_a , which are real functions of space-time. This parametrization ensures that $\varphi = 0$ corresponds to the

vacuum. Using the isospin transformation rule Eq. (5.27), we can perform an infinitesimal transformation of the Goldstone fields,

$$\Sigma \rightarrow U_V \Sigma U_V^\dagger \sim \left(1 + i\eta_a \frac{1}{2} \lambda_a\right) \left(1 + i\frac{1}{f} \varphi_b \lambda_b\right) \left(1 - i\eta_c \frac{1}{2} \lambda_c\right) \sim 1 + i\frac{\varphi_a}{f} \lambda_a + i\frac{\varphi_a}{f} \eta_b f_{abc} \lambda_c, \quad (5.53)$$

or

$$\varphi_a \rightarrow [\delta_{ab} + i\eta_c(-if_{abc})]\varphi_b. \quad (5.54)$$

That is, φ_a transforms under the adjoint representation of $\mathfrak{su}(3)$, which is made up of elements of the form $\eta_c(-if_{abc})$. The $\mathfrak{su}(3)$ Lie algebra has three $\mathfrak{su}(2)$ sub-algebras. We introduce the matrices

$$\lambda_Q = \lambda_3 + \frac{1}{\sqrt{3}}\lambda_8, \quad \lambda_K = -\lambda_3 + \frac{1}{\sqrt{3}}\lambda_8, \quad (5.55)$$

From the structure constants, Eq. (A.32), we can conclude that they commute, i.e., $[\lambda_Q, \lambda_K] = 0$. Furthermore, we find the commutation relations

$$[\lambda_i, \lambda_j] = 2i\epsilon_{ijk}\lambda_k, \quad ijk \in \{1, 2, 3\}, \{4, 5, Q\}, \text{ or } \{6, 7, K\}. \quad (5.56)$$

We here define the Levi-Civita symbol by $\epsilon_{123} = \epsilon_{34Q} = \epsilon_{67K} = 1$. This is the defining commutation relation of $\mathfrak{su}(2)$. The first subalgebra, spanned by $\{\lambda_1, \lambda_2, \lambda_3\}$, corresponds to isospin transformations, which are rotations of the up and down quark into each other. Consider the transformation where $\eta_3 \neq 0$, while $\eta_a = 0$ for $a \neq 3$. Acting on the quarks, this transformation is generated by λ_3 , while in the adjoint representation the generator is f_{3ab} . Under this transformation, $\varphi_3\lambda_3$ is invariant. We can see this from the fact that the structure constants f_{abc} is totally antisymmetric, and thus $f_{33b} = 0$. This means that φ_3 has the quantum number $I_3 = 0$. $\varphi_1\lambda_1$ and $\varphi_2\lambda_2$ do not have definite values of the third component of isospin as they are not eigenvectors of f_{3ab} , but they do have definite values for the first and second component. The linear combinations $\pi^\pm (\lambda_1 \mp \lambda_2)$, on the other hand, do. This shows the relationship between our fields φ_a , and the observed, charged pions π^+ and π^- , as they have definite values for I_3 .¹ The full relationship between the φ_a -fields and the observed pseudoscalar mesons is [50]

$$\varphi_a \lambda_a = \begin{pmatrix} \varphi_3 + \frac{1}{\sqrt{3}}\varphi_8 & \varphi_1 - i\varphi_2 & \varphi_4 - i\varphi_5 \\ \varphi_1 + i\varphi_2 & -\varphi_3 + \frac{1}{\sqrt{3}}\varphi_8 & \varphi_6 - i\varphi_7 \\ \varphi_4 + i\varphi_5 & \varphi_6 + i\varphi_7 & -\frac{2}{\sqrt{3}}\varphi_8 \end{pmatrix} = \begin{pmatrix} \pi^0 + \frac{1}{\sqrt{3}}\eta & \sqrt{2}\pi^+ & \sqrt{2}K^+ \\ \sqrt{2}\pi^- & -\pi^0 + \frac{1}{\sqrt{3}}\eta & \sqrt{2}K^0 \\ \sqrt{2}K^- & \sqrt{2}\bar{K}^0 & -\frac{2}{\sqrt{3}}\eta \end{pmatrix}.$$

5.3.1 Ground state

When we take into account chemical potentials, we need to pick a new parametrization. We will start the analysis by assuming $e = 0$ and then reintroduce electromagnetic interactions later. The covariant derivative is then

$$\nabla_\mu \Sigma = \partial_\mu \Sigma - i[v_\mu, \Sigma], \quad v_\mu = \mu \delta_\mu^0. \quad (5.57)$$

The chemical potential matrix μ has three independent degrees of freedom, one for each quark, and is

$$\begin{aligned} \mu &= \begin{pmatrix} \mu_u & 0 & 0 \\ 0 & \mu_d & 0 \\ 0 & 0 & \mu_s \end{pmatrix} = \begin{pmatrix} \frac{1}{3}\mu_B + \frac{1}{2}\mu_I & 0 & 0 \\ 0 & \frac{1}{3}\mu_B - \frac{1}{2}\mu_I & 0 \\ 0 & 0 & \frac{1}{3}\mu_B - \mu_S \end{pmatrix} \\ &= \frac{1}{3}(\mu_B - \mu_S)\mathbb{1} + \frac{1}{2}\mu_I\lambda_3 + \frac{1}{\sqrt{3}}\mu_S\lambda_8, \end{aligned} \quad (5.58)$$

¹Authors differ if they define $\sqrt{2}\pi^\pm = \varphi_1 \pm i\varphi_2$, or with opposite signs, $\sqrt{2}\pi^\pm = \varphi_1 \mp i\varphi_2$. We choose the latter, so that $\pi_+ |0\rangle$ is the state with the quantum numbers of the positive pion.

where we have defined $\mu_B = \frac{3}{2}(\mu_u + \mu_d)$, $\mu_I = \mu_u - \mu_d$ and $\mu_S = \frac{1}{2}(\mu_u + \mu_d) - \mu_s$. Here, μ_u , μ_d , and μ_s are the up, down, and strange quark chemical potentials, while μ_B , μ_I , and μ_S are the baryon number, isospin, and strangeness chemical potentials. Σ transforms as $\Sigma \rightarrow \Sigma$ under $U(1)_V$, the symmetry corresponding to the baryon number; it is a baryon number singlet. This reflects the fact that the baryon number of mesons, and thus the φ_a 's, is zero. Therefore, the chemical potential corresponding to the baryon number, μ_B , should not affect the final result. We can also see this because μ_B only appears with the identity matrix $\mathbb{1}$ in μ . Any dependence on μ_B in $\nabla_\mu \Sigma$ will vanish as $\mathbb{1}$ commutes with everything.

We will assume the ground state is a spatially independent configuration, $\varphi_a^0 = \text{const}$. This configuration must then minimize the free energy, to leading order, is equivalent to minimizing the static Hamiltonian, i.e., $\mathcal{H}^{(0)} = \mathcal{H}[\varphi^0]$. To this end, we define

$$\Sigma_\alpha = \exp \{i\alpha n_a \lambda_a\}, \quad \alpha = \frac{1}{f} \sqrt{\varphi_a^0 \varphi_a^0}, \quad n_a = \frac{\varphi_a^0}{\sqrt{\varphi_b^0 \varphi_b^0}}. \quad (5.59)$$

We show how to derive the correct parametrization of the ground state in the case of two flavors in section B.1, as was first done in [25]. For $\mu_S = 0$, we expect to recover this result, in which $n_1^2 + n_2^2 = 1$, and thus $n_a = 0$ for $a > 2$. Furthermore, we showed that we may choose $n_1 = 0$ without loss of generality, in which case the ground state becomes

$$\Sigma_\alpha^\pm = \exp \{i\alpha \lambda_2\} = (\mathbb{1} - \lambda_2^2) + \lambda_2^2 \cos \alpha + i\lambda_2 \sin \alpha. \quad (5.60)$$

The ground state is thus parameterized by α only. As we will show in Chapter 6, when the isospin chemical potential exceeds a critical value, $\mu_I \geq \mu_I^c$, the system undergoes a phase transition from the vacuum phase to a phase in which $\alpha \neq 0$, and the charged pions form a condensate. It is only when we reach this phase that the equation of state is non-trivial at $T = 0$, which makes it possible for pion stars to form.

If we define $\mu_{K^\pm} = \mu_S + \frac{1}{2}\mu_I$ and $\mu_{K^0} = \mu_S - \frac{1}{2}\mu_I$, then we can write the terms of the QCD Lagrangian made up of μ_I and μ_S and their corresponding currents densities as

$$\bar{q}\gamma^0 \left(\frac{1}{2}\mu_I \lambda_3 + \frac{1}{\sqrt{3}}\mu_S \lambda_8 \right) q = \bar{q}\gamma^0 \left(\frac{1}{2}\mu_{K^\pm} \lambda_Q + \frac{1}{2}\mu_{K^0} \lambda_K \right) q. \quad (5.61)$$

Analogously to how a higher μ_I leads to a condensate in the first $\mathfrak{su}(2)$ subalgebra, we can expect these chemical potentials to lead to different condensates in their respective subalgebras. If we assume $\mu_{K^0} = 0$, we would expect the new ground state to take the form

$$\Sigma_\alpha^{K^\pm} = \exp \{i\alpha \lambda_5\} = (\mathbb{1} - \lambda_5^2) + \lambda_5^2 \cos \alpha + i\lambda_5 \sin \alpha. \quad (5.62)$$

This analysis extends to all four quadrants of the $\mu_I - \mu_S$ plane. If we set $\mu_{K^\pm} = 0$, we would expect a ground state of the form $e^{i\alpha \lambda_7}$. Further calculations show that this analysis is right, there are no simultaneous condensations and these states are local minima of the static Lagrangian [72, 73]. However, the domains of the different condensates overlap, so there is a phase transition between the condensates. We will study the different condensates and the transition between them in Chapter 6.

5.3.2 The pion-condensed phase

The new ground state Σ_α is a rotation of the vacuum state $\Sigma_0 = \mathbb{1}$ by $U_A = A_\alpha^i$. To parameterize excitations from this new field, we must then rotate the excitations $U(x)$ accordingly. The procedure is shown in detail for the two-flavor case in section B.1. This new parameterization is

$$\Sigma(x) = A_\alpha^i U(x) \Sigma_0 U(x) A_\alpha^i, \quad U(x) = \exp \left\{ i \frac{\varphi_a \lambda_a}{2f} \right\}, \quad A_\alpha^i = \exp \left\{ i \frac{\alpha \lambda_i}{2} \right\}, \quad (5.63)$$

where $i = 2, 5, 7$ depending on which phase we are in. We begin the analysis of the pion-condensed phase, so $i = 2$, and assume $\mu_I > 0$ and $e = 0$. Inserting this into Eq. (5.47), and expanding up to and including $\mathcal{O}((\pi/f)^2)$, we get

$$\mathcal{L}_2^{(0)} = \frac{1}{2}f^2 (\mu_I^2 \sin^2 \alpha + 2\bar{m}^2 \cos \alpha + m_S^2), \quad (5.64)$$

$$\mathcal{L}_2^{(1)} = -f\mu_I \partial_0 \varphi_1 \sin \alpha + f \sin \alpha (\mu_I^2 \cos \alpha - \bar{m}^2) \varphi_2, \quad (5.65)$$

$$\mathcal{L}_2^{(2)} = \frac{1}{2} \partial_\mu \varphi_a \partial^\mu \varphi_a + \frac{1}{2} m_{ab} \varphi_a \partial_0 \varphi_b - \frac{1}{2} m_a^2 \varphi_a^2 - \frac{1}{\sqrt{3}} \Delta m^2 \varphi_3 \varphi_8. \quad (5.66)$$

Here, we have introduced a number of mass parameters, which will in general be functions of α and the chemical potentials. The diagonal mass terms are

$$m_1^2 = \bar{m}^2 \cos \alpha - \mu_I^2 \cos^2 \alpha, \quad (5.67)$$

$$m_2^2 = \bar{m}^2 \cos \alpha - \mu_I^2 \cos 2\alpha, \quad (5.68)$$

$$m_3^2 = \bar{m}^2 \cos \alpha + \mu_I^2 \sin^2 \alpha, \quad (5.69)$$

$$m_4^2 = m_5^2 = m_-^2 - m_{\mu+}^2, \quad (5.70)$$

$$m_6^2 = m_7^2 = m_+^2 - m_{\mu-}^2, \quad (5.71)$$

$$m_8^2 = \frac{1}{3}(\bar{m}^2 \cos \alpha + 2m_S^2), \quad (5.72)$$

where

$$m_\pm^2 = \frac{1}{2}(\bar{m}^2 \cos \alpha \pm \Delta m^2 + m_S^2), \quad m_{\mu\pm}^2 = \left(\mu_S \pm \frac{1}{2} \mu_I \cos \alpha \right)^2 - \frac{1}{4} \mu_I^2 \sin^2 \alpha, \quad (5.73)$$

and the off-diagonal terms are

$$m_{12} = 2\mu_I \cos \alpha, \quad (5.74)$$

$$m_{45} = 2 \left(\mu_S + \frac{1}{2} \mu_I \cos \alpha \right), \quad (5.75)$$

$$m_{67} = 2 \left(\mu_S - \frac{1}{2} \mu_I \cos \alpha \right). \quad (5.76)$$

Here, $m_{ab} = -m_{ba}$, and terms not defined above are zero. These terms mean that the basis φ_a does not correspond to mass eigenstates. This is to be expected, as they are not eigenstates of isospin nor strangeness.

At $\mu_S = \mu_I = 0$ and $\alpha = 0$, we obtain the well-known, tree-level masses of the pseudoscalar mesons [67],

$$m_{\pi,0}^2 = \bar{m}^2 = B_0(m_u + m_d) \quad (5.77)$$

$$m_{K^\pm,0}^2 = \frac{1}{2}(\bar{m}^2 - \Delta m^2 + m_S^2) = B_0(m_u + m_s), \quad (5.78)$$

$$m_{K^0,0}^2 = \frac{1}{2}(\bar{m}^2 + \Delta m^2 + m_S^2) = B_0(m_d + m_s), \quad (5.79)$$

$$m_{\eta,0}^2 = \frac{1}{3}(\bar{m}^2 + 2m_S^2) = \frac{1}{3}B_0(m_u + m_d + 4m_s). \quad (5.80)$$

To leading order, these are the physical masses of the pions, charged kaons, neutral kaons, and the η -particle. The values used in this thesis are given in section A.1. Similarly, the f -constant is, to leading order, given by $f = f_\pi$.

To find the physical masses in the pion-condensed phase, we must analyze the propagator and the spectrum of the theory. We follow [70, 74]. The spectrum is given by the zero of the inverse

propagator, which has a block diagonal form. In momentum space, it reads

$$D_{ab}^{-1} = \frac{\delta^2 S}{\delta\varphi_a \delta\varphi_b} = (p^2 - m_a^2)\delta_{ab} - ip_0 m_{ab} = \begin{pmatrix} D_{12}^{-1} & 0 & 0 & 0 & 0 \\ 0 & p^2 - m_3^2 & 0 & 0 & 0 \\ 0 & 0 & D_{45}^{-1} & 0 & 0 \\ 0 & 0 & 0 & D_{67}^{-1} & 0 \\ 0 & 0 & 0 & 0 & p^2 - m_3^2 \end{pmatrix}. \quad (5.81)$$

where

$$D_{12}^{-1} = \begin{pmatrix} p^2 - m_1^2 & -ip_0 m_{12} \\ ip_0 m_{12} & p^2 - m_1^2 \end{pmatrix}, \quad (5.82)$$

$$D_{45}^{-1} = \begin{pmatrix} p^2 - m_4^2 & -ip_0 m_{45} \\ ip_0 m_{45} & p^2 - m_5^2 \end{pmatrix}, \quad (5.83)$$

$$D_{67}^{-1} = \begin{pmatrix} p^2 - m_6^2 & -ip_0 m_{67} \\ ip_0 m_{67} & p^2 - m_7^2 \end{pmatrix}. \quad (5.84)$$

We have chosen to neglect the $\pi^0 - \eta$ -mixing terms $D_{83}^{-1} = D_{38}^{-1} = -\Delta m^2/\sqrt{3}$. We will, however, keep $\Delta m \neq 0$ in the other mass contribution. The spectrum of the theory is given by the zeros of the determinant of the propagator,

$$\det(D^{-1}) = (p^2 - m_3^2)(p^2 - m_8^2) [(p^2 - m_1^2)(p^2 - m_2^2) - p_0^2 m_{12}^2] \\ \times [(p^2 - m_4^2)(p^2 - m_5^2) - p_0^2 m_{45}^2] [(p^2 - m_6^2)(p^2 - m_7^2) - p_0^2 m_{67}^2] = 0. \quad (5.85)$$

Solving $\det(D^{-1}) = 0$ for p_0^2 gives eight roots E_i^2 , one for each particle. Writing the four-momentum as $p^\mu = (p_0, \vec{p})$, these zeros are

$$E_{\pi^0}^2 = |\vec{p}|^2 + m_3^2, \quad (5.86)$$

$$E_\eta^2 = |\vec{p}|^2 + m_8^2, \quad (5.87)$$

$$E_{\pi^\pm}^2 = |\vec{p}|^2 + \frac{1}{2}(m_1^2 + m_2^2 + m_{12}^2) \mp \frac{1}{2}\sqrt{4|\vec{p}|^2 m_{12}^2 + (m_1^2 + m_2^2 + m_{12}^2)^2 - 4m_1^2 m_2^2}, \quad (5.88)$$

$$E_{K^\pm}^2 = |\vec{p}|^2 + m_4^2 + \frac{1}{2}m_{45}^2 \mp \frac{1}{2}m_{45}\sqrt{4|\vec{p}|^2 + 4m_4^2 + m_{45}^2}, \quad (5.89)$$

$$E_{K^0}^2 = |\vec{p}|^2 + m_6^2 + \frac{1}{2}m_{67}^2 \pm \frac{1}{2}m_{67}\sqrt{4|\vec{p}|^2 + 4m_6^2 + m_{67}^2}. \quad (5.90)$$

The masses of the particles are given by the energy at $\vec{p} = 0$. For $\alpha = 0$, which we will later show is valid for low μ 's, we get a Zeeman-like splitting of the energies of the pions,

$$E_0 = \sqrt{|\vec{p}|^2 + \bar{m}^2}, \quad E_{\pi^\pm} = \sqrt{|\vec{p}|^2 + \bar{m}^2} \mp \mu_I. \quad (5.91)$$

The kaons have a similar splitting, only due to the kaon chemical potentials μ_{K^\pm} and μ_{K^0} instead. The masses of the various mesons are shown in Figure 5.1. These results use the relationship between μ_I and α , which we derive in the next chapter. In the lower plot, we see the Zeeman splitting of the pion masses, which persists until the mass of the positive pion vanishes. As we explore further in the next chapter, this happens as the exact isospin symmetry $U(1)_{I_3} \subset SU(3)_V$ is broken spontaneously by the pion condensate, and π^+ is the corresponding Goldstone boson. On the top, we see that the kaons also get this Zeeman splitting in the vacuum phase.

If we adjust the strangeness chemical potential instead, while the isospin chemical potential remains constant, then the kaons will get a similar splitting, as shown in Figure 5.2, while the pions are unaffected. For $\mu_I > 0$, the mass of the positive kaon will reach zero first, at the point of transition into the charged kaon condensate. At this point, the results obtained in this section will become invalid, as $\Sigma = \exp\{i\alpha\lambda_2\}$ no longer is the ground state.

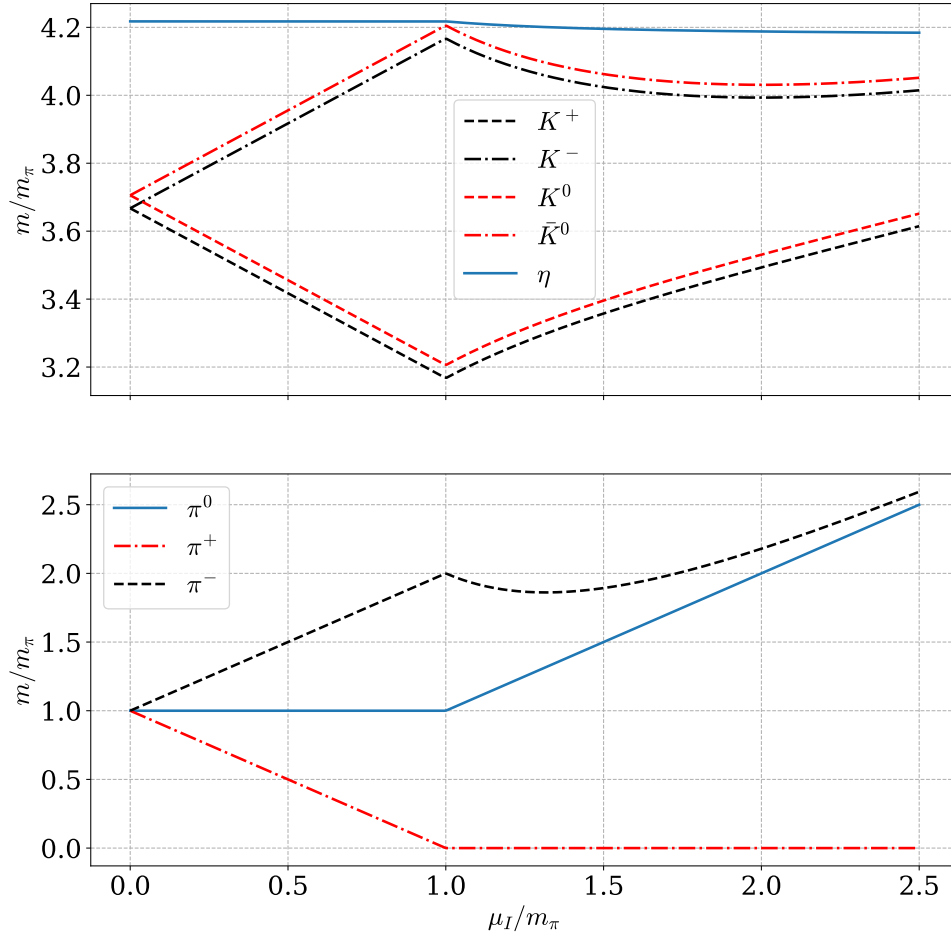


Figure 5.1: The leading order masses of the pseudoscalar mesons, as functions of the isospin chemical potential. Both the masses and chemical potential are normalized to the pion mass. These results are at $\mu_S = 0$. The difference between the kaons at $\mu_I = 0$ is a result of the fact that $\Delta m \neq 0$.

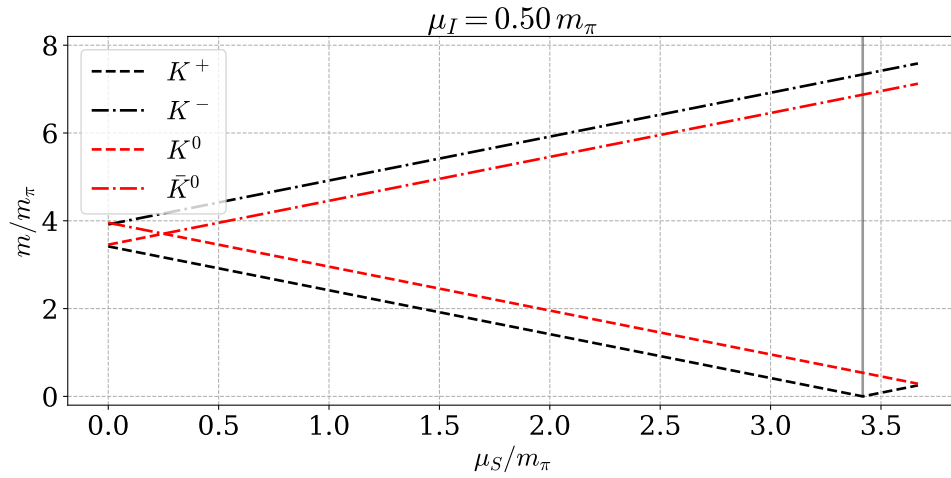


Figure 5.2: The kaon masses as a function of μ_S , both in units of m_π , evaluated at $\mu_I = 0.5 m_\pi$. These results are only valid to the left of the gray line at $\mu_S \approx 3.3 m_\pi$, where m_{K^+} reaches zero.

5.3.3 The kaon condensed phase

In the K^\pm -condensate, we get

$$\mathcal{L}_2^{(0)} = \frac{1}{2}f^2 \left(\mu_{K^\pm}^2 \sin^2 \alpha + 2m_{K^\pm,0}^2 \cos \alpha + \bar{m}^2 + \Delta m^2 \right), \quad (5.92)$$

$$\mathcal{L}_2^{(1)} = -\frac{1}{2}f\mu_{K^\pm}\partial_0\varphi_4 \sin \alpha + f \sin \alpha \left(\mu_{K^\pm}^2 \cos \alpha - m_{K^\pm,0}^2 \right) \varphi_5 \quad (5.93)$$

$$\mathcal{L}_2^{(1)} = \frac{1}{2}\partial_\mu\varphi_a\partial^\mu\varphi_a + \frac{1}{2}m'_{ab}\varphi_a\partial_0\varphi_a - \frac{1}{2}m_a'^2\varphi_a^2 - \frac{1}{2}\Delta_{\eta\pi}\varphi_3\varphi_8. \quad (5.94)$$

The new mass parameters are

$$m_1'^2 = m_2^2 = m_+'^2 + m_{\mu+}'^2, \quad (5.95)$$

$$m_3'^2 = \frac{1}{4} \left(\mu_{K^\pm}^2 \sin^2 \alpha + 2m_{K^\pm,0}^2 \cos \alpha + 3\bar{m}^2 + \Delta m^2 - m_S^2 \right), \quad (5.96)$$

$$m_4'^2 = m_{K^\pm,0}^2 \cos \alpha - \mu_{K^\pm} \cos^2 \alpha, \quad (5.97)$$

$$m_5'^2 = m_{K^\pm,0}^2 \cos \alpha - \mu_{K^\pm} \cos 2\alpha, \quad (5.98)$$

$$m_6'^2 = m_7^2 = m_-'^2 + m_{\mu-}'^2, \quad (5.99)$$

$$m_8'^2 = \frac{1}{12} \left[\frac{9}{4}\mu_{K^\pm}^2 \sin^2 \alpha + 5m_{K^\pm,0}^2 \cos \alpha - \bar{m}^2 + 5\Delta m^2 + 3m_S^2 \right], \quad (5.100)$$

$$\Delta_{\eta\pi} = \frac{1}{2\sqrt{3}} \left[\sqrt{3}\mu_{K^\pm}^2 \sin^2 \alpha + m_{K^\pm,0}^2 \cos \alpha - \bar{m}^2 - \sqrt{3}\Delta m^2 - m_S^2 \right], \quad (5.101)$$

$$(5.102)$$

where we have defined

$$m_\pm'^2 = \frac{1}{4} \left[2m_{K^\pm,0}^2 \cos \alpha + (2 \pm 1)\bar{m}^2 + (2 \mp 1)\Delta m^2 \pm m_S^2 \right], \quad (5.103)$$

$$m_{\mu\pm}'^2 = \frac{1}{2} \left[\mu_{K^\pm}^2 \sin^2 \alpha - \mu_{K^0}^2 (1 \mp \cos \alpha) - \mu_I^2 (1 \pm \cos \alpha) \right]. \quad (5.104)$$

The off-diagonal terms are

$$m'_{12} = 2(\mu_{K^\pm} \cos \alpha + \mu_I + \mu_{K^0}) \quad (5.105)$$

$$m'_{45} = 2\mu_{K^\pm} \cos \alpha, \quad (5.106)$$

$$m'_{67} = 2(\mu_{K^\pm} \cos \alpha - \mu_I - \mu_{K^0}). \quad (5.107)$$

We see that both the Lagrangian and the masses have a similar structure to the pion condensate, only with φ_4 and φ_5 taking the roles of φ_1 and φ_2 , and μ_{K^\pm} and m_{K^\pm} the roles of μ_I and \bar{m} . The phase with a K^0 -condensate, with the ground state $\Sigma = \exp \{i\lambda_7\alpha\}$ has a very similar structure. The static Lagrangian is

$$\mathcal{L}_2^{(0)} = \frac{1}{2}f^2 \left(\mu_{K^0}^2 \sin^2 \alpha + 2m_{K^0,0}^2 \cos \alpha + \bar{m}^2 - \Delta m^2 \right). \quad (5.108)$$

5.3.4 Electromagnetic effects

We now reintroduce e . First, we set $\mu_I = \mu_S = 0$, so we are in the vacuum phase, $\Sigma = U^2 = \exp \{i\varphi_a\lambda_a/f\}$, and the covariant derivative is

$$\nabla_\mu \Sigma = \partial_\mu \Sigma - ie\mathcal{A}_\mu[Q, \Sigma], \quad (5.109)$$

where Q is the charge matrix Eq. (5.51). Inserting this into the terms of the leading-order Lagrangian, Eq. (5.47), and expanding to and including $\mathcal{O}((\pi/f)^2)$ yields

$$\begin{aligned} \mathcal{L}_2 = & f^2 \left(\bar{m}^2 + \frac{1}{2} m_S^2 + \frac{2}{3} \frac{C e^2}{f^2} \right) + \frac{1}{2} \partial_\mu \varphi_a \partial^\mu \varphi_a - \frac{1}{2} (m_a^2 + \Delta m_{\text{EM},a}^2) \varphi_a^2 - \frac{\Delta m^2}{\sqrt{3}} \varphi_3 \varphi_8 \\ & + e \mathcal{A}^\mu (\varphi_1 \partial_\mu \varphi_2 - \varphi_2 \partial_\mu \varphi_1 + \varphi_4 \partial_\mu \varphi_5 - \varphi_5 \partial_\mu \varphi_4) + \frac{1}{2} e^2 \mathcal{A}^2 (\varphi_1^2 + \varphi_2^2 + \varphi_4^2 + \varphi_5^2). \end{aligned} \quad (5.110)$$

Here, m_a are the leading order masses without the electromagnetic contribution, as we found in Eqs. (5.67) to (5.72), for $\mu_I = \mu_S = \alpha = 0$, which is given in Eqs. (5.77) to (5.80). $\Delta m_{\text{EM},a}$ is the new electromagnetic contribution to the masses. This only affects the charged pions π^\pm , which are linear combinations φ_1 and φ_2 , and the charged kaons, K^\pm , which are linear combinations of φ_4 and φ_5 . The contributions to the mass squared from electromagnetic effects are the same to leading order for these particles,

$$\Delta m_{\text{EM},a}^2 = 2C \frac{e^2}{f^2} := \Delta m_{\text{EM}}^2, \quad a \in \{1, 2, 4, 5\}. \quad (5.111)$$

This is known as Dashen's theorem [75]. We can express C in terms of the pion decay constant and the mass and decay constant of the ρ -meson. This was first done in [76], using the then newly derived Weinberg sum rules relating the masses of heavier mesons [77]. This yields

$$C = \frac{3m_\rho^2 f_\rho^2}{32\pi^2} \ln \left(\frac{f_\rho^2}{f_\rho^2 - f_\pi^2} \right). \quad (5.112)$$

Urech, using the values $f_\pi = 93.3 \text{ MeV}$, $f_\rho = 154 \text{ MeV}$ and $m_\rho = 770 \text{ MeV}$, gets the numerical result $6.11 \times 10^{-5} (\text{GeV})^4$ [69]. With the value $f_\pi = 92.1 \text{ MeV}$ as used in the rest of this text, we obtain $C = 5.91 \times 10^{-5} (\text{GeV})^4$. As C is the sole source of difference in the masses of the neutral and charged pions to leading order, it can also be obtained directly from these masses. Using the values listed in section A.1, we find

$$C = \frac{f^2}{2e^2} (m_{\pi^\pm}^2 - m_\pi^2) = 5.824 \times 10^{-5} (\text{GeV})^4, \quad (5.113)$$

or in the characteristic units of the system, $C = 0.3771 u_0$. This corresponds to $\Delta m_{\text{EM}}^2 = (35.50 \text{ MeV})^2$. We see that the numerical differences between these results are small. When choosing the numerical values to use, we must take care to use a consistent set of values. Formulas such as Eq. (5.112) mean that the decay constants and masses are over-constrained. In this text, we use the masses and the decay constant listed in section A.1 and therefore choose the value in Eq. (5.113) for C .

These results allow us to derive a set of leading-order relations between the physical masses and discuss—in a loose sense—where the mass originates from. The contribution to the pion mass from electromagnetic interactions is

$$m_{\pi^\pm} - m_\pi = \sqrt{m_\pi^2 + \Delta m_{\text{EM}}^2} - m_\pi = 3.401 \times 10^{-2} m_\pi = 4.590 \text{ MeV}. \quad (5.114)$$

Even though the contribution to the *square* of the masses of the charged pion and kaons are the same, we see that the absolute difference between the neutral and charged pion depends on $\Delta m_{\text{EM}}/m_\pi$. We, therefore, expect the mass contribution from electromagnetic interactions to be lower for the heavier charged kaon. From the values in section A.1, however, we see that the mass difference between the charged and neutral pions masses is very close to that of the charged and neutral kaons. This is because the difference in mass of the kaons is not only due to the electric charge at leading order, unlike the pions, but also due to Δm ,

$$m_{K^0}^2 - m_{K^\pm}^2 = \Delta m^2 - \Delta m_{\text{EM}}^2. \quad (5.115)$$

We notice that the two contributions work in opposite directions. As we already have an independent way of determining Δm_{EM}^2 , we can disentangle these contributions. To leading order,

$$\Delta m^2 = m_{K^0}^2 - (m_{K^\pm}^2 - \Delta m_{\text{EM}}^2) = (0.5320 m_\pi)^2 = (71.80 \text{ MeV})^2. \quad (5.116)$$

This is consistent with the fact that the down quark is around twice as heavy as the light quark [78]. The electromagnetic contribution to the mass of the charged kaon is

$$m_{K^\pm} - \sqrt{m_{K^\pm}^2 - \Delta m_{\text{EM}}^2} = 9.443 \times 10^{-3} m_\pi = 1.278 \text{ MeV}. \quad (5.117)$$

The difference due to Δm , on the other hand, is

$$m_{K^0} - \sqrt{m_{K^\pm}^2 - \Delta m_{\text{EM}}^2} = 3.858 m_\pi = 5.208 \text{ MeV}. \quad (5.118)$$

We analyze how electromagnetic interactions affect the condensed phases. In the pion condensate, the covariant derivative is

$$\nabla_\mu \Sigma = \partial_\mu \Sigma - i[v_\mu, \Sigma], \quad v_\mu = \mu \delta_\mu^0 + e \mathcal{A}_\mu Q. \quad (5.119)$$

The ground state field parametrization is still $\Sigma = e^{i\alpha\lambda_2}$. Inserting this in the leading-order Lagrangian Eq. (5.47), and setting $\mathcal{A}_\mu = 0$ gives us the static Lagrangian including electromagnetic effects,

$$\mathcal{L}_{\text{EM},2}^{(0)} = \frac{1}{2} f^2 \left[(\mu_I^2 - \Delta m_{\text{EM}}^2) \sin^2 \alpha + 2\bar{m}^2 \cos \alpha + \frac{2}{3} \Delta m_{\text{EM}}^2 + m_S^2 \right]. \quad (5.120)$$

Similarly, the static Lagrangian in the charged kaon condensate is

$$\mathcal{L}_{\text{EM},2}^{(0)} = \frac{1}{2} f^2 \left[(\mu_{K^\pm}^2 - \Delta m_{\text{EM}}^2) \sin^2 \alpha + 2m_{K^\pm,0}^2 \cos \alpha + \frac{2}{3} \Delta m_{\text{EM}}^2 + \bar{m}^2 + \Delta m^2 \right]. \quad (5.121)$$

In the neutral kaon condensate, on the other hand, the static Lagrangian remains unchanged. In the pion condensate, the α -dependent masses we found in subsection 5.3.2 are also affected by the inclusion of electromagnetic effects. The diagonal mass terms are now

$$m_1^2 = \bar{m}^2 \cos \alpha - (\mu_I^2 - \Delta m_{\text{EM}}^2) \cos^2 \alpha, \quad (5.122)$$

$$m_2^2 = \bar{m}^2 \cos \alpha - (\mu_I^2 - \Delta m_{\text{EM}}^2) \cos 2\alpha, \quad (5.123)$$

$$m_3^2 = \bar{m}^2 \cos \alpha + (\mu_I^2 - \Delta m_{\text{EM}}^2) \sin^2 \alpha, \quad (5.124)$$

$$m_4^2 = m_5^2 = m_-^2 - m_{\mu+}^2 + \frac{1}{2} \cos \alpha (\cos \alpha + 1) \Delta m_{\text{EM}}^2, \quad (5.125)$$

$$m_6^2 = m_7^2 = m_+^2 - m_{\mu-}^2 + \frac{1}{2} \cos \alpha (\cos \alpha - 1) \Delta m_{\text{EM}}^2, \quad (5.126)$$

$$m_8^2 = \frac{1}{3} (\bar{m}^2 \cos \alpha + 2m_S^2), \quad (5.127)$$

where m_\pm and $m_{\mu\pm}$ are defined as in Eq. (5.73). This reduces to $m_a^2 + \Delta m_{\text{EM},a}^2$ in the case of $\mu_I = \mu_S = \alpha = 0$. The masses, as functions of the isospin chemical potential, are illustrated in Figure 5.3.

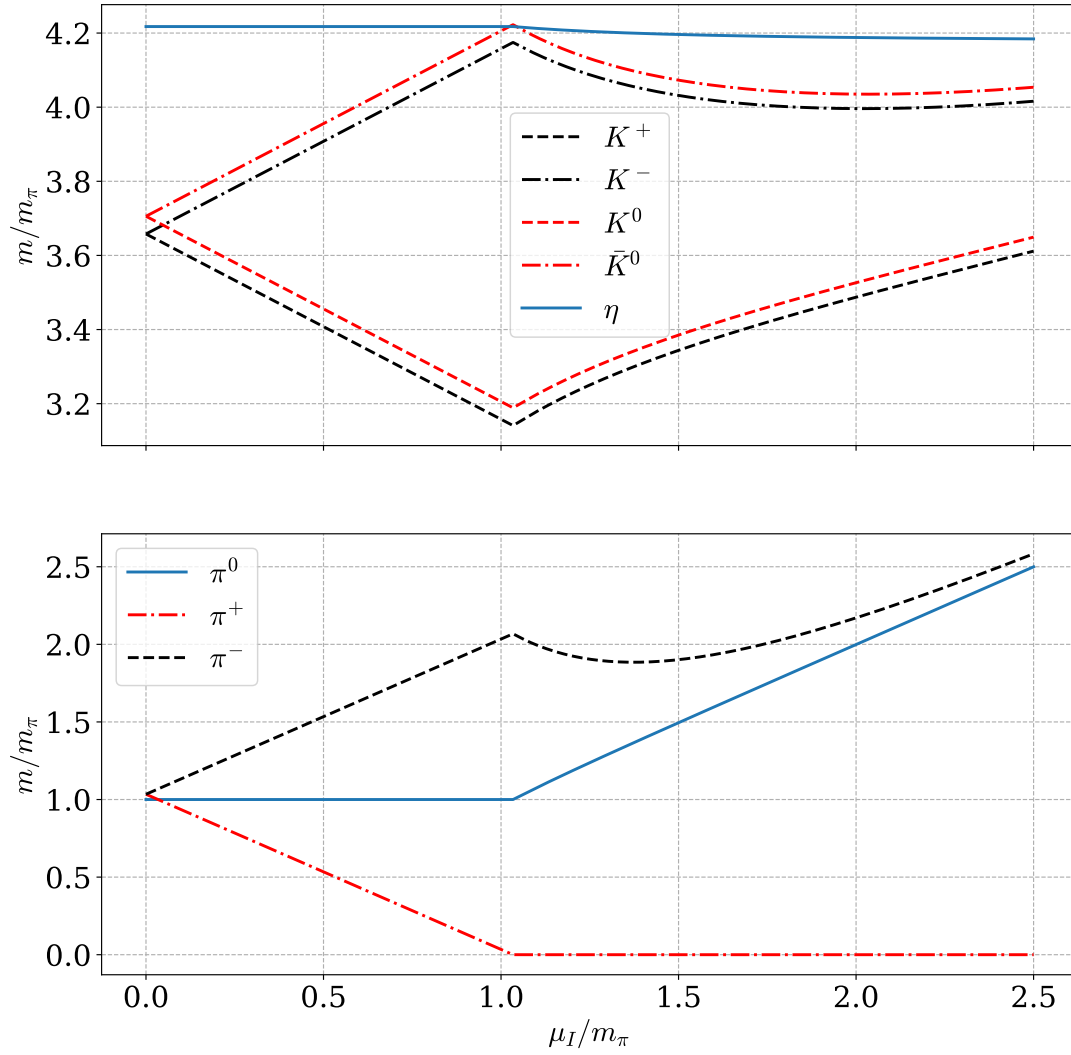


Figure 5.3: The leading order masses of the pseudoscalar mesons, as functions of the isospin chemical potential, including electromagnetic effects. Both the masses and chemical potential are normalized to the pion mass. These results are at $\mu_S = 0$. The difference between the kaons at $\mu_I = 0$ is a result of the fact that $\Delta m \neq 0$.

5.4 Next-to-leading order Lagrangian

To construct the next-to-leading order Lagrangian, one follows the same approach of combining the building blocks we used in section 5.2 into locally $SU(3)_R \times SU(3)_L$ -invariant terms. However, a naïve approach will lead to redundant terms in the Lagrangian which, on the face of it might seem independent, but are, in fact, equivalent to linear combinations of other terms. Such terms may be eliminated by reparametrization and the use of the equation of motion, as shown for two-flavors in section B.3. Furthermore, trace relations allow for different but equivalent forms of the Lagrangian. In section B.4, we show how two different choices of next-to-leading order, two-flavor Lagrangians are equivalent. Although the naïve identification of invariant terms is the same for $N_f = 2$ and $N_f = 3$, such trace relations mean that there are fewer independent terms in the two-flavor case [50].

We do not need to include terms with the field strength tensors $f_{\mu\nu}^{(r)}$ and $f_{\mu\nu}^{(l)}$, as in our case, they will vanish. Furthermore, we will not consider electromagnetic interactions to higher orders, and therefore will not consider terms including the fundamental charge e . With this, the NLO Lagrangian is [52]

$$\begin{aligned} \mathcal{L}_4 = & L_1 \text{Tr} \left\{ \nabla_\mu \Sigma \nabla^\mu \Sigma^\dagger \right\}^2 + L_2 \text{Tr} \left\{ \nabla_\mu \Sigma \nabla_\nu \Sigma^\dagger \right\} \text{Tr} \left\{ \nabla^\mu \Sigma \nabla^\nu \Sigma^\dagger \right\} \\ & + L_3 \text{Tr} \left\{ \left(\nabla_\mu \Sigma \nabla^\mu \Sigma^\dagger \right)^2 \right\} + L_4 \text{Tr} \left\{ \nabla_\mu \Sigma \nabla^\mu \Sigma^\dagger \right\} \text{Tr} \left\{ \chi \Sigma^\dagger + \Sigma \chi^\dagger \right\} \\ & + L_5 \text{Tr} \left\{ \nabla_\mu \Sigma \nabla^\mu \Sigma^\dagger \left(\chi \Sigma^\dagger + \Sigma \chi^\dagger \right) \right\} + L_6 \text{Tr} \left\{ \chi \Sigma^\dagger + \Sigma \chi^\dagger \right\}^2 \\ & + L_7 \text{Tr} \left\{ \chi \Sigma^\dagger - \Sigma \chi^\dagger \right\}^2 + L_8 \text{Tr} \left\{ \left(\chi^\dagger \Sigma \right)^2 + \left(\chi \Sigma^\dagger \right)^2 \right\} + H_2 \text{Tr} \left\{ \chi \chi^\dagger \right\}. \end{aligned} \quad (5.128)$$

Here, L_i and H_i are coupling constants. As discussed, these are needed to parametrize all possible effective Lagrangians. As long as we are unable to solve low-energy QCD, they must be measured experimentally. The L_i 's are called *low-energy constants*. The H_i 's only couple to external fields, but they are needed for renormalization [52].

The pion-condensed phase is still parametrized as described in subsection 5.3.2. We obtained the next-to-leading order static Lagrangian by substituting the vacuum-parametrization $\Sigma_\alpha^{\pi^\pm}$ into Eq. (5.128), which yields

$$\begin{aligned} \mathcal{L}_4 = & 2(2L_1 + 2L_2 + L_3) \mu_I^4 \sin^4 \alpha + 4L_4 (2\bar{m}^2 \cos \alpha + m_S^2) \mu_I^2 \sin^2 \alpha \\ & + 4L_5 \bar{m}^2 \mu_I^2 \cos \alpha \sin^2 \alpha + 4L_6 (2\bar{m}^2 \cos \alpha + m_S^2)^2 \\ & + 2L_8 (2\bar{m}^4 \cos 2\alpha + 2\Delta m^4 + m_S^4) + H_2 (2\bar{m}^4 + 2\Delta m^4 + m_S^4). \end{aligned} \quad (5.129)$$

These results, as well as some earlier calculations, were calculated using CAS software. This is discussed in section D.2, where a link to an online repository with the code used is available.

L_i and H_i are bare coupling constants, which are unobservable, but they are related to the renormalized coupling constants L_i^r and H_i^r . We will perform renormalization by using dimensional regularization, in which the divergent integrals are generalized to d -dimensions, and the $\overline{\text{MS}}$ -scheme. This is discussed in more detail in subsection C.3.3. In this case, the bare and renormalized constants are related by

$$L_i = L_i^r - \frac{1}{2} \frac{\mu^{-2\epsilon}}{(4\pi)^2} \left(\frac{1}{\epsilon} + 1 \right) \Gamma_i, \quad (5.130)$$

$$H_i = H_i^r - \frac{1}{2} \frac{\mu^{-2\epsilon}}{(4\pi)^2} \left(\frac{1}{\epsilon} + 1 \right) \Delta_i. \quad (5.131)$$

Here, $d = 3 - 2\epsilon$ and μ is a parameter of mass-dimension one, which is introduced so that the action integral remains dimensionless in dimensional regularization. The dimensionless constants

Table 5.1: The renormalized coupling constants of the next-to-leading order Lagrangian of three-flavor chiral perturbation theory, measured at the mass of the rho meson, $M = m_\rho$.

constant	value [$\times 10^{-3}$]	source
$L_1^r(M)$	1.0 ± 0.1	[79]
$L_2^r(M)$	-1.6 ± 0.2	[79]
$L_3^r(M)$	-3.8 ± 0.3	[79]
$L_4^r(M)$	0.0 ± 0.3	[79]
$L_5^r(M)$	1.2 ± 0.1	[79]
$L_6^r(M)$	0.0 ± 0.4	[79]
$L_8^r(M)$	0.5 ± 0.2	[79]
$H_2^r(M)$	-3.4 ± 1.5	[80]

Γ_i and Δ_i are found by insisting that the divergent $1/\epsilon$ -factors cancel, leaving a finite result. These have been calculated for $\mu_I = 0$ [52]. They are independent of μ_I , and we can therefore use them in this calculation. They are

$$\Gamma_1 = \frac{3}{32}, \Gamma_2 = \frac{3}{16}, \Gamma_3 = 0, \Gamma_4 = \frac{1}{8}, \Gamma_5 = \frac{3}{8}, \Gamma_6 = \frac{11}{144}, \Gamma_8 = \frac{5}{48}, \Delta_2 = \frac{5}{24}. \quad (5.132)$$

The bare coupling constants L_i and H_i are independent of our renormalization scale μ . From this we obtain the renormalization group equations for the running coupling constants,

$$\mu \frac{dL_i^r}{d\mu} = -\frac{\mu^{-2\epsilon}}{(4\pi)^2} \Gamma_i + \mathcal{O}(\epsilon), \quad \mu \frac{dH_i^r}{d\mu} = -\frac{\mu^{-2\epsilon}}{(4\pi)^2} \Delta_i + \mathcal{O}(\epsilon). \quad (5.133)$$

Inserting the solutions back into the bare coupling constants, Eq. (5.130) yields, to $\mathcal{O}(\epsilon)$,

$$L_i = L_i^r(M) - \frac{1}{2} \frac{\mu^{-2\epsilon}}{(4\pi)^2} \left(\frac{1}{\epsilon} + 1 + \ln \frac{\tilde{\mu}^2}{M^2} \right) \Gamma_i, \quad (5.134)$$

$$H_i = H_i^r(M) - \frac{1}{2} \frac{\mu^{-2\epsilon}}{(4\pi)^2} \left(\frac{1}{\epsilon} + 1 + \ln \frac{\tilde{\mu}^2}{M^2} \right) \Delta_i. \quad (5.135)$$

We have introduced the dimensional constant $\tilde{\mu}$, related to μ by $\tilde{\mu}^2 = 4\pi e^{-\gamma_E} \mu^2$ where γ_E is the Euler-Mascheroni constant, to match up with the contribution from loop integrals. This is the “modified” of “modified minimal subtraction”, $\overline{\text{MS}}$, as discussed in subsection C.3.3. $L_i^r(M)$ and $H_i^r(M)$ are the constants of integration of the renormalization group equations. These must be measured at some energy M . This only applies if the numerical constants Γ_i/Δ_i are non-zero. If they are zero, then the coupling is not running, and the measured value can be applied at all energies. The values used in this text are given in Table 5.1, at the ρ -meson mass, $m_\rho = 770 \text{ MeV}$.

After inserting the renormalized coupling constants into the Lagrangian Eq. (5.129), we get

$$\begin{aligned} \mathcal{L}_4 = & 2(2L_1^r + 2L_2^r + L_3^r) \mu_I^4 \sin^4 \alpha + 4L_4^r (2\bar{m}^2 \cos \alpha + m_S^2) \mu_I^2 \sin^2 \alpha \\ & + 4L_5^r (\bar{m}^2 \cos \alpha) (\mu_I^2 \sin^2 \alpha) + 4L_6^r (2\bar{m}^2 \cos \alpha + m_S^2)^2 \\ & + 2L_8^r (2\bar{m}^4 \cos 2\alpha + 2\Delta m^4 + m_S^4) + H_2^r (2\bar{m}^4 + 2\Delta m^4 + m_S^4) \\ & - \frac{1}{2} \frac{\mu^{-2\epsilon}}{(4\pi)^2} \left(\frac{1}{\epsilon} + 1 + \ln \frac{\tilde{\mu}^2}{M^2} \right) \\ & \times \left[\frac{37}{15} (\bar{m}^2 \cos \alpha)^2 + \frac{5}{2} (\bar{m}^2 \cos \alpha) (\mu_I^2 \sin^2 \alpha) + \frac{9}{8} (\mu_I^2 \sin^2 \alpha)^2 \right. \\ & \left. + \frac{11}{9} (\bar{m}^2 \cos \alpha) m_S^2 + \frac{1}{2} (\mu_I^2 \sin^2 \alpha) m_S^2 + \frac{5}{6} \Delta m^4 + \frac{13}{18} m_S^4 \right]. \end{aligned} \quad (5.136)$$

With this Lagrangian, we can perform loop calculations and obtain next-to-leading order results from χ PT. We will now use the results from this chapter to calculate the thermodynamic properties of the pion-condensed phase in the next chapter.

Chapter 6

Thermodynamics

In Chapter 5, we built up machinery to do calculations in chiral perturbation theory in the case of a non-zero isospin chemical potential μ_I . Our ultimate goal is to model pion stars, in which condensed pions form a gravitationally bound astrophysical object. As we saw in section 4.3, we need the equation of state, $u = u(p)$, for this. In this chapter, we will use the results from χ PT to calculate the thermodynamic properties of our system, such as the phase diagram, pressure, and energy density. We will study how the inclusion of electromagnetic interactions, charged leptons and neutrinos, and higher-order calculations affect these properties.

6.1 Free energy in a homogenous system

The key to the thermodynamic behavior of our system is its free energy, F . We use the grand canonical ensemble, so this is the grand canonical free energy, also called the grand canonical potential. In our case, we are working with a homogenous system, in which we may write the free energy as $F = V\mathcal{F}$, where \mathcal{F} is the free energy density. It is related to the partition function of statistical mechanics, \mathcal{Z} , by

$$\mathcal{F} = -\frac{1}{V\beta} \ln \mathcal{Z}. \quad (6.1)$$

Here, V is the volume and $\beta = 1/T$ is the inverse temperature. In Appendix C, we show using the imaginary-time formalism for thermal field theory that the partition function is given by the path integral of the *Euclidean* Lagrange density, as shown in equation Eq. (C.20). In the zero temperature limit $\beta \rightarrow \infty$, the partition function is related to the generating functional $Z = Z[j]$, as described in section 3.1, by a Wick rotation. The free energy density at zero temperature is therefore

$$\mathcal{F} = \frac{i}{VT} \ln Z, \quad (6.2)$$

where VT is the volume of space-time. As we found in Eq. (3.16), this equals the effective potential in the ground state. In section 3.2, we found an explicit formula for this to one-loop order, Eq. (3.38). This loop expansion must, as we will discuss later, be used in conjunction with the Weinberg power counting scheme. In section A.4, we show how to expand free energy density and other thermodynamic quantities in a self-consistent way.

We are after the equation of state, to which the free energy density will give us access. Thermodynamically, grand canonical free energy is defined as a Legendre transformation of the internal energy U ,

$$F(T, V, \mu_i) = U - TS - \sum_i \mu_i Q_i, \quad dF = -SdT - pdV - \sum_i Q_i d\mu_i. \quad (6.3)$$

Here S is the entropy, Q_i are conserved charges, in our case the isospin and strangeness charge, and μ_i their corresponding chemical potentials. In this thesis, we will assume $T = 0$. From Eq. (6.3), the pressure is given by

$$p = - \left(\frac{\partial F}{\partial V} \right)_{T, \mu} = -\mathcal{F}. \quad (6.4)$$

The total charges are proportional to volume, which means that the corresponding densities are

$$n_i = \frac{Q_i}{V} = -\frac{1}{V} \left(\frac{\partial F}{\partial \mu_i} \right)_{T, V, \mu \neq \mu_i} = -\frac{\partial \mathcal{F}}{\partial \mu_i}, \quad i = I, S. \quad (6.5)$$

From Eq. (6.3) we get the energy density, $u = U/V$, at $T = 0$, is given by

$$u(\mu_I) = -p(\mu_i) + \sum_i \mu_i n_i(\mu_i), \quad (6.6)$$

The equation of state, $u = u(p)$, is now implicitly defined through the parametrization by the chemical potential.

6.2 Leading order analysis

We begin by computing the thermodynamic properties to leading order. This will give an accurate first approximation, which we can verify by next-to-leading order results later. As we start to calculate terms to next-to-leading order, we must be careful distinguishing between bare constants, such as $m_{\pi,0} = \bar{m}$ and f , and the physical (or empirical) constants, such as m_π and f_π . The value of bare constants defined at a given order, such as $m_{\pi,0} = m_\pi$ at leading order, but are modified at higher orders. We will always use bare constants in expressions of, for example, the Lagrangian or the energy density, but use physical constants to define units, such as $u_0 = f_\pi^2 m_\pi^2$, or when stating relationships that hold to all orders

6.2.1 Pure pion condensate

The leading order contribution to free energy is given by the static Lagrangian, to first order in Weinberg's power counting scheme. We start by assuming $e = 0$, i.e., no electromagnetic interactions, which means the relevant static Lagrangian is given by Eq. (5.64), and the free energy density is therefore

$$\mathcal{F} = -\frac{1}{2} f^2 (\mu_I^2 \sin^2 \alpha + 2m_{\pi,0}^2 \cos \alpha + m_S^2). \quad (6.7)$$

The parameter α is determined by minimizing \mathcal{F} for a given value of μ_I ,

$$\frac{\partial \mathcal{F}}{\partial \alpha} = f^2 (m_{\pi,0}^2 - \mu_I^2 \cos \alpha) \sin \alpha = 0. \quad (6.8)$$

This gives an explicit formula for α in terms of μ_I . As long as the chemical potential is lower than the critical value $\mu_I^c = m_{\pi,0}$, the only solution to this equation is $\alpha = 0$. As the chemical potential reaches this critical value, the system undergoes a phase transition from the vacuum phase to the *pion-condensed* phase. In this new phase, the solution is

$$\cos \alpha = \frac{m_{\pi,0}^2}{\mu_I^2}. \quad (6.9)$$

Substituting this back into the free energy, we get

$$\mathcal{F} = -\frac{u_0}{2} \left(\frac{m_{\pi,0}^2}{\mu_I^2} + \frac{\mu_I^2}{m_{\pi,0}^2} \right) + \text{const.} \quad (6.10)$$

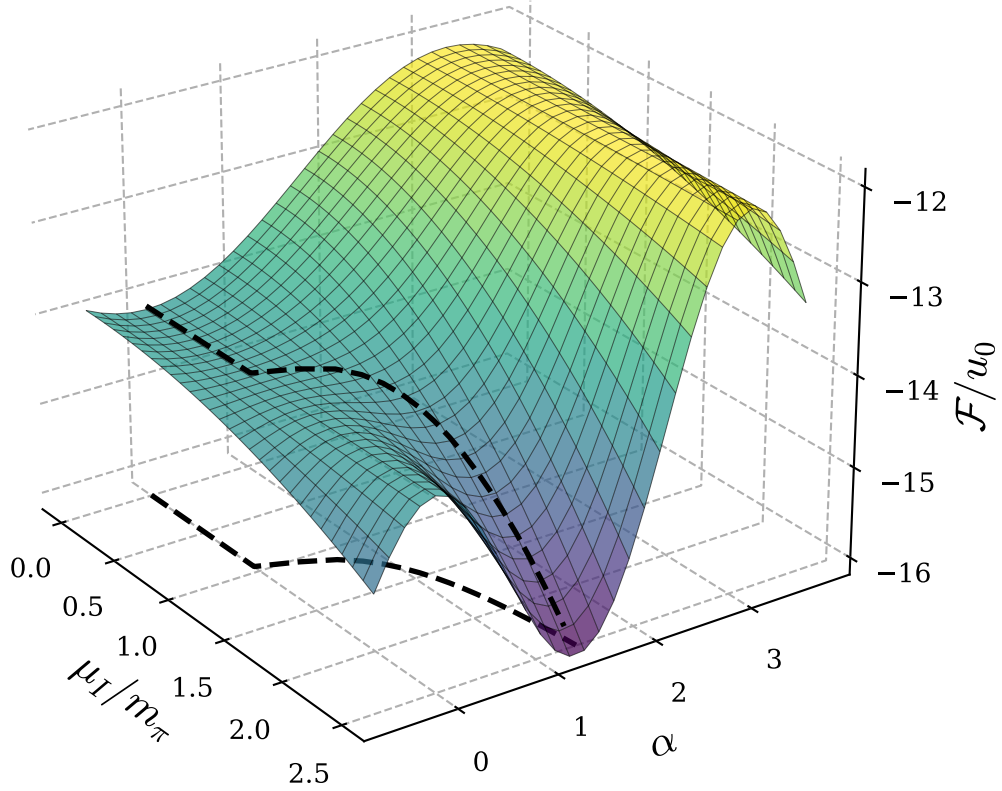


Figure 6.1: The surface is the free energy as a function of α and μ_I . The black dashed line illustrates the value of α which minimizes the free energy for a given value of μ_I .

We have introduced the characteristic energy density $u_0 = m_\pi^2 f_\pi^2$. This process of minimizing free energy for a given μ_I is illustrated in Figure 6.1.

As we found in the last section, the pressure is given by negative the free energy density. We normalized the pressure to $\mu_I = m_\pi$, and choose $p_0 = u_0$, so the pressure is

$$p = -(\mathcal{F} - \mathcal{F}_{\mu_I=m_{\pi,0}}) = u_0 \frac{1}{2} \frac{\mu_I^2}{m_{\pi,0}^2} \left(1 - \frac{m_{\pi,0}^2}{\mu_I^2} \right)^2. \quad (6.11)$$

The charge density corresponding to a chemical potential is given by minus the derivative of the free energy with respect to that chemical potential. We must, however, not assume any dependence of α on μ_I when taking this derivative. The isospin density is

$$n_I = -\frac{\partial \mathcal{F}}{\partial \mu_I} = f^2 \mu_I \sin^2 \alpha = n_0 \frac{\mu_I}{m_{\pi,0}} \left(1 - \frac{m_{\pi,0}^4}{\mu_I^4} \right). \quad (6.12)$$

where $n_0 = u_0/m_\pi = m_\pi f_\pi^2$, while the strangeness is zero. With this, the energy density at $T = 0$ is

$$u = -p + \mu_I n_I = u_0 \frac{1}{2} \frac{\mu_I^2}{m_{\pi,0}^2} \left(1 - \frac{m_{\pi,0}^2}{\mu_I^2} \right) \left(1 + 3 \frac{m_{\pi,0}^2}{\mu_I^2} \right). \quad (6.13)$$

The ratio of pressure to energy density is

$$\frac{p}{u} = \frac{\mu_I^2 - m_{\pi,0}^2}{\mu_I^2 + 3m_{\pi,0}^2}, \quad (6.14)$$

which matches earlier results [25]. In the ultrarelativistic limit, where $\mu_I \rightarrow \infty$, we get $p/u = 1$, or $u_{\text{UR}} = p$. The non-relativistic limit is $\mu_I^2 = m_{\pi,0}^2(1 + \epsilon)$, $\epsilon \ll 1$. With this we get $\tilde{p} = \epsilon^2/2$, and $\tilde{u} = 2\epsilon$, so the equation of state is $\tilde{u}_{\text{NR}} = \sqrt{8\sqrt{\tilde{p}}}$. The isospin density, and thus the pion number density, is $n_I = 2(u_0/m_{\pi,0})\epsilon$, and we can therefore write the energy density in this limit as $u = m_{\pi,0}n_I + \mathcal{O}(\epsilon^2)$. The energy density is thus dominated by the rest mass as $\epsilon \rightarrow 0$, as we expect from the non-relativistic limit. Figure 6.2 shows the equation of state in two different regimes and compares it with the ultrarelativistic and non-relativistic limits.

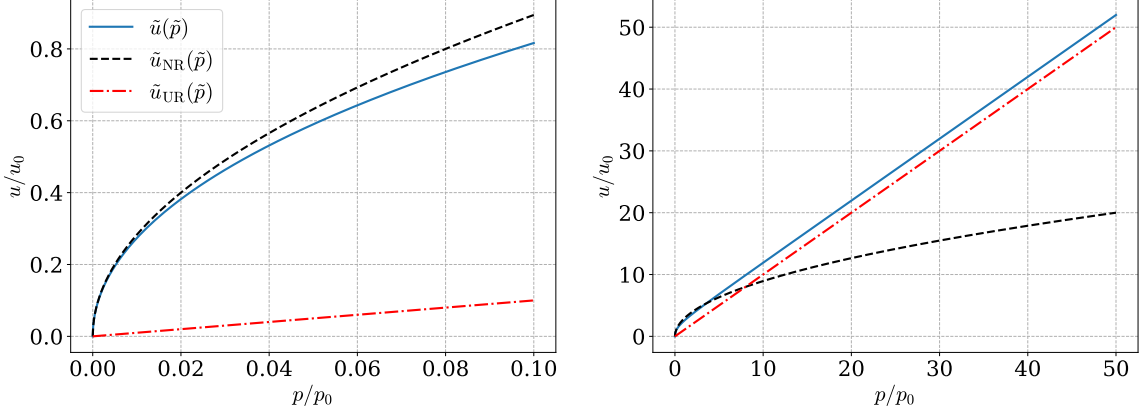


Figure 6.2: The leading order equation of state from two-flavor chiral perturbation theory, in two different regimes. The full equation is shown as a solid line and is compared to the ultrarelativistic and non-relativistic limits shown as dashed lines. The y -axis shows the energy density normalized to u_0 , x -axis shows the pressure normalized to p_0 . We have chosen $p_0 = u_0$.

6.2.2 Including electromagnetism

From Eq. (5.120), the free energy density, including electromagnetic interactions, is

$$\mathcal{F} = -\frac{1}{2}f^2 \left[(\mu_I^2 - \Delta m_{\text{EM}}^2) \sin^2 \alpha + 2m_{\pi,0}^2 \cos \alpha + \frac{2}{3}\Delta m_{\text{EM}}^2 + m_S^2 \right]. \quad (6.15)$$

Free energy minimization now gives

$$\frac{1}{u_0} \frac{\partial \mathcal{F}}{\partial \alpha} = \left[\left(\frac{\mu_I^2}{m_{\pi,0}^2} - \Delta \right) \cos \alpha - 1 \right] \sin \alpha = 0. \quad (6.16)$$

Here, x is defined as before, and we introduced the new quantity $\Delta = \Delta m_{\text{EM}}^2/m_{\pi}^2 = 0.06916$. We see that the phase transition is raised, the critical chemical potential is now $\mu_I^c = m_{\pi,0}\sqrt{1 + \Delta}$, the mass of the charged pions. Below this value, $\alpha = 0$ remains the only solution. In the pion condensate phase, the solution is

$$\cos \alpha = \frac{1}{\frac{\mu_I^2}{m_{\pi,0}^2} - \Delta}. \quad (6.17)$$

This reduces to our old solution for $\Delta = 0$, as it should. With the same procedure as in the last section, we get

$$\tilde{p}_{\text{EM}} = \frac{1}{2} \frac{\mu_I^2 - \Delta m_{\text{EM}}^2}{m_{\pi,0}^2} \left(1 - \frac{m_{\pi,0}^2}{\mu_I^2 - \Delta m_{\text{EM}}^2} \right)^2, \quad (6.18)$$

$$\tilde{n}_{I,\text{EM}} = \frac{\mu_I}{m_{\pi,0}} \left[1 - \frac{m_{\pi,0}^4}{(\mu_I^2 - \Delta m_{\text{EM}}^2)^2} \right], \quad (6.19)$$

$$\tilde{u}_{\text{EM}} = \frac{1}{2} \left[\frac{\mu_I^2 + \Delta m_{\text{EM}}^2}{m_{\pi,0}^2} + 2 - m_{\pi,0}^2 \frac{3\mu_I^2 - \Delta m_{\text{EM}}^2}{(\mu_I^2 - \Delta m_{\text{EM}}^2)^2} \right]. \quad (6.20)$$

The ratio between pressure and energy is now

$$\frac{p_{\text{EM}}}{u_{\text{EM}}} = \frac{\mu_I^4 - (2\Delta + 1)\mu_I^2 m_{\pi,0}^2 + \Delta(\Delta + 1)m_{\pi,0}^4}{\mu_I^4 + 3\mu_I^2 m_{\pi,0}^2 - \Delta(\Delta + 1)m_{\pi,0}^4}. \quad (6.21)$$

In the limit $\Delta = 0$, these results reduce to those we found in the last section. In the ultra-relativistic limit, the behavior is the same as before, and we again approach $p = u$. As the mass of the charged pions have changed, the non-relativistic limit is now obtained by substituting $\mu_I^2/m_{\pi,0}^2 = 1 + \Delta + \epsilon$, for $\epsilon \ll 1$. To first order in ϵ we get $\tilde{p} = \epsilon/2$, which is the same as before. However, the energy density limit is perturbed by the inclusion of electromagnetism and is now $\tilde{u} = 2(1 + \Delta)\epsilon$. The non-relativistic equation of state is thus still a polytrope of the form $\tilde{p} = K\tilde{u}^2$, however the constant is now $K^{-1} = 8(1 + \Delta)^2$.

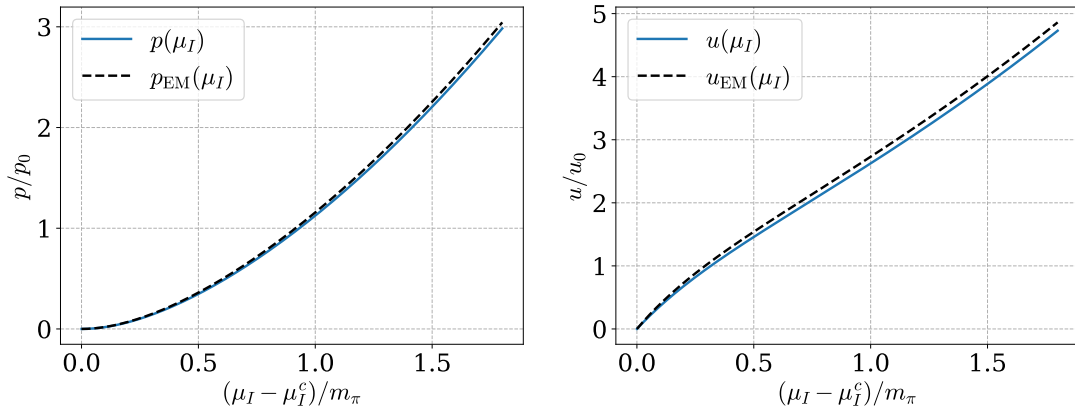


Figure 6.3: Left: The pressure as a function of the chemical potential above the critical value. Right: The energy density also as a function of the chemical potential. Results with electromagnetic interaction are shown as dashed lines, u, p and μ_I are normalized to u_0 , p_0 and m_π , respectively.

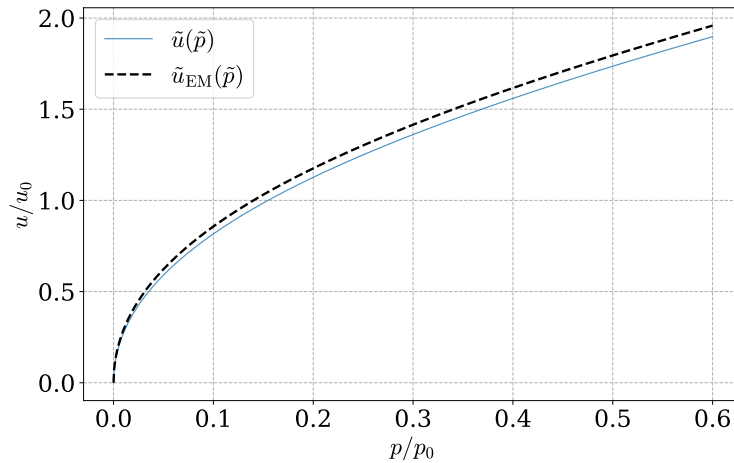


Figure 6.4: The equation of state in the pion condensate phase. Results with electromagnetic interactions are shown as dashed lines. The energy density and pressure is normalized to u_0 and $p_0 = u_0$.

6.3 Phase transitions

To study the phase transition from the vacuum phase, at $\mu_I < m_\pi$, to the condensed phase, we apply Landau theory [40]. In this theory, we make the general assumption that close to the point of a phase transition at $x = x_c$ for some thermodynamic variable x , the free energy may be Taylor-expanded in an order parameter, α . The order parameter is a quantity that changes from a zero to a non-zero expectation value over the phase transition. Furthermore, we assume the system is invariant under the transformation $\alpha = -\alpha$. We may then write

$$\mathcal{F} = \text{const.} + a(x)\alpha^2 + \frac{1}{2}b(x)\alpha^4 + \mathcal{O}(\alpha^6). \quad (6.22)$$

The order parameter is then given by minimizing the free energy, and must therefore solve

$$\frac{\partial \mathcal{F}}{\partial \alpha} = 2[a(x) + b(x)\alpha^2]\alpha^2 = 0. \quad (6.23)$$

We assume b does not vanish close to the phase transition. Assuming $b > 0$, the value of α depends on the sign of a . If $a > 0$, the only solution is $\alpha = 0$, while for $a < 0$ a new solution becomes available. The criterion of phase transition is therefore $a(x) = 0$, and we may write $a(x) = -a_0(x - x_c) + \mathcal{O}((x - x_c)^2)$ where $a_0 > 0$ and $b(\mu) = b_0 + \mathcal{O}(x - x_c)$ where $b_0 > 0$ close to $x = x_c$. The new solution in the $\alpha \neq 0$ phase is

$$\alpha(x) = \sqrt{\frac{a_0}{b_0}}(x - x_c)^{1/2}. \quad (6.24)$$

As the order parameter changes continuously, this is a *second-order* phase transition. The power-law behavior, $\alpha \propto (x - x_c)^\beta$ is ubiquitous near such phase transitions. The exponent β , in our case $\beta = \frac{1}{2}$, is known as a *critical exponent*. If $b_0 < 0$, we must expand the free energy further and might get a first-order phase transition in which the order parameter changes discontinuously.

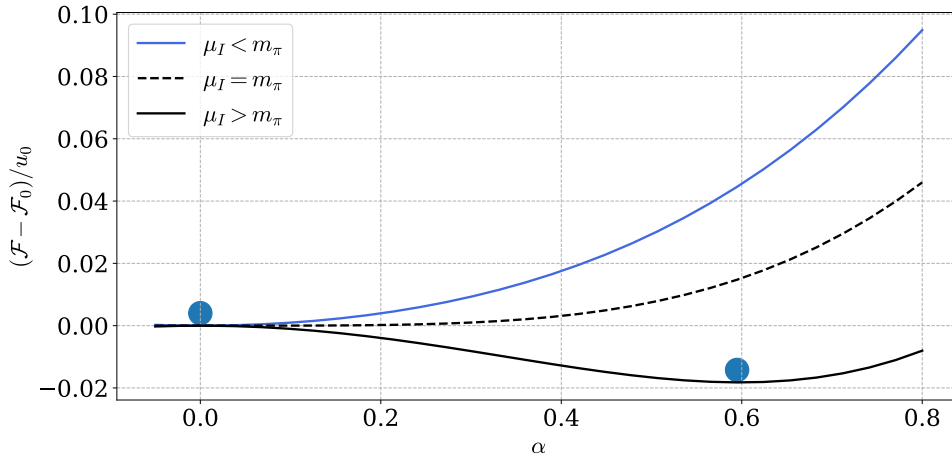


Figure 6.5: The normalized free energy, as a function of α , close to the point of phase transition. As the system undergoes a phase transition, the ground state is shifted away from $\alpha = 0$. Each line is a $\mu_I = \text{const.}$ slice of the surface in Figure 6.1.

We now apply this theory to the pion condensate by Taylor expanding the free energy for a pure pion-condensate, Eq. (6.7), around the point $\alpha = 0$,

$$\mathcal{F} = \mathcal{F}(\mu_I = 0) - \frac{1}{2}f^2(\mu_I^2 - m_{\pi,0}^2)\alpha^2 + \frac{1}{24}f^2(4\mu_I^2 - m_{\pi,0}^2)\alpha^4 + \mathcal{O}(\alpha^6). \quad (6.25)$$

This fulfills the assumptions made earlier, with $x = \mu_I^2$, $a_0 = f^2/2$, $b_0 = f^2 m_{\pi,0}^2/8$, and $x^c = m_{\pi,0}^2$. The phase transition from the vacuum phase, where $\alpha = 0$, into the pion-condensed

phase, where $\alpha \neq 1$, thus a second-order phase transition, and it happens at $\mu_I = m_\pi$, to leading order. The change in the shape of the free energy is illustrated in Figure 6.5.

As discussed in subsection 5.1.3, the full Lagrangian has an approximate $SU(3)_V \times SU(3)_A$ -symmetry. The axial part is broken by the quark condensate, which results in the pseudo-Goldstone bosons φ_a , but the $SU(3)_V$ -symmetry remains. The mass term $\bar{q}mq$, where

$$m = \frac{1}{3}(m_u + m_d + m_s)\mathbb{1} + \frac{1}{2}(m_u - m_d)\lambda_3 + \frac{1}{2\sqrt{3}}(m_u + m_d - 2m_s)\lambda_8, \quad (6.26)$$

explicitly breaks this symmetry. However, as $[\lambda_3, \lambda_8] = 0$, the transformations generated by λ_3 and λ_8 , or linear combinations such as λ_K and λ_Q , are *exact*. We focus on the subgroup generated by λ_3 , $U(1)_{I_3}$. In the vacuum phase, the ground-state is given by $\Sigma_0 = \mathbb{1}$. From Eq. (5.27), we see that $\Sigma \rightarrow V\Sigma V^\dagger$ under $SU(3)_V$. Σ_0 is thus invariant under this transformation, and the symmetry remains intact. In the pion-condensed phase, however, the ground state is $\Sigma_\alpha = \exp\{-i\alpha\lambda_2\}$. This is *not* invariant under λ_3 , the $U(1)_{I_3}$ has been spontaneously broken. The resulting Goldstone boson is the π^+ , which as we see from Figure 5.1, becomes massless at the point of phase transition.

A similar treatment will show that λ_Q and λ_K are broken in the charged and neutral kaons-condensed phases and that the K^+ and K^0 , respectively, are the resulting Goldstone bosons. We defined the order parameter as $\alpha = \sqrt{\pi_a \pi_a}/f$. This thus indicates a condensation of pseudoscalar mesons, although which depend on the ground state. This analysis, however, only says if we are in the vacuum phase or a condensed phase. To find which condensate we are in, we must compare the free energy between condensed phases.

6.3.1 Transition between condensates

As the static Lagrangian has the same form in the kaon condensed phase as in the pion condensed phase, the analysis of the phase transition and α as a function of μ_{K^\pm} will be the same as in the pion condensate. The system will be in the phase whose static Lagrangian minimizes the free energy, or equivalently, maximizes the pressure. Therefore, we can find the transition line between the condensates by setting the pressure of the two condensates equal. Using Eq. (6.11), and the similar expression for the charged kaon-condensed phase, we get

$$p = \frac{1}{2}f^2 m_{K^\pm,0}^2 \left(\frac{\mu_{K^\pm}}{m_{K^\pm,0}} - \frac{m_{K^\pm,0}}{\mu_{K^\pm}} \right)^2 = \frac{1}{2}f^2 m_{\pi,0}^2 \left(\frac{\mu_I}{m_{\pi,0}} - \frac{m_{\pi,0}}{\mu_I} \right)^2. \quad (6.27)$$

Solving for μ_{K^\pm} , we get

$$\mu_{K^\pm} = \frac{1}{2\mu_I} \left(\mu_I^2 - m_{\pi,0}^2 + \sqrt{(\mu_I^2 - m_{\pi,0}^2)^2 + 4\mu_I^2 m_{K^\pm,0}^2} \right). \quad (6.28)$$

The transitions into the condensates are at $\mu_I = m_{\pi,0}$, and $\mu_{K^\pm} = m_{K^\pm,0}$. This point, $(\mu_I, \mu_S) = (m_{\pi,0}, m_{K^\pm,0} - m_{\pi,0}/2)$, satisfies Eq. (6.28), and is thus a triple point between the vacuum phase, π^\pm condensate and the K^\pm condensate. Similarly, the line between the charged and neutral kaon condensed phase is defined by

$$\frac{1}{2}f^2 m_{K^\pm,0}^2 \left(\frac{\mu_{K^\pm}}{m_{K^\pm,0}} - \frac{m_{K^\pm,0}}{\mu_{K^\pm}} \right)^2 = \frac{1}{2}f^2 m_{K^0,0}^2 \left(\frac{\mu_{K^0}}{m_{K^0,0}} - \frac{m_{K^0,0}}{\mu_{K^0}} \right)^2. \quad (6.29)$$

The solution is

$$\begin{aligned} \mu_{K^\pm} &= \frac{1}{2\mu_{K^0}} \left(\mu_{K^0}^2 - m_{K^0,0}^2 + \sqrt{(\mu_{K^0}^2 - m_{K^0,0}^2)^2 + 4\mu_{K^0}^2 m_{K^\pm,0}^2} \right) \\ &= \mu_{K^0} \left(1 - \frac{\Delta m^2}{\mu_{K^0}^2 + m_{K^0,0}^2} \right) + \mathcal{O} \left(\frac{\Delta m^4}{(\mu_{K^0}^2 + m_{K^0,0}^2)^2} \right). \end{aligned} \quad (6.30)$$

We here expanded in the mass difference of the kaons, $m_{K^0,0}^2 - m_{K^\pm,0}^2 = \Delta m^2$. The expansion in Δm is an excellent approximation, as $\Delta m^4/4m_{K^0,0}^4 \approx 4 \times 10^{-4}$. The triple point is in this case at $\mu_{K^\pm} = m_{K^\pm,0}$, $\mu_{K^0} = m_{K^0,0}$ or $(\mu_I, \mu_S) = (m_{K^\pm,0} - m_{K^0,0}, [m_{K^\pm,0} + m_{K^0,0}]/2)$. If we consider $\Delta m = 0$, then this reduces to $\mu_{K^\pm} = \mu_{K^0}$, or $\mu_S = 0$, as obtained in [72]. A similar analysis gives the transition line between all phases. Figure 6.6 shows the phase diagram in the $\mu_I - \mu_S$ -plane.

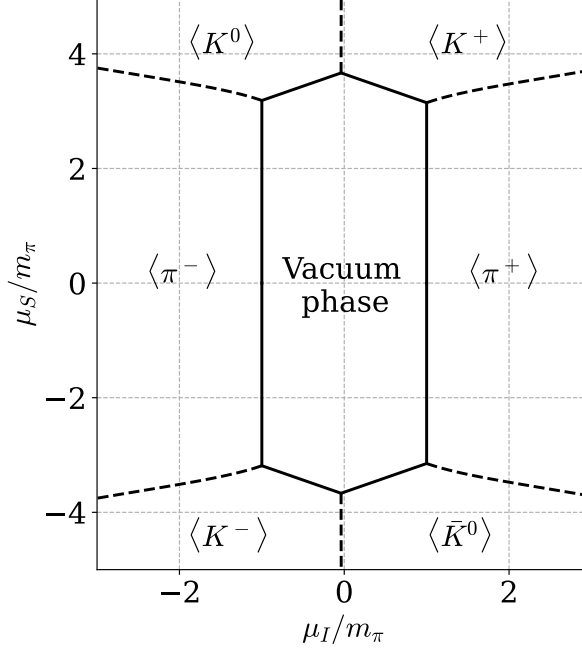


Figure 6.6: Phase diagram of χ PT in the $\mu_I - \mu_S$ -plane. Chemical potentials are given in units of the pion mass. The expectation values indicate which particles form condensates. The dashed lines are first-order transitions and the solid lines are second-order transitions.

In the pion phase, the isospin and strangeness densities are

$$n_I = -\frac{\partial \mathcal{F}}{\partial \mu_I} = f^2 \mu_I \left(1 - \frac{m_{\pi,0}^4}{\mu_I^4} \right), \quad n_S = -\frac{\partial \mathcal{F}}{\partial \mu_S} = 0. \quad (6.31)$$

In the charged kaon condensed phase, they are

$$n_I = -\frac{\partial \mathcal{F}}{\partial \mu_I} = \frac{1}{2} \frac{\partial \mathcal{F}}{\partial \mu_{K^\pm}} = \frac{1}{2} f_\pi^2 \mu_{K^\pm} \left(1 - \frac{m_{K^\pm,0}^4}{\mu_{K^\pm}^4} \right), \quad (6.32)$$

$$n_S = -\frac{\partial \mathcal{F}}{\partial \mu_S} = f^2 \mu_{K^\pm} \left(1 - \frac{m_{K^\pm,0}^4}{\mu_{K^\pm}^4} \right). \quad (6.33)$$

At the line of phase transition, $\mu_{K^\pm} > m_{K^\pm,0}$. The strangeness density thus jumps discontinuously to a non-zero value. This phase transition is, therefore, of first order. In the neutral kaon condensed phase, the isospin density is

$$n_I = -\frac{\partial \mathcal{F}}{\partial \mu_I} = -\frac{1}{2} \frac{\partial \mathcal{F}}{\partial \mu_{K^\pm}} = -\frac{1}{2} f_\pi^2 \mu_{K^\pm} \left(1 - \frac{m_{K^\pm,0}^4}{\mu_{K^\pm}^4} \right). \quad (6.34)$$

This, too, will change discontinuously between the two kaon condensed phases. Similar arguments hold between all condensates. This indicates that the transitions between condensates are of *first order*.

6.3.2 Electromagnetic contribution

We can describe the effect of electromagnetic interactions on the pressure, as obtained subsection 6.2.2, by modifying the isospin chemical potential by $\mu_I^2 \rightarrow \mu_I^2 - \Delta m_{\text{EM}}^2$. From the structure of the Lagrangian Eq. (5.121), the same will happen in the case of the charged kaon, only the change will be $\mu_{K^\pm}^2 \rightarrow \mu_{K^\pm}^2 - \Delta m_{\text{EM}}^2$, while from Eq. (5.108) we see that the results will be unchanged by electromagnetic interactions. We define the effective chemical potential by $\mu'^2 = \mu^2 - \Delta m_{\text{EM}}^2$. The transitions between the vacuum phase and the condensed phase will now be $\mu'_I = m_{\pi,0}$ and $\mu'_{K^\pm} = m_{K^\pm,0}$, while the line between these condensed phases is now

$$m_{K^\pm,0}^2 \left(\frac{\mu'_{K^\pm}}{m_{K^\pm,0}} - \frac{m_{K^\pm,0}}{\mu'_{K^\pm}} \right)^2 = m_{\pi,0}^2 \left(\frac{\mu'_I}{m_{\pi,0}} - \frac{m_{\pi,0}}{\mu'_I} \right)^2, \quad (6.35)$$

The neutral kaon condensate, on the other hand, remains unchanged by the inclusion of electromagnetic interactions. The line between the kaon condensates is thus given by

$$m_{K^\pm,0}^2 \left(\frac{\mu'_{K^\pm}}{m_{K^\pm,0}} - \frac{m_{K^\pm,0}}{\mu'_{K^\pm}} \right)^2 = m_{K^0,0}^2 \left(\frac{\mu_{K^0}}{m_{K^0,0}} - \frac{m_{K^0,0}}{\mu_{K^0}} \right)^2. \quad (6.36)$$

The new phase diagram is shown in Figure 6.7 in red, where it is compared with the results without electromagnetic interactions in black. The change is very small. However, it affects the pion condensation more than the charged kaon. This is because, as we discussed earlier, the *square* of the mass is the same by Dashen's theorem, Δm_{EM}^2 , while the absolute shift will depend on the ratio between Δm_{EM} and the non-electromagnetic mass. This is thus lower for the heavier kaon. The line between the kaon condensates is moved slightly closer to $\mu_I = 0$, as the electromagnetic contribution to the lighter charged kaon mass reduces the difference between its and the neutral kaon's mass.

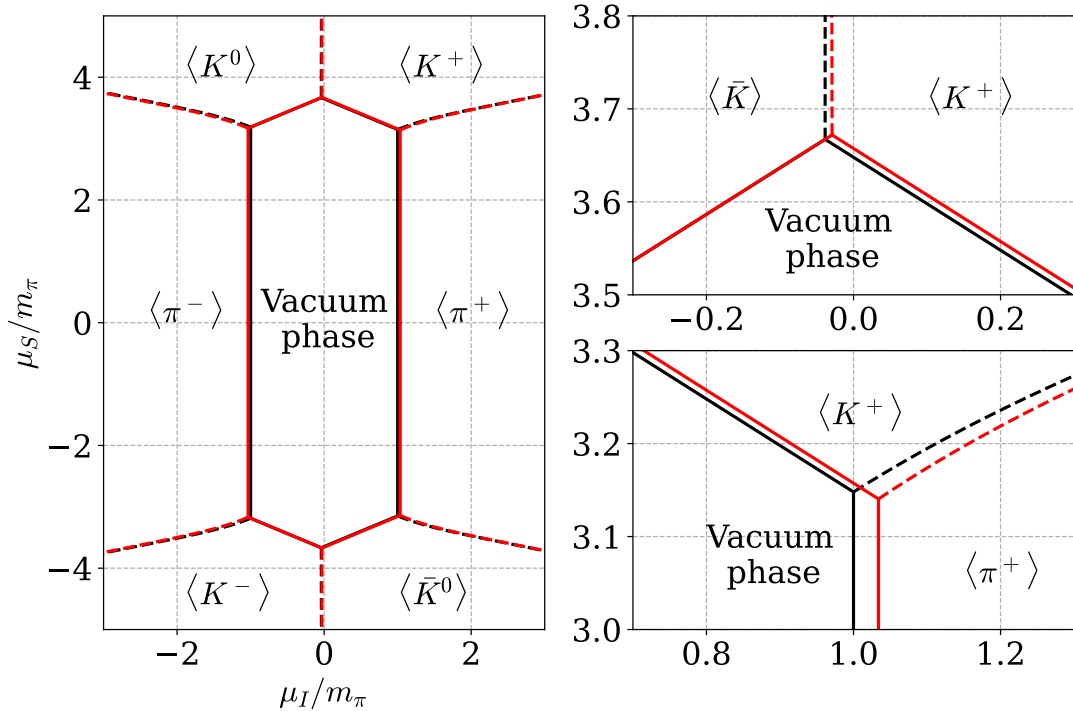


Figure 6.7: The phase diagram of χ PT in the $\mu_I - \mu_S$ -plane. The black lines are results without the electromagnetic interactions, while red lines are results including them. To the right, we have expanded around two of the triple points.

6.4 Electric charge neutrality

A pion condensate will have an electric charge. In the grand canonical ensemble, the QCD Lagrangian will have the term $\mu_Q e \bar{q} \gamma^0 Q q$, where $e \bar{q} \gamma^\mu Q q$ is the electric current density, Q the quark charge matrix Eq. (5.51), and $e \mu_Q = \mu_I + 2\mu_S$ is the electric charge chemical potential. In the case of $\mu_S = 0$, the charge density is

$$n_Q = -\frac{\partial \mathcal{F}}{\partial \mu_Q} = e n_I. \quad (6.37)$$

A realistic astrophysical object will not have a macroscopic electric charge. This is due to the long-range nature of the Coulomb force, which ensures that any macroscopically charged objects will neutralize each other, given that the total amount of charge is zero. Therefore, we will model pion stars with the additional constraint of charge neutrality by including charged leptons, muons or electrons, as free fermions. These leptons have an electric charge of $-e$. As we saw in subsection 5.2.1, e has a chiral dimension. Strictly speaking, then, we should include self-interactions in one-loop order for a consistent expansion scheme. However, as QED converges quickly this will be a very small correction and we will only include leading order effects. We may therefore use the results from section 4.4. The electric charge density of the leptons is given $-e n_\ell$, where n_ℓ is the particle number, in this case, the lepton number. In Eq. (4.89), we found the expression

$$n_\ell = \frac{8}{3} \frac{u_{\ell,0}}{m_\ell} x_f^3, \quad (6.38)$$

where $x_f = \sqrt{\mu_\ell^2/m_\ell^2 - 1}$ is the dimensionless Fermi momentum, m_ℓ the lepton mass, and μ_ℓ the lepton chemical potential. This formula is valid for $\mu_\ell \geq m_\ell$. We have introduced the characteristic energy density of leptons,

$$u_{\ell,0} = \frac{m_\ell^4}{8\pi^2}. \quad (6.39)$$

The criterion for charge neutrality is then

$$n_I = n_\ell. \quad (6.40)$$

With this, we can determine the lepton chemical potential as a function of the isospin chemical potential, $\mu_\ell = \mu_\ell(\mu_I)$. The leading order result for the isospin density of the pion condensate is given in Eq. (6.12). Inserting the expressions for these densities into Eq. (6.40), we get

$$A \left(\frac{\mu_\ell^2}{m_\ell^2} - 1 \right)^{3/2} = \frac{\mu_I}{m_{\pi,0}} \left(1 - \frac{m_{\pi,0}^4}{\mu_I^4} \right). \quad (6.41)$$

Both densities vanish at the point $(\mu_I, \mu_\ell) = (m_{\pi,0}, m_\ell)$, which we have seen earlier is the point where the pressure and energy density of both the Fermi gas and the pion condensate vanish. We have introduced the dimensionless constant

$$A = \frac{8}{3} \frac{m_{\pi,0}}{m_\ell} \frac{u_{0,\ell}}{u_0} = \frac{1}{3\pi^2} \frac{m_\ell^3}{m_{\pi,0} f^2}. \quad (6.42)$$

Setting the lepton mass equal the electron mass or muon mass gives, respectively, $A = 3.9 \times 10^{-9}$ and $A = 3.5 \times 10^{-2}$. In this case, we can write the expression for $\mu_\ell(\mu_I)$ as an explicit function,

$$\frac{\mu_\ell}{m_\ell} = \sqrt{1 + A^{-2/3} \left[\frac{\mu_I}{m_{\pi,0}} \left(1 - \frac{m_{\pi,0}^4}{\mu_I^4} \right) \right]^{2/3}}. \quad (6.43)$$

These relationships are illustrated in Figure 6.8. The plot on the left is the electron chemical potential as a function of isospin chemical potential, both normalized to the masses of their

corresponding particles, while the muon chemical potential is on the right. We see that both lepton potentials are suppressed, relative to the isospin chemical potential, by the A constant in Eq. (6.41). The electron is much lighter than the pion and therefore grows much faster than the muon chemical potential.

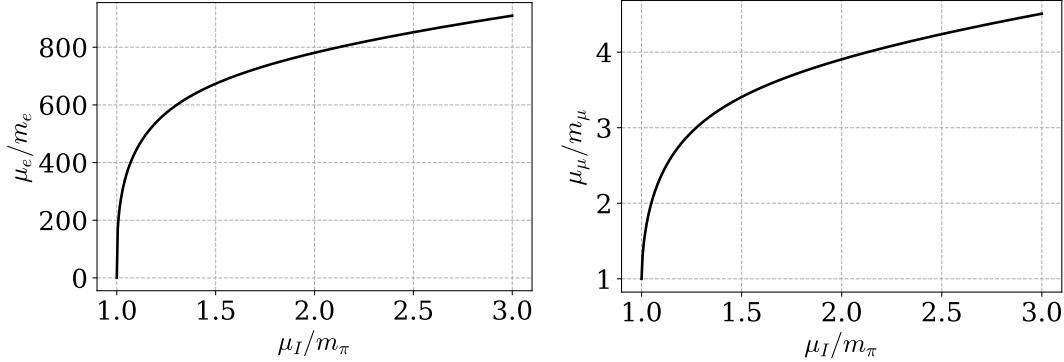


Figure 6.8: The lepton chemical potentials as functions of the isospin chemical potential normalized to their respective particle masses. The electron chemical potential is shown to the left, the muon to the right.

The total pressure and energy density will now be the sum of the contributions from the pion condensate and the leptons. The lepton contribution to these, which we found in Eq. (4.90) and Eq. (4.91), is

$$p_\ell = \frac{1}{3} u_{\ell,0} \left[(2x_f^3 - 3x_f) \sqrt{1 + x_f^2} + 3 \operatorname{arcsinh}(x_f) \right], \quad (6.44)$$

$$u_\ell = u_{\ell,0} \left[(2x_f^3 + x_f) \sqrt{1 + x_f^2} - \operatorname{arcsinh}(x_f) \right]. \quad (6.45)$$

$$(6.46)$$

The contribution from the pion condensate is, as we found in Eq. (6.11) and Eq. (6.13), is

$$p_\pi = u_0 \frac{1}{2} \frac{\mu_I^2}{m_{\pi,0}^2} \left(1 - \frac{m_{\pi,0}^2}{\mu_I^2} \right)^2, \quad (6.47)$$

$$u_\pi = u_0 \frac{1}{2} \frac{\mu_I^2}{m_{\pi,0}^2} \left(1 - \frac{m_{\pi,0}^2}{\mu_I^2} \right) \left(1 + 3 \frac{m_{\pi,0}^2}{\mu_I^2} \right). \quad (6.48)$$

This leads to a total pressure and energy

$$p = p_\pi + p_\ell, \quad u = u_\pi + u_\ell. \quad (6.49)$$

As Eq. (6.40) gives μ_ℓ as a function of μ_I , these are both parameterized by the isospin chemical potential, and we can extract the equation of state $u = u(p)$. The full equation of state in different regimes is shown in Figure 6.9. On the top left, the addition of the electron results in a much stiffer equation of state than the addition of the muon. We have seen that the low-pressure energy density of the pion is $m_\pi n_I$, while for the lepton, it is $m_\ell n_\ell$. As $n_I = n_\ell$, the low-pressure limit of the energy density is $(m_\pi + m_\ell) n_I$, which explains why the muon, where $m_\mu \approx m_\pi$, contributes a lot more to the energy density than the electron, for which $m_e \ll m_\pi$. We see that the pion contribution dominates the high-pressure regime in the top right plot. However, as chiral perturbation assumes small pion energies and small external currents, this result must be used carefully. The equation of state in an intermediate range is shown on the bottom. It is not very sensitive to the lepton mass, at least as long as it is less than the pion mass.

We can find the ultrarelativistic limit by letting $\mu_I^2/m_\pi^2 = y$, $y \gg 1$. From Eq. (6.43), we find that the lepton chemical potential to leading order in y is $\mu_\ell^2 \propto y^{1/3}$. In section 4.4, we found

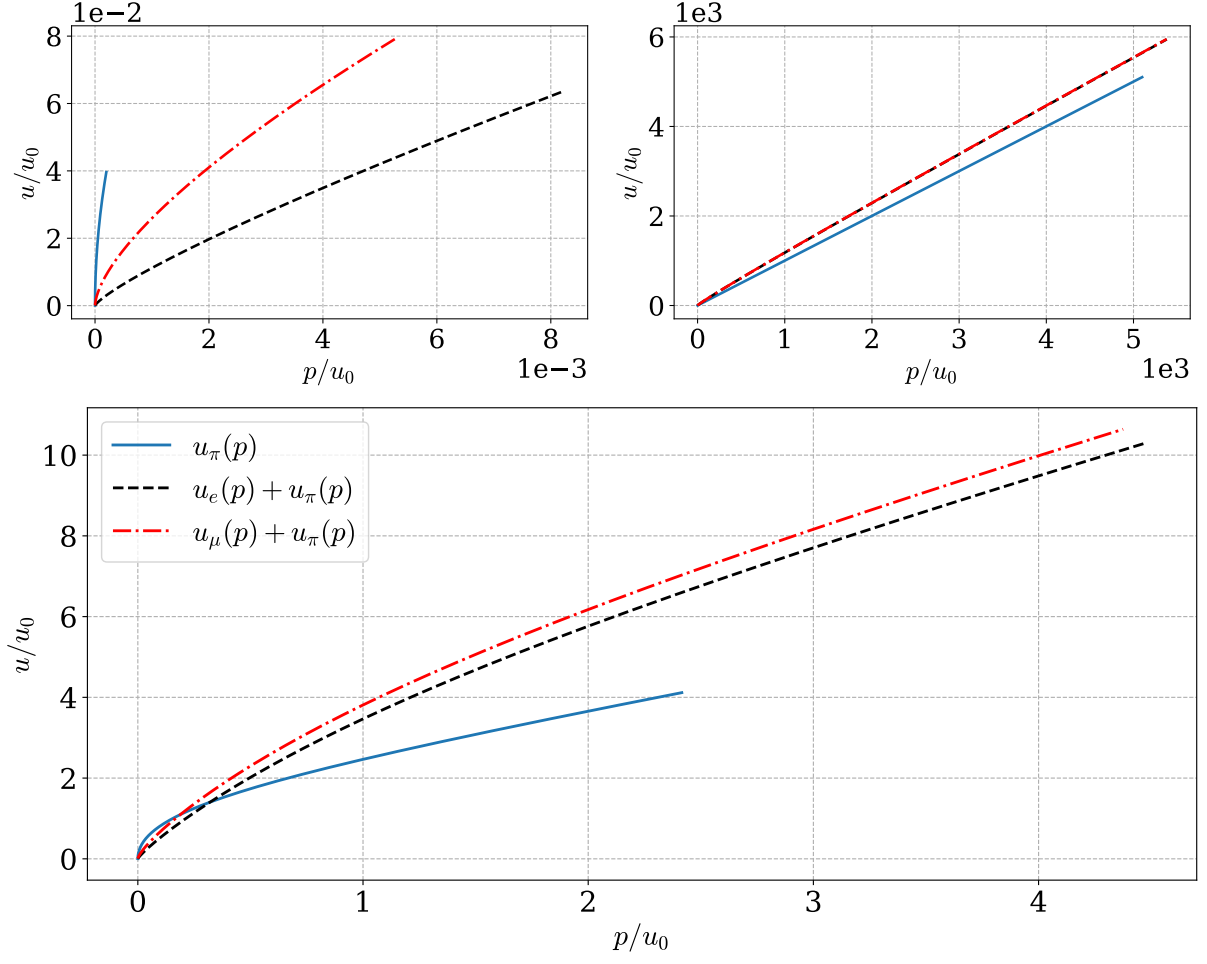


Figure 6.9: The equation of state including a lepton is compared with the equation of state of only the pion condensate in two different regimes. The pressure and energy density is normalized to $u_0 = f_\pi^2 m_\pi^2$.

that in the ultrarelativistic limit of non-interacting fermions, both the pressure and energy is proportional to $x_f^4 \propto y^{2/3}$. In the case of the pion, however, both are proportional to $\mu_I^2 \propto y$. Therefore, the ultrarelativistic limit of the combined system is, to leading order, given by the ultrarelativistic limit of the pion condensate alone.

As before, we can find the non-relativistic limit by letting $\mu_I^2/m_\pi^2 = 1 + \epsilon$. Inserting this into Eq. (6.43) and expanding to first order in ϵ , we get $\mu_\ell^2/m_\ell^2 = 1 + (2A^{-1}\epsilon)^{2/3}$. This is equivalent to $x_f = (2A^{-1}\epsilon)^{1/3}$. In section 4.4, we found the non-relativistic limit of the pressure and energy of the Fermi gas, i.e., the lowest order contribution in x_f , as $x_f \rightarrow 0$. Inserting this new result into these limits, we get the leading low energy limits of the pressure and energy,

$$u_{\ell,\text{NR}} = \frac{8}{3} \frac{2}{A} u_{\ell,0} \epsilon, \quad p_{\ell,\text{NR}} = \frac{8}{15} \left(\frac{2}{A} \right)^{5/3} u_{\ell,0} \epsilon^{5/3}. \quad (6.50)$$

From section 6.2, we have the equivalent expressions for the pion condensate,

$$u_{\pi,\text{NR}} = 2u_0 \epsilon, \quad p_{\pi,\text{NR}} = \frac{1}{2} u_0 \epsilon^2. \quad (6.51)$$

As we see, the energy density of the pion condensate and the leptons are of the same order, and both will therefore contribute to the leading order energy density. However, the lepton pressure is of a lower order, and *only* this will contribute to the leading order pressure. At low enough

isospin chemical potential, then, the leading order behavior of the combined system is

$$u_{\text{NR}} = 2u_0 \left(1 + \frac{1}{2} \frac{m_\ell}{m_\pi}\right) \epsilon, \quad p_{\text{NR}} = \frac{8}{15} u_{\ell,0} \left(\frac{2}{A}\right)^{5/3} \epsilon^{5/3}. \quad (6.52)$$

The equation of state is now a polytrope with $\gamma = \frac{5}{3}$, different from the $\gamma = 2$ polytrope of only the pion condensate. For a heavy lepton, $m_\ell \gg m_\pi$, the factor $A^{-\frac{5}{3}}$ would suppress the leading order of the lepton contribution to the pressure. Thus, the equation of state would have an intermediate range in which it would be well approximated as a polytrope with $\gamma = 2$, and a modified poly tropic constant $K'^{-1} = 8(1 + \frac{1}{2}m_\ell/m_\pi)^2$. The full equation of state is compared to the non-relativistic limit in Figure 6.10.

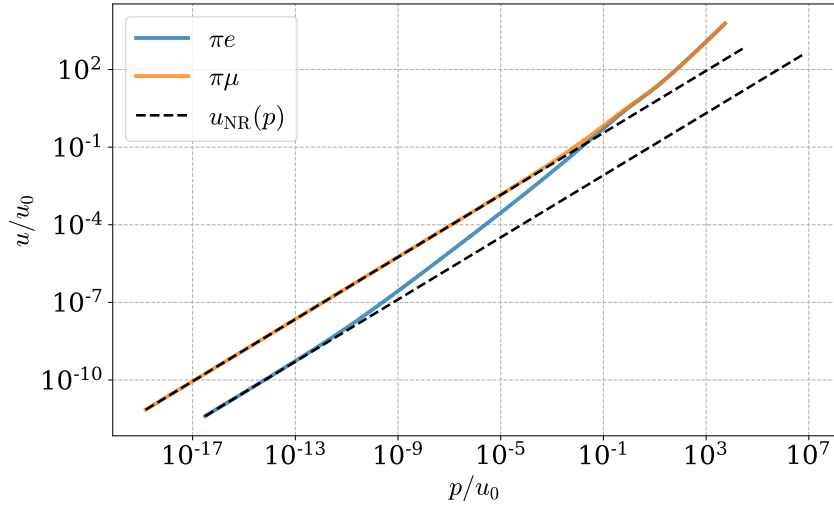
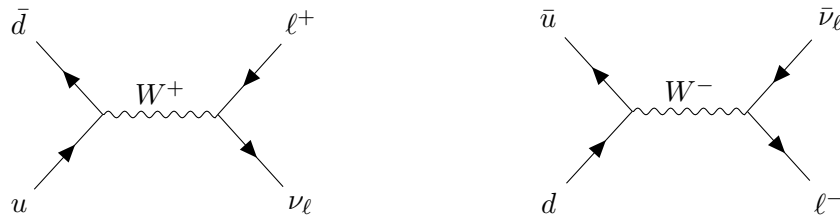


Figure 6.10: The full equation of state of the pion + lepton systems, compared with the non-relativistic limit. Both the energy density and the pressure is given in units of $u_0 = m_\pi^2 f_\pi^2$.

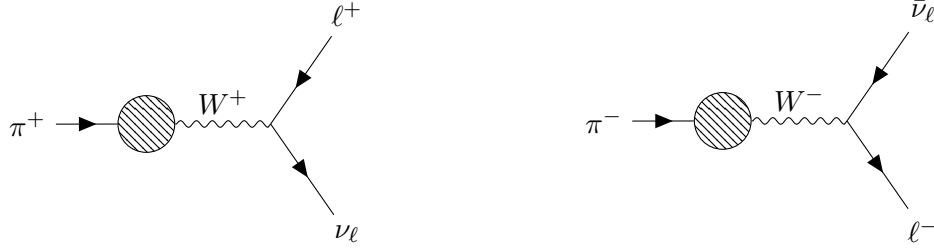
6.4.1 Neutrinos

The primary decay mode for charged pions is via the weak force. The W^\pm bosons, which together with the Z boson mediate the weak force, couple to quarks, charged leptons ℓ and their corresponding neutrinos ν_ℓ . Neutrinos are very light leptons that only interact via the weak force. The exact nature of the mass of neutrinos is still an open problem [9]. In this thesis, we will regard the neutrinos as massless. The leading order diagrams for the relevant interactions are



The W^\pm boson only couples to left-handed fermions, $\psi_L = P_L \psi$, as discussed in subsection 5.1.3. Therefore, the coupling has the form $W_\mu^\pm \bar{\psi}_L \gamma^\mu \psi_L$. This will result in effective interactions of

the form



Here, the shaded circle represents the effective interaction between the pions and the W^\pm bosons. Although the $\pi \rightarrow e\nu_e$ decay has a larger phase-space than $\pi \rightarrow \mu\nu_\mu$ due to the lighter mass of the electron, the latter decay mode is dominating. This is due to *helicity suppression*. In the zero-mass limit, the helicity of a particle, i.e., the alignment of spin and momentum, is given by its chirality. A left-handed, massless particle has helicity $h = -1$ and the corresponding antiparticle has $h = 1$. The decay product from a weak interaction has the same chirality and thus opposite helicity, which is forbidden by the conservation of linear and angular momentum. This effect suppresses the decay into the light electron [10].

We treat neutrinos ν_ℓ as free, massless fermions, with chemical potentials μ_{ν_ℓ} . In chemical equilibrium, the processes $\pi^+ \leftrightarrow \ell^+\nu_\ell$ and $\pi^- \leftrightarrow \ell^-\bar{\nu}_\ell$ are balanced, and the chemical potentials therefore obey

$$\mu_I = \mu_{\nu_\ell} - \mu_\ell. \quad (6.53)$$

Even though we regard the neutrinos as massless when working with the dynamics, the non-zero mass will affect the results via *neutrino oscillations*. As the mass eigenstates of neutrinos are not the same as the flavor eigenstates, the neutrino spontaneously and continuously undergoes processes of the form $\nu_\ell \rightarrow \nu_{\ell'}$. As a result, neither the individual lepton particle numbers n_{ν_ℓ} and n_ℓ , nor individual lepton numbers $L_\ell = n_\ell + n_{\nu_\ell}$ are conserved. However, the sum of all lepton numbers is conserved. In chemical equilibrium, neutrino oscillations will result in the relationship

$$\mu_{\nu_e} = \mu_{\nu_\mu}. \quad (6.54)$$

Or, using Eq. (6.53), $\mu_e = \mu_\mu$. The equation for charge neutrality now becomes $n_I = n_e + n_\mu$, or

$$\frac{\mu_I}{m_{\pi,0}} \left(1 - \frac{m_{\pi,0}^4}{\mu_I^4} \right) = \theta(\mu_e - m_e) A_e \sqrt{\frac{\mu_e^2}{m_e^2} - 1} + \theta(\mu_e - m_\mu) A_\mu \sqrt{a^2 \frac{\mu_e^2}{m_e^2} - 1}, \quad (6.55)$$

where $a = m_e/m_\mu \approx 1/200$. Thus, for $\mu_e < m_\mu$, there will be no muons. The relationship between μ_e and μ_I is the same as with only pions and electrons, while it deviates for $\mu_e > m_\mu$. These results are compared in Figure 6.11. The plot also illustrates the derivative of μ_e with respect to μ_I , which remains continuous even at the point where muons start to contribute.

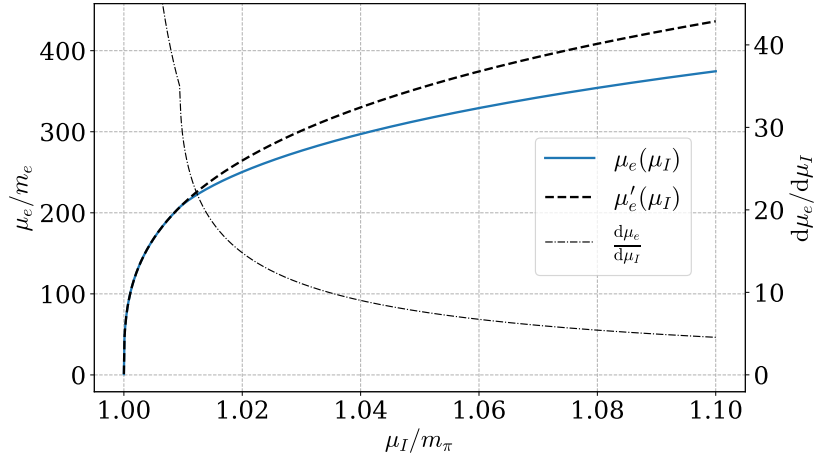


Figure 6.11: The electron chemical potential as a function of isospin chemical potential when including only electrons, μ'_e , and when including neutrinos and weak interactions, μ_e , and its derivative. The chemical potentials are normalized to their respective masses.

The pressure and energy from the neutrinos are given by the ultrarelativistic limit of the free fermion results, which we found in section 4.4. These results are divided by two, as there are only left-handed neutrinos, and thus only half as many degrees of freedom as fermions where both chiralities appear. The chemical potential of a massless particle equals its Fermi momentum, so the result is

$$u_{\nu_\ell} = \frac{\mu_{\nu_\ell}^4}{8\pi^2}, \quad p_{\nu_\ell} = \frac{\mu_{\nu_\ell}^4}{24\pi^2}. \quad (6.56)$$

The total pressure and energy density are now, as before, the sum of the individual contribution from each species.

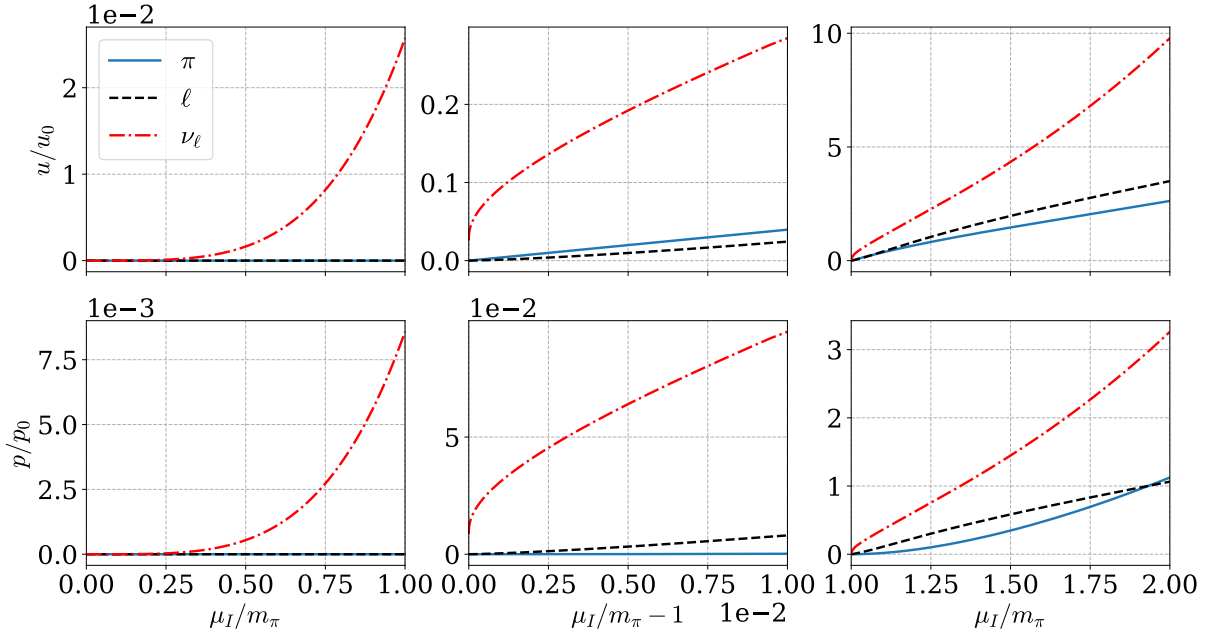


Figure 6.12: The contributions to energy density and pressure from the pion condensate, π , the charged leptons ℓ and the corresponding neutrinos ν_ℓ , in various domains.

The various contributions to the energy density and pressure are shown in Figure 6.12. As before, the criterion of charge neutrality Eq. (6.55) ensures that the transition to the vacuum phase for the pion condensate, at $\mu_I = m_\pi$, happens simultaneously as the charged lepton

density vanishes, here at $\mu_e = m_e$. However, due to the weak-interaction chemical equilibrium, Eq. (6.53), the neutrino chemical potential and thus the neutrino pressure will be non-zero even with no pion condensate nor any charged leptons. As both the electron and muon neutrino contributes, the pressure is

$$p_{\min} = \frac{(m_\pi + m_e)^4}{12\pi^2}. \quad (6.57)$$

After this point, μ_I and μ_ℓ do not have a strict functional relationship, as Eq. (6.55) no longer applies. The equation of state is then given only by the neutrinos and is $u = 3p$. This is not correct for arbitrarily low pressure, as the finite neutrino mass will at some point become relevant. The equation of state of the full system is shown in Figure 6.13, where it is compared to the equation of state of only neutrinos.

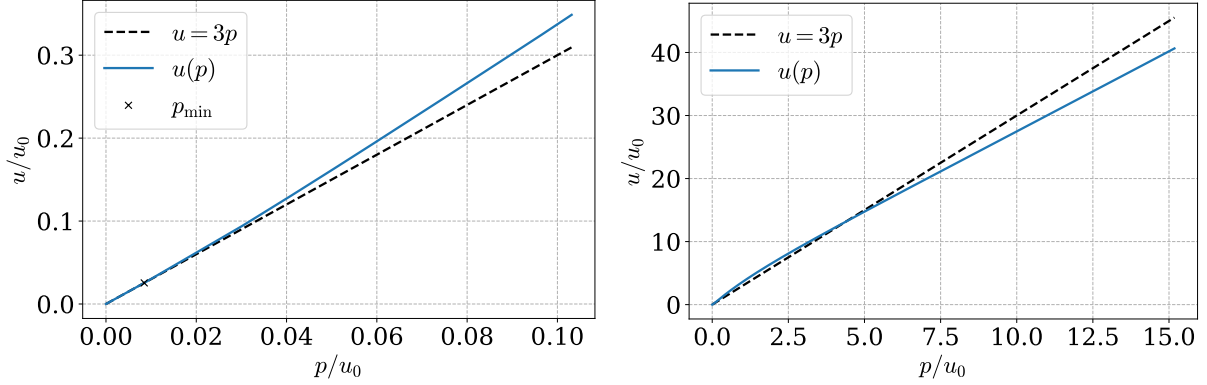


Figure 6.13: The equation of state for a system of pions, charged leptons and neutrinos in chemical equilibrium, solid line, is compared to the equation of state of only neutrinos, $u = 3p$.

6.5 Next-to-leading order results

In section 5.4, we found the most general Lagrangian at next-to-leading order in Weinberg's power counting scheme, that is, of chiral dimension $D = 4$. The parameters in this Lagrangian contained divergences of the form $1/\epsilon$. These are to counteract the divergences which now will appear as we start to calculate the loop contributions to the free energy from the $D = 2$ Lagrangian. As we showed in subsection 5.2.1, all term of chiral dimension D scale as t^D when the external momenta are scaled as $Q \rightarrow tQ$, chemical momentum as $\mu \rightarrow t\mu$, quark masses as $m_q \rightarrow t^2 m_q$ and electric charge as $e \rightarrow te$. The tree-level contributions from \mathcal{L}_D are thus of chiral dimension D . The n -loop corrections to these results, however, will be suppressed by p^{2n} , and are therefore of chiral dimension $D + 2n$. As such, they can be renormalized by the sum of the $n - 1$ -loop contributions of \mathcal{L}_{D-2} , $n - 2$ -loop contributions of \mathcal{L}_{D-4} and so on. [1, 51]. This expansion in both loops and chiral dimension, which is used to evaluate all physical quantities, is elaborated on in section A.4. As a result, the next-to-leading order contribution consists of tree-level contributions for \mathcal{L}_4 and one-loop contribution from \mathcal{L}_2 . In this section, we will calculate the NLO contribution to the free energy density using this technique.

6.5.1 One-loop contribution

We now calculate the one-loop contribution to the free energy due to \mathcal{L}_2 , following the procedure used in [70, 74, 81]. The loop integrals will diverge, and we must therefore regularize them. As discussed in section 5.4, will use dimensional regularization, in which the integral is generalized to d dimensions, and employ the $\overline{\text{MS}}$ -scheme. From the formula for the effective potential,

Eq. (3.38), we have that the one loop-contribution to one-loop order is

$$\mathcal{F}^{(1)} = -\frac{i}{VT} \frac{1}{2} \text{Tr} \{ \ln(-D_{ab}^{-1}) \}, \quad (6.58)$$

where D_{ab}^{-1} is the inverse propagator. In subsection 5.3.2, we found the inverse propagator to be in a block-diagonal form. The trace is then a sum of the trace of each block,

$$\begin{aligned} \text{Tr} \{ \ln(-D_{ab}^{-1}) \} &= \text{Tr} \{ \ln(-p^2 + m_3^2) \} + \text{Tr} \{ \ln(-p^2 + m_8^2) \} \\ &+ \text{Tr} \{ \ln(-D_{12}^{-1}) \} + \text{Tr} \{ \ln(-D_{45}^{-1}) \} + \text{Tr} \{ \ln(-D_{67}^{-1}) \}. \end{aligned} \quad (6.59)$$

The sub-matrices are defined in Eqs. (5.82) to (5.84). The trace, in this case, is not only a sum over the matrix-indices of the propagator, but is an operator trace, as discussed in section C.3. Writing the trace in integral form, the contributions from the neutral pion and the η -particle are

$$\mathcal{F}_{\pi^0}^{(1)} = -i \frac{1}{2} \int \frac{d^4 p}{(2\pi)^4} \ln(-p^2 + m_3^2), \quad \mathcal{F}_{\eta}^{(1)} = -i \frac{1}{2} \int \frac{d^4 p}{(2\pi)^4} \ln(-p^2 + m_8^2). \quad (6.60)$$

As shown in subsection A.5.2, we may rewrite integrals of this form as

$$-i \frac{1}{2} \int \frac{d^4 p}{(2\pi)^4} \ln(-p_0^2 + \vec{p}^2 + m^2) = \frac{1}{2} \int \frac{d^3 p}{(2\pi)^3} \sqrt{\vec{p}^2 + m^2}. \quad (6.61)$$

We see that the result is what we would expect physically; the total energy is the integral of the energy of each mode. This also agrees with the result from Appendix C in the zero-temperature limit $\beta \rightarrow \infty$. We discuss dimensional regularization and perform this integral in section A.5. The results are

$$\mathcal{F}_{\pi^0}^{(1)} = -\frac{1}{4} \frac{\mu^{-2\epsilon}}{(4\pi)^2} \left(\frac{1}{\epsilon} + \frac{3}{2} + \ln \frac{\tilde{\mu}^2}{m_3^2} \right) m_3^4 + \mathcal{O}(\epsilon), \quad (6.62)$$

$$\mathcal{F}_{\eta}^{(1)} = -\frac{1}{4} \frac{\mu^{-2\epsilon}}{(4\pi)^2} \left(\frac{1}{\epsilon} + \frac{3}{2} + \ln \frac{\tilde{\mu}^2}{m_8^2} \right) m_8^4 + \mathcal{O}(\epsilon). \quad (6.63)$$

Here, $d = 3 - 2\epsilon$, and μ is the renormalization scale, a parameter with mass-dimension 1, introduced to ensure the action integral remains dimensionless during dimensional regularization. The scale $\tilde{\mu}$ is related to μ as described in Eq. (A.112).

Using the identity $\ln\{\det(A)\} = \text{Tr} \{ \ln(A) \}$, and the spectrum we found in subsection 5.3.2, write the charged pion contribution as

$$\begin{aligned} \mathcal{F}_{\pi^\pm}^{(1)} &= -\frac{i}{VT} \frac{1}{2} \text{Tr} \{ \ln(-D_{12}^{-1}) \} \\ &= -\frac{i}{VT} [\text{Tr} \{ \ln(-p_0^2 + E_{\pi^+}^2) \} + \text{Tr} \{ \ln(-p_0^2 + E_{\pi^-}^2) \}] \\ &= -i \int \frac{d^4 p}{(2\pi)^2} [\ln(-p_0^2 + E_{\pi^+}^2) \ln(-p_0^2 + E_{\pi^-}^2)] \end{aligned} \quad (6.64)$$

$$= \frac{1}{2} \int \frac{d^3 p}{(2\pi)^3} (E_{\pi^+} + E_{\pi^-}). \quad (6.65)$$

Here, we again rewrote the integral as shown in subsection A.5.2. However, the similarities stop here, as the spectra of the charged pions are much more complicated,

$$E_{\pi^\pm} = \sqrt{|\vec{p}|^2 + \frac{1}{2} (m_1^2 + m_2^2 + m_{12}^2) \mp \frac{1}{2} \sqrt{4|\vec{p}|^2 m_{12}^2 + (m_1^2 + m_2^2 + m_{12}^2)^2 - 4m_1^2 m_2^2}}. \quad (6.66)$$

This is not an integral we can easily do in dimensional regularization. Instead, we will seek a function $f(|\vec{p}|)$ with the same UV-behavior, that is, behavior for large \vec{p} , as $E_{\pi^+} + E_{\pi^-}$. If we then add $0 = f(|\vec{p}|) - f(|\vec{p}|)$ to the integrand, we can isolate the divergent behavior

$$\mathcal{F}_{\pi^\pm}^{(1)} = \frac{1}{2} \int \frac{d^3p}{(2\pi)^3} [E_{\pi^+} + E_{\pi^-} - f(|\vec{p}|)] + \frac{1}{2} \int \frac{d^3p}{(2\pi)^3} f(|\vec{p}|) = \mathcal{F}_{\text{fin},\pi^\pm}^{(1)} + \mathcal{F}_{\text{div},\pi^\pm}^{(1)}. \quad (6.67)$$

This results in a finite integral, $\mathcal{F}_{\text{fin},\pi^\pm}^{(1)}$, which can be evaluated numerically, and a divergent integral $\mathcal{F}_{\text{div},\pi^\pm}^{(1)}$, which we hope can be evaluated in dimensional regularization.

We can explore the UV-behavior of $E_{\pi^+} + E_{\pi^-}$ by expanding it in powers of $1/|\vec{p}|$,

$$\begin{aligned} E_{\pi^+} + E_{\pi^-} &= 2|\vec{p}| + \frac{m_{12} + 2(m_1^2 + m_2^2)}{4} |\vec{p}|^{-1} \\ &\quad - \frac{m_{12}^4 + 4m_{12}^2(m_1^2 + m_2^2) + 8(m_1^4 + m_2^4)}{64} |\vec{p}|^{-3} + \mathcal{O}(|\vec{p}|^{-5}) \\ &= a_1 |\vec{p}| + a_2 |\vec{p}|^{-1} + a_3 |\vec{p}|^{-3} + \mathcal{O}(|\vec{p}|^{-5}). \end{aligned} \quad (6.68)$$

We have defined new constants a_i for brevity of notation. As

$$\int_{\mathbb{R}^3} \frac{d^3p}{(2\pi)^3} |\vec{p}|^n = C \int_0^\infty dp p^{2+n} \quad (6.69)$$

is UV divergent for $n \geq -3$, f need to match the expansion of $E_{\pi^+} + E_{\pi^-}$ up to and including $\mathcal{O}(|\vec{p}|^{-3})$ for $\mathcal{F}_{\text{fin},\pi^\pm}^{(1)}$ to be finite. The most obvious choice for f is

$$f(|\vec{p}|) = a_1 |\vec{p}| + a_2 |\vec{p}|^{-1} + a_3 |\vec{p}|^{-3}. \quad (6.70)$$

However, this introduces a new problem. f has the same UV behavior as $E_{\pi^+} + E_{\pi^-}$, but the last term diverges in the IR, that is, for low $|\vec{p}|$. This can be amended by introducing a mass term. If we substitute $|\vec{p}|^2 \rightarrow |\vec{p}|^2 + m^2$, the function retains its UV behavior. However, for $|\vec{p}| \rightarrow 0$, it remains finite, so the IR-divergence is gone. As f is both added and subtracted, any final result will be independent of the value of m .

We can, however, tame the IR divergence without introducing any new mass parameter by defining $E_i = \sqrt{|\vec{p}|^2 + \tilde{m}_i^2}$, where $\tilde{m}_i^2 = m_i^2 + \frac{1}{4}m_{12}^2$. Then, we define $f(|\vec{p}|) = E_1 + E_2$, which differ from $E_{\pi^+} + E_{\pi^-}$ by $\mathcal{O}(|\vec{p}|^{-5})$ and is well-behaved in the IR. This leads to a divergent integral of the same form as in the case of a free scalar, and we may again use the result from section A.5. With this, the divergent part of the free energy is

$$\mathcal{F}_{\text{div},\pi^\pm}^{(1)} = -\frac{1}{4} \frac{\mu^{-2\epsilon}}{(4\pi)^2} \left(\frac{1}{\epsilon} + \frac{3}{2} + \ln \frac{\tilde{\mu}^2}{\tilde{m}_1^2} \right) \tilde{m}_1^4 - \frac{1}{4} \frac{\mu^{-2\epsilon}}{(4\pi)^2} \left(\frac{1}{\epsilon} + \frac{3}{2} + \ln \frac{\tilde{\mu}^2}{\tilde{m}_2^2} \right) \tilde{m}_2^4 + \mathcal{O}(\epsilon), \quad (6.71)$$

and the remaining finite part is

$$\mathcal{F}_{\text{fin},\pi^\pm}^{(1)} = \frac{1}{2} \int \frac{d^3p}{(2\pi)^3} (E_{\pi^+} + E_{\pi^-} - E_1 - E_2). \quad (6.72)$$

Lastly, the charged kaon contribution is

$$\mathcal{F}_{K^\pm}^{(1)} = -\frac{i}{VT} \frac{1}{2} \ln \{ \det(-D_{45}^{-1}) \} = -\frac{i}{VT} \frac{1}{2} \ln \{ \det [(-p^2 + m_4)(-p^2 + m_5) - p_0^2 m_{45}^2] \}, \quad (6.73)$$

where we have used the original form of the determinant which we found in subsection 5.3.2. To

perform the integral, we will use the following rewritings

$$\begin{aligned}
(-p^2 + m_4^2)(-p^2 + m_5^2) - p_0^2 m_{45}^2 &= \left[-p^2 + \frac{1}{2}(m_4^2 + m_5^2) \right]^2 - p_0^2 m_{45}^2 - \frac{1}{4}(m_4^2 - m_5^2)^2, \\
\left[-p^2 + \frac{1}{2}(m_4^2 + m_5^2) \right]^2 - p_0^2 m_{45}^2 &= \left[-p^2 + \frac{1}{2}(m_4^2 + m_5^2) - p_0 m_{45} \right] \\
&\quad \times \left[-p^2 + \frac{1}{2}(m_4^2 + m_5^2) + p_0 m_{45} \right], \\
-p^2 + \frac{1}{2}(m_4^2 + m_5^2) \pm p_0 m_{45} &= - \left(p_0 \mp \frac{1}{2} m_{45} \right)^2 + |\vec{p}|^2 + \tilde{m}_{45}^2,
\end{aligned}$$

where we have defined $\tilde{m}_{45}^2 = \frac{1}{2}(m_4^2 + m_5^2) + \frac{1}{4}m_{45}^2$. As $m_4 = m_5$, we can then write the free energy integrals on the form

$$\begin{aligned}
\mathcal{F}_{K^\pm}^{(1)} &= \frac{1}{2} \int \frac{d^4 p}{(2\pi^4)} \ln \left[- \left(p_0 + \frac{1}{2} m_{45} \right)^2 + |\vec{p}|^2 + \tilde{m}_{45}^2 \right] \\
&\quad + \frac{1}{2} \int \frac{d^4 p}{(2\pi^4)} \ln \left[- \left(p_0 - \frac{1}{2} m_{45} \right)^2 + |\vec{p}|^2 + \tilde{m}_{45}^2 \right]
\end{aligned} \tag{6.74}$$

After shifting the integration variable p_0 , we can again use Eq. (A.105). The result is therefore

$$\mathcal{F}_{K^\pm}^{(1)} = -\frac{1}{2} \frac{\mu^{-2\epsilon}}{(4\pi)^2} \left(\frac{1}{\epsilon} + \frac{3}{2} + \ln \frac{\tilde{\mu}^2}{\tilde{m}_{45}^2} \right) \tilde{m}_{45}^4. \tag{6.75}$$

The approach for the neutral kaon is the same, only with different masses. The result is

$$\mathcal{F}_{K^0}^{(1)} = -\frac{1}{2} \frac{\mu^{-2\epsilon}}{(4\pi)^2} \left(\frac{1}{\epsilon} + \frac{3}{2} + \ln \frac{\tilde{\mu}^2}{\tilde{m}_{67}^2} \right) \tilde{m}_{67}^4. \tag{6.76}$$

where $\tilde{m}_{67}^2 = \frac{1}{2}(m_6^2 + m_7^2) + \frac{1}{4}m_{67}^2$. In conclusion, the total leading-order, one-loop contribution to the free energy is

$$\begin{aligned}
\mathcal{F}_2^{(1)} &= -\frac{1}{2} \frac{\mu^{-2\epsilon}}{(4\pi)^2} \left[\left(\frac{1}{\epsilon} + \frac{3}{2} + \ln \frac{\tilde{\mu}^2}{m_3^2} \right) m_3^4 + \frac{1}{2} \left(\frac{1}{\epsilon} + \frac{3}{2} + \ln \frac{\tilde{\mu}^2}{m_8^2} \right) m_8^4 + \frac{1}{2} \left(\frac{1}{\epsilon} + \frac{3}{2} + \ln \frac{\tilde{\mu}^2}{\tilde{m}_1^2} \right) \tilde{m}_1^4 \right. \\
&\quad \left. + \left(\frac{1}{\epsilon} + \frac{3}{2} + \ln \frac{\tilde{\mu}^2}{\tilde{m}_{45}^2} \right) \tilde{m}_{45}^4 + \left(\frac{1}{\epsilon} + \frac{3}{2} + \ln \frac{\tilde{\mu}^2}{\tilde{m}_{67}^2} \right) \tilde{m}_{67}^4 \right] + \mathcal{O}(\epsilon) + \mathcal{F}_{\pi^\pm, \text{fin}}^{(1)}
\end{aligned}$$

6.5.2 Renormalization

The second-order, tree-level contribution to free energy is given by the second-order static Lagrangian,

$$\mathcal{F}_4^{(0)} = -\mathcal{L}_4^{(0)}, \tag{6.77}$$

which we found in Eq. (5.136). In combination with the results from the last subsection, this gives the total next-to-leading order contribution to the free energy,

$$\begin{aligned}
\mathcal{F}_{\text{NLO}} &= -\frac{1}{2} f^2 \left(2\bar{m}^2 \cos \alpha + \mu_I^2 \sin^2 \alpha + m_S^2 \right) + \mathcal{F}_{\pi^\pm, \text{fin}} \\
&\quad - 2(2L_1^r + 2L_2^r + L_3^r) \mu_I^4 \sin^4 \alpha - 4L_4^r (2\bar{m}^2 \cos \alpha + m_S^2) \mu_I^2 \sin^2 \alpha \\
&\quad - 4L_5^r \bar{m}^2 \mu_I^2 \cos \alpha \sin^2 \alpha - 4L_6^r (2\bar{m}^2 \cos \alpha + m_S^2)^2 \\
&\quad - 2L_8^r (2\bar{m}^4 \cos 2\alpha + 2\Delta m^4 + m_S^4) - H_2^r (2\bar{m}^4 + 2\Delta m^4 + m_S^4)
\end{aligned}$$

$$\begin{aligned}
& -\frac{1}{2} \frac{1}{(4\pi)^2} \left[\left(\frac{1}{2} + \ln \frac{M^2}{m_3^2} \right) m_3^2 + \frac{1}{2} \left(\frac{1}{2} + \ln \frac{M^2}{m_8^2} \right) m_8^4 + \frac{1}{2} \left(\frac{1}{2} + \ln \frac{M^2}{\tilde{m}_1^2} \right) \tilde{m}_1^4 \right. \\
& \quad \left. + \left(\frac{1}{2} + \ln \frac{M^2}{\tilde{m}_{45}^2} \right) \tilde{m}_{45}^4 + \left(\frac{1}{2} + \ln \frac{M^2}{\tilde{m}_{67}^2} \right) \tilde{m}_{67}^4 \right]. \tag{6.78}
\end{aligned}$$

Here, the mass terms are

$$\tilde{m}_1^2 = \bar{m}^2 \cos \alpha, \tag{6.79}$$

$$\tilde{m}_2 = m_3^2 = \bar{m}^2 \cos \alpha + \mu_I^2 \sin^2 \alpha, \tag{6.80}$$

$$m_8^2 = \frac{1}{3}(\bar{m}^2 \cos \alpha + 2m_S^2), \tag{6.81}$$

$$\tilde{m}_{45}^2 = \frac{1}{2}(\bar{m}^2 \cos \alpha - \Delta m^2 + m_S^2) + \frac{1}{4}\mu_I^2 \sin^2 \alpha, \tag{6.82}$$

$$\tilde{m}_{67}^2 = \frac{1}{2}(\bar{m}^2 \cos \alpha + \Delta m^2 + m_S^2) + \frac{1}{4}\mu_I^2 \sin^2 \alpha. \tag{6.83}$$

Notice that divergent $1/\epsilon$ -terms cancel exactly, and the total NLO contribution is therefore finite even as $\epsilon \rightarrow 0$, as expected. Furthermore, all dependence on the unphysical parameter μ has vanished, and only the renormalized coupling constants and the mass M at which they are defined remain.

When evaluating the free energy and quantities derived from it, we need the NLO relationship between the bare parameters that appear in the Lagrangian and the experimental values. For numerical results, we will consider $\Delta m = 0$. This is done in the QCD-lattice research and allows for easier comparison with those results [6]. Furthermore, we expect this to have marginal effects on our results, as Δm does not affect the results until NLO. After setting $\Delta m = 0$, we are left with three independent bare parameters, \bar{m} , m_S , and f . We must therefore use physical values of three constants, as more would lead to an overdetermined system of equations. As we work with a pion condensate without electromagnetic interactions, it is natural to choose the neutral pion mass m_π and the pion decay f_π . As we assume $\Delta m = 0$ and no electromagnetic interaction, the charged and neutral kaon masses are equal. We, therefore, define $m_{K,0}^2 := (\bar{m} + m_S)/2$, and choose the neutral kaon mass, m_{K^0} , as the last physical constant. The value use for the physical constants can be found in section A.1. The NLO relationships that determine the bare parameters are [52]

$$\begin{aligned}
m_\pi^2 = m_{\pi,0}^2 & \left[1 + \left(16L_8^r - 8L_5^r + 24L_6^r - 12L_4^r + \frac{1}{2(4\pi)^2} \ln \frac{m_{\pi,0}^2}{M^2} \right) \frac{m_{\pi,0}^2}{f^2} \right. \\
& \quad \left. + \left(24L_6^r - 12L_4^r - \frac{1}{6(4\pi)^2} \ln \frac{m_{\eta,0}^2}{M^2} \right) \frac{m_{\eta,0}^2}{f^2} \right], \tag{6.84}
\end{aligned}$$

$$\begin{aligned}
m_{K^0} = m_{K,0}^2 & \left[1 + 8(2L_6^r - L_4^r) \frac{m_{\pi,0}^2}{f^2} \right. \\
& \quad \left. + 8(2L_8^r - L_5^r + 4L_6^r - 2L_4^r) \frac{m_{K,0}^2}{f^2} + \left(\frac{1}{3(4\pi)^2} \ln \frac{m_{\eta,0}^2}{M^2} \right) \frac{m_{\eta,0}^2}{f^2} \right], \tag{6.85}
\end{aligned}$$

$$\begin{aligned}
f_\pi^2 = f^2 & \left[1 + \left(8L_4^r + 8L_5^r - \frac{2}{(4\pi)^2} \ln \frac{m_{\pi,0}^2}{M^2} \right) \frac{m_{\pi,0}^2}{f^2} \right. \\
& \quad \left. + \left(16L_4^r - \frac{1}{(4\pi)^2} \ln \frac{m_{K,0}^2}{M^2} \right) \frac{m_{K,0}^2}{f^2} \right]. \tag{6.86}
\end{aligned}$$

These three equations allow us to determine \bar{m} , m_S and f to next-to-leading order. The numerical results are shown in Table 6.1.

Table 6.1: The leading order and next-to-leading order values for the bare masses and decay constant. These values are for $\Delta m = 0$.

Bare constant	LO [MeV]	NLO [MeV]	NLO/LO
f	92.07	78.55	0.853
\bar{m}	134.98	135.53	1.004
m_S	664.17	743.48	1.119

The next-to-leading order relation between α and μ_I is given by, as discussed in section A.4,

$$\left[\frac{\partial}{\partial \alpha} \mathcal{F}_{\text{NLO}}(\mu_I, \alpha) \right]_{\alpha=\alpha_{\text{NLO}}} = 0. \quad (6.87)$$

The result is compared to the leading order result in Figure 6.14, together with the derived thermodynamic quantities n_I , p and u . The LO and NLO results for α are very close. It has been shown analytically that the phase transition happens at $\mu_I = m_\pi$ also at next-to-leading order [70]. This amounts to showing that the free energy has the form

$$\mathcal{F}_{\text{NLO}} = \text{const.} - \frac{1}{2} f_\pi^2 (\mu_I^2 - m_\pi^2) \alpha^2 + \mathcal{O}(\alpha^4). \quad (6.88)$$

We expect this to hold to all orders in perturbation theory. One cannot, however, expect no deviation numerically, as higher-order terms have been neglected. Such numerical deviations are observed, as we found $\mu_I^c \approx 1.001 m_\pi$. The NLO results for the thermodynamic quantities are close to the LO results for values of μ_I close to m_π , however, the results start to deviate as μ_I increases. This is to be expected, as we are expanding perturbatively in particle energies, and thus also chemical potential. As discussed subsection 5.2.1, we see that $4\pi f_\pi \approx 8.6 m_\pi$ is the energy scale that determines convergence. As μ_I approaches this point, the NLO corrections are no longer small. These results indicate that, at least for $\mu_I < 2 m_\pi$, χPT converges quickly. The NLO equation of state is shown in Figure 6.15, where it is compared to the leading order result. The NLO equation of state is less stiff than the LO equation of state, and they deviate more as the pressure increases. With the NLO results for u_π and p_π as functions of μ_I , we can obtain the NLO results for the $\pi\ell\nu_\ell$ -system by using these results in the total pressure and energy density, as laid out in subsection 6.4.1. The NLO and LO results are compared in Figure 6.16 for two different regimes. As the neutrino contribution to the pressure dominates, the change to the equation of state is minimal. It is still well approximated by $u = 3p$. At the top, we see that the NLO equation of state is ever so slightly stiffer for low pressures, while at the bottom we see that the relationship reverses for higher pressures. Finally, we compare the different equations of state in Figure 6.17.

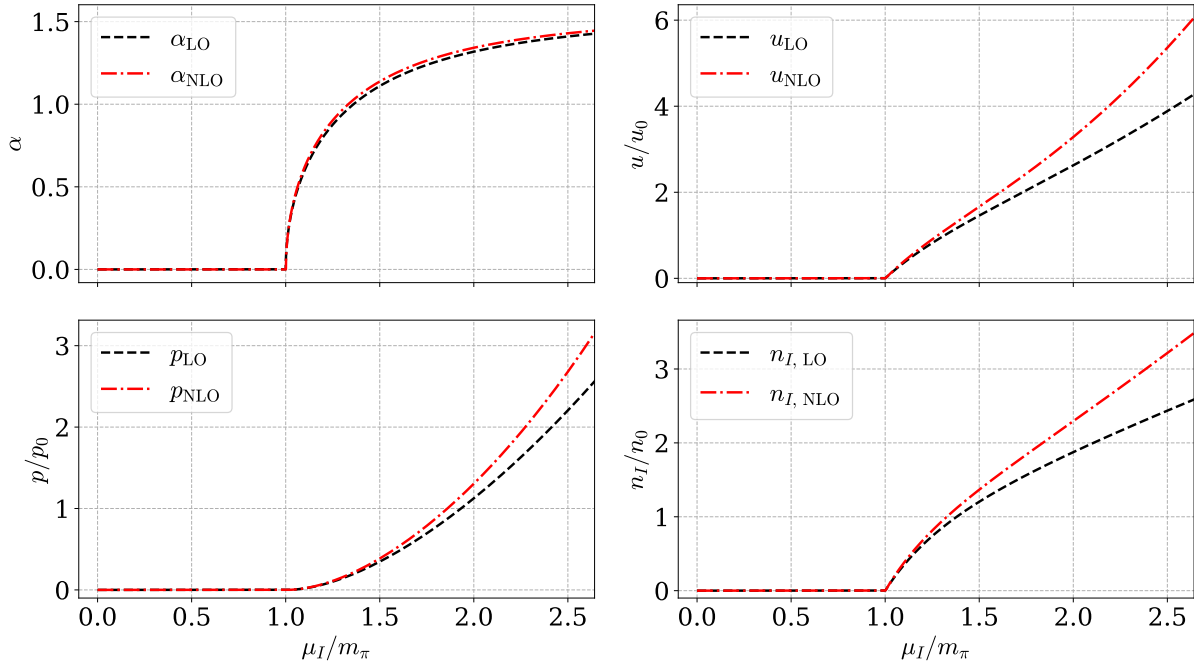


Figure 6.14: The next-to-leading order results of various thermodynamic quantities, compared to the leading order results. The characteristic quantities are $p_0 = u_0 = m_\pi n_0 = f_\pi^2 m_\pi^2$, and μ_I is given in units of m_π .

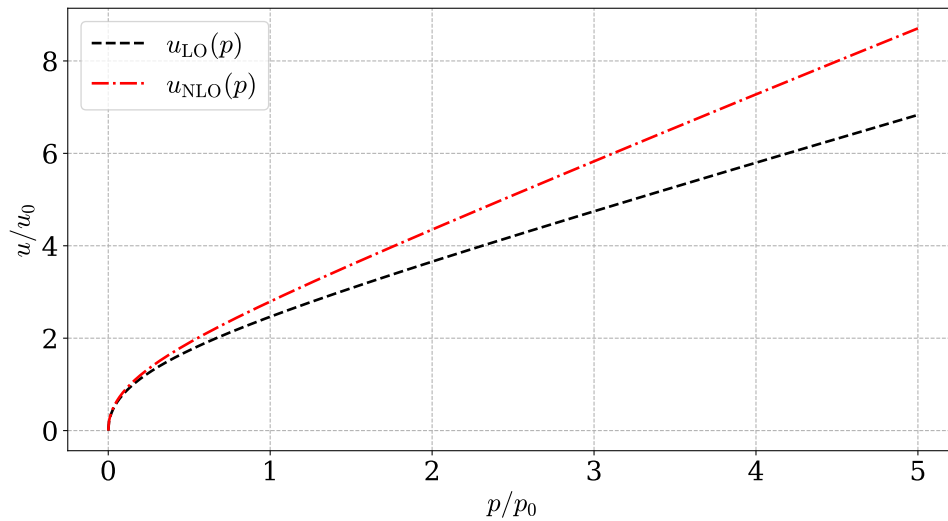


Figure 6.15: The NLO equation of state compared to the LO results. The characteristic quantities are $u_0 = p_0 = m_\pi^2 f_\pi^2$.

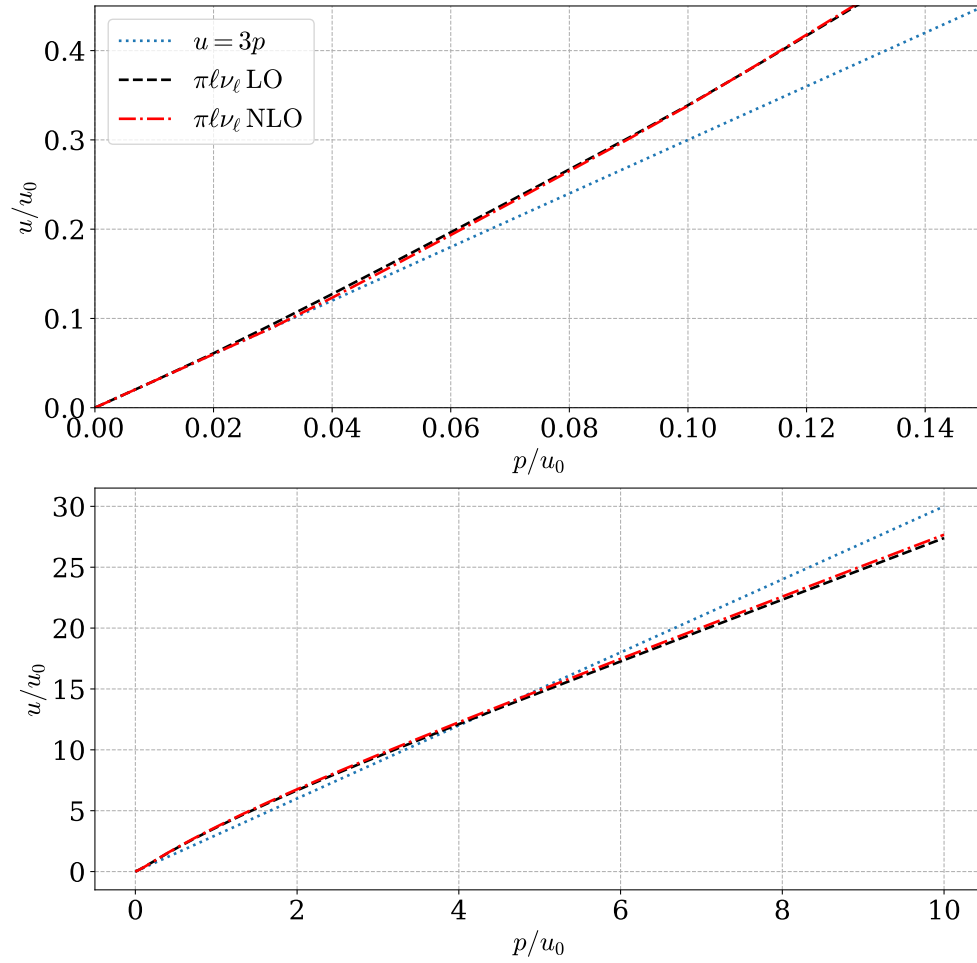


Figure 6.16: The NLO and LO equation of state for the $\pi\ell\nu_\ell$ system are compared for two different regimes. Energy density and pressure are normalized to their characteristic quantities, $p_0 = u_0 = f_\pi^2 m_\pi^2$.

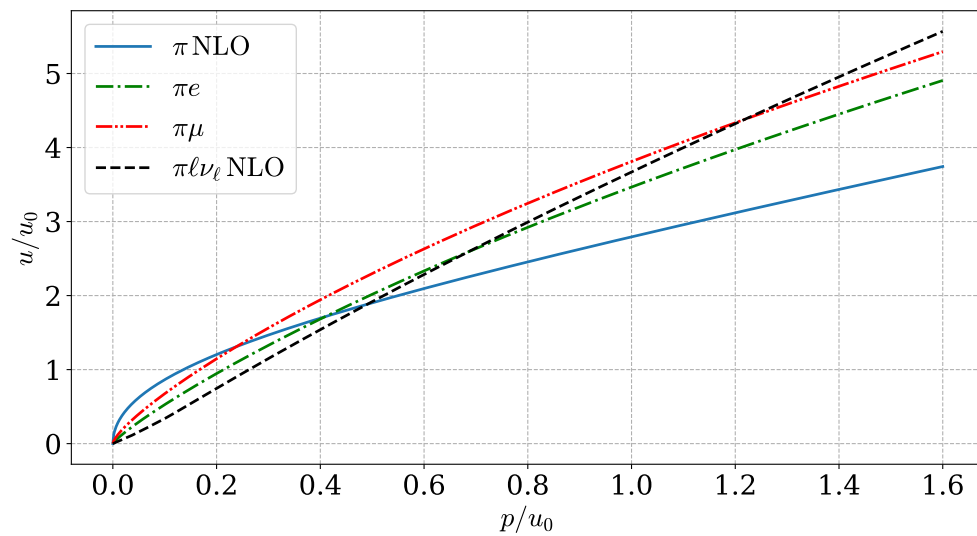


Figure 6.17: The equation of state of pion condensate alone, and including leptons. Both the pressure and the energy density are normalized to $u_0 = f_\pi^2 m_\pi^2$.

Part III

Pion stars

Chapter 7

Pion stars

As we found in section 4.3, the Tolman-Oppenheimer-Volkoff equation, Eq. (4.42), determines the pressure as a function of the radius of a star given the equation of state and the central pressure. From Chapter 6, we have various equations of state for the pion condensate. In this chapter, we will apply these results to study pion stars, bosonic stars composed of a gravitationally bound pion condensate. As these results are analytical, as opposed to earlier numerical results, we can derive limiting behavior. Separate the contributions to equations of state from various sources. This will allow us a more informed discussion on the physical properties of pion stars. At the end, we will compare our results with earlier studies.

7.1 Units and limiting radius

We can gain some insights by reviewing the characteristic quantities of the problem. The characteristic mass and length, as discussed in section 4.3, are found by setting $k_1 = k_2 = k_3 = 1$. These are the dimensionless constants of the TOV equation, Eq. (4.53). Using the values for f_π and m_π as given in section A.1 and reinstating c and \hbar , these quantities are given by

$$u_0 = m_\pi^2 f_\pi^2 \frac{c}{\hbar^3} = 3.216 \cdot 10^{33} \text{ J m}^{-3}, \quad (7.1)$$

$$m_0 = \frac{c^4}{\sqrt{\frac{4\pi}{3} u_0 G^3}} = 64.21 M_\odot, \quad (7.2)$$

$$r_0 = \frac{G}{c^2} m_0 = 94.79 \text{ km}. \quad (7.3)$$

We expect a pion star made up of a pure pion condensate to have dimensions of this order of magnitude, around one order of magnitude larger than the star made up of cold neutrons. However, when we introduce leptons there is not just one characteristic energy scale, and it becomes harder to anticipate the scale of the stars.

In section 6.2, we found that the leading order, the non-relativistic limit of the equation of state of a pure pion-condensate, without electromagnetic interaction, is $\tilde{p} = 8^{-1} \tilde{u}^2$. That is, it is a polytrope with $\gamma = 2$. As discussed in subsection 4.3.1, this corresponds to a situation where the radius of the star is independent of the central pressure, at least in the Newtonian limit of gravity. When simulating the Newtonian, non-relativistic limit of the pion star, we should expect the radius to be constant. From Eq. (4.59), the radius is $R = C\xi_1$, where

$$C = \frac{1}{\sqrt{4(4\pi)Gu_0}} = \frac{1}{\sqrt{12}} r_0, \quad (7.4)$$

and ξ_1 is the root of the Lane-Emden function $\theta(\xi)$ for polytrope index $n = 1$, the solution to

$$\theta'' + \frac{2}{\xi}\theta' + \theta = 0. \quad (7.5)$$

By substituting θ for its power series expansion, $\theta = \sum_n a_n \xi^n$, we get

$$\sum_n [(n+2)(n+1)a_{n+2} + 2(n+1)a_{n+1}\xi^{-1} + a_n] \xi^n = 0. \quad (7.6)$$

This must be obeyed for arbitrary ξ . We therefore get the recursion relation $a_{n+2} = -a_n/(n+1)(n+2)$. With our boundary conditions, the solution is

$$\theta(\xi) = \frac{\sin(\xi)}{\xi}, \quad (7.7)$$

and the first root is therefore $\xi_1 = \pi$. With this, we get a closed-form expression for the stellar radius of this non-relativistic and Newtonian limit—which we expect the full theory to approach as the central pressure decreases—namely

$$R = \frac{\pi}{\sqrt{12}} r_0 = 85.97 \text{ km}. \quad (7.8)$$

When including electromagnetic interactions, as done in subsection 6.2.2, the non-relativistic equation of state remains a polytrope with $\gamma = 2$, however with a new constant by a factor $(1 + \Delta)^2$, where $\Delta = \Delta m_{\text{EM}}^2/m_\pi^2$. This affects the limiting radius, which now is

$$R = \frac{\pi}{\sqrt{12}(1 + \Delta)} r_0 = 80.40 \text{ km}. \quad (7.9)$$

These limits are only available when considering the pion condensate alone, without leptons. As we found, the inclusion of leptons will change the low-density limit of the equation of state, and it is only for $\gamma = 2$ where the Lane-Emden equation admits a finite limit radius of this sort.

7.2 Leading order results

In this section and the next, we present the results of numerically integrating the TOV equation using the various equations of state we have obtained. The computer code used to obtain these results is discussed in Appendix D.

7.2.1 Pion star of pure pion condensate

We start with the simplest case of a pure pion condensate, in which there are only strong interactions, to leading order as described in subsection 6.2.1. The equation of state of this system is shown in Figure 6.2. Figure 7.1 shows the pressure and mass as a function of radius for varying values of central pressure. The quantities are normalized to the central pressure, stellar mass, and stellar radius, respectively. The black dashed line corresponds to the configuration with the maximum mass. We see that both the pressure and mass distribution are very similar for stars with a mass less than the maximum. As the central pressure increase beyond that of the star with maximum mass, the pressure close to the center grows sharply. This is similar to what we saw in the case of an incompressible fluid, subsection 4.3.2.

Figure 7.2 shows the mass-radius relation for the pion star. As in the case of the neutron star it has a maximum mass, $M_{\text{max}} = 10.47 M_\odot$, and a corresponding radius $R = 55.44 \text{ km}$. However, in contrast to the case of the neutron star, the stellar radius approaches a maximum

radius as the central pressure decreases. This matches our expectation from the non-relativistic, Newtonian limit. We see that the largest radius in our results, corresponding to $p_c = 10^{-6} p_0$, is $R = 85.91$ km, an excellent fit with our earlier analysis, Eq. (7.8). Figure 7.3 compares the mass-radius relation from the full equation of state and TOV equation with various limits. In the non-relativistic, Newtonian limit, the stellar radius is independent of the mass, as we found in our earlier analysis.

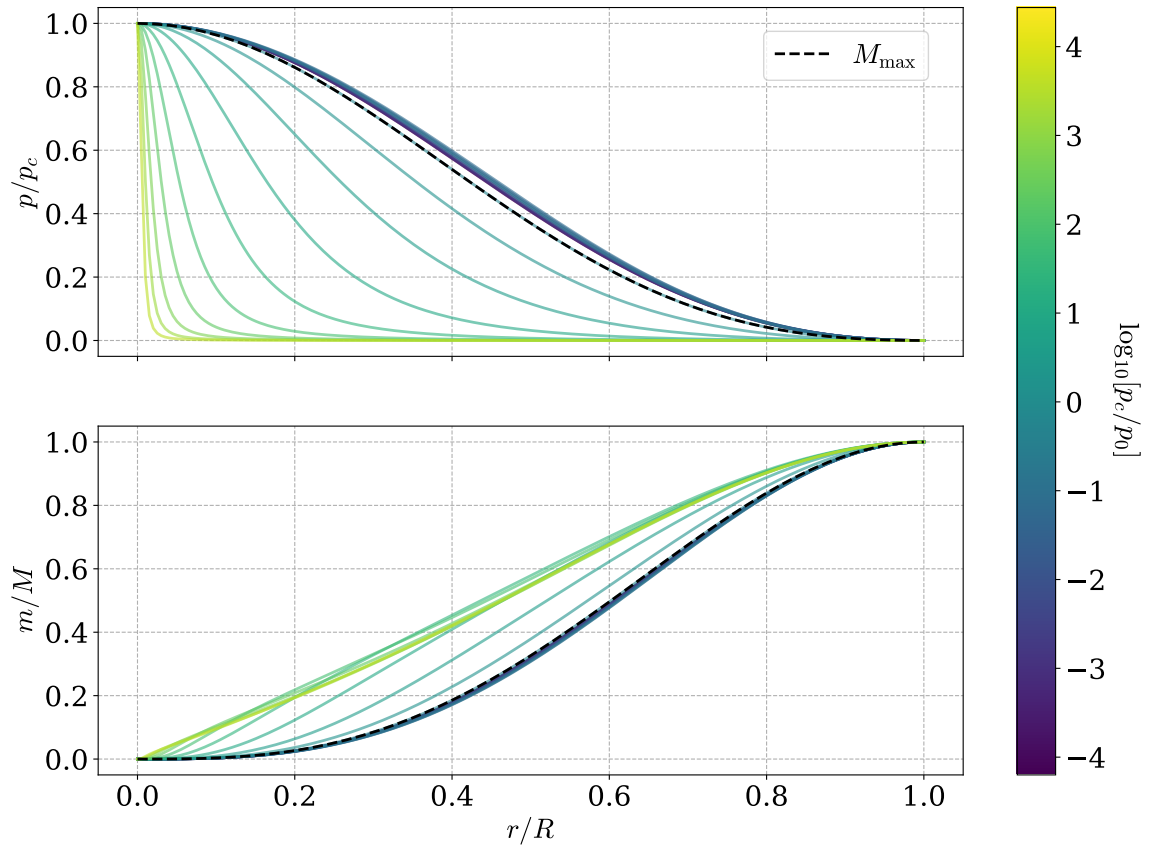


Figure 7.1: Top: The pressure normalized to the central pressure. Bottom: The mass, normalized to the stellar mass. Both are functions of radius r , normalized to the stellar radius, and the plots show a range of stars with different central pressures, indicated by the color. The black dashed line corresponds to the star with the largest mass.

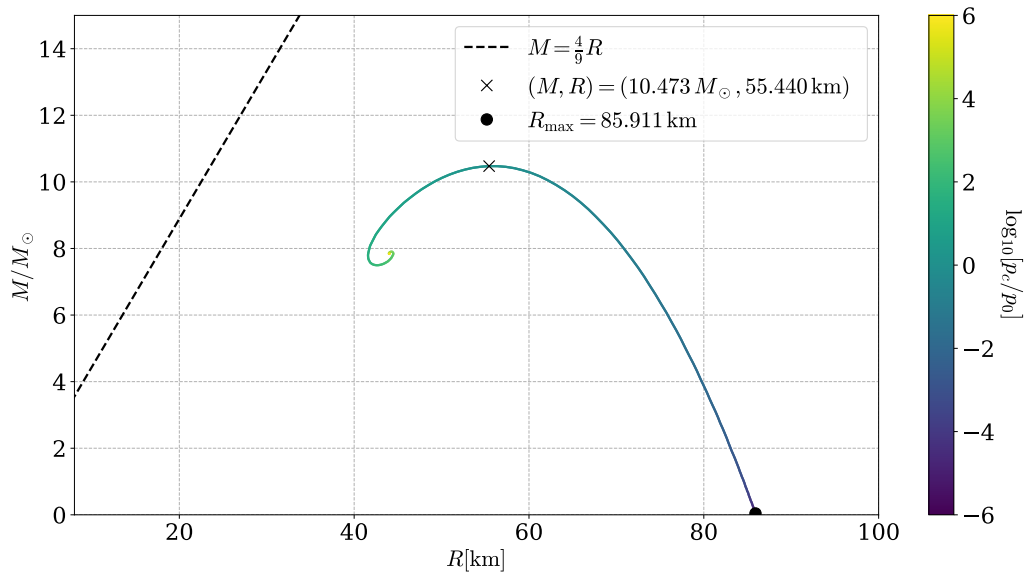


Figure 7.2: The mass-radius relation of a pion star of a pure pion condensate, to the lowest order using χ PT. The mass is given in units of solar masses, while the radius is measured in kilometers. This line is parameterized by the central pressure p_c of the star, as indicated by the color gradient. The dashed black line indicates the theoretical maximum mass for a given radius, and any configuration above it will collapse to form a black hole.

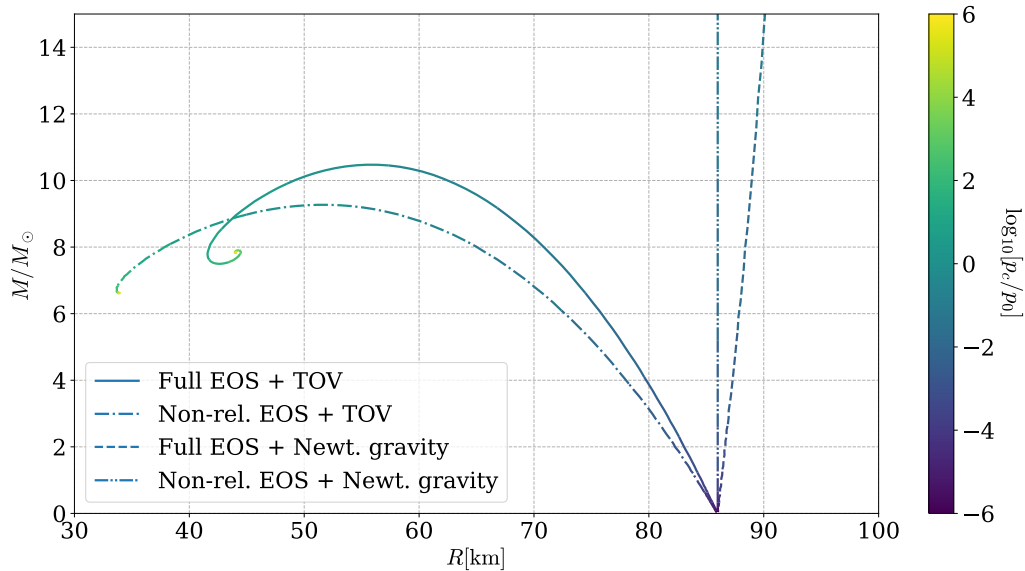


Figure 7.3: The mass-radius relationship of the pion star using the full, leading-order equation of state from χ PT and the TOV equation, compared with results in various limits.

7.2.2 Including electromagnetic contributions

As we found in subsection 6.2.2, the electromagnetic interaction of the pseudoscalar mesons contributes to the equation of state, even at leading order. Figure 6.3 shows the pressure and energy density, normalized to their characteristic quantities, as a function of chemical potential above the critical value, normalized to m_π . Figure 6.4 shows the equation of state. The results with and without electromagnetic results are compared. We see that the inclusion of electromagnetic contributions results in a less stiff equation of state; a given pressure corresponds to a higher energy density when including electromagnetic interactions.

Figure 7.4 shows the mass-radius relation of the pion star when the electromagnetic interaction is taken into account and compares it with our earlier result. We see that the shape of the curve has not changed much from the earlier result. Both the maximum mass and radius are slightly smaller. As discussed in section 4.4, we expect a stiffer equation of state to correspond to a more massive star, as happens in this case. The new result for maximum radius, $R = 80.40$ km, is in excellent agreement with our expectation, Eq. (7.9).

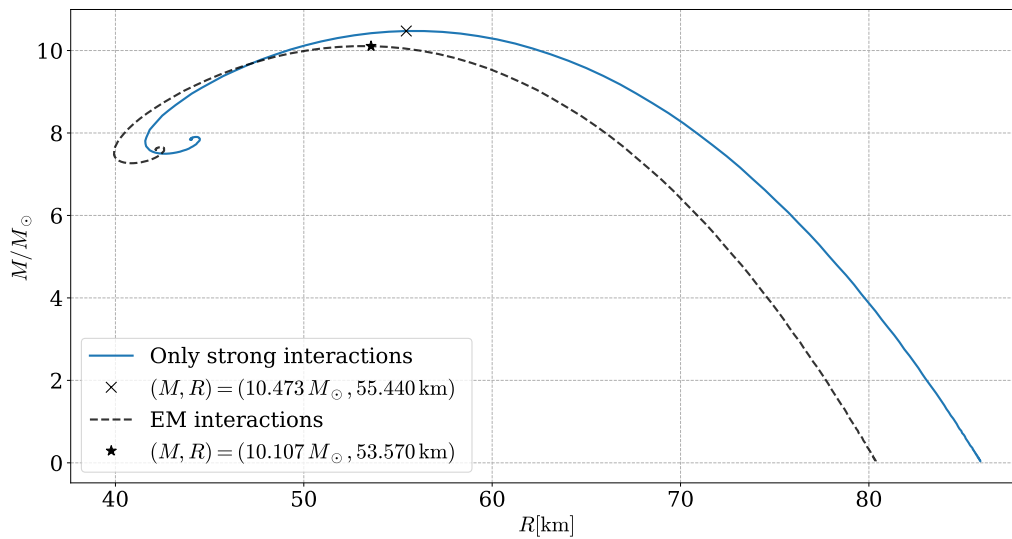


Figure 7.4: The mass-radius relation of pion stars with and without the effects of electromagnetism. The mass is in units of solar masses, the radius in kilometers. The marked points are the maximum mass and corresponding radius of the stars.

7.2.3 Charge neutral stars

We now apply the results from section 6.4, where we added a lepton to enforce charge neutrality. As the electromagnetic force is long-range, we should expect any macroscopic astronomical object to be charge neutral. First, we apply the system of pions and one charged lepton. The star with electrons is shown in Figure 7.5. We see that this star is much larger than those made of only pions. This is because the light electrons make the equation of state stiffer at low pressures. The non-relativistic equation of state is now a polytrope with $\gamma = \frac{5}{3}$, instead of $\gamma = 2$, and there is no upper limit on the radius. The maximum mass is now $239 M_\odot$, and the corresponding maximum radius is 3.2×10^4 km.

The mass-radius relation for a star where the lepton is a muon is shown in Figure 7.6. This has a similar form to the one with the electron, only smaller and lighter, as the equation of state, in this case, is less stiff. The maximum mass is now $18.6 M_\odot$, and the corresponding maximum radius is 262 km.

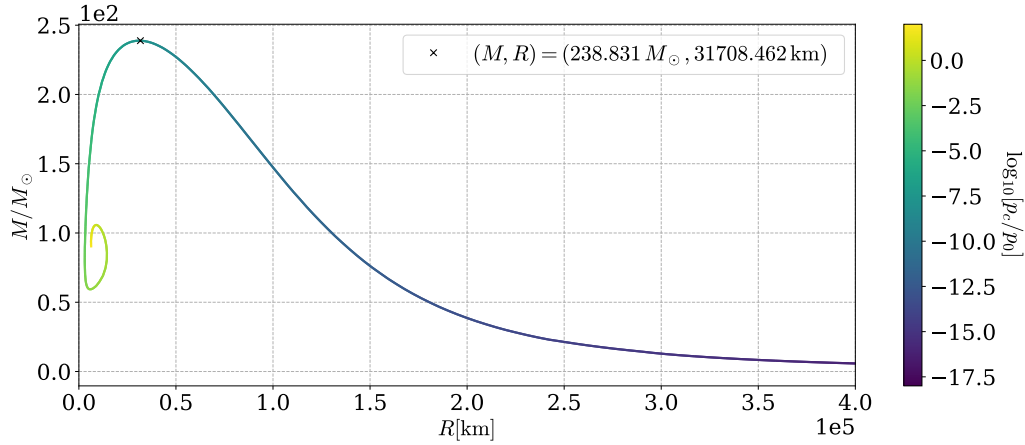


Figure 7.5: The mass-radius relation of pion stars, including electrons to enforce charge neutrality, is parameterized by the central pressure. The mass in units of solar masses, the radius in kilometers, and the pressure in $p_0 = f_\pi^2 m_\pi^2$.

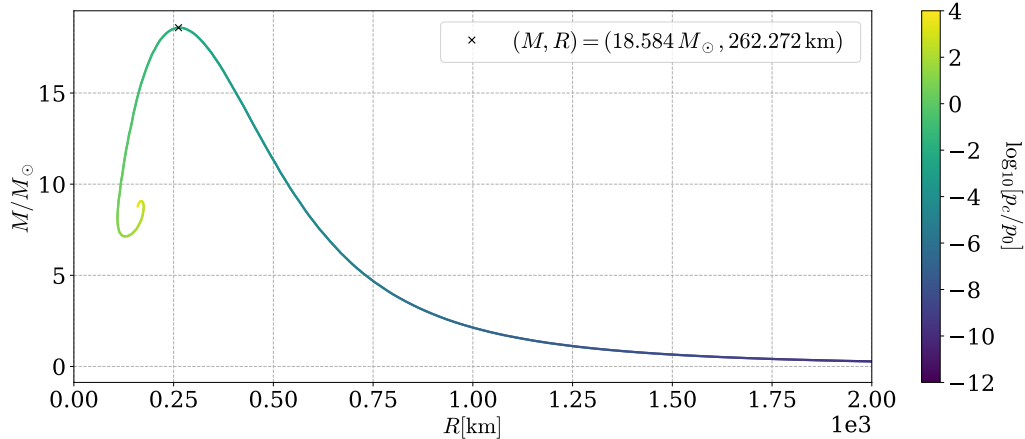


Figure 7.6: The mass-radius relation of pion stars, including muons to enforce charge neutrality, is parameterized by the central pressure. The mass in units of solar masses, the radius in kilometers, and the pressure in $p_0 = f_\pi^2 m_\pi^2$.

7.2.4 Neutrinos

As discussed in subsection 6.4.1, a more realistic charge-neutral pion condensate includes weak decay, in which case both electrons and muons will be present and in chemical equilibrium with their respective neutrinos. The equation of state is dominated by the neutrinos, as illustrated in Figure 6.13, and is therefore well approximated by $u = 3p$. Below the point where the pion condensate vanishes, at $p_{\min} = 1.84 \times 10^{-2} u_0$, the equation of state is exactly $u = 3p$. A star with such an equation of state will not have a finite radius where the pressure vanishes. However, as the isospin density vanishes at p_{\min} , we define the stellar radius R by $p(R) = p_{\min}$. Such a star will therefore have an atmosphere of ultrarelativistic neutrinos. When we defined the stellar radius by $p(R) = 0$, the $p + u$ factor in the TOV equation, Eq. (4.42), vanishes as we approach the surface of the star, while for this new definition, $p + u \geq 4p_{\min}$ at all radii. Close to the surface, the pressure will therefore fall faster. The resulting mass-radius relation is shown in Figure 7.7. We see that, in contrast to the earlier results, both the mass and radius approach zero as $p_c \rightarrow p_{\min}$. The maximum mass is now $M_{\max} = 18.8M_{\odot}$, with a corresponding radius $R = 125$ km. At the bottom of Figure 7.7, the pion stars including charged leptons and neutrinos are compared to a family of stars with $u = 3p$ but different values for p_{\min} . As p_{\min} increases, the mass-radius relation is scaled down, and as it approaches zero, the maximum mass will diverge. We see that the mass-radius relation of the pion star closely resembles that of such a star, and, therefore, is mostly set by p_{\min} . The equation of state of the $\pi\ell\nu_{\ell}$ -system is somewhat less stiff than $u = 3p$, at least for central pressures below that of the maximum mass star, and we see that the result is a smaller and lighter star for the same value of p_{\min} .

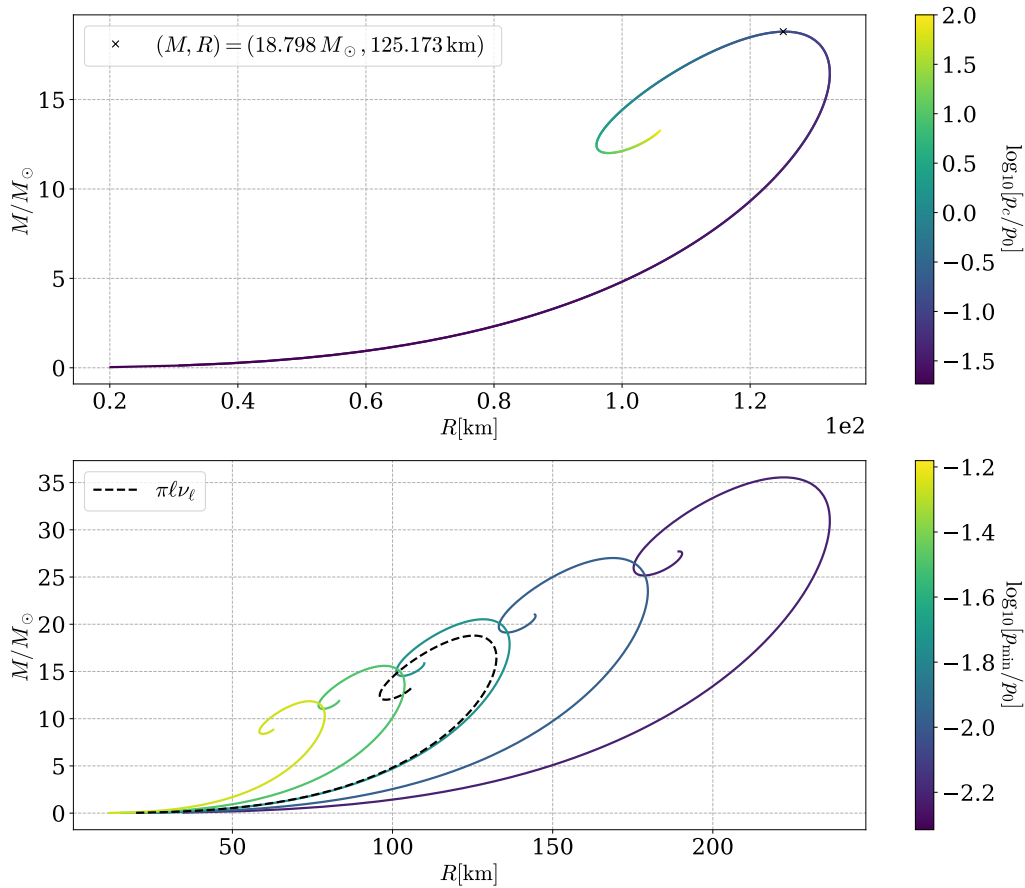


Figure 7.7: The mass-radius relation of pion stars, including leptons and neutrinos in equilibrium. The radius is given in kilometers and the mass in units of solar masses. Top: The full $\pi\ell\nu_{\ell}$ -system, with maximum mass marked by a cross. Bottom: The $\pi\ell\nu_{\ell}$ -system is compared to results using $u = 3p$, and different values of p_{\min}

7.3 Next-to-leading order results

In section 6.5, we calculated the NLO free energy of the pion condensate, and with this, we found the NLO equation of state of the pure pion condensate as well as the $\pi\ell\nu_\ell$ -system. We now use these equations of state to obtain the corresponding NLO mass-radius relations. Figure 7.8 shows the NLO mass-radius relation of a pion star composed of a pure pion condensate and compares it to the LO result. The results are similar, however, the next-to-leading order star is smaller and less massive, as is expected for a less stiff equation of state. The maximum mass of the NLO star is $M_{\text{max}} = 9.64 M_0$, and the corresponding radius is $R = 54.09 \text{ km}$.

The NLO mass-radius relation of pion stars including charged leptons and neutrinos are shown in Figure 7.9. As discussed in section 6.5, the change in the equation of state from LO to NLO is small, and as a consequence, the difference in the mass-radius relations is too. However, for $p < 0.1p_0$, the NLO equation of state is slightly stiffer. From Figure 7.7, we see that this is the relevant range for stars with a central pressure less than that of the maximum mass star. As expected the NLO pion star is therefore slightly larger and more massive. This relationship is still well approximated by a $u = 3p$ equation of state with some cut-off pressure p_{min} .

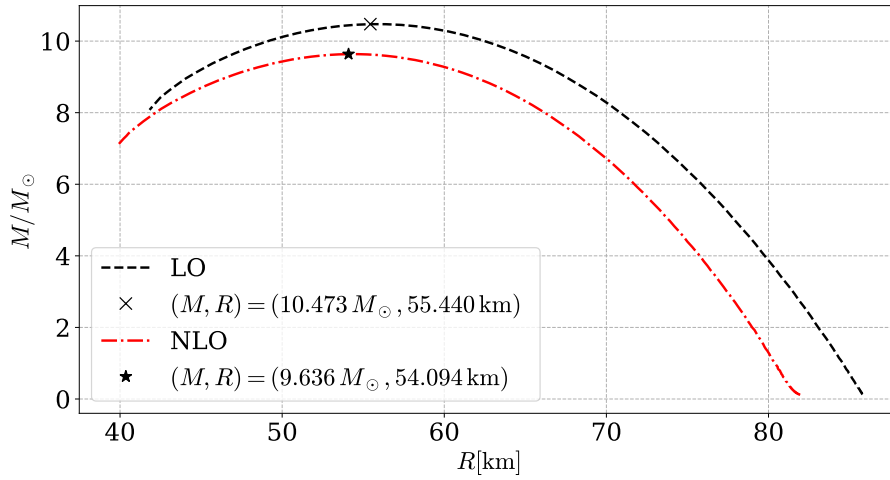


Figure 7.8: The LO and NLO mass-radius relation of pion stars composed of a pure pion condensate are compared. The mass is given in solar masses and the radius in kilometers.

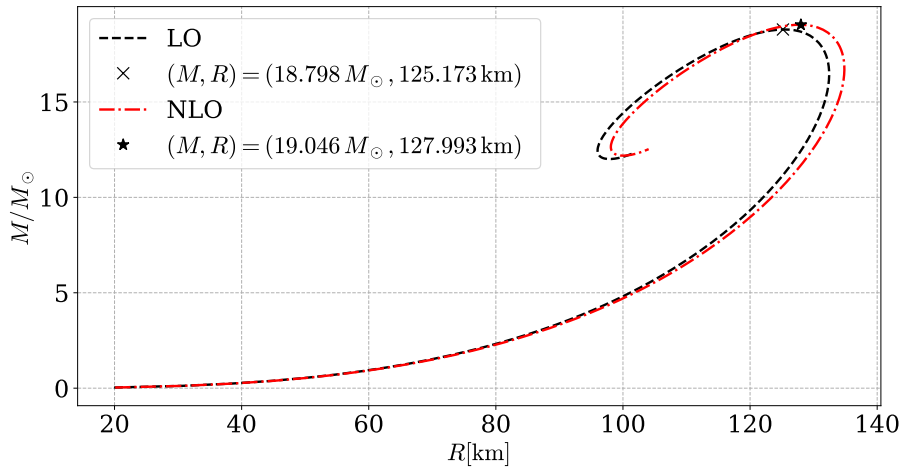


Figure 7.9: The LO and NLO mass-radius relation of pion stars composed of a pion condensate including leptons and neutrinos are compared. The mass is given in solar masses and the radius in kilometers.

7.4 Key values and results

We have modeled pion stars using the equation of state of pion condensates including various effects such as electromagnetism, loop-corrections, charge neutrality and weak interactions. These various compositions create stars of wildly different sizes and masses. In this section, we compile the main results. In Table 7.1 we have combined some key figures for the maximum mass configuration for the different equations of state. For all the star families, except those of a pion condensate and only electrons, the masses and radii are within an order of magnitude of m_0 and r_0 . We can explain this by considering that for all these systems, the only energy scales are f_π , m_π and m_μ , which all are close to 100 MeV. This is true even for the $\pi\ell\nu_\ell$ -system, as in this case the energy scale is $p_{\min}^{1/4} \propto m_\pi$. The πe -system, on the other hand, has a different, much lower energy scale, $m_e \approx 0.5\text{MeV}$, which leads to a corresponding much larger radius and mass for the resulting star.

We see that, for all the different stars, μ_I is well below the threshold $4\pi f_\pi \approx 8.6 m_\pi$ for the convergence of chiral perturbation theory. The range of validity is somewhat smaller than this, as new degrees of freedom that we have not taken into account come into play. The lightest particle not in our model is the ρ -meson, with mass $m_\rho = 770\text{ MeV} \approx 5.7 m_\pi$, which is still well above the energies in our result. For the most realistic composition, the $\pi\ell\nu_\ell$ -system, the isospin chemical potential at the center for the maximum mass star is around $0.02 m_\pi$. This means that the pion condensate throughout this star, and all those with a lower central pressure, is only slightly above the point of phase transition.

In Figure 7.10 we compare the mass-radius relations of the different stars. We only include the next-to-leading order result for pure pion condensation and the $\pi\ell\nu_\ell$ -system. This is a logarithmic plot, as both the masses and radii vary over several orders of magnitude. Figure 7.11 shows the mass and pressure distributions of the maximum mass configurations of the various stars. Among the mass distributions, the $\pi\ell\nu_\ell$ -system stands out as the mass increases in a straight line, as opposed to the other distributions, which taper off towards the surface of the star. In the bottom plot, we see that the pressure of all the stars approaches 0 as r approaches R except for the $\pi\ell\nu_\ell$ -system which approaches $p_{\min} > 0$. All stars obey the necessary criterion for stability, as discussed in subsection 4.4.5, for central pressures below that of the maximum mass star. Stability analysis done in [6] shows that, as we expect, the stars are stable in this case.

Table 7.1: The values of some key quantities for the maximum mass configurations of the various stars.

system	M_{\max}/M_\odot	R/km	u/u_0	p/u_0	$\mu_I/m_\pi - 1$
π LO	10.47	55.47	2.865	1.318	1.100
π NLO	9.64	54.09	3.020	1.139	0.9256
π EM	10.11	53.57	2.930	1.318	1.116
πe	238.8	3.171×10^4	2.550×10^{-6}	1.995×10^{-8}	6.222×10^{-7}
$\pi\mu$	18.58	262.3	0.1411	1.202×10^{-2}	1.732×10^{-2}
$\pi\ell\nu_\ell$	18.80	125.2	0.5399	0.1492	2.030×10^{-2}
$\pi\ell\nu_\ell$ NLO	19.05	128.0	0.4960	0.1391	1.801×10^{-2}

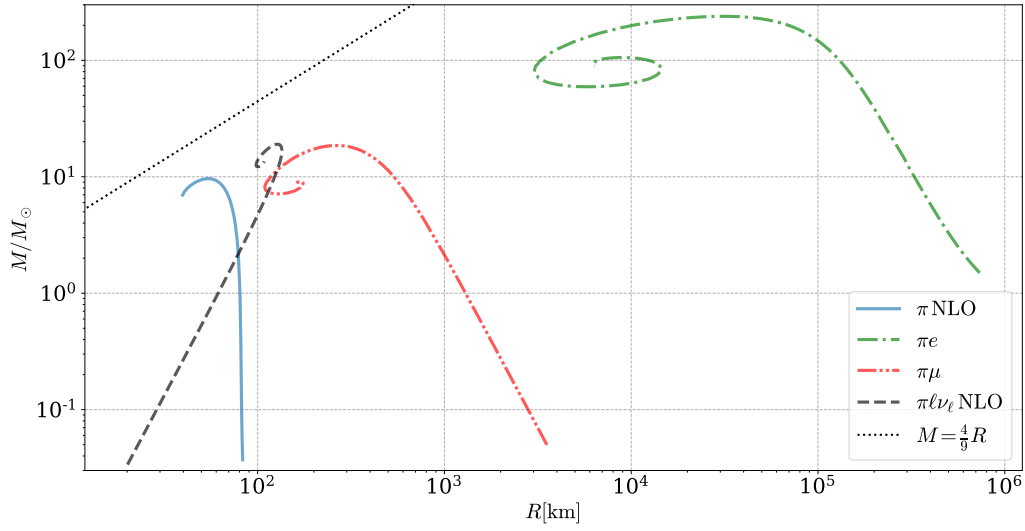


Figure 7.10: The mass-radius relations of pion stars of various compositions are compared. The radius is given in kilometers and the mass in units of solar masses.

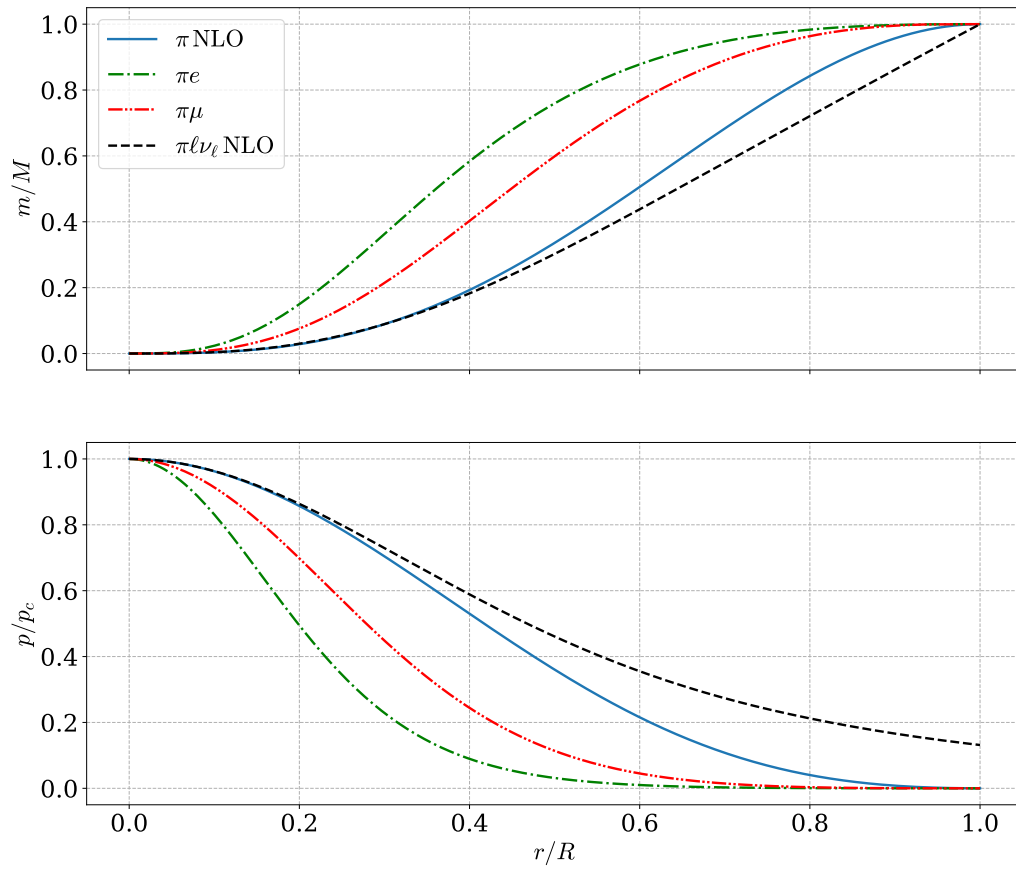


Figure 7.11: The pressure and mass of the maximum-mass configuration of pion stars of various compositions. The mass, pressure, and radius are normalized to the star's stellar mass, central pressure and stellar radius.

7.5 Comparison with lattice QCD results

In this section, we compare our results with earlier results obtained using lattice QCD methods. These are first-principle numerical methods that use QCD directly without any assumption of symmetry breaking or the construction of an effective theory. The results of Brandt et al. for the equation of state of the pion condensate and the system with pions and electrons or muons, presented in [6], are shown and compared with our results in Figure 7.12. With these equations of state, they obtained the mass-radius relations of pion stars. We compare our results for the various mass-radius relations with theirs, including uncertainties, in Figure 7.13.

Brandt et al. do not use the values of physical constants from the Particle Data Group (PDG) [78], as we have used in this thesis. Instead, they use the central values [74]

$$m_\pi = 131 \text{ MeV}, \quad (7.10)$$

$$f_\pi = 90.5 \text{ MeV}, \quad (7.11)$$

$$m_K = 481 \text{ MeV}. \quad (7.12)$$

Changing these constants will shift the equations of state, and consequently the mass-radius relations. To leading order, the energy density and pressure of the pure pion condensate are

$$\frac{p}{p_0} = \frac{1}{2} \left(\frac{\mu_I}{m_\pi} - \frac{m_\pi}{\mu_I} \right)^2, \quad \frac{u}{u_0} = \frac{1}{2} \left(2 + \frac{\mu_I^2}{m_\pi^2} - 3 \frac{m_\pi^2}{\mu_I^2} \right). \quad (7.13)$$

The change in constants therefore only leads to a scaling of the equation of state, and consequently a scaling of the mass-radius relations. The dependence of the characteristic radius and mass on the energy density is

$$r_0 \propto m_0 \propto \frac{1}{\sqrt{u_0}} = \frac{1}{m_\pi f_\pi}. \quad (7.14)$$

As a result, r_0 and m_0 increase about 5% if we use the lattice constants instead of those from the PDG. When including other leptons and thus other mass scales or higher-order corrections, the exact effect of changing these constants becomes more complicated than a simple scaling, as there are several scales. However, the magnitude of the shift is similar. In Figure 7.14, we compare both leading order and next-to-leading order results using both the constants from the PDG and those used by Brandt et al. On the top are the results of the pure pion condensate and on the bottom the $\pi\ell\nu_\ell$ -system. These results are compared with the those of Brandt et al. from [6]. In all cases, we see that lowering constants results in larger and heavier stars.

There is, in general, good agreement between the results of Brandt et al. and our results. In the case of the pure pion-condensate using lattice constants, we see that the next-to-leading order equation of state is a significantly better fit than the leading order results, at least for $p < 0.5u_0$. This is within the region where we noted chiral perturbation theory seems to converge quickly. The different constants here do not affect the results significantly, as we compared normalized pressure and energy density. For the mass-radius relation of the pure pion star, we see that the next-to-leading order results using the constants from the lattice simulation are in very good agreement with the numerical results, and are a significant improvement over the leading order results. The fact that the results using the PDG constants become a less good fit from LO to NLO suggests that the lattice constants give a better comparison. In the case of the $\pi\ell\nu_\ell$ -system, the results using lattice constants are the best fit. Here, the leading order results alone are in good agreement as the neutrino is dominating. There is a modest improvement in the agreement at the next-to-leading order.

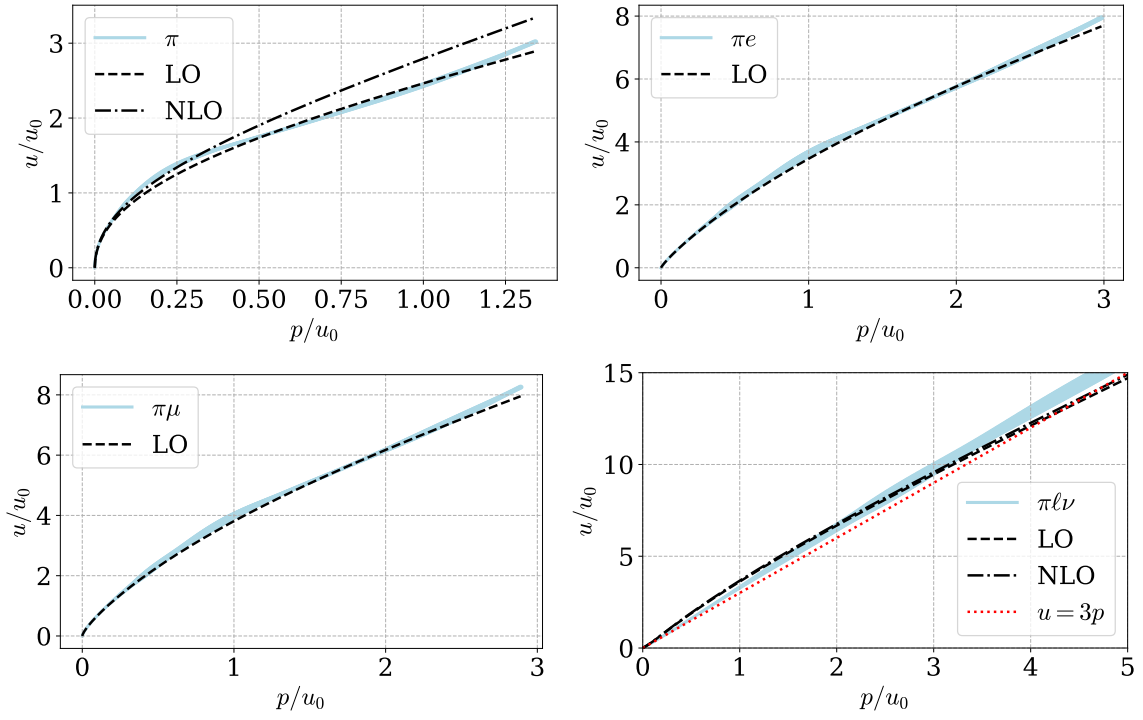


Figure 7.12: The equation of state of the pion condensate with and without charged leptons. The results of Brandt et al., in solid color incorporating uncertainty, are compared to the results presented in Chapter 6. Both energy density and pressure are shown in units of $u_0 = f_\pi^2 m_\pi^2$. The data was provided by the authors [6].

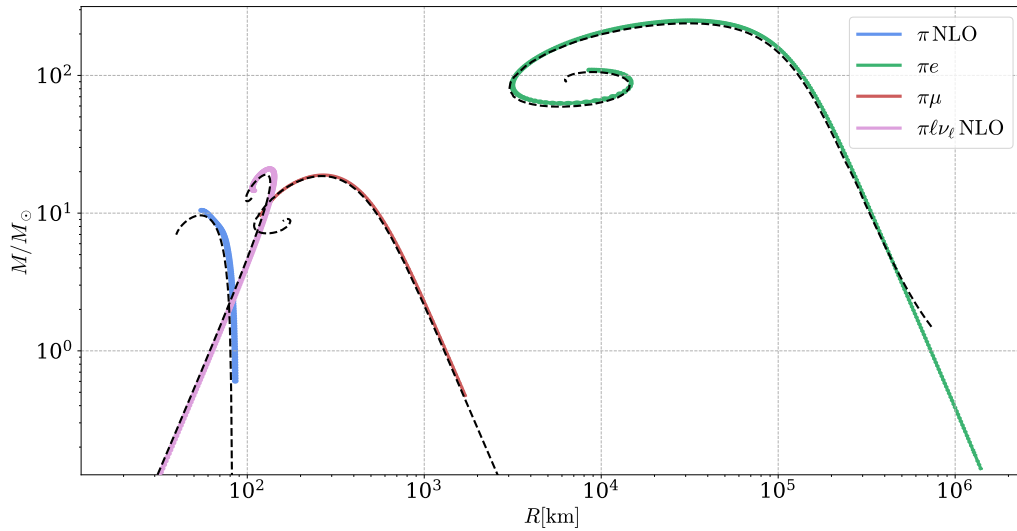


Figure 7.13: The mass-radius relations for the various pion stars. The results of Brandt et al., solid color incorporating uncertainty, are compared with our LO results, dashed lines. The radius is in units of km, while mass is in solar masses, M_\odot . The data was provided by the authors [6].

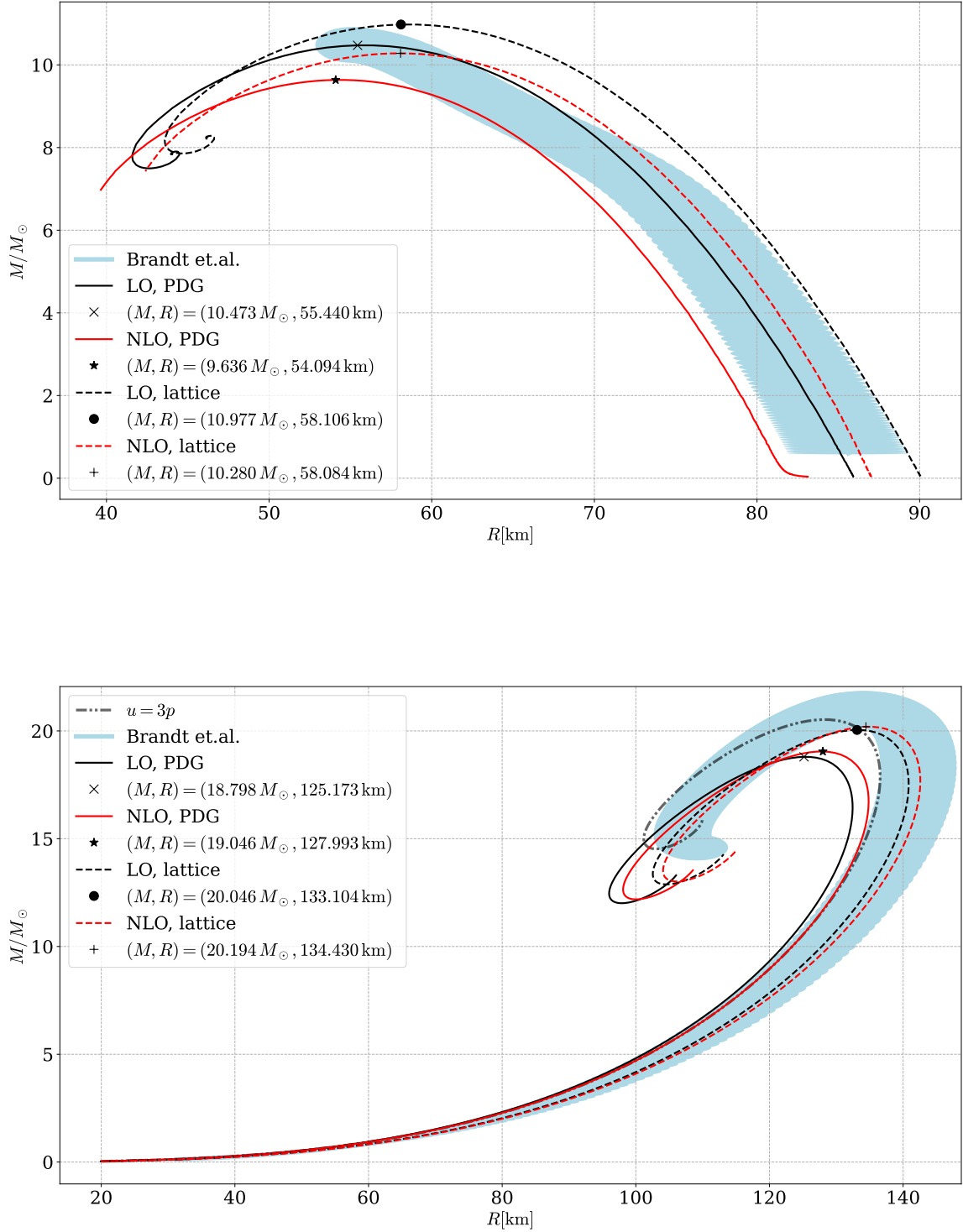


Figure 7.14: The mass-radius relations, using the constants from the PDG [78] or as used in lattice QCD calculations [6]. The results are compared with the results of [6]. On the top are the results from a pure pion condensate, while at the bottom are the results of the $\pi l \nu_l$ -system.

Chapter 8

Concluding remarks

8.1 Summary

In this thesis, we have investigated the ground state of QCD for isospin chemical potential greater than the pion mass—the pion condensed phase. The results have been applied to model how a pion condensate might form compact astronomical objects, pion stars. These objects were first proposed by Carignano et al. in [7] and investigated by Brandt et al. in [6] using QCD lattice methods.

8.1.1 Pion condensate

We investigated the meson sector of zero-temperature quantum chromodynamics using three-flavor chiral perturbation theory. By exploiting the spontaneous breaking of the approximate $SU(3)_L \times SU(3)_R$ symmetry of the three lightest quarks, the up, down and strange quarks, one can construct an effective field theory of the resulting pseudo-Goldstone bosons. With this effective theory, we calculated the phase diagram in the $\mu_S - \mu_I$ -plane at $T = 0$. At $\mu_I = m_\pi$, a second-order phase transition from the vacuum phase to the pion-condensed phase occurs. Similar second-order transitions occur between the vacuum phase and the charged kaon- and neutral kaon-condensed phase. These condensed phases are separated by first-order phase transitions. We calculated the effects of electromagnetic interactions on this phase diagram.

Focusing on the pion-condensed phase, we found the equation of state to leading order, next-to-leading order, and including the effects of electromagnetism. Furthermore, we found the equations of state of systems of a pion condensate together with charged leptons. This ensures charge-neutrality, which is more realistic as a basis for astronomical objects. Lastly, we included the effects of weak interactions and calculated the equation of state of the $\pi\ell\nu_\ell$ -system in which the pion condensate, charged leptons, and neutrinos are in chemical equilibrium at next-to-leading order.

8.1.2 Pion stars

The equations of state for the various configurations were used, in conjunction with the TOV equation, to model pion stars. We calculated their energy and pressure profiles, and thus obtained the mass-radius relations. The size and mass of pion stars vary greatly based on their composition, and so did how the radius changes as the mass increases. We showed analytically that the limiting radius of a pion star composed of a pure pion condensate with only strong interactions is $R = 85.97$ km, and becomes $R = 80.40$ km when including electromagnetic

interactions. We further showed that the equation of state of the $\pi\ell\nu_\ell$ -system is closely approximated by that of ultrarelativistic fermions or electromagnetic radiation for $T > 0$, $u = 3p$, as the neutrino contribution to the equation of state dominates. The resulting mass-radius relation is therefore mostly defined by the pressure p_{\min} at the surface of the star, where the pion condensate vanishes and the neutrino atmosphere begins.

8.1.3 Comparison with data

Large parts of the low-temperature QCD phase diagram are inaccessible for investigation from first principles. Asymptotic freedom allows for some results at asymptotically high temperatures or densities, such as the color superconducting phase at high densities. However, due to the running of the strong coupling constant, perturbation theory breaks down below around 1 GeV. Currently, the only method available for this regime is QCD lattice methods, numerical schemes which calculate the path integral on a discrete lattice using the Metropolis-Hastings algorithm. At finite baryon densities, this method fails due to the sign problem. The zero baryon number sector, however, can be and has been investigated with QCD lattice methods. This allows us to test our effective theories, such as chiral perturbation theory. We compare our results with those of Brandt et al., in which they calculated the equation of state of the pion-condensed phase, as well as the resulting pion star mass-radius relations [6].

When comparing with the results for the pion star mass-radius relations, we have to take into account the fact that the pion mass is slightly different in the lattice QCD system. Using the lattice values, we find very good agreement in all cases. Here too, the agreement improves using the next-to-leading order results, in comparison with the leading order results. The good agreement between χ PT and QCD lattice methods increases our confidence in both methods, and as a consequence the confidence in our understanding of pion stars.

8.2 Outlook and further research

We have made several approximations in the calculation of the equation of state in this thesis. Improving on these calculations will yield more accurate results. Although we included the effects of electromagnetism in the pure pion condensate, we have not carried these effects over to the $\pi\ell\nu_\ell$ -system. The next-to-leading order Lagrangian including electromagnetic effects has been derived [69], which could in principle be used to calculate the NLO equation of state, although this might prove to be prohibitively difficult. The phase diagram could also be improved by a next-to-leading order treatment. A fully consistent power counting entails, in the case of the leading order pion condensate, calculating electromagnetic effects in the lepton sector to and including $\mathcal{O}(e^2)$. In the case of the next-to-leading order pion condensate, one should include one-loop effects. A further improvement to the accuracy of the pion condensate calculation would be to take into account the effects due to $\Delta m \neq 0$. This leads to different masses for the charged and neutral kaons, as well as a mixing of the neutral pion and the η -particle.

By themselves, pions are unstable particles. The neutral pion decays mainly via $\pi^0 \rightarrow \gamma\gamma$, and has a mean lifetime of $\tau = 8.45 \times 10^{-17}$ s [78]—incredibly short. The decay of the charged pions is suppressed due to the conservation of electric charge, and their main decay process is $\pi^\pm \rightarrow \mu\nu_\mu$ as discussed in section 6.4. Still, their mean lifetime is only $\tau = 2.60 \times 10^{-8}$ s [78]. These timescales are much smaller than that of astronomical objects, which immediately casts some doubt on the research project of pion stars. However, these results are for the vacuum state. In the $\pi\ell\nu_\ell$ -case the electrons and muons fill the Fermi-sphere up to their Fermi momentum, as we are considering $T = 0$, and the decay is thus Pauli-blocked. Even if the final decay-states are available, in the pion condensate they are suppressed by μ_I^{-3} [6]. For a more complete understanding of pion stars, research into time evolution is required. An investigation of the

decay of the pion condensate is then necessary. The most realistic case, the $\pi\ell\nu_\ell$ -system, has a neutrino atmosphere. In the creation of neutron stars, the escape of neutrinos plays a vital role in cooling the system down [54]. We similarly expect the neutrino atmosphere of the pion star to evaporate. This will change the conditions at the surface of the star, such as the surface pressure p_{\min} . We found that this was crucial for the mass-radius relation, so a more realistic model must take this into account. Here, finite temperature effects might play a vital role.

Pion stars, like neutron stars, are compact objects. This allows us to approximate them as having zero temperature, as $T \ll m_\pi$ while $\mu \approx m_\pi$. A more realistic model would take into account thermal effects. This is especially important in the case of the $\pi\ell\nu_\ell$ -system. Due to the dominating contribution to the equation of state from the neutrinos, the isospin density remains small even at the core of the most massive star. The isospin chemical potential is just $0.02 m_\pi$ above the pion condensation transition. Calculations of thermodynamic properties of the pion condensate at non-zero temperatures using chiral perturbation theory have shown good agreement with lattice results [82]. This could allow for the modeling of pion stars at non-zero temperature, which is a more realistic model.

For now, the pion star has been a purely theoretical research project. For any such object to form, a strong isospin asymmetry must be present. Such circumstances, as we saw in the section on electric neutrality, can arise due to lepton asymmetry through the weak interaction. It has been shown that high neutrino densities can cause the condensation of pions [83]. The lepton asymmetry of the universe, the abundance of leptons over anti-leptons, is not well known. It has been shown that, within current experimental limits, the trajectory of the early universe through the QCD phase diagram as it cooled and expanded might have entered the pion-condensed phase. If that is the case, pion stars might have formed and left observable traces in cosmological data such as the cosmological background gravitational radiation [37, 38].

Appendices

Appendix A

A.1 Constants and units

All values in this section, except m_ρ , are from the Particle Data Group [78]. To obtain results in the SI-system, we use the following conversion factors, as given by

$$c = 2.998 \cdot 10^8 \text{ m s}^{-1}, \quad (\text{A.1})$$

$$\hbar = 1.055 \cdot 10^{-34} \text{ J s}, \quad (\text{A.2})$$

$$k_B = 1.380 \cdot 10^{-23} \text{ J K}^{-1}, \quad (\text{A.3})$$

$$G = 6.674 \cdot 10^{-11} \text{ m}^3 \text{ kg}^{-1} \text{ s}^{-2}, \quad (\text{A.4})$$

where G is Newton's gravitational constant. The conversion factor between MeV and SI-units is

$$1 \text{ MeV} = 1.60218 \cdot 10^{-19} \text{ J}. \quad (\text{A.5})$$

The fine structure constant and the elementary charge is

$$\alpha = 7.297 \cdot 10^{-3}, \quad (\text{A.6})$$

$$e := \sqrt{4\pi\alpha} = 3.028 \cdot 10^{-1}. \quad (\text{A.7})$$

In astronomical calculation, the solar mass is used, which is

$$M_\odot = 1.988 \cdot 10^{30} \text{ kg}. \quad (\text{A.8})$$

The physical parameters we use are

$$f_\pi = 92.07 \text{ MeV}, \quad (\text{A.9})$$

$$m_{\pi^0} = 134.98 \text{ MeV}, \quad (\text{A.10})$$

$$m_{\pi^\pm} = 139.57 \text{ MeV}, \quad (\text{A.11})$$

$$m_{K^\pm} = 493.68 \text{ MeV}, \quad (\text{A.12})$$

$$m_{K^0} = 497.61 \text{ MeV}, \quad (\text{A.13})$$

$$m_\eta = 547.86 \text{ MeV}, \quad (\text{A.14})$$

$$m_e = 0.5110 \text{ MeV}, \quad (\text{A.15})$$

$$m_\mu = 105.7 \text{ MeV}, \quad (\text{A.16})$$

$$m_N = 939.57 \text{ MeV}. \quad (\text{A.17})$$

The mass of the ρ -meson is used as the energy scale for the low-energy constants, and the value used is

$$m_\rho = 770 \text{ MeV}. \quad (\text{A.18})$$

A.2 Algebra bases

A.2.1 Pauli matrices

The Pauli matrices are

$$\tau_1 = \begin{pmatrix} 0 & 1 \\ 1 & 0 \end{pmatrix}, \quad \tau_2 = \begin{pmatrix} 0 & -i \\ i & 0 \end{pmatrix}, \quad \tau_3 = \begin{pmatrix} 1 & 0 \\ 0 & -1 \end{pmatrix}. \quad (\text{A.19})$$

They obey

$$[\tau_a, \tau_b] = 2i\varepsilon_{abc}\tau_c, \quad (\text{A.20})$$

$$\{\tau_a, \tau_b\} = 2\delta_{ab}\mathbb{1}, \quad (\text{A.21})$$

$$\text{Tr}\{\tau_a\} = 0, \quad (\text{A.22})$$

$$\text{Tr}\{\tau_a\tau_b\} = 2\delta_{ab}, \quad (\text{A.23})$$

$$\text{Tr}\{\tau_a\tau_b\tau_c\tau_d\} = 2(\delta_{ab}\delta_{cd} - \delta_{ac}\delta_{cb} + \delta_{ad}\delta_{cb}). \quad (\text{A.24})$$

Together with the identity matrix $\mathbb{1}$, the Pauli matrices form a basis for the vector space of all 2-by-2 matrices. An arbitrary 2-by-2 matrix M may be written

$$M = M_0\mathbb{1} + M_a\tau_a, \quad M_0 = \frac{1}{2}\text{Tr}\{M\}, \quad M_a = \frac{1}{2}\text{Tr}\{\tau_a M\}. \quad (\text{A.25})$$

A.2.2 Gell-Mann matrices

The Gell-Mann matrices are

$$\begin{aligned} \lambda_1 &= \begin{pmatrix} 0 & 1 & 0 \\ 1 & 0 & 0 \\ 0 & 0 & 0 \end{pmatrix}, \quad \lambda_2 = \begin{pmatrix} 0 & -i & 0 \\ i & 0 & 0 \\ 0 & 0 & 0 \end{pmatrix}, \quad \lambda_3 = \begin{pmatrix} 1 & 0 & 0 \\ 0 & -1 & 0 \\ 0 & 0 & 0 \end{pmatrix}, \quad \lambda_4 = \begin{pmatrix} 0 & 0 & 1 \\ 0 & 0 & 0 \\ 1 & 0 & 0 \end{pmatrix}, \\ \lambda_5 &= \begin{pmatrix} 0 & 0 & -i \\ 0 & 0 & 0 \\ i & 0 & 0 \end{pmatrix}, \quad \lambda_6 = \begin{pmatrix} 0 & 0 & 0 \\ 0 & 0 & 1 \\ 0 & 1 & 0 \end{pmatrix}, \quad \lambda_7 = \begin{pmatrix} 0 & 0 & 0 \\ 0 & 0 & -i \\ 0 & i & 0 \end{pmatrix}, \quad \lambda_8 = \frac{1}{\sqrt{3}} \begin{pmatrix} 1 & 0 & 0 \\ 0 & 1 & 0 \\ 0 & 0 & -2 \end{pmatrix}. \end{aligned}$$

They obey

$$[\lambda_a, \lambda_b] = 2if^{abc}\lambda_c, \quad (\text{A.26})$$

$$\{\lambda_a, \lambda_b\} = \frac{4}{3}\mathbb{1}\delta_{ab} + 2d_{abc}\lambda_c, \quad (\text{A.27})$$

$$\text{Tr}\{\lambda_a\} = 0, \quad (\text{A.28})$$

$$\text{Tr}\{\lambda_a\lambda_b\} = 2\delta_{ab}, \quad (\text{A.29})$$

$$\text{Tr}\{\lambda_a\lambda_b\lambda_c\lambda_d\} = \frac{4}{3}\delta_{ab}\delta_{cd} + 2(d_{abe} + if_{abe})(d_{cde} + if_{cde}). \quad (\text{A.30})$$

where

$$f_{abc} = -\frac{i}{4}\text{Tr}\{\lambda_a[\lambda_b, \lambda_c]\}, \quad d_{abc} = -\frac{i}{4}\text{Tr}\{\lambda_a\{\lambda_b, \lambda_c\}\}. \quad (\text{A.31})$$

where the non-zero elements of f_{abc} and d_{abc} are

$$f_{123} = 1, \quad f_{147} = f_{246} = f_{257} = f_{345} = -f_{156} = -f_{367} = \frac{1}{2}, \quad f_{458} = f_{678} = \frac{\sqrt{3}}{2}, \quad (\text{A.32})$$

$$\begin{aligned} d_{146} &= d_{157} = d_{256} = -d_{247} = d_{355} = -d_{366} = -d_{377} = \frac{1}{2} \\ d_{118} &= d_{228} = d_{338} = -d_{888} = \frac{1}{\sqrt{3}}, \quad d_{448} = d_{558} = d_{668} = d_{778} = -\frac{1}{2\sqrt{3}}, \end{aligned} \quad (\text{A.33})$$

or a permutation of the indices. The indices of f are totally antisymmetric, while those of d are totally symmetric [84].

A.2.3 Gamma matrices

The gamma matrices γ^μ , $\mu \in \{0, 1, 2, 3\}$, obey

$$\{\gamma^\mu, \gamma^\nu\} = 2g^{\mu\nu}\mathbb{1}, \quad (\text{A.34})$$

$$\gamma^{0\dagger} = \gamma^0, \quad \gamma^{i\dagger} = -\gamma^i. \quad (\text{A.35})$$

These matrices, together with

$$\sigma^{\mu\nu} = \frac{1}{2}[\gamma^\mu, \gamma^\nu], \quad (\text{A.36})$$

$$\gamma_A^\mu = \gamma^\mu \gamma^5, \quad (\text{A.37})$$

$$\gamma^5 = \frac{i}{4!} \epsilon_{\mu\nu\rho\sigma} \gamma^\mu \gamma^\nu \gamma^\rho \gamma^\sigma, \quad (\text{A.38})$$

form the Clifford algebra $\text{Cl}_{1,3}$, also known as the *space-time algebra*. The subscripts (1, 3) denotes the signature of the metric. The “fifth γ -matrix”, which can be expressed as $\gamma^5 = \gamma^0 \gamma^1 \gamma^2 \gamma^3$, obey

$$\{\gamma^5, \gamma^\mu\} = 0, \quad (\gamma^5)^2 = \mathbb{1}. \quad (\text{A.39})$$

The Euclidian counterpart of the space-time algebra, Cl_4 , is defined by the “Euclidian gamma matrices”, which obey

$$\{\tilde{\gamma}_a, \tilde{\gamma}_b\} = 2\delta_{ab}\mathbb{1}. \quad (\text{A.40})$$

These can be related to the regular Minkowski-matrices by

$$\tilde{\gamma}_0 = \gamma^0, \quad \tilde{\gamma}_j = -i\gamma^j. \quad (\text{A.41})$$

These then obey

$$\tilde{\gamma}_a^\dagger = \tilde{\gamma}_a. \quad (\text{A.42})$$

The Euclidean $\tilde{\gamma}_5$ is defined as

$$\tilde{\gamma}_5 = \gamma_0 \gamma_1 \gamma_2 \gamma_3 = i\gamma^0 \gamma^1 \gamma^2 \gamma^3 = \gamma^5. \quad (\text{A.43})$$

It thus also anti-commutes with the Euclidean γ -matrices,

$$\{\tilde{\gamma}_5, \tilde{\gamma}_a\} = 0. \quad (\text{A.44})$$

A.3 Functionals

The principle of stationary action and the path integral method relies on functional calculus, where ordinary, n -dimensional calculus is generalized to an infinite-dimensional calculus on a space of functions. A functional, S , takes in a function $\varphi(x)$, and returns a real number $S[\varphi]$. We will be often be dealing with functionals of the form

$$S[\varphi] = \int_{\mathcal{M}} d^n x \mathcal{L}[\varphi](x), \quad (\text{A.45})$$

Here, $\mathcal{L}[\varphi](x)$, the Lagrangian density, is a functional which takes in a function φ , and returns a real number $\mathcal{L}[\varphi](x)$ for each point $x \in \mathcal{M}$. \mathcal{L} thus returns a real-valued function, not just a number. \mathcal{M} is the manifold, in our case space-time, of which both $\varphi(x)$ and $\mathcal{L}[\varphi](x)$ are functions. The function φ can, in general, take on the value of a scalar, complex number, spinor, vector, etc..., while $\mathcal{L}[\varphi](x)$ must be a scalar-valued function. This strongly constraints the form of any Lagrangian and is an essential tool in constructing quantum field theories. Although this section is written with a single scalar-valued function φ , this can easily be generalized by adding an index, $\varphi \rightarrow \varphi_\alpha$, enumerating all the degrees of freedom, then summing over this index when restating the arguments [2, 9, 40].

A.3.1 Functional derivative

The functional derivative is based on an arbitrary *variation* η of the function φ . The variation η , often written $\delta\varphi$, is an arbitrary function only constrained to vanish *quickly enough* at the boundary $\partial\mathcal{M}$.¹ The variation of the functional S is defined as

$$\delta_\eta S[\varphi] = \lim_{\epsilon \rightarrow 0} \frac{1}{\epsilon} (S[\varphi + \epsilon\eta] - S[\varphi]) = \frac{d}{d\epsilon} S[\varphi + \epsilon\eta]|_{\epsilon=0}. \quad (\text{A.46})$$

We can regard the variation of a functional as the generalization of the differential of a function, Eq. (2.18), as the best linear approximation around a point. In regular differential geometry, a function f can be approximated around a point x by

$$f(x + \epsilon v) = f(x) + \epsilon df(v), \quad (\text{A.47})$$

where v is a vector in the tangent space at x . In functional calculus, the functional S is analogous to f , φ to x , and η to v . We can more clearly see the resemblance by writing

$$\frac{d}{d\epsilon} f(x + \epsilon v) = df(v) = \frac{\partial f}{\partial x^\mu} v^\mu. \quad (\text{A.48})$$

In the last line we expanded the differential using the basis-representation, $v = v^\mu \partial_\mu$. To generalize this to functional, we define the *functional derivative*, by

$$\delta_\eta S[\varphi] = \int_{\mathcal{M}} d^n x \frac{\delta S[\varphi]}{\delta \eta(x)} \eta(x). \quad (\text{A.49})$$

If we let $S[\varphi] = \varphi(x)$, for some fixed x , the variation becomes

$$\delta_\eta S[\varphi] = \eta(x) = \int d^n y \delta(x - y) \eta(y), \quad (\text{A.50})$$

which leads to the identity

$$\frac{\delta \varphi(x)}{\delta \varphi(y)} = \delta(x - y). \quad (\text{A.51})$$

There is also a generalized chain rule for functional derivatives. If ψ is some new functional variable, then

$$\frac{\delta S[\varphi]}{\delta \varphi(x)} = \int_{\mathcal{M}} d^n y \frac{\delta S[\varphi]}{\delta \psi(y)} \frac{\delta \psi(y)}{\delta \varphi(x)}. \quad (\text{A.52})$$

Higher functional derivatives are defined in terms of higher-order variations,

$$\delta_\eta^m S[\varphi] = \frac{d}{d\epsilon} \delta_\eta^{m-1} S[\varphi + \epsilon\eta]|_{\epsilon=0} = \int_{\mathcal{M}} \left(\prod_{i=1}^m d^n x_i \eta(x_i) \right) \frac{\delta^m S[\varphi]}{\delta \varphi(x_1) \dots \delta \varphi(x_m)}. \quad (\text{A.53})$$

With this, we can write the functional Taylor expansion,

$$S[\varphi_0 + \varphi] = S[\varphi_0] + \int_{\mathcal{M}} d^n x \varphi(x) \frac{\delta S[\varphi_0]}{\delta \varphi(x)} + \frac{1}{2} \int_{\mathcal{M}} d^n x d^n y \varphi(x) \varphi(y) \frac{\delta^2 S[\varphi_0]}{\delta \varphi(x) \delta \varphi(y)} + \dots \quad (\text{A.54})$$

Here, the notation $\frac{\delta S[\varphi_0]}{\delta \varphi}$ indicate that $S[\varphi]$ is first differentiated with respect to φ , then evaluated at $\varphi = \varphi_0$ [9, 40].

¹The condition of “quickly enough” is to ensure that we can integrate by parts and ignore the boundary condition, which we will do without remorse.

A.3.2 *Gaussian integrals and the stationary phase approximation

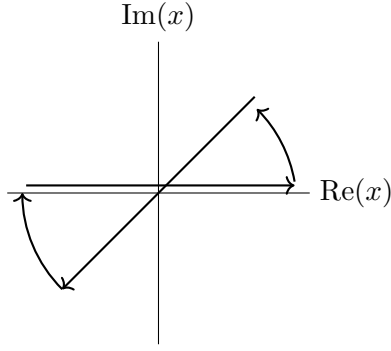


Figure A.1: Wick rotation

An integral that we will use a lot is the Gaussian integral,

$$\int_{\mathbb{R}} dx \exp \left\{ -\frac{1}{2} ax^2 \right\} = \sqrt{\frac{2\pi}{a}}, \quad (\text{A.55})$$

for $a \in \mathbb{R}$. The imaginary version,

$$\int_{\mathbb{R}} dx \exp \left\{ i\frac{1}{2} ax^2 \right\} \quad (\text{A.56})$$

does not converge. However, if we change $a \rightarrow a + i\epsilon$, the integrand is exponentially suppressed.

$$f(x) = \exp \left\{ i\frac{1}{2} ax^2 \right\} \rightarrow \exp \left\{ i\frac{1}{2} ax^2 - \frac{1}{2} \epsilon x^2 \right\}. \quad (\text{A.57})$$

As the integrand falls exponentially for $x \rightarrow \infty$ and contains no poles in the upper right nor lower left quarter of the complex plane, we may perform a wick rotation by closing the contour as shown in Figure A.1. This gives the result

$$\begin{aligned} \int_{\mathbb{R}} dx \exp \left\{ i\frac{1}{2} (a + i\epsilon) x^2 \right\} &= \int_{\sqrt{i}\mathbb{R}} dx \exp \left\{ i\frac{1}{2} ax^2 \right\} \\ &= \sqrt{i} \int_{\mathbb{R}} dy \exp \left\{ -\frac{1}{2} (-a) y^2 \right\} \\ &= \sqrt{\frac{2\pi i}{(-a)}}, \end{aligned} \quad (\text{A.58})$$

where we have made the change of variable $y = (1 + i)/\sqrt{2}x = \sqrt{i}x$. In n dimensions, the Gaussian integral formula generalizes to

$$\int_{\mathbb{R}^n} d^n x \exp \left\{ -\frac{1}{2} x_n A_{nm} x_m \right\} = \sqrt{\frac{(2\pi)^n}{\det(A)}}, \quad (\text{A.59})$$

where A is a matrix with n real, positive eigenvalues. We may also generalize Eq. (A.58),

$$\int_{\mathbb{R}^n} d^n x \exp \left\{ i\frac{1}{2} x_n (A_{nm} + i\epsilon \delta_{nm}) x_m \right\} = \sqrt{\frac{(2\pi i)^n}{\det(-A)}}. \quad (\text{A.60})$$

The final generalization is to functional integrals. If $A(x, x')$ is a linear operator, then

$$\begin{aligned} \int \mathcal{D}\varphi \exp \left\{ -\frac{1}{2} \int dx dx' \varphi(x) A(x, x') \varphi(x') \right\} &= C \det(A)^{-1/2}, \\ \int \mathcal{D}\varphi \exp \left\{ i\frac{1}{2} \int dx dx' \varphi(x) A(x, x') \varphi(x') \right\} &= C' \det(-A)^{-1/2}. \end{aligned} \quad (\text{A.61})$$

C and C' are divergent constants but will either fall away as we are only looking at the logarithm of I_∞ and can throw away additive constants, or ratios between quantities that are both multiplied by C or C^* .

The Gaussian integral can be used for the stationary phase approximation. By Taylor expanding around a stationary point x_0 , we may approximate

$$\int dx \exp \{i\alpha f(x)\} \sim \sqrt{\frac{2\pi}{\alpha f''(x_0)}} \exp \{\alpha f(x_0)\}, \quad \alpha \rightarrow \infty, \quad (\text{A.62})$$

where the point x_0 is defined by $f'(x_0) = 0$. The functional generalization of this is

$$\int \mathcal{D}\varphi \exp \{i\alpha S[\varphi]\} \sim C \det \left(-\frac{1}{\alpha} \frac{\delta^2 S[\varphi_0]}{\delta \varphi^2} \right)^{-1/2} \exp \{i\alpha S[\varphi_0]\}, \quad (\text{A.63})$$

Here, $S[\varphi]$ is a general functional of φ , we have used the Taylor expansion, and φ_0 obeys

$$\frac{\delta S[\varphi_0]}{\delta \varphi(x)} = 0. \quad (\text{A.64})$$

A.3.3 The Euler-Lagrange equation

The Lagrangian may also be written as a scalar function of the field-values at x , $\varphi(x)$, as well as its derivatives, $\partial_\mu \varphi(x)$, for example

$$\mathcal{L}(\varphi, \partial_\mu \varphi) = \frac{1}{2} \partial_\mu \varphi \partial^\mu \varphi - \frac{1}{2} m^2 \varphi^2 - \frac{1}{4!} \lambda \varphi^4 + \dots \quad (\text{A.65})$$

We have omitted the evaluation at x for the brevity of notation. We use this to evaluate the variation of a functional in the of Eq. (A.45),

$$\delta_\eta S[\varphi] = \frac{d}{d\epsilon} \int_{\mathcal{M}} d^n x \mathcal{L}[\varphi + \epsilon \eta](x), \quad (\text{A.66})$$

by Taylor expanding the Lagrangian density as a function of φ and its derivatives,

$$\mathcal{L}[\varphi + \epsilon \eta] = \mathcal{L}(\varphi + \epsilon \eta, \partial_\mu \{\varphi + \epsilon \eta\}) = \mathcal{L}[\varphi] + \epsilon \left(\frac{\partial \mathcal{L}}{\partial \varphi} \eta + \frac{\partial \mathcal{L}}{\partial (\partial_\mu \varphi)} \partial_\mu \eta \right) + \mathcal{O}(\epsilon^2). \quad (\text{A.67})$$

Inserting this into Eq. (A.66) and partially integrating the last term allows us to write the variation on the form Eq. (A.49). The functional derivative is

$$\frac{\delta S}{\delta \varphi} = \frac{\partial \mathcal{L}}{\partial \varphi} - \partial_\mu \frac{\partial \mathcal{L}}{\partial (\partial_\mu \varphi)}. \quad (\text{A.68})$$

The principle of stationary action says that the equation of motion of a field obeys $\delta_\eta S = 0$. As η is arbitrary, this is equivalent to setting the functional derivative of S equal to zero. The result is the Euler-Lagrange equations of motion [9],

$$\frac{\partial \mathcal{L}}{\partial \varphi} - \partial_\mu \frac{\partial \mathcal{L}}{\partial (\partial_\mu \varphi)} = 0. \quad (\text{A.69})$$

A.3.4 Functional calculus on a curved manifold

As discussed in subsection 2.1.3, when integrating a scalar on a curved manifold, we must include the $\sqrt{|g|}$ -factor to get a coordinate-independent result. The action in curved spacetime is therefore

$$S[g, \varphi] = \int_{\mathcal{M}} d^n x \sqrt{|g|} \mathcal{L}[g, \varphi], \quad (\text{A.70})$$

where the action and the Lagrangian now is a functional of both the matter-field φ and the metric $g_{\mu\nu}$. Our example Lagrangian from last section now takes the form

$$\mathcal{L}(g_{\mu\nu}, \varphi, \nabla_\mu \varphi) = \frac{1}{2} g^{\mu\nu} \nabla_\mu \varphi \nabla_\nu \varphi - \frac{1}{2} m^2 \varphi^2 - \frac{1}{4!} \lambda \varphi^4 \dots, \quad (\text{A.71})$$

where partial derivatives are substituted with covariant derivatives following the minimal coupling rule. We define the functional derivative as

$$\delta_\eta S = \int_{\mathcal{M}} d^n x \sqrt{|g|} \frac{\delta S}{\delta \eta(x)} \eta(x). \quad (\text{A.72})$$

If this is a variation in φ only, this gives the same result as before. However, in general relativity, the metric itself is a dynamic field, and we may therefore vary it. Consider $g_{\mu\nu} \rightarrow g_{\mu\nu} + \delta g_{\mu\nu}$. The variation of the action is then assuming \mathcal{L} only depends on g and not its derivatives, we get

$$\delta_g S = \int_{\mathcal{M}} d^n x \left[\left(\delta \sqrt{|g|} \right) \mathcal{L}[g] + \sqrt{|g|} \delta \mathcal{L}[g] \right] \quad (\text{A.73})$$

The variation of the $\sqrt{|g|}$ -factor can be evaluated using the Levi-Civita symbol $\varepsilon_{\mu_1 \dots \mu_n}$. The determinant of a $n \times n$ -matrix may be written as

$$\det(A) = \frac{1}{n!} \varepsilon_{\mu_1 \dots \mu_n} \varepsilon^{\nu_1 \dots \nu_n} A^{\mu_1}_{\nu_1} \dots A^{\mu_n}_{\nu_n}. \quad (\text{A.74})$$

For a matrix M , then, we can write

$$\begin{aligned} \det(\mathbb{1} + \varepsilon M) &= \frac{1}{n!} \varepsilon_{\mu_1 \dots \mu_n} \varepsilon^{\nu_1 \dots \nu_n} (\mathbb{1} + \varepsilon M)^{\mu_1}_{\nu_1} (\mathbb{1} + \varepsilon M)^{\mu_2}_{\nu_2} \dots \\ &= \frac{1}{n!} \varepsilon_{\mu_1 \dots \mu_n} \varepsilon^{\nu_1 \dots \nu_n} [\delta^{\mu_1}_{\nu_1} \delta^{\mu_2}_{\nu_2} \dots + \varepsilon (M^{\mu_1}_{\nu_1} \delta^{\mu_2}_{\nu_2} \dots + M^{\mu_2}_{\nu_2} \delta^{\mu_1}_{\nu_1} \dots + \dots) + \mathcal{O}(\varepsilon^2)] \\ &= 1 + M^\mu_\mu + \mathcal{O}(\varepsilon^2). \end{aligned} \quad (\text{A.75})$$

Using

$$\det(g^\mu_\nu + \varepsilon \eta^\mu_\nu) = \det(g^\mu_\rho [\delta^\rho_\nu + \varepsilon g^{\rho\lambda} \eta_{\lambda\nu}]) = \det(g^\mu_\rho) (1 + \varepsilon g^{\nu\lambda} \eta_{\lambda\nu}), \quad (\text{A.76})$$

we get

$$\delta \sqrt{|g|} = \frac{1}{2} \frac{1}{\sqrt{|g|}} \frac{g}{|g|} \delta \det(g^\mu_\nu) = -\frac{1}{2} \sqrt{|g|} g^{\mu\nu} \delta g_{\mu\nu} \quad (\text{A.77})$$

The minus sign is due to the determinant of a Lorentzian metric being negative. Assuming the Lagrangian only depends on the metric directly, and not its derivatives, the variation of the action is

$$\delta_g S = \int_{\mathcal{M}} d^n x \sqrt{|g|} \left(\frac{\partial \mathcal{L}}{\partial g^{\mu\nu}} - \frac{1}{2} g_{\mu\nu} \mathcal{L} \right) \delta g^{\mu\nu}. \quad (\text{A.78})$$

With the Lagrangian in Eq. (A.71), we get

$$\frac{\delta S}{\delta g^{\mu\nu}} = \frac{\partial \mathcal{L}}{\partial g^{\mu\nu}} - \frac{1}{2} g_{\mu\nu} \mathcal{L} = -\frac{1}{2} \left(\frac{1}{2} \nabla_\mu \varphi \nabla_\nu \varphi + \frac{1}{2} m^2 \varphi^2 g_{\mu\nu} + \dots \right). \quad (\text{A.79})$$

We recognize the $(\mu, \nu) = (0, 0)$ -component as negative half the Hamiltonian density, which supports the definition of the definition of the stress-energy tensor Eq. (4.9) [2].

A.3.5 Functional derivative of the Einstein-Hilbert action

In the Einstein-Hilbert action, Eq. (4.6), the Lagrangian density is $\mathcal{L} = kR = kg^{\mu\nu}R_{\mu\nu}$, where k is a constant and $R_{\mu\nu}$ the Ricci tensor, Eq. (2.43). As the Ricci tensor is dependent on both the derivative and second derivative of the metric, the variation is

$$\delta S_{\text{EH}} = k \int_{\mathcal{M}} d^n x \sqrt{|g|} \left(\delta R - \frac{1}{2} g_{\mu\nu} \delta g^{\mu\nu} R \right). \quad (\text{A.80})$$

The variation of the Ricci scalar is

$$\delta R = R_{\mu\nu} \delta g^{\mu\nu} + g^{\mu\nu} \delta R_{\mu\nu}, \quad (\text{A.81})$$

We can write the variation of the Ricci scalar, and thus the Riemann curvature tensor, in terms of variations in Christoffel symbols, $\delta\Gamma_{\mu\nu}^\rho$ using the explicit formula for a symmetric, metric-compatible covariant derivative, Eq. (2.39). As $\delta\Gamma = \Gamma - \Gamma'$, it is a tensor, and we may write

$$\begin{aligned} \delta R^\rho_{\sigma\mu\nu} &= \delta(\partial_\mu \Gamma_{\nu\sigma}^\rho - \partial_\nu \Gamma_{\mu\sigma}^\rho + \Gamma_{\lambda\mu}^\rho \Gamma_{\nu\sigma}^\lambda - \Gamma_{\lambda\nu}^\rho \Gamma_{\mu\sigma}^\lambda) \\ &= \partial_\mu \delta\Gamma_{\nu\sigma}^\rho + \Gamma_{\lambda\mu}^\rho \delta\Gamma_{\nu\sigma}^\lambda - \Gamma_{\mu\sigma}^\lambda \delta\Gamma_{\lambda\nu}^\rho - \left(\partial_\nu \delta\Gamma_{\mu\sigma}^\rho + \Gamma_{\lambda\nu}^\rho \delta\Gamma_{\mu\sigma}^\lambda - \Gamma_{\nu\sigma}^\lambda \delta\Gamma_{\lambda\mu}^\rho \right) \\ &\quad + (\Gamma_{\mu\nu}^\lambda \delta\Gamma_{\lambda\sigma}^\rho - \Gamma_{\mu\sigma}^\lambda \delta\Gamma_{\lambda\nu}^\rho) \\ &= \nabla_\mu \delta\Gamma_{\nu\sigma}^\rho - \nabla_\nu \delta\Gamma_{\mu\sigma}^\rho = \nabla_\eta (g^\eta_\mu \delta\Gamma_{\nu\sigma}^\rho - g^\eta_\nu \delta\Gamma_{\mu\sigma}^\rho) := \nabla_\eta K^{\rho\eta}_{\mu\rho\nu}, \end{aligned}$$

where K is a tensorial quantity, which vanishes at the boundary of our spacetime. Using the generalized divergence theorem, Eq. (2.64), we see the contribution to the action from this quantity vanish. The contribution comes from an integral over $g^{\mu\nu} \delta R_{\mu\nu} = g^{\mu\nu} \delta R^\rho_{\mu\rho\nu} = g^{\mu\nu} \nabla_\eta K^{\rho\eta}_{\mu\rho\nu}$. Using metric compatibility, we can exchange the covariant derivative and the metric, and we have $g^{\mu\nu} \delta R_{\mu\nu} = \nabla_\eta [g^{\mu\nu} K^{\rho\eta}_{\mu\rho\nu}]$. The contribution to the action therefore becomes

$$\int_{\mathcal{M}} d^4 x \sqrt{|g|} g^{\mu\nu} \delta R_{\mu\nu} = \int_{\mathcal{M}} d^4 x \sqrt{|g|} \nabla_\eta K^{\eta\rho\mu}_{\rho\mu} = \int_{\partial\mathcal{M}} d^3 y \sqrt{|\gamma|} n_\eta K^{\eta\rho\mu}_{\rho\mu} = 0, \quad (\text{A.82})$$

where we used the fact that $\delta g_{\mu\nu}$, and thus K , vanish at $\partial\mathcal{M}$, and the generalized form of the divergence theorem, Eq. (2.64). The variation of the action is therefore

$$\delta S_{\text{EH}} = k \int_{\mathcal{M}} d^n x \sqrt{|g|} \left[R_{\mu\nu} - \frac{1}{2} R g_{\mu\nu} \right] \delta g^{\mu\nu}, \quad (\text{A.83})$$

and by the definition of the functional derivative,

$$\frac{\delta S_{\text{EH}}}{\delta g^{\mu\nu}} = k \left(R_{\mu\nu} - \frac{1}{2} R g_{\mu\nu} \right). \quad (\text{A.84})$$

A.4 *Consistent series expansion of observables

As with all other quantities, we calculate using χPT , the free energy density \mathcal{F} must be expanded in chiral dimension, as explained in subsection 5.2.1, as well as an expansion in loops. We write

$$\mathcal{F} = \mathcal{F}_2^{(0)} + \mathcal{F}_2^{(1)} + \mathcal{F}_2^{(2)} + \mathcal{F}_4^{(0)} \dots, \quad (\text{A.85})$$

where $\mathcal{F}_D^{(n)}$ is the n -loop contribution from the Lagrangian with chiral dimension D , \mathcal{L}_D . In Chapter 6, we found a relationship between α and μ_I , using the leading-order result for \mathcal{F} . To calculate any thermodynamic quantities to leading order, at tree-level, we must use this result. When using the NLO result for the free energy, we must consistently calculate this and other quantities to the same order. As we have seen in section 3.2, when replacing the action by

$S[\varphi] \rightarrow g^{-1}S[\varphi]$, the L -loop contribution is proportional to g^{L-1} . In Weinberg's power counting scheme, we scale $p \rightarrow tp$ the quark masses as $m_q \rightarrow t^2 m_q$, and so forth. Then, the n th term in the expansion is proportional to t^{2n} . Using both these scalings, the expansion of the free energy becomes

$$\mathcal{F} = t^2 g^{-1} \mathcal{F}_2^{(0)} + t^2 \mathcal{F}_2^{(1)} + t^4 g^{-1} \mathcal{F}_4^{(0)} + \dots \quad (\text{A.86})$$

We consider terms where $k = L + n$ has the same value to be of same order. This expansion can be written as

$$\mathcal{F} = \sum_{k=0}^{\infty} \sum_{n+L=k} t^{2n} g^{L-1} \mathcal{F}_{2n}^{(L)}. \quad (\text{A.87})$$

If we now define

$$\tilde{\mathcal{F}}_k = \sum_{n+L=k} t^{2n} g^{L-1} \mathcal{F}_{2n}^{(L)}, \quad (\text{A.88})$$

then scale $t \rightarrow \sqrt{s}t$ and $g \rightarrow sg$, where s is some real number, then $t^{2n} g^{L-1}$ scales as $s^{n+L-1} = s^{m-1}$. All expansions are now done in this new parameter s . The free energy expansion is

$$\mathcal{F} = \sum_{k=0}^{\infty} \tilde{\mathcal{F}}_k s^{k-1}. \quad (\text{A.89})$$

As argued earlier, α must minimize the free energy and therefore satisfy

$$\frac{\partial \mathcal{F}}{\partial \alpha} = 0, \quad (\text{A.90})$$

to all orders. Inserting the expansion in of the solution to this equation, $\alpha = \alpha_0 + \alpha_1 s + \dots$, into the expansion of \mathcal{F} , we get

$$\begin{aligned} 0 &= \frac{\partial}{\partial \alpha} \left[s^{-1} \tilde{\mathcal{F}}_0 + \tilde{\mathcal{F}}_1 + \mathcal{O}(s) \right] \Big|_{\alpha=\alpha_0+\alpha_1 s+\mathcal{O}(s)} \\ &= s^{-1} \left[\tilde{\mathcal{F}}'_0(\alpha_0) + \alpha_1 s \tilde{\mathcal{F}}''_0(\alpha_0) + \mathcal{O}(s^2) \right] + \tilde{\mathcal{F}}'_1(\alpha_0) + \mathcal{O}(s) \\ &= s^{-1} \tilde{\mathcal{F}}'_1(\alpha_0) + s^0 \left[\alpha_1 \tilde{\mathcal{F}}''_0(\alpha_0) + \tilde{\mathcal{F}}'_1(\alpha_0) \right] + \mathcal{O}(s). \end{aligned} \quad (\text{A.91})$$

Here, the prime indicates partial derivatives with respect to α . The equality in Eq. (A.91) has to hold term for term. The leading order relation is

$$\tilde{\mathcal{F}}'_0(\alpha_0) = 0, \quad \tilde{\mathcal{F}}_0 = \mathcal{F}_2^{(0)}.$$

This is what we have used as the leading-order result. The first correction is on this result is

$$\alpha_1 = -\frac{\tilde{\mathcal{F}}'_1(\alpha_0)}{\tilde{\mathcal{F}}''_0(\alpha_0)}, \quad \tilde{\mathcal{F}}_1 = \mathcal{F}_4^{(0)} + \mathcal{F}_2^{(1)}. \quad (\text{A.92})$$

The next to leading order results for the free energy and α are

$$\mathcal{F}_{\text{NLO}} = \tilde{\mathcal{F}}_0 + \tilde{\mathcal{F}}_1, \quad \alpha_{\text{NLO}} = \alpha_0 + \alpha_1. \quad (\text{A.93})$$

We have that

$$\mathcal{F}'_{\text{NLO}}(\alpha_{\text{NLO}}) = \tilde{\mathcal{F}}'_0(\alpha_0) + \alpha_1 \tilde{\mathcal{F}}''_0(\alpha_0) + \dots + \tilde{\mathcal{F}}'_1(\alpha_0) + \dots, \quad (\text{A.94})$$

where the excluded terms are beyond next-to-leading order. Using Eq. (A.92), we see that this vanishes and we, therefore, use the criterion

$$\frac{\partial \mathcal{F}_{\text{NLO}}}{\partial \alpha} \Big|_{\alpha=\alpha_{\text{NLO}}} = 0 \quad (\text{A.95})$$

to calculate α_{NLO} .

We can use the expansion in s to consistently evaluate any observable to any power in perturbation theory. Assume that f is some observable, and a function of α . We then expand in s ,

$$f(\alpha) = f_0(\alpha) + sf_1(\alpha) + s^2f_2(\alpha) + \dots \quad (\text{A.96})$$

Taylor expanding around the leading order result for α , we get

$$f(\alpha) = f_0(\alpha_0) + s\alpha_1 f'_0(\alpha_0) + sf_1(\alpha_0) + \mathcal{O}(s^2) = f_0(\alpha_0 + s\alpha_1) + sf_1(\alpha_0) + \mathcal{O}(s^2).$$

To get a consistent expansion, we must evaluate the leading order result for the function f_0 at next-to-leading order in α , while next-to-leading order correction can be evaluated at leading order. However, as

$$f_1(\alpha_0 + s\alpha_1) = f_1(\alpha_0) + \mathcal{O}(s), \quad (\text{A.97})$$

we also get a consistent expansion if we evaluate the leading-order result and its correction at next-to-leading order in α . This is what we do to obtain all results in this thesis.

A.5 *Integrals in dimensional regularization

When applying dimensional regularization, we will encounter integrals on the form

$$\Phi_n(m, d, \alpha) := \int_{\mathbb{R}^d} \frac{d^d p}{(2\pi)^d} (p^2 + m^2)^{-\alpha}. \quad (\text{A.98})$$

We will use the formula for integration of spherically symmetric function in d -dimensions,

$$\int_{\mathbb{R}^d} d^d x f(r) = \frac{2\pi^{d/2}}{\Gamma(d/2)} \int_{\mathbb{R}} dr r^{d-1} f(r), \quad (\text{A.99})$$

where $r = \sqrt{x_i x_i}$ is the radial distance and Γ is the Gamma function. The factor in the front of the integral is the solid angle. By extending this formula from integer-valued d to real numbers, we get

$$\Phi_n = \frac{2\pi^{d/2}}{\Gamma(d/2)} \int_{\mathbb{R}} dp \frac{p^{d-1}}{(p^2 + m^2)^\alpha} = \frac{m^{n-2\alpha} m^{d-n}}{(4\pi)^{d/2} \Gamma(d/2)} 2 \int_{\mathbb{R}} dz \frac{z^{d-1}}{(1+z)^\alpha}, \quad (\text{A.100})$$

where we have made the change of variables $mz = p$. We make one more change of variable to the integral,

$$I = 2 \int_{\mathbb{R}} dz \frac{z^{d-1}}{(1+z)^\alpha}. \quad (\text{A.101})$$

Let

$$z^2 = \frac{1}{s} - 1 \implies 2zdz = -\frac{ds}{s^2} \quad (\text{A.102})$$

Thus,

$$I = \int_0^a ds s^{\alpha-d/2-1} (1-z)^{d/2-1}. \quad (\text{A.103})$$

This is the beta function, which can be written in terms of Gamma functions [40]

$$I = B\left(\alpha - \frac{d}{2}, \frac{d}{2}\right) = \frac{\Gamma\left(\alpha - \frac{d}{2}\right) \Gamma\left(\frac{d}{2}\right)}{\Gamma(\alpha)}. \quad (\text{A.104})$$

Combining this gives

$$\Phi_n(m, d, \alpha) = \mu^{n-d} \frac{m^{n-2\alpha}}{(4\pi)^{d/2}} \frac{\Gamma\left(\alpha - \frac{d}{2}\right)}{\Gamma(\alpha)} \left(\frac{m^2}{\mu^2}\right)^{(d-n)/2}. \quad (\text{A.105})$$

In the last step, we have introduced a parameter μ with mass dimension 1, that is, $[\mu] = [m]$. This is done to be able to series expand around $d-n$ in a dimensionless variable. This parameter is arbitrary, and all physical quantities should therefore be independent of it.

A.5.1 A special case

A special case of this integral, which shows up in calculations of free energy, is

$$\mathcal{F} = \int \frac{d^3 p}{(2\pi)^3} \sqrt{\vec{p}^2 + m^2}. \quad (\text{A.106})$$

Which corresponds to $n = 3$, $d = 3 - 2\epsilon$ and $\alpha = -1/2$, or $\mathcal{F} = \Phi_3(m, 3 - 2\epsilon, -1/2)$. Inserting this into Eq. (A.105), we get

$$\mathcal{F} = \frac{m^4 \mu^{-2\epsilon}}{(4\pi)^{d/2} \Gamma(-1/2)} \Gamma(-2 + \epsilon) \left(\frac{m^2}{\mu^2} \right)^{-\epsilon} = -\mu^{-2\epsilon} \frac{m^4}{(4\pi)^2} \left(\frac{m^2}{4\pi \mu^2} \right)^{-\epsilon} \frac{\Gamma(\epsilon)}{(\epsilon - 2)(\epsilon - 1)}, \quad (\text{A.107})$$

where we have used the defining property $\Gamma(z + 1) = z\Gamma(z)$ and $\Gamma(1/2) = \sqrt{\pi}$. Expanding around $\epsilon = 0$ gives

$$\left(\frac{m^2}{4\pi \mu^2} \right)^{-\epsilon} \sim 1 + \epsilon \ln \left(4\pi \frac{\mu^2}{m^2} \right), \quad (\text{A.108})$$

$$\Gamma(\epsilon) \sim \frac{1}{\epsilon} - \gamma, \quad (\text{A.109})$$

$$\frac{1}{(\epsilon - 2)(\epsilon - 1)} \sim \frac{1}{2} \left(1 + \frac{3}{2}\epsilon \right). \quad (\text{A.110})$$

The result is therefore

$$\mathcal{F} = -\mu^{-2\epsilon} \frac{1}{4} \frac{m^4}{(4\pi)^2} \left[\frac{1}{\epsilon} - \gamma + \frac{3}{2} + \ln \left(4\pi \frac{\mu^2}{m^2} \right) \right] + \mathcal{O}(\epsilon). \quad (\text{A.111})$$

With this regulator, one can then add counter-terms to cancel the ϵ^{-1} -divergence. The exact form of the counter-term is convention. One may also cancel the finite contribution due to the regulator. The minimal subtraction (MS) scheme involves only subtracting the divergent term, as the name suggests. We will use the modified minimal subtraction, or $\overline{\text{MS}}$, scheme. In this scheme, one also removes the $-\gamma$ and $\ln(4\pi)$ term, by defining a new mass scale $\tilde{\mu}$ by

$$-\gamma + \ln \left(4\pi \frac{\mu^2}{m^2} \right) = \ln \left(4\pi e^{-\gamma} \frac{\mu^2}{m^2} \right) := \ln \left(\frac{\tilde{\mu}^2}{m^2} \right). \quad (\text{A.112})$$

The result is thus

$$\mathcal{F} = -\mu^{-2\epsilon} \frac{1}{4} \frac{m^4}{(4\pi)^2} \left(\frac{1}{\epsilon} + \frac{3}{2} + \ln \frac{\tilde{\mu}^2}{m^2} \right) + \mathcal{O}(\epsilon). \quad (\text{A.113})$$

A.5.2 Rewriting a real-time integral

We seek to rewrite the integral

$$I = \int \frac{d^4 p}{(2\pi)^2} \ln(-p_0^2 + E^2), \quad (\text{A.114})$$

where E is some function of the 3-momentum \vec{p} , but not p_0 . We use the trick

$$\frac{\partial}{\partial \alpha} (-p_0^2 + E^2)^{-\alpha} \Big|_{\alpha=0} = \frac{\partial}{\partial \alpha} \exp \{ -\alpha \ln(-p_0^2 + E^2) \} \Big|_{\alpha=0} = \ln(-p_0^2 + E^2), \quad (\text{A.115})$$

and then perform a Wick-rotation of the p_0 -integral to write the integral on the form

$$I = i \frac{\partial}{\partial \alpha} \int \frac{d^4 p}{(2\pi)^4} (p_0^2 + E^2)^{-\alpha} \Big|_{\alpha=0}, \quad (\text{A.116})$$

where p now is a Euclidean four-vector. The p_0 integral equals $\Phi_1(E, 1, \alpha)$, as defined in Eq. (A.98). The result is therefore given by Eq. (A.105),

$$\int \frac{dp_0}{2\pi} (p_0^2 + E)^{-\alpha} = \frac{E^{1-2\alpha}}{\sqrt{4\pi}} \frac{\Gamma(\alpha - \frac{1}{2})}{\Gamma(\alpha)}. \quad (\text{A.117})$$

The derivative of the Gamma function is $\Gamma'(\alpha) = \psi(\alpha)\Gamma(\alpha)$, where $\psi(\alpha)$ is the digamma function. Using

$$\left. \frac{\Gamma(\alpha - \frac{1}{2})}{\Gamma(\alpha)} \right|_{\alpha=0} = 0, \quad \left. \frac{\partial}{\partial \alpha} \frac{\Gamma(\alpha - \frac{1}{2})}{\Gamma(\alpha)} \right|_{\alpha=0} = \Gamma\left(\alpha - \frac{1}{2}\right) \frac{\psi(\alpha - \frac{1}{2}) - \psi(\alpha)}{\Gamma(\alpha)} \Big|_{\alpha=0} = \sqrt{4\pi}, \quad (\text{A.118})$$

we get

$$I = i \int \frac{d^3 p}{(2\pi)^3} E. \quad (\text{A.119})$$

When the energy is on the simple form $E^2 = \vec{p}^2 + m^2$, we can use the result from subsection A.5.1,

Appendix B

*Two flavor results

In this appendix, we give a short summary of some of the results from the specialization project on which this thesis builds. The specialization project focused on the thermodynamics of χ PT but included only two flavors, i.e., quark types. In addition, we give examples of some derivations which is readily generalized to three flavors.

B.1 *Two-flavour χ PT to leading order

In this section, we will assume $N_f = 2$, which means the generators are $T_a = \frac{1}{2}\tau_a$, where τ_a are the Pauli Matrices, as described in section A.2. The leading order Lagrangian in Winberg's power counting scheme, with $e = 0$, is

$$\mathcal{L}_2 = \frac{1}{4}f^2\text{Tr}\left\{\nabla_\mu\Sigma(\nabla^\mu\Sigma)^\dagger\right\} + \frac{1}{4}f^2\text{Tr}\left\{\chi^\dagger\Sigma + \Sigma^\dagger\chi\right\}. \quad (\text{B.1})$$

The covariant derivative is

$$\nabla_\mu\Sigma = \partial_\mu\Sigma - i[v_\mu, \Sigma], \quad v_\mu = \frac{1}{2}\mu_I\delta_\mu^0\tau_3, \quad (\text{B.2})$$

and we have defined

$$\chi = 2B_0\begin{pmatrix} m_u & 0 \\ 0 & m_d \end{pmatrix} = \begin{pmatrix} \bar{m} - \Delta m & 0 \\ 0 & \bar{m} + \Delta m \end{pmatrix}. \quad (\text{B.3})$$

To incorporate a finite isospin density, we must parametrize the Goldstone manifold differently than in the vacuum. We follow the analysis in [70]. We assume the ground state is independent of space, $\pi_a(x) = \pi_a^0$, and write it as

$$\Sigma_\alpha := \exp\{i\alpha n_a\tau_a\} = \cos\alpha + in_a\tau_a\sin\alpha, \quad (\text{B.4})$$

where

$$\alpha = \frac{1}{f}\sqrt{\pi_a^0\pi_a^0}, \quad n_a = \frac{\pi_a^0}{\sqrt{\pi_a^0\pi_a^0}}. \quad (\text{B.5})$$

With this, the covariant derivative is $\nabla_\mu\Sigma_\alpha = -iv_\mu^a[\tau_a, \Sigma_\alpha]$, and the two terms in the first order Lagrangian are

$$\text{Tr}\left\{\nabla_\mu\Sigma_\alpha(\nabla^\mu\Sigma_\alpha)^\dagger\right\} = 2\mu_I^2(n_1^2 + n_2^2)\sin^2\alpha, \quad \text{Tr}\left\{\chi^\dagger\Sigma_\alpha + \Sigma_\alpha^\dagger\chi\right\} = 4\bar{m}^2\cos\alpha. \quad (\text{B.6})$$

We see that, to first order, all results are independent of Δm . To find the new ground state, we minimize the Hamiltonian density. With the assumption that the fields are constant, the first order Hamiltonian density is

$$\mathcal{H}_2 = -\mathcal{L}_2 = -f^2\left[\bar{m}^2\cos\alpha + \frac{1}{2}\mu_I^2(n_1^2 + n_2^2)\sin^2\alpha\right]. \quad (\text{B.7})$$

For $\mu_I = 0$, this is independent of n_a , and minimized by $\alpha = 0$. Now, as $n_i n_i = 1$, we have that $n_1^2 + n_2^2 = 1 - n_3^2$. This means that, for $\mu_I \neq 0$, the energy is minimized by $n_3 = 0$. We can write $n_1 = \cos \phi$, $n_2 = \sin \phi$, for some real number ϕ , which gives the ground state

$$\Sigma_\alpha = \mathbb{1} \cos \alpha + i(\tau_1 \cos \phi + \tau_2 \sin \phi) \sin \alpha. \quad (\text{B.8})$$

We can choose, without loss of generality, $\phi = 0$ [25]. This corresponds to a change of basis of $\mathfrak{su}(2)$, $\tau_1 \rightarrow \tilde{\tau}_1 = \tau_1 \cos \phi + \tau_2 \sin \phi$ and $\tau_2 \rightarrow \tilde{\tau}_2 = -\tau_1 \sin \phi + \tau_2 \cos \phi$. With this, the new ground state is

$$\Sigma_\alpha = \exp \{i\alpha\tau_1\}. \quad (\text{B.9})$$

Any excited state is a transformation of the ground state by $\text{SU}(2)_A$. For $\mu_I = 0$, this corresponds to

$$\Sigma(x) = U_R(x)\Sigma_0 U_L^\dagger(x) = U(x)\Sigma_0 U(x). \quad (\text{B.10})$$

where

$$U(x) = \exp \left\{ i \frac{\tau_a \pi_a(x)}{2f} \right\}. \quad (\text{B.11})$$

We see that this recovers the parametrization vacuum parametrization. For $\mu_I \neq 0$, the ground state may be shifted, and so $U(x)$ must be too. The groundstate transforms as

$$\Sigma_0 \rightarrow \Sigma_\alpha = \hat{U}_L \Sigma_0 \hat{U}_R^\dagger = A_\alpha \Sigma_0 A_\alpha. \quad (\text{B.12})$$

where

$$A_\alpha := \exp \left\{ i \frac{1}{2} \alpha \tau_1 \right\} = \cos \frac{\alpha}{2} + i \tau_1 \sin \frac{\alpha}{2}. \quad (\text{B.13})$$

This induces the following transformations for the fluctuations,

$$U_L \rightarrow \hat{U}_L U_L \hat{U}_L^\dagger = A_\alpha U_L A_\alpha^\dagger, \quad (\text{B.14})$$

$$U_R \rightarrow \hat{U}_R U_R \hat{U}_R^\dagger = A_\alpha^\dagger U_R A_\alpha. \quad (\text{B.15})$$

The new parameterization is thus

$$\Sigma(x) = A_\alpha [U(x)\Sigma_0 U(x)] A_\alpha. \quad (\text{B.16})$$

With this, we can expand the first order Lagrangian, Eq. (B.1), in powers of π/f . We will use this expansion to calculate the free energy density. Expanding Σ to $\mathcal{O}((\pi/f)^5)$, we get

$$\begin{aligned} \Sigma = & \left(1 - \frac{\pi_a^2}{2f^2} + \frac{\pi_a^2 \pi_b^2}{24f^4} \right) (\cos \alpha + i\tau_1 \sin \alpha) \\ & + \left(\frac{\pi_a}{f} - \frac{\pi_b^2 \pi_a}{6f^3} \right) \left(i\tau_a - 2i\delta_{a1}\tau_1 \sin^2 \frac{\alpha}{2} - \delta_{a1} \sin \alpha \right). \end{aligned} \quad (\text{B.17})$$

The kinetic term in the χPT Lagrangian is

$$\nabla_\mu \Sigma (\nabla^\mu \Sigma)^\dagger = \partial_\mu \Sigma \partial^\mu \Sigma^\dagger - i \left(\partial_\mu \Sigma [v^\mu, \Sigma^\dagger] - \text{h.c.} \right) - [v_\mu, \Sigma] [v_\mu, \Sigma^\dagger]. \quad (\text{B.18})$$

Using Eq. (B.17) we find the expansion of the constitutive parts of the kinetic term to be

$$\begin{aligned} \partial_\mu \Sigma = & \left[\left(\frac{-1}{f^2} + \frac{\pi_b^2}{6f^4} \right) (\pi_a \partial_\mu \pi_a) \cos \alpha - \left(\frac{\partial_\mu \pi_1}{f} - \frac{\pi_b^2 \partial_\mu \pi_1 + 2\pi_1 \pi_b \partial_\mu \pi_b}{6f^3} \right) \sin \alpha \right] \\ & - \left[\left(\frac{-1}{f^2} + \frac{\pi_b^2}{6f^4} \right) (\pi_a \partial_\mu \pi_a) \sin \alpha - \left(\frac{\partial_\mu \pi_1}{f} - \frac{\pi_b^2 \partial_\mu \pi_1 + 2\pi_1 \pi_b \partial_\mu \pi_b}{6f^3} \right) 2 \sin^2 \frac{\alpha}{2} \right] i\tau_1 \\ & + \left(\frac{\partial_\mu \pi_a}{f} - \frac{\pi_b^2 \partial_\mu \pi_a + 2\pi_a \pi_b \partial_\mu \pi_b}{6f^3} \right) i\tau_a, \end{aligned} \quad (\text{B.19})$$

and

$$[v_\mu, \Sigma] = -\mu_I \delta_\mu^0 \left\{ \left[\left(1 - \frac{\pi_a^2}{2f^2} + \frac{\pi_a^2 \pi_b^2}{24f^4} \right) \sin \alpha + \left(\frac{\pi_1}{f} - \frac{\pi_b^2 \pi_1}{6f^3} \right) \cos \alpha \right] \tau_2 - \left(\frac{\pi_2}{f} - \frac{\pi_b^2 \pi_2}{6f^3} \right) \tau_1 \right\}. \quad (\text{B.20})$$

Combining Eq. (B.19) and Eq. (B.20) gives the following terms

$$\text{Tr} \left\{ \partial_\mu \Sigma \partial^\mu \Sigma^\dagger \right\} = \frac{2}{f^2} \partial_\mu \pi_a \partial^\mu \pi_a + \frac{2}{3f^4} [(\pi_a \partial_\mu \pi_a)(\pi_b \partial^\mu \pi_b) - (\pi_a \partial_\mu \pi_b)(\pi_b \partial^\mu \pi_a)], \quad (\text{B.21})$$

$$\begin{aligned} -i \text{Tr} \left\{ \partial^\mu \Sigma [v_\mu, \Sigma^\dagger] - \text{h.c.} \right\} \\ = 4\mu_I \frac{\partial_0 \pi_2}{f} + 8\mu_I \frac{\pi_3}{3f^3} \sin \alpha (\pi_2 \partial_0 \pi_3 - \pi_3 \partial_0 \pi_2) \sin \alpha \\ + \left(\frac{4\mu_I}{f^2} \cos \alpha - \frac{8\mu_I \pi_1}{3f^3} \sin \alpha - \frac{4\mu_I \pi_a \pi_a}{3f^4} \cos \alpha \right) (\pi_1 \partial_0 \pi_2 - \pi_2 \partial_0 \pi_1), \end{aligned} \quad (\text{B.22})$$

$$\begin{aligned} -\text{Tr} \left\{ [v_\mu, \Sigma] [v^\mu, \Sigma^\dagger] \right\} \\ = \mu_I^2 \left[2 \sin^2 \alpha + \left(\frac{2}{f} - \frac{4\pi_a \pi_a}{3f^3} \right) \pi_1 \sin 2\alpha + \left(\frac{2}{f^2} - \frac{2\pi_a \pi_a}{3f^4} \right) \pi_a \pi_b k_{ab} \right], \end{aligned} \quad (\text{B.23})$$

$$\begin{aligned} \text{Tr} \left\{ \chi^\dagger \Sigma + \Sigma^\dagger \chi \right\} \\ = \bar{m}^2 \left(4 \cos \alpha - \frac{4\pi_1}{f} \sin \alpha - \frac{2\pi_a \pi_a}{f^2} \cos \alpha + \frac{2\pi_1 \pi_a \pi_a}{3f^3} \sin \alpha + \frac{(\pi_a \pi_a)^2}{6f^4} \cos \alpha \right), \end{aligned} \quad (\text{B.24})$$

where $k_{ab} = \delta_{a1} \delta_{b1} \cos 2\alpha + \delta_{a2} \delta_{b2} \cos^2 \alpha - \delta_{a3} \delta_{b3} \sin^2 \alpha$. Notice that the mass term is independent of the difference in quark masses, Δm . If we write the Lagrangian Eq. (B.1) as $\mathcal{L}_2 = \mathcal{L}_2^{(0)} + \mathcal{L}_2^{(1)} + \mathcal{L}_2^{(2)} + \dots$, where $\mathcal{L}_2^{(n)}$ contains all terms of order $(\pi/f)^n$, then the result of the series expansion is

$$\mathcal{L}_2^{(0)} = f^2 \left(\bar{m}^2 \cos \alpha + \frac{1}{2} \mu^2 \sin^2 \alpha \right), \quad (\text{B.25})$$

$$\mathcal{L}_2^{(1)} = f(\mu_I^2 \cos \alpha - \bar{m}^2) \pi_1 \sin \alpha + f\mu_I \partial_0 \pi_2 \sin \alpha, \quad (\text{B.26})$$

$$\mathcal{L}_2^{(2)} = \frac{1}{2} \partial_\mu \pi_a \partial^\mu \pi_a + \mu_I \cos \alpha (\pi_1 \partial_0 \pi_2 - \pi_2 \partial_0 \pi_1) - \frac{1}{2} \bar{m}^2 \pi_a \pi_a \cos \alpha + \frac{1}{2} \mu_I^2 \pi_a \pi_b k_{ab}, \quad (\text{B.27})$$

$$\begin{aligned} \mathcal{L}_2^{(3)} = \frac{\pi_a \pi_a \pi_1}{6f} (\bar{m}^2 \sin \alpha - 2\mu_I^2 \sin 2\alpha) \\ - \frac{2\mu_I}{3f} [\pi_1 (\pi_1 \partial_0 \pi_2 - \pi_2 \partial_0 \pi_1) + \pi_3 (\pi_3 \partial_0 \pi_2 - \pi_2 \partial_0 \pi_3)] \sin \alpha, \end{aligned} \quad (\text{B.28})$$

$$\begin{aligned} \mathcal{L}_2^{(4)} = \frac{1}{6f^2} \left\{ \frac{1}{4} \bar{m}^2 (\pi_a \pi_a)^2 \cos \alpha - [(\pi_a \pi_a)(\partial_\mu \pi_b \partial^\mu \pi_b) - (\pi_a \partial_\mu \pi_a)(\pi_b \partial^\mu \pi_b)] \right\} \\ - \frac{\mu_I \pi_a \pi_a}{3f^2} \left[(\pi_1 \partial_0 \pi_2 - \pi_2 \partial_0 \pi_1) \cos \alpha + \frac{1}{2} \mu_I \pi_a \pi_b k_{ab} \right]. \end{aligned} \quad (\text{B.29})$$

B.2 *Next-to-leading order Lagrangian

Constructing the next-to-leading order (NLO) Lagrangian is a business of combining the building blocks we found in section 5.2 into locally $\text{SU}(N_f)$ invariant terms. We must include all terms that obey all symmetries and that are fourth-order in Weinberg's power counting scheme and remove possible redundant terms, as discussed in section B.3. We will quote the result from

[50],

$$\begin{aligned}
\mathcal{L}_4 = & \frac{l_1}{4} \text{Tr} \left\{ \nabla_\mu \Sigma (\nabla^\mu \Sigma)^\dagger \right\}^2 + \frac{l_2}{4} \text{Tr} \left\{ \nabla_\mu \Sigma (\nabla_\nu \Sigma)^\dagger \right\} \text{Tr} \left\{ \nabla^\mu \Sigma (\nabla^\nu \Sigma)^\dagger \right\} \\
& + \frac{l_3 + l_4}{16} \text{Tr} \left\{ \chi \Sigma^\dagger + \Sigma \chi^\dagger \right\}^2 + \frac{l_4}{8} \text{Tr} \left\{ \nabla_\mu \Sigma (\nabla^\mu \Sigma)^\dagger \right\} \text{Tr} \left\{ \chi \Sigma^\dagger + \Sigma \chi^\dagger \right\} \\
& - \frac{l_7}{16} \text{Tr} \left\{ \chi \Sigma^\dagger - \Sigma \chi^\dagger \right\}^2 + \frac{h_1 + h_3 - l_4}{4} \text{Tr} \left\{ \chi \chi^\dagger \right\} \\
& + \frac{h_1 - h_3 - l_4}{16} \left[\text{Tr} \left\{ \chi \Sigma^\dagger + \Sigma \chi^\dagger \right\}^2 + \text{Tr} \left\{ \chi \Sigma^\dagger - \Sigma \chi^\dagger \right\}^2 - 2 \text{Tr} \left\{ \left(\chi \Sigma^\dagger \right)^2 + \left(\Sigma \chi^\dagger \right)^2 \right\} \right].
\end{aligned} \tag{B.30}$$

We have ignored terms containing the field strength tensors for external fields, as they vanish in our case. The parameters l_i and h_i are called low energy constants, or LEO. In section B.3, we show how to rewrite the Lagrangian to match the one used in [70, 81]. To obtain \mathcal{L}_4 to $\mathcal{O}((\pi/f)^3)$, we use the result from Eq. (B.19) and Eq. (B.20), which gives

$$\begin{aligned}
\text{Tr} \left\{ \partial_\mu \Sigma \partial_\nu \Sigma^\dagger \right\} &= 2 \frac{\partial_\mu \pi_a \partial_\nu \pi_a}{f^2} \\
-i \text{Tr} \left\{ \partial_\mu \Sigma [v_\nu, \Sigma^\dagger] - \text{h.c.} \right\} &= \frac{2\mu_I \pi_2}{f} (\delta_\mu^0 \partial_\nu + \delta_\nu^0 \partial_\mu) \sin \alpha \\
&\quad + \frac{2\mu_I}{f^2} [\pi_1 (\delta_\mu^0 \partial_\nu + \delta_\nu^0 \partial_\mu) \pi_2 - \pi_2 (\delta_\mu^0 \partial_\nu + \delta_\nu^0 \partial_\mu) \pi_1] \cos \alpha \\
-\text{Tr} \left\{ [v_\nu, \Sigma] [v_\nu, \Sigma^\dagger] \right\} &= 2\mu_I^2 \delta_\mu^0 \delta_\nu^0 \left[\sin^2 \alpha + \frac{\pi_1}{f} \sin 2\alpha + \frac{\pi_a \pi_b}{f^2} k_{ab} \right],
\end{aligned}$$

up to $\mathcal{O}((\pi/f)^3)$. Inserting $\chi = 2B_0 m = \bar{m}^2 \mathbb{1} + \Delta m^2 \tau_3$ gives

$$\begin{aligned}
\chi \Sigma^\dagger + \Sigma \chi^\dagger &= 2(\bar{m}^2 + \Delta m^2 \tau_3) \left[\left(1 - \frac{\pi_a^2}{2f^2} \right) \cos \alpha - \frac{\pi_1}{f} \sin \alpha \right] \\
&\quad + 2\Delta m^2 \left[\left(1 - \frac{\pi_a^2}{2f^2} \right) \tau_2 \sin \alpha + \frac{\pi_a}{f} (\delta_{a1} \tau_2 \cos \alpha - \delta_{a2} \tau_1) \right], \\
\chi \Sigma^\dagger - \Sigma \chi^\dagger &= -2i\bar{m}^2 \left[\left(1 - \frac{\pi_a^2}{2f^2} \right) \tau_1 \sin \alpha + \frac{\pi_a}{f} \left(\tau_a - 2\delta_{1a} \tau_1 \sin^2 \frac{\alpha}{2} \right) \right] - 2i\Delta m^2 \frac{\pi_3}{f}.
\end{aligned}$$

Combining these results gives all the terms in \mathcal{L}_4 , to $\mathcal{O}((\pi/f)^3)$:

$$\begin{aligned}
\text{Tr} \left\{ \nabla_\mu \Sigma (\nabla^\mu \Sigma)^\dagger \right\}^2 &= \text{Tr} \left\{ \partial_\mu \Sigma \partial^\mu \Sigma^\dagger - i \left(\partial_\mu \Sigma [v^\mu, \Sigma^\dagger] - \text{h.c.} \right) - [v_\mu, \Sigma] [v^\mu, \Sigma^\dagger] \right\}^2 \\
&= \frac{8\mu_I^2}{f^2} (\partial_\mu \pi_a \partial^\mu \pi_a + 2\partial_\mu \pi_2 \partial^\mu \pi_2) \sin^2 \alpha \\
&\quad + 16\mu_I^3 \left[\frac{\partial_0 \pi_2}{f} \sin^3 \alpha + \frac{1}{f^2} (3\pi_1 \partial_0 \pi_2 - \pi_2 \partial_0 \pi_1) \cos \alpha \sin^2 \alpha \right] \\
&\quad + 4\mu_I^4 \left\{ \sin^4 \alpha + 2 \sin^2 \alpha \left[\frac{\pi_1}{f} \sin 2\alpha + \frac{\pi_a \pi_b}{f^2} (k_{ab} + 2\delta_{a1} \delta_{a2} \cos^2 \alpha) \right] \right\},
\end{aligned} \tag{B.31}$$

$$\begin{aligned}
&\text{Tr} \left\{ \nabla_\mu \Sigma (\nabla_\nu \Sigma)^\dagger \right\} \text{Tr} \left\{ \nabla^\mu \Sigma (\nabla^\nu \Sigma)^\dagger \right\} \\
&= \frac{4\mu_I^2}{f^2} (\partial_0 \pi_a \partial_0 \pi_a + \partial_0 \pi_2 \partial_0 \pi_2 + \partial_\mu \pi_2 \partial^\mu \pi_2) \sin^2 \alpha \\
&\quad + 16\mu_I^3 \left[\frac{\partial_0 \pi_2}{f} \sin^3 \alpha + \frac{1}{f^2} (3\pi_1 \partial_0 \pi_2 - \pi_2 \partial_0 \pi_1) \cos \alpha \sin^2 \alpha \right] \\
&\quad + 4\mu_I^4 \left\{ \sin^4 \alpha + 2 \sin^2 \alpha \left[\frac{\pi_1}{f} \sin 2\alpha + \frac{\pi_a \pi_b}{f^2} (k_{ab} + 2\delta_{a1} \delta_{a2} \cos^2 \alpha) \right] \right\},
\end{aligned} \tag{B.32}$$

$$\text{Tr} \left\{ \nabla_\mu \Sigma (\nabla^\mu \Sigma)^\dagger \right\} \text{Tr} \left\{ \chi \Sigma^\dagger + \Sigma \chi^\dagger \right\}$$

$$\begin{aligned}
&= 4\bar{m}^2 \left\{ 2 \frac{\partial_\mu \pi_a \partial^\mu \pi_a}{f^2} \cos \alpha + 4\mu_I \left[\frac{\partial_0 \pi_2}{2f} \sin 2\alpha + \frac{1}{f^2} (\pi_1 \partial_0 \pi_2 \cos 2\alpha - \pi_2 \partial_0 \pi_1 \cos^2 \alpha) \right] \right. \\
&\quad + \mu_I^2 \left[2 \cos \alpha \sin^2 \alpha - 2 \frac{\pi_1}{f} \sin \alpha (2 - 3 \sin^2 \alpha) \right. \\
&\quad \left. \left. + \frac{1}{f^2} (\pi_1^2 [2 - 9 \sin^2 \alpha] + \pi_2^2 [2 - 3 \sin^2 \alpha] - 3\pi_3^2 \sin^2 \alpha) \cos \alpha \right] \right\}, \tag{B.33}
\end{aligned}$$

$$\text{Tr} \left\{ \chi \Sigma^\dagger + \Sigma \chi^\dagger \right\}^2 = 16\bar{m}^4 \left[\cos^2 \alpha - \frac{\pi_1}{f} \sin 2\alpha + \frac{1}{f^2} (\pi_1^2 \sin^2 \alpha - \pi_a \pi_a \cos^2 \alpha) \right], \tag{B.34}$$

$$\text{Tr} \left\{ \chi \Sigma^\dagger - \Sigma \chi^\dagger \right\}^2 = -16 \left(\frac{\Delta m^2 \pi_3}{f} \right)^2, \tag{B.35}$$

$$\begin{aligned}
&\text{Tr} \left\{ \left(\chi \Sigma^\dagger \right)^2 + \left(\Sigma \chi^\dagger \right)^2 \right\} \\
&= 4\bar{m}^4 \left(\cos 2\alpha - 2 \frac{\pi_1}{f} \sin 2\alpha - 2 \frac{\pi_a \pi_a}{f^2} \cos^2 \alpha + 2 \frac{\pi_1^2}{f^2} \sin^2 \alpha \right) + 4\Delta m^4 \left(1 - 2 \frac{\pi_3^2}{f^2} \right), \tag{B.36}
\end{aligned}$$

$$\text{Tr} \left\{ \chi^\dagger \chi \right\} = 2\bar{m}^4 + 2\Delta m^4. \tag{B.37}$$

The different terms of the NLO Lagrangian are

$$\begin{aligned}
\mathcal{L}_4^{(0)} &= (l_1 + l_2) \mu_I^4 \sin^4 \alpha + (l_3 + l_4) \bar{m}^2 \cos^2 \alpha \\
&\quad + l_4 \bar{m} \mu_I^2 \cos \alpha \sin^2 \alpha + (h_1 - l_4) \bar{m}^4 + h_3 \Delta m^4, \tag{B.38}
\end{aligned}$$

$$\begin{aligned}
\mathcal{L}_4^{(1)} &= 4\mu_I^3 \frac{l_1 + l_2}{f} (\partial_0 \pi_2 + \mu_I \cos \alpha \pi_1) \sin^3 \alpha - \frac{l_3 + l_4}{f} \bar{m}^4 \pi_1 \sin 2\alpha \\
&\quad + \bar{m}^2 \frac{l_4}{f} [\mu_I \partial_0 \pi_2 \sin 2\alpha - \mu_I^2 \pi_1 \sin \alpha (3 \sin^2 \alpha - 2)], \tag{B.39}
\end{aligned}$$

$$\begin{aligned}
\mathcal{L}_4^{(2)} &= 2\mu_I^2 \frac{l_1}{f^2} (\partial_\mu \pi_a \partial^\mu \pi_a + 2\partial_0 \pi_2 \partial_0 \pi_2) \sin^2 \alpha \\
&\quad + \mu_I^2 \frac{l_2}{f^2} (\partial_\mu \pi_2 \partial^\mu \pi_2 + 2\partial_0 \pi_a \partial_0 \pi_a + 2\partial_0 \pi_2 \partial_0 \pi_2) \sin^2 \alpha \\
&\quad + 2 \frac{l_1 + l_2}{f^2} [2\mu_I^3 (3\pi_1 \partial_0 \pi_2 - \pi_2 \partial_0 \pi_1) \cos \alpha + \mu_I^4 \pi_a \pi_b (k_{ab} + 2\delta_{a1} \delta_{a2} \cos^2 \alpha)] \sin^2 \alpha \\
&\quad + \frac{l_3 + l_4}{f^2} \bar{m}^2 (\pi_1^2 \sin^2 \alpha - \pi_a \pi_a \cos^2 \alpha) \\
&\quad + \frac{l_4}{f^2} \bar{m}^2 \left[\partial_\mu \pi_a \partial^\mu \pi_a \cos \alpha + 4\mu_I (\pi_1 \partial_0 \pi_2 \cos 2\alpha - \pi_2 \partial_0 \pi_1 \cos^2 \alpha) \right. \\
&\quad \left. + \frac{1}{2} \mu_I^2 (\pi_1^2 [2 - 9 \sin^2 \alpha] + \pi_2^2 [2 - 3 \sin^2 \alpha] - 3\pi_3^2 \sin^2 \alpha) \cos \alpha \right] + \frac{l_7}{f^2} \Delta m^2 \pi_3^2. \tag{B.40}
\end{aligned}$$

B.3 *Rewriting terms

This section shows how to rewrite terms in the Lagrangian of Chiral perturbation theory. These techniques and more are used to reduce the total number of terms and to change between different conventions. Changing the field parametrization that appears in the Lagrangian does not affect any of the physics, as it corresponds to a change of variables in the path integral [50, 85, 86]. However, a change of variables can result in new terms in the Lagrangian. As a result of this, terms that appear independent on their face may be redundant. These terms can be eliminated by using the classical equations of motion. In this section, we show first the derivation of the equations of motion, then use this result to identify redundant terms which need not be included in the most general Lagrangian.

We derive the equations of motion for the leading order Lagrangian using the principle of least action. Choosing the parametrization $\Sigma = \exp \{i\pi_a \tau_a\}$, a variation $\pi_a \rightarrow \pi_a + \delta\pi_a$ results in a variation in Σ , $\delta\Sigma = i\tau_a \delta\pi_a \Sigma$. The variation of the leading order action $S_2 = \int_\Omega d^4x \mathcal{L}_2$, when varying π_a is

$$\delta S = \int_\Omega dx \frac{f^2}{4} \text{Tr} \left\{ (\nabla_\mu \delta\Sigma)(\nabla^\mu \Sigma)^\dagger + (\nabla_\mu \Sigma)(\nabla^\mu \delta\Sigma)^\dagger + \chi \delta\Sigma^\dagger + \delta\Sigma \chi^\dagger \right\}.$$

Using the properties of the covariant derivative to do partial integration as well as $\delta(\Sigma\Sigma^\dagger) = (\delta\Sigma)\Sigma^\dagger + \Sigma(\delta\Sigma)^\dagger = 0$, the variation of the action can be written

$$\begin{aligned} \delta S &= \frac{f^2}{4} \int_\Omega dx \text{Tr} \left\{ -\delta\Sigma \nabla^2 \Sigma^\dagger + (\nabla^2 \Sigma)(\Sigma^\dagger \delta\Sigma \Sigma^\dagger) - \chi(\Sigma^\dagger \delta\Sigma \Sigma^\dagger) + \delta\Sigma \chi^\dagger \right\} \\ &= \frac{f^2}{4} \int_\Omega dx \text{Tr} \left\{ \delta\Sigma \Sigma^\dagger \left[(\nabla^2 \Sigma) \Sigma^\dagger - \Sigma \nabla^2 \Sigma^\dagger - \chi \Sigma^\dagger + \Sigma \chi^\dagger \right] \right\} \\ &= i \frac{f^2}{4} \int_\Omega dx \text{Tr} \left\{ \tau_a \left[(\nabla^2 \Sigma) \Sigma^\dagger - \Sigma \nabla^2 \Sigma^\dagger - \chi \Sigma^\dagger + \Sigma \chi^\dagger \right] \right\} \delta\pi_a. \end{aligned}$$

As the variation is arbitrary, the equations of motion to leading order is

$$\text{Tr} \left\{ \tau_a \left[(\nabla^2 \Sigma) \Sigma^\dagger - \Sigma \nabla^2 \Sigma^\dagger - \chi \Sigma^\dagger + \Sigma \chi^\dagger \right] \right\} = 0. \quad (\text{B.41})$$

We define

$$\mathcal{O}_{\text{EOM}}^{(2)} = (\nabla^2 \Sigma) \Sigma^\dagger - \Sigma \nabla^2 \Sigma^\dagger - \chi \Sigma^\dagger + \Sigma \chi^\dagger. \quad (\text{B.42})$$

The next step in eliminating redundant terms is to change the parametrization of Σ by $\Sigma(x) \rightarrow \Sigma'(x)$. Here, $\Sigma(x) = e^{iS(x)} \Sigma'(x)$, $S(x) \in \mathfrak{su}(2)$. This change leads to a new Lagrange density, $\mathcal{L}[\Sigma] = \mathcal{L}[\Sigma'] + \Delta\mathcal{L}[\Sigma']$. We are free to choose $S(x)$, as long Σ' still obey the required transformation properties. Any terms in the Lagrangian $\Delta\mathcal{L}$ due to a reparametrization can be neglected, as argued earlier. When demanding that Σ' obey the same symmetries as Σ , the most general transformation to second order in Weinberg's power counting scheme is [50]

$$S_2 = i\alpha_2 \left[(\nabla^2 \Sigma') \Sigma'^\dagger - \Sigma' (\nabla^2 \Sigma')^\dagger \right] + i\alpha_2 \left[\chi \Sigma'^\dagger - \Sigma' \chi^\dagger - \frac{1}{2} \text{Tr} \left\{ \chi \Sigma'^\dagger - \Sigma' \chi^\dagger \right\} \right]. \quad (\text{B.43})$$

α_1 and α_2 are arbitrary real numbers. As Eq. (B.43) is second-order, $\Delta\mathcal{L}$ is fourth-order in Weinberg's power counting scheme. Inserting this gives

$$\begin{aligned} \mathcal{L}_2 [e^{iS_2} \Sigma'] &= \frac{f^2}{4} \text{Tr} \left\{ [\nabla_\mu (1 + iS_2) \Sigma'] [\nabla^\mu \Sigma'^\dagger (1 - iS_2)] \right\} + \frac{f^2}{4} \text{Tr} \left\{ \chi \Sigma'^\dagger (1 - iS_2) + (1 + iS_2) \Sigma' \chi^\dagger \right\} \\ &= \mathcal{L}[\Sigma'] + i \frac{f^2}{4} \text{Tr} \left\{ [\nabla_\mu (S_2 \Sigma')] [\nabla^\mu \Sigma']^\dagger - [\nabla_\mu \Sigma'] [\nabla^\mu (\Sigma'^\dagger S_2)] \right\} \\ &\quad - i \frac{f^2}{4} \text{Tr} \left\{ \chi \Sigma'^\dagger S_2 - S_2 \Sigma' \chi^\dagger \right\}. \end{aligned}$$

Using the properties of the covariant derivative, we may use the product rule and partial integration to write the difference between the two Lagrangians to fourth-order as

$$\begin{aligned} \Delta\mathcal{L}[\Sigma'] &= i \frac{f^2}{4} \text{Tr} \left\{ (\nabla_\mu S_2) (\Sigma' \nabla^\mu \Sigma'^\dagger - (\nabla^\mu \Sigma') \Sigma'^\dagger) \right\} - i \frac{f^2}{4} \text{Tr} \left\{ \chi \Sigma'^\dagger S_2 - S_2 \Sigma' \chi^\dagger \right\} \\ &= \frac{f^2}{4} \text{Tr} \left\{ i S_2 \mathcal{O}_{\text{EOM}}^{(2)} \right\}. \end{aligned} \quad (\text{B.44})$$

Any term that can be written in the form of Eq. (B.44) for arbitrary $\alpha_1, \alpha_2 \in \mathbb{R}$ is redundant, as we argued earlier, and may therefore be discarded. $\Delta\mathcal{L}_2$ is of fourth-order, and it can thus be used to remove terms from \mathcal{L}_4 or higher order.

B.4 *Rewriting NLO Lagrangian

The NLO Lagrangian used in this Appendix is given in Eq. (B.30) and is

$$\begin{aligned}\mathcal{L}_4 = & \frac{l_1}{4} \text{Tr} \left\{ \nabla_\mu \Sigma (\nabla^\mu \Sigma)^\dagger \right\}^2 + \frac{l_2}{4} \text{Tr} \left\{ \nabla_\mu \Sigma (\nabla_\nu \Sigma)^\dagger \right\} \text{Tr} \left\{ \nabla^\mu \Sigma (\nabla^\nu \Sigma)^\dagger \right\} + \frac{l_3 + l_4}{16} \text{Tr} \left\{ \chi \Sigma^\dagger + \Sigma \chi^\dagger \right\}^2 \\ & + \frac{l_4}{8} \text{Tr} \left\{ \nabla_\mu \Sigma (\nabla^\mu \Sigma)^\dagger \right\} \text{Tr} \left\{ \chi \Sigma^\dagger + \Sigma \chi^\dagger \right\} - \frac{l_7}{16} \text{Tr} \left\{ \chi \Sigma^\dagger - \Sigma \chi^\dagger \right\}^2 + \frac{h_1 + h_3 - l_4}{4} \text{Tr} \left\{ \chi \chi^\dagger \right\} \\ & + \frac{h_1 - h_3 - l_4}{16} \left[\text{Tr} \left\{ \chi \Sigma^\dagger + \Sigma \chi^\dagger \right\}^2 + \text{Tr} \left\{ \chi \Sigma^\dagger - \Sigma \chi^\dagger \right\}^2 - 2 \text{Tr} \left\{ \left(\chi \Sigma^\dagger \right)^2 + \left(\Sigma \chi^\dagger \right)^2 \right\} \right].\end{aligned}$$

We can rewrite it to match the one used in [70, 81], starting with

$$\begin{aligned}& \frac{h_1 - h_3 - l_4}{16} \left(\text{Tr} \left\{ \chi \Sigma^\dagger - \Sigma \chi^\dagger \right\}^2 - 2 \text{Tr} \left\{ \left(\chi \Sigma^\dagger \right)^2 + \left(\Sigma \chi^\dagger \right)^2 \right\} \right) \\ & = \frac{h_1 - h_3 - l_4}{16} \left(\text{Tr} \left\{ \chi \Sigma^\dagger \right\}^2 - 2 \text{Tr} \left\{ \chi \Sigma^\dagger \right\} \text{Tr} \left\{ \Sigma \chi^\dagger \right\} + \text{Tr} \left\{ \Sigma \chi^\dagger \right\}^2 \right. \\ & \quad \left. - 2 \text{Tr} \left\{ \left(\chi \Sigma^\dagger \right)^2 \right\} - 2 \text{Tr} \left\{ \left(\Sigma \chi^\dagger \right)^2 \right\} \right).\end{aligned}$$

Using $\text{Tr} \{A^2\} = \text{Tr} \{A\}^2 - \det(A) \text{Tr} \{1\}$, we get

$$\begin{aligned}& = -\frac{h_1 - h_3 - l_4}{16} \left(\text{Tr} \left\{ \chi \Sigma^\dagger \right\}^2 + 2 \text{Tr} \left\{ \chi \Sigma^\dagger \right\} \text{Tr} \left\{ \Sigma \chi^\dagger \right\} + \text{Tr} \left\{ \Sigma \chi^\dagger \right\}^2 - 4 \det(\chi \Sigma^\dagger) - 4 \det(\Sigma \chi^\dagger) \right) \\ & = -\frac{h_1 - h_3 - l_4}{16} \left(\text{Tr} \left\{ \chi \Sigma^\dagger + \Sigma \chi^\dagger \right\}^2 - 4 \det(\chi \Sigma^\dagger) - 4 \det(\Sigma \chi^\dagger) \right).\end{aligned}$$

Furthermore, as $\det(\Sigma) = 1$,

$$\begin{aligned}\mathcal{L}_4 = & \frac{l_1}{4} \text{Tr} \left\{ \nabla_\mu \Sigma (\nabla^\mu \Sigma)^\dagger \right\}^2 + \frac{l_2}{4} \text{Tr} \left\{ \nabla_\mu \Sigma (\nabla_\nu \Sigma)^\dagger \right\} \text{Tr} \left\{ \nabla^\mu \Sigma (\nabla^\nu \Sigma)^\dagger \right\} + \frac{l_3 + l_4}{16} \text{Tr} \left\{ \chi \Sigma^\dagger + \Sigma \chi^\dagger \right\}^2 \\ & + \frac{l_4}{8} \text{Tr} \left\{ \nabla_\mu \Sigma (\nabla^\mu \Sigma)^\dagger \right\} \text{Tr} \left\{ \chi \Sigma^\dagger + \Sigma \chi^\dagger \right\} - \frac{l_7}{16} \text{Tr} \left\{ \chi \Sigma^\dagger - \Sigma \chi^\dagger \right\}^2 + \frac{h_1 + h_3 - l_4}{4} \text{Tr} \left\{ \chi \chi^\dagger \right\} \\ & + \frac{h_1 - h_3 - l_4}{4} (\det \chi + \det \chi^\dagger).\end{aligned}$$

For real χ , we have $\text{Tr} \{ \chi \chi^\dagger \} = \det(\chi) + \det(\chi^\dagger)$, and we can define $h'_1 = h_1 - l_4$ to get

$$\begin{aligned}\mathcal{L}_4 = & \frac{l_1}{4} \text{Tr} \left\{ \nabla_\mu \Sigma (\nabla^\mu \Sigma)^\dagger \right\}^2 + \frac{l_2}{4} \text{Tr} \left\{ \nabla_\mu \Sigma (\nabla_\nu \Sigma)^\dagger \right\} \text{Tr} \left\{ \nabla^\mu \Sigma (\nabla^\nu \Sigma)^\dagger \right\} + \frac{l_3 + l_4}{16} \text{Tr} \left\{ \chi \Sigma^\dagger + \Sigma \chi^\dagger \right\}^2 \\ & + \frac{l_4}{8} \text{Tr} \left\{ \nabla_\mu \Sigma (\nabla^\mu \Sigma)^\dagger \right\} \text{Tr} \left\{ \chi \Sigma^\dagger + \Sigma \chi^\dagger \right\} - \frac{l_7}{16} \text{Tr} \left\{ \chi \Sigma^\dagger - \Sigma \chi^\dagger \right\}^2 + \frac{h'_1}{2} \text{Tr} \left\{ \chi \chi^\dagger \right\}.\end{aligned}$$

If one assumes $\Delta m = 0$, i.e., what is called the chiral limit, then the term l_7 falls away, as $\chi = \chi^\dagger$.

Appendix C

*Thermal field theory

This appendix is based on [62, 63, 87].

In this appendix, we will give a brief overview of the basics of thermal field theory using imaginary-time formalism. We will derive the relevant scalar path integral, discuss the operator determinant and regularization, derive the Feynman rules for a φ^4 -theory and discuss the fermionic theory. The theory laid out in this appendix is referenced throughout the thesis.

C.1 *Statistical mechanics

In classical mechanics, a thermal system at temperature $T = 1/\beta$ is described as an ensemble state, which have a probability P_n of being in state n , with energy E_n . In the canonical ensemble, the probability is proportional to $e^{-\beta E_n}$, so $P_n = C e^{-\beta E_n}$. The expectation value of some quantity A , with value A_n in the state n , is

$$\langle A \rangle = \sum_n A_n P_n = \frac{1}{Z} \sum_n A_n e^{-\beta E_n}, \quad Z = \sum_n e^{-\beta E_n}. \quad (\text{C.1})$$

Z is called the partition function. In quantum mechanics, an ensemble configuration is described by a non-pure density operator,

$$\hat{\rho} = \sum_n P_n |n\rangle \langle n|, \quad (\text{C.2})$$

where $|n\rangle$ is some basis for the relevant Hilbert space. Assuming $|n\rangle$ are energy eigenvectors, i.e., $\hat{H} |n\rangle = E_n |n\rangle$, the density operator for the canonical ensemble is

$$\hat{\rho} = \sum_n C e^{-\beta E_n} |n\rangle \langle n| = C e^{-\beta \hat{H}} \sum_n |n\rangle \langle n| = C e^{-\beta \hat{H}}. \quad (\text{C.3})$$

The expectation value in the ensemble state of a quantity corresponding to the operator \hat{A} is given by

$$\langle A \rangle = \frac{\text{Tr} \{ \hat{\rho} \hat{A} \}}{\text{Tr} \{ \hat{\rho} \}} = \frac{1}{Z} \text{Tr} \{ \hat{A} e^{-\beta \hat{H}} \}. \quad (\text{C.4})$$

The partition function Z ensures that the probabilities add up to 1, and is defined as

$$Z = \text{Tr} \{ e^{-\beta \hat{H}} \}. \quad (\text{C.5})$$

The grand canonical ensemble takes into account the conserved charges of the system, which are a result of Nöther's theorem, as discussed in section 3.3. In the grand canonical ensemble,

a system with n conserved charges Q_i has probability proportional to $e^{-\beta(H-\mu_i Q_i)}$. Here, μ_i are the chemical potentials corresponding to conserved charge Q_i . This leads to the partition function

$$Z = \text{Tr} \left\{ e^{-\beta(\hat{H}-\mu_i \hat{Q}_i)} \right\}. \quad (\text{C.6})$$

The free energy in the grand canonical ensemble, also called grand potential, is

$$F = -\frac{1}{\beta} \ln(Z). \quad (\text{C.7})$$

C.2 *Imaginary-time formalism

The partition function may be calculated similarly to the path integral approach, in what is called the imaginary-time formalism. This formalism is restricted to time-independent problems and is used to study fields in a volume V . This volume is taken to infinity in the thermodynamic limit. As an example, take a scalar quantum field theory with the Hamiltonian

$$\hat{H} = \int_V d^3x \hat{\mathcal{H}}[\hat{\varphi}(\vec{x}), \hat{\pi}(\vec{x})], \quad (\text{C.8})$$

where $\hat{\varphi}(\vec{x})$ is the field operator, and $\hat{\pi}(\vec{x})$ is the corresponding canonical momentum operator. These field operators have time-independent eigenvectors, $|\varphi\rangle$ and $|\pi\rangle$, defined by

$$\hat{\varphi}(\vec{x}) |\varphi\rangle = \varphi(\vec{x}) |\varphi\rangle, \quad \hat{\pi}(\vec{x}) |\pi\rangle = \pi(\vec{x}) |\pi\rangle. \quad (\text{C.9})$$

In analogy with regular quantum mechanics, they obey the relations¹

$$\mathbb{1} = \int \mathcal{D}\varphi(\vec{x}) |\varphi\rangle \langle\varphi| = \int \mathcal{D}\pi(\vec{x}) |\pi\rangle \langle\pi|, \quad (\text{C.10})$$

$$\langle\varphi|\pi\rangle = \exp \left\{ i \int_V d^3x \varphi(\vec{x}) \pi(\vec{x}) \right\}, \quad (\text{C.11})$$

$$\langle\pi_a|\pi_b\rangle = \delta(\phi_a - \phi_b), \quad \langle\varphi_a|\varphi_b\rangle = \delta(\varphi_a - \varphi_b). \quad (\text{C.12})$$

The functional integral is defined by starting with M degrees of freedom, $\{\varphi_m\}_{m=1}^M$ located at a finite grid $\{\vec{x}_m\}_{m=1}^M \subset V$. The integral is then the limit of the integral over all degrees of freedom, as $M \rightarrow \infty$:

$$\lim_{M \rightarrow \infty} \int \left(\prod_{m=1}^M d\varphi_m \right) := \int \mathcal{D}\varphi(\vec{x}).$$

The functional Dirac-delta $\delta(f) = \prod_x \delta(f(x))$ is generalization of the familiar Dirac delta function. Given a functional $\mathcal{F}[f]$, it is defined by the relation

$$\int \mathcal{D}f(x) \mathcal{F}[f] \delta(f - g) = \mathcal{F}[g]. \quad (\text{C.13})$$

The Hamiltonian is the limit of a sum of Hamiltonians \hat{H}_m for each point \vec{x}_m

$$\hat{H} = \lim_{M \rightarrow \infty} \sum_{m=1}^M \frac{V}{M} \hat{H}_m(\{\hat{\varphi}_m\}, \{\hat{\pi}_m\}). \quad (\text{C.14})$$

H_m may depend on the local degrees of freedom $\hat{\varphi}_m, \hat{\pi}_m$ as well as those at neighboring points. By inserting the completeness relations Eq. (C.10) N times into the definition of the partition

¹Some authors write $\mathcal{D}\pi/2\pi$. This extra factor 2π is a convention that we leave out for notational clarity.

function, it may be written as

$$\begin{aligned} Z &= \int \mathcal{D}\varphi(\vec{x}) \left\langle \varphi \left| e^{-\beta \hat{H}} \right| \varphi \right\rangle \\ &= \prod_{n=1}^N \left(\int \mathcal{D}\varphi_n(\vec{x}) \int \mathcal{D}\pi_n(\vec{x}) \right) \prod_{n=1}^N \langle \varphi_n | \pi_n \rangle \left\langle \pi_n \left| e^{-\epsilon \hat{H}} \right| \varphi_{n+1} \right\rangle \langle \varphi_1 | \varphi_{N+1} \rangle, \end{aligned} \quad (\text{C.15})$$

where $\epsilon = \beta/N$. The last term ensures that $\varphi_1 = \varphi_{N+1}$. Bosons such as the scalar field φ , follow the periodic boundary condition $\varphi(0, \vec{x}) = \varphi(\beta, \vec{x})$. Fermions, as we will show later, follow the anti-periodic boundary condition $\psi(0, \vec{x}) = -\psi(\beta, \vec{x})$. We now want to exploit the fact that $|\pi\rangle$ and $|\varphi\rangle$ are the eigenvectors of the operators that define the Hamiltonian. In our case, as the Hamiltonian density \mathcal{H} can be written as a sum of functions of φ and π separately, $\mathcal{H}[\varphi(\vec{x}), \pi(\vec{x})] = \mathcal{F}_1[\varphi(\vec{x})] + \mathcal{F}_2[\pi(\vec{x})]$ we may evaluate it as $\langle \pi_n | \mathcal{H}[\hat{\varphi}(\vec{x}), \hat{\pi}(\vec{x})] | \varphi_{n+1} \rangle = \mathcal{H}[\varphi_{n+1}(\vec{x}), \pi_n(\vec{x})] \langle \pi_n | \varphi_{n+1} \rangle$. This relationship does not, however, hold for more general functions of the field operators. In that case, one has to be more careful about the ordering of the operators, for example, by using *Weyl ordering* [40]. By series expanding $e^{-\epsilon \hat{H}}$ and exploiting this relationship, the partition function can be written as, to second order in ϵ ,

$$\begin{aligned} Z &= \prod_{n=1}^N \left(\int \mathcal{D}\varphi_n(\vec{x}) \int \mathcal{D}\pi_n(\vec{x}) \right) \\ &\quad \times \exp \left\{ -\epsilon \sum_{n=1}^N \int_V d^3x \left(\mathcal{H}[\varphi_n(\vec{x}), \pi_n(\vec{x})] - i\pi_n(\vec{x}) \frac{\varphi_n(\vec{x}) - \varphi_{n+1}(\vec{x})}{\epsilon} \right) \right\}. \end{aligned} \quad (\text{C.16})$$

We denote $\varphi_n(\vec{x}) = \varphi(\tau_n, \vec{x})$, $\tau_n = n\epsilon \in [0, \beta]$ and likewise with $\pi_n(\vec{x})$. In the limit $N \rightarrow \infty$, the expression for the partition function becomes

$$Z = \int_S \mathcal{D}\varphi(\tau, \vec{x}) \int \mathcal{D}\pi(\tau, \vec{x}) \exp \left\{ - \int_0^\beta d\tau \int_V d\vec{x} \left(\mathcal{H}[\varphi(\tau, \vec{x}), \pi(\tau, \vec{x})] - i\pi(\tau, \vec{x}) \dot{\varphi}(\tau, \vec{x}) \right) \right\}, \quad (\text{C.17})$$

where S is the set of field configurations φ such that $\varphi(\beta, \vec{x}) = \varphi(0, \vec{x})$. With a Hamiltonian density of the form $\mathcal{H} = \frac{1}{2}\pi^2 + \frac{1}{2}(\nabla\varphi)^2 + \mathcal{V}(\varphi)$, we can evaluate the integral over the canonical momentum π by discretizing $\pi(\tau_n, \vec{x}_m) = \pi_{m,n}$,

$$\begin{aligned} &\int \mathcal{D}\pi \exp \left\{ - \int_0^\beta d\tau \int_V d^3x \left(\frac{1}{2}\pi^2 - i\pi\dot{\varphi} \right) \right\} \\ &= \lim_{M,N \rightarrow \infty} \int \left(\prod_{m,n=1}^{M,N} \frac{d\pi_{m,n}}{2\pi} \right) \exp \left\{ - \sum_{m,n} \frac{V\beta}{MN} \left[\frac{1}{2}(\pi_{m,n} - i\dot{\varphi}_{m,n})^2 + \frac{1}{2}\dot{\varphi}_{m,n}^2 \right] \right\} \\ &= \lim_{M,N \rightarrow \infty} \left(\frac{MN}{2\pi V\beta} \right)^{MN/2} \exp \left\{ - \int_0^\beta d\tau \int_V d^3x \frac{1}{2}\dot{\varphi}^2 \right\}, \end{aligned}$$

where $\dot{\varphi}_{m,n} = (\varphi_{m,n+1} - \varphi_{m,n})/\epsilon$. The partition function is then,

$$Z = C \int \mathcal{D}\varphi \exp \left\{ - \int_0^\beta d\tau \int_V d^3x \left[\frac{1}{2} (\dot{\varphi}^2 + \nabla\varphi^2) + \mathcal{V}(\varphi) \right] \right\}. \quad (\text{C.18})$$

Here, C is the divergent constant that results from the π -integral. In the last line, we exploited the fact that the variable of integration $\pi_{n,m}$ may be shifted by a constant without changing the integral, and used the Gaussian integral

$$\int_{-\infty}^{\infty} dx e^{-ax^2/2} = \sqrt{\frac{2\pi}{a}}. \quad (\text{C.19})$$

The partition function resulting from this procedure may also be obtained by starting with the ground state path integral

$$Z_g = \int \mathcal{D}\varphi \mathcal{D}\pi \exp \left\{ i \int_{\Omega'} d^4x (\pi \dot{\varphi} - \mathcal{H}[\varphi, \pi]) \right\} = C' \int \mathcal{D}\varphi \exp \left\{ i \int_{\Omega'} d^4x \mathcal{L}[\varphi, \partial_\mu \varphi] \right\},$$

and follow a formal procedure. First, the action integral is modified by performing a Wick-rotation of the time coordinate t . This involves changing the domain of t from the real line to the imaginary line by closing the contour at infinity and changing variable $it \rightarrow \tau$. The new variable is then restricted to the interval $\tau \in [0, \beta]$, and the domain of the functional integral $\int \mathcal{D}\varphi$ is restricted from *all* (smooth enough) field configurations $\varphi(t, \vec{x})$, to only those that obey $\varphi(\beta, \vec{x}) = e^{i\theta} \varphi(0, \vec{x})$, which is denoted S . Here, $\theta \in \{0, \pi\}$, depending on if the particle is a boson or fermion. This procedure motivates the introduction of the Euclidean Lagrange density, $\mathcal{L}_E(\tau, \vec{x}) = -\mathcal{L}(-i\tau, \vec{x})$, as well as the name “imaginary-time formalism”. The result is the same partition function as before,

$$\begin{aligned} Z &= C \int_S \mathcal{D}\varphi \int \mathcal{D}\pi \exp \left\{ - \int_0^\beta d\tau \int_V d^3x [-i\dot{\varphi}\pi + \mathcal{H}(\varphi, \pi)] \right\} \\ &= C' \int_S \mathcal{D}\varphi \exp \left\{ - \int_0^\beta d\tau \int_V d^3x \mathcal{L}_E(\varphi, \pi) \right\}. \end{aligned} \quad (\text{C.20})$$

C.2.1 Fourier series

Due to the finite range of the imaginary-time coordinate $\tau \in [0, \beta]$, the momentum-space fields in imaginary-time formalism have a discrete coordinate. We define the Matsubara-frequencies as $\omega_n = 2n\pi/\beta$ for bosons and $\omega_n = (2n+1)\pi/\beta$ for fermions. They together form the reciprocal space $\tilde{\Omega} = \{\omega_n\} \times \tilde{V}$, where \tilde{V} is reciprocal to V . To get a more economical notation, we denote the Euclidean real-space coordinates as $X = (\tau, \vec{x})$ and the reciprocal space coordinates as $K = (\omega_n, \vec{k})$. The dot product is $X \cdot K = \omega_n \tau + \vec{k} \cdot \vec{x}$. In the limit $V \rightarrow \infty$, we follow the prescription

$$\frac{1}{V} \sum_{\vec{k} \in \tilde{V}} \rightarrow \int_{\mathbb{R}^3} \frac{d^3k}{(2\pi)^3}. \quad (\text{C.21})$$

The sum over all degrees of freedom, and the corresponding integrals for the thermodynamic limit are

$$\frac{\beta V}{NM} \sum_{n=1}^N \sum_{\vec{x}_m \in V} \xrightarrow{N, M \rightarrow \infty} \int_0^\beta d\tau \int_{\mathbb{R}^3} d^3x = \int_\Omega dX, \quad (\text{C.22})$$

$$\frac{1}{V} \sum_{n=-\infty}^{\infty} \sum_{\vec{k} \in \tilde{V}} \xrightarrow{V \rightarrow \infty} \sum_{n=-\infty}^{\infty} \int_{\mathbb{R}^3} \frac{d^3k}{(2\pi)^3} = \int_{\tilde{\Omega}} dK. \quad (\text{C.23})$$

The convention used for the Fourier expansion of thermal fields is in accordance with [63]. The prefactor is chosen to make the Fourier components of the field dimensionless, which makes it easier to evaluate the trace correctly. For bosons, the Fourier expansion is

$$\varphi(X) = \sqrt{V\beta} \int_{\tilde{\Omega}} dK \tilde{\varphi}(K) e^{iX \cdot K} = \sqrt{\frac{\beta}{V}} \sum_{n=-\infty}^{\infty} \sum_{\vec{k} \in \tilde{V}} \tilde{\varphi}_n(\vec{k}) \exp \left\{ i(\omega_n \tau + \vec{x} \cdot \vec{k}) \right\}, \quad (\text{C.24})$$

$$\tilde{\varphi}(K) = \sqrt{\frac{1}{V\beta^3}} \int_{\tilde{\Omega}} dX \tilde{\varphi}(X) e^{-iX \cdot K}, \quad (\text{C.25})$$

while for Fermions, it is

$$\psi(X) = \sqrt{V} \int_{\tilde{\Omega}} dK \tilde{\psi}(K) e^{iX \cdot K} = \frac{1}{\sqrt{V}} \sum_{n=-\infty}^{\infty} \sum_{\vec{k} \in \tilde{V}} \psi(\omega_n, \vec{k}) \exp \left\{ i(\omega_n \tau + \vec{x} \cdot \vec{k}) \right\}. \quad (\text{C.26})$$

Two often-used identities are

$$\int_{\Omega} dX e^{iX \cdot (K-K')} = \beta \delta_{nn'} (2\pi)^3 \delta^3(\vec{k} - \vec{k}') := \beta \delta(K - K'), \quad (\text{C.27})$$

$$\int_{\tilde{\Omega}} dK e^{iK(X-X')} = \beta \delta(\tau - \tau') \delta^3(\vec{x} - \vec{x}') := \beta \delta(X - X'). \quad (\text{C.28})$$

C.3 *Free scalar field

The procedure for obtaining the thermal properties of an interacting scalar field is similar to that used in scattering theory. One starts with a free theory, which can be solved exactly. Then an interaction term is added, which is accounted for perturbatively by using Feynman diagrams. The Euclidean Lagrangian for a free scalar gas is, after integrating by parts,

$$\mathcal{L}_E = \frac{1}{2} \varphi(X) (-\partial_E^2 + m^2) \varphi(X) \quad (\text{C.29})$$

Here, $X = (\tau, \vec{x})$ is the Euclidean coordinate resulting from the Wick-rotation as described in the last section. We have also introduced the Euclidean Laplace operator, $\partial_E^2 = \partial_\tau^2 + \nabla^2$. Following the procedure to obtain the thermal partition function yields

$$Z = C \int_S \mathcal{D}\varphi(X) \exp \left\{ - \int_{\Omega} dX \frac{1}{2} \varphi(X) (-\partial_E^2 + m^2) \varphi(X) \right\}. \quad (\text{C.30})$$

Here, Ω is the domain $[0, \beta] \times V$. We then insert the Fourier expansion of φ and change the functional integration variable to the Fourier components. The integration measures are related by

$$\mathcal{D}\varphi(X) = \det \left(\frac{\delta\varphi(X)}{\delta\tilde{\varphi}(K)} \right) \mathcal{D}\tilde{\varphi}(K),$$

where $K = (\omega_n, \vec{k})$ is the Euclidean Fourier-space coordinate. The determinant factor which appears may be absorbed into the constant C , as the integration variables are related by a linear transform. The action becomes

$$\begin{aligned} S &= - \int_{\Omega} dX \mathcal{L}_E = - \frac{1}{2} V \beta \int_{\Omega} dX \int_{\tilde{\Omega}} dK \int_{\tilde{\Omega}} dK' \tilde{\varphi}(K') (\omega_n^2 + \vec{k}^2 + m^2) \tilde{\varphi}(K) e^{iX \cdot (K-K')} \\ &= - \frac{1}{2} V \beta^2 \int_{\tilde{\Omega}} dK \tilde{\varphi}(K)^* (\omega_n^2 + \omega_k^2) \tilde{\varphi}(K), \end{aligned}$$

where $\omega_k^2 = \vec{k}^2 + m^2$. $\tilde{\Omega}$ is the reciprocal space corresponding to Ω . We used the fact that φ is real, which implies that $\tilde{\varphi}(-K) = \tilde{\varphi}(K)^*$, as well as the identity Eq. (C.27). This gives the partition function

$$Z = C \int_{\tilde{S}} \mathcal{D}\tilde{\varphi}(K) \exp \left\{ - \frac{1}{2} V \int_{\tilde{\Omega}} dK \tilde{\varphi}(K)^* [\beta^2 (\omega_n^2 + \omega_k^2)] \tilde{\varphi}(K) \right\}. \quad (\text{C.31})$$

Going back to before the continuum limit, this integral can be written as a product of Gaussian integrals and may therefore be evaluated

$$Z = C \prod_{n=-\infty}^{\infty} \prod_{k \in \tilde{V}} \left(\int d\tilde{\varphi}_{n,\vec{k}} \exp \left\{ - \frac{1}{2} \tilde{\varphi}_{n,\vec{k}}^* [\beta^2 (\omega_n^2 + \omega_k^2)] \tilde{\varphi}_{n,\vec{k}} \right\} \right) = C \prod_{n=-\infty}^{\infty} \prod_{k \in \tilde{V}} \sqrt{\frac{2\pi}{\beta^2 (\omega_n^2 + \omega_k^2)}}.$$

The partition function is related to free energy F through

$$\frac{F}{TV} = - \frac{\ln(Z)}{V} = \frac{1}{2} \int_{\tilde{\Omega}} dK \ln[\beta^2 (\omega_n^2 + \omega_k^2)] + \frac{F_0}{TV}, \quad (\text{C.32})$$

where F_0 is a constant.

A faster and more formal way to get to this result is to compare the partition function to the multidimensional version of the Gaussian integral [40, 63]. The partition function has the form

$$I_n = \int_{\mathbb{R}^n} d^n x \exp \left\{ -\frac{1}{2} \langle x, D_0^{-1} x \rangle \right\}, \quad (\text{C.33})$$

where D_0^{-1} is a linear operator, and $\langle \cdot, \cdot \rangle$ an inner product on the corresponding vector space. By diagonalizing D_0^{-1} , we get the result

$$I_n = \sqrt{\frac{(2\pi)^n}{\det(D_0^{-1})}}. \quad (\text{C.34})$$

We may then use the identity

$$\det(D_0^{-1}) = \prod_i \lambda_i = \exp \left\{ \text{Tr}[\ln(D_0^{-1})] \right\}, \quad (\text{C.35})$$

where λ_i are the eigenvalues of D_0^{-1} . The trace in this context is defined by the vector space D_0^{-1} acts on. For given an orthonormal basis x_n , such that $\langle x_n, x_{n'} \rangle = \delta_{nn'}$ the trace can be evaluated as $\text{Tr} \{ D_0^{-1} \} = \sum_n \langle x_n, D_0^{-1} x_n \rangle$. Identifying

$$\langle x, D_0^{-1} x \rangle = \int_{\Omega} dX \varphi(X) (-\partial_E^2 + m^2) \varphi(X), \quad (\text{C.36})$$

we get the formal result

$$Z = \det(-\partial_E^2 + m^2)^{-1/2}, \quad (\text{C.37})$$

and

$$\beta F = \frac{1}{2} \text{Tr} \{ \ln(-\partial_E^2 + m^2) \}. \quad (\text{C.38})$$

The logarithm may then be evaluated by using the eigenvalues of the linear operator. This is found by diagonalizing the operator,

$$\langle x, D_0^{-1} x \rangle = \int_{\Omega} dX \varphi(X) (-\partial_E^2 + m^2) \varphi(X) = V \int_{\tilde{\Omega}} dK \tilde{\varphi}(K)^* [\beta^2(\omega_k^2 + \omega_n^2)] \tilde{\varphi}(K), \quad (\text{C.39})$$

leaving us with the same result as we obtained in Eq. (C.32),

$$\beta F = \frac{1}{2} \text{Tr} \{ \ln(-\partial_E^2 + m^2) \} = \frac{1}{2} V \int_{\tilde{\Omega}} dK \ln[\beta^2(\omega_n^2 + \omega_k^2)]. \quad (\text{C.40})$$

Sums similar to this show up a lot, and we show how to evaluate them in the next section.

C.3.1 Thermal sum

When evaluating thermal integral, we will often encounter sums of the form

$$j(\omega, \mu) = \frac{1}{2\beta} \sum_{\omega_n} \ln \{ \beta^2 [(\omega_n + i\mu) + \omega^2] \} + g(\beta), \quad (\text{C.41})$$

where the sum is over either the bosonic Matsubara frequencies $\omega_n = 2n\pi/\beta$, $n \in \mathbb{Z}$, or the fermionic ones, $\omega_n = (2n+1)\pi/\beta$, $n \in \mathbb{Z}$. Furthermore, $\mu \in \mathbb{R}$ is chemical potential, and g may be a function of β , but we assume it is independent of ω . Thus, the factor β^2 could strictly be dropped, but it is kept to make the argument within the logarithm dimensionless. We define the function

$$i(\omega, \mu) = \frac{1}{\omega} \frac{d}{d\omega} j(\omega, \mu) = \frac{1}{\beta} \sum_{\omega_n} \frac{1}{(\omega_n + i\mu)^2 + \omega^2}. \quad (\text{C.42})$$

We will first work with the sum over bosonic Matsubara frequencies. Assume $f(z)$ is an analytic function, except perhaps on a set of isolated poles $\{z_i\}$ located outside the real line. We can exploit this using the properties of the Bose-distribution $n_B(z)$. The Bose distribution is defined as

$$n_B(\omega) = \frac{1}{e^{\beta\omega} - 1}. \quad (\text{C.43})$$

This function obeys

$$n_B(-i\omega) = -1 - n_B(i\omega). \quad (\text{C.44})$$

We can expand it around the Bose Matsubara frequencies on the imaginary line:

$$in_B[i(\omega_n + \epsilon)] = \frac{i}{e^{i\beta\epsilon + 2\pi i n} - 1} = i[i\beta\epsilon + \mathcal{O}(\epsilon)]^{-1} \sim \frac{1}{\epsilon\beta}. \quad (\text{C.45})$$

This means that $in_B(i\omega)$ has a pole on all Matsubara-frequencies, with residue $1/\beta$. Using this, we can rewrite the sum over Matsubara frequencies as a contour integral

$$\frac{1}{\beta} \sum_{\omega_n} f(\omega_n) = \oint_{\gamma} \frac{dz}{2\pi i} f(z) in_B(iz),$$

where γ is a contour that goes from $-\infty - i\epsilon$ to $+\infty - i\epsilon$, crosses the real line at ∞ , goes from $+\infty - i\epsilon$ to $-\infty + i\epsilon$ before closing the curve. The contour γ and the new contours are illustrated in Figure C.1. This result exploits Cauchy's integral formula by letting the poles of $in_B(iz)$ at the Matsubara frequencies “pick out” the necessary residues. The integral over γ is equivalent to two integrals along $\mathbb{R} \pm i\epsilon$,

$$\begin{aligned} \frac{1}{\beta} \sum_{\omega_n} f(\omega_n) &= \left(\int_{\infty + i\epsilon}^{-\infty + i\epsilon} \frac{dz}{2\pi} + \int_{-\infty - i\epsilon}^{\infty - i\epsilon} \frac{dz}{2\pi} \right) f(z) n_B(iz), \\ &= \int_{-\infty - i\epsilon}^{\infty - i\epsilon} \frac{dz}{2\pi} \{ -f(-z) + [f(z) - f(-z)] n_B(iz) \} \\ &= \int_{-\infty}^{\infty} \frac{dz}{2\pi} f(z) + \int_{-\infty - i\epsilon}^{\infty - i\epsilon} \frac{dz}{2\pi} [f(z) + f(-z)] n_B(iz). \end{aligned} \quad (\text{C.46})$$

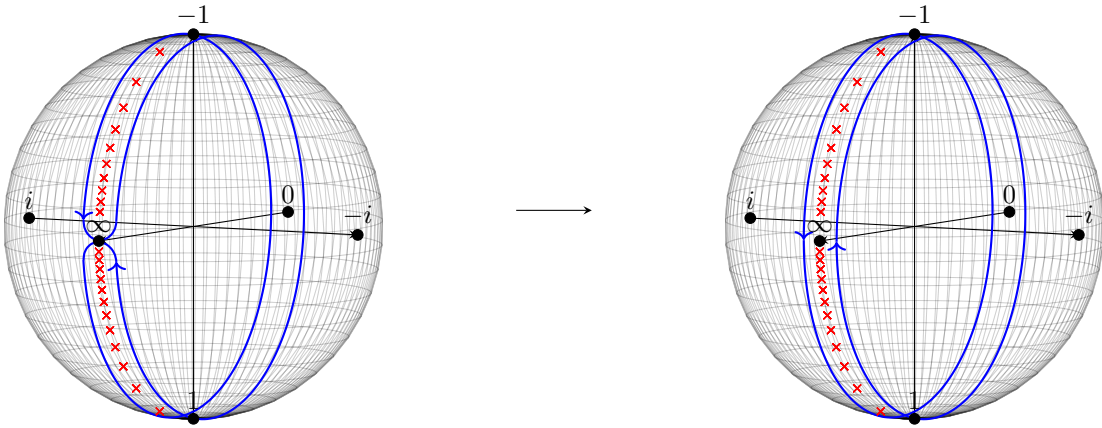


Figure C.1: The integral contour γ , and the result of deforming it into contours close to the real line. The red crosses illustrate the poles of n_B .

In the second line, we have changed variables $z \rightarrow -z$ in the first integral, and exploited the property $n_B(-iz) = -1 - n_B(iz)$. In the last line, we use the assumption that $f(z)$ is analytic on the real line, and therefore also in a neighborhood of it. This allows us to shift the first integral back to the real line. As $n_B(iz)$ is analytic outside the real line, the result of the second integral is the sum of residues of $f(z) + f(-z)$ in the lower half-plane. The function

$$f(z) = \frac{1}{(z + i\mu)^2 + \omega^2} = \frac{i}{2\omega} \left(\frac{1}{z + i(\mu + \omega)} - \frac{1}{z + i(\mu - \omega)} \right). \quad (\text{C.47})$$

obeys the assumed properties, as it has poles at $z = -i(\mu \pm \omega)$ with residue $1/(2\omega)$, so the function defined in Eq. (C.42) may be written

$$i(\omega, \mu) = \frac{1}{2\omega} [1 + n_B(\omega - \mu) + n_B(\omega + \mu)]. \quad (\text{C.48})$$

Using the antiderivative of the Bose distribution,

$$\frac{d}{d\omega} \ln(1 - e^{-\beta\omega}) = \beta n_B(\omega), \quad (\text{C.49})$$

we get the final form of Eq. (C.41),

$$j(\omega, \mu) = \int d\omega' \omega' i(\omega', \mu) = \frac{1}{2}\omega + \frac{1}{2\beta} \left[\ln(1 - e^{-\beta(\omega-\mu)}) + \ln(1 - e^{-\beta(\omega+\mu)}) \right] + g'(\beta). \quad (\text{C.50})$$

The extra ω -independent term $g'(\beta)$ is an integration constant. We see there are temperature-dependent terms, one due to the particle and one due to the anti-particle and one due to the antiparticle, with opposite signs in front of chemical potentials.

We now consider the sum over fermionic frequencies, which we for clarity denote $\tilde{\omega}_n$ in this chapter. The procedure, in this case, is the same, except that we have to use a function with poles at the fermionic Matsubara frequencies. This is done by the Fermi distribution, $n_F(z)$. The Fermi distribution is

$$n_F(\omega) = \frac{1}{e^{\beta\omega} + 1}. \quad (\text{C.51})$$

It obeys

$$\frac{d}{d\omega} \ln(1 + e^{-\beta\omega}) = -\beta n_F(\omega), \quad (\text{C.52})$$

$$n_F(-i\omega) = 1 - n_F(i\omega). \quad (\text{C.53})$$

With this, the sum over fermionic Matsubara frequencies gives

$$\begin{aligned} \frac{1}{\beta} \sum_{\tilde{\omega}_n} f(\tilde{\omega}_n) &= \left(\int_{\infty+i\epsilon}^{-\infty+i\epsilon} \frac{dz}{2\pi} + \int_{-\infty-i\epsilon}^{\infty-i\epsilon} \frac{dz}{2\pi} \right) f(z) n_B(iz) \\ &= \int_{-\infty}^{\infty} \frac{dz}{2\pi} f(z) - \int_{-\infty-i\epsilon}^{\infty-i\epsilon} \frac{dz}{2\pi} [f(z) - f(-z)] n_F(iz), \end{aligned} \quad (\text{C.54})$$

and

$$i(\omega, \mu) = \frac{1}{2\omega} [1 - n_F(\omega - \mu) - n_F(\omega + \mu)]. \quad (\text{C.55})$$

Using the antiderivative of the Fermi distribution, we get

$$j(\omega, \mu) = \frac{1}{2}\omega + \frac{1}{2\beta} \left[\ln(1 + e^{-\beta(\omega-\mu)}) + \ln(1 + e^{-\beta(\omega+\mu)}) \right]. \quad (\text{C.56})$$

C.3.2 Low-temperature limit

Using the result from subsection C.3.1 and the result for the free energy density of the free scalar field, Eq. (C.20), we get an expression for the free energy density, $\mathcal{F} = F/V$,

$$\mathcal{F} = \frac{\ln(Z)}{\beta V} = \frac{1}{2} \int_{\tilde{V}} \frac{d^3 k}{(2\pi)^3} \left[\omega_k + \frac{2}{\beta} \ln(1 - e^{-\beta\omega_k}) \right]. \quad (\text{C.57})$$

The free energy density thus has two contributions from two parts; the first part is dependent on temperature, and the other part is a temperature-independent vacuum contribution. Noticing that the integral is spherically symmetric, we may write the two contributions as

$$\mathcal{F}_0 = \frac{1}{2} \frac{1}{2\pi^2} \int_{\mathbb{R}} dk k^2 \sqrt{k^2 + m^2}, \quad \mathcal{F}_T = \frac{T^4}{2\pi^2} \int_{\mathbb{R}} dx x^2 \ln \left(1 - \exp \left\{ -\sqrt{x^2 + (m/T)^2} \right\} \right). \quad (\text{C.58})$$

The temperature-independent part, \mathcal{F}_0 , is divergent, and we must impose a regulator and then add counter-terms. \mathcal{F}_T , however, is convergent. To see this, we use the series expansion $\ln(1 + \epsilon) \sim \epsilon + \mathcal{O}(\epsilon)$ to find the leading part of the integrand for large k 's,

$$x^2 \ln \left(1 - \exp \left\{ -\sqrt{x^2 + (\beta m)^2} \right\} \right) \sim -x^2 e^{-x}, \quad (\text{C.59})$$

which is exponentially suppressed, making the integral convergent. In the limit of $T \rightarrow 0$, we get

$$\mathcal{F}_T \sim \frac{T^4}{2\pi^2} \int_{\mathbb{R}} dx x^2 \ln(1 - e^{-x}) = -\frac{T^4}{2\pi^2} \sum_{n=1} \frac{1}{n} \frac{\partial^2}{\partial n^2} \int dx e^{-nx} = -\frac{T^4}{2\pi^2} \sum_{n=1} \frac{2}{n^4} = -\frac{T^4}{\pi^2} \zeta(4),$$

where ζ is the Riemann-zeta function. Using $\zeta(4) = \frac{\pi^4}{90}$, we get

$$\mathcal{F}_T \sim -\frac{\pi^2}{90} T^4, \quad T \rightarrow 0. \quad (\text{C.60})$$

C.3.3 Regularization and renormalization

Returning to the temperature-independent part, we use dimensional regularization to control its divergent behavior. This is discussed in section A.5. Using the definition Eq. (A.98), we can write $\mathcal{F}_0 = \Phi_3(m, 3, -1/2)/2$. This integral is calculated in subsection A.5.1, with the result

$$\mathcal{F}_0 = -\mu^{-2\epsilon} \frac{1}{4} \frac{m^4}{(4\pi)^2} \left(\frac{1}{\epsilon} + \frac{3}{2} + \ln \frac{\tilde{\mu}^2}{m^2} \right) + \mathcal{O}(\epsilon). \quad (\text{C.61})$$

As detailed in section A.5, this result uses the $\overline{\text{MS}}$ -scheme. Now that we have applied a regulator, we can handle the divergence in a well-defined way. When $\epsilon \neq 0$, we can subtract terms that are proportional to ϵ^{-1} , and be left with a term that is finite in the limit $\epsilon \rightarrow 0$.

We can subtract the divergences by performing *renormalization*. Consider an arbitrary Lagrangian,

$$\mathcal{L}[\varphi] = \sum_n \lambda_n \mathcal{O}_n[\varphi]. \quad (\text{C.62})$$

Here, $\mathcal{O}_n[\varphi]$ are operators consisting of φ and $\partial_\mu \varphi$, and λ_n are coupling constants. In d dimensions, the action integral is

$$S[\varphi] = \sum_n \int d^d x \lambda_n \mathcal{O}_n[\varphi]. \quad (\text{C.63})$$

The action has mass dimension 0. This means that all terms $\lambda_n \mathcal{O}_n$ must have mass dimension d , as $[d^d x] = -d$. We are free to choose the coupling constant corresponding to $\mathcal{O}_0 = \partial_\mu \varphi \partial^\mu \varphi$ to be of mass dimension 0, and set $\lambda_0 = 1/2$ to get canonical normalization. This allows us to deduce the dimensionality of φ . As $[\partial_\mu] = 1$, we have that $[\varphi] = (d-2)/2$. Assume \mathcal{O}_n consists of k_n factors of φ , and l_n factors of $\partial_\mu \varphi$. We must then have

$$[\lambda_n] + [\mathcal{O}_n] - d = [\lambda_n] + (k_n + l_n)(d-2)/2 + l_n - d = 0, \quad (\text{C.64})$$

$$\implies D_n := [\lambda_n] = d - k_n \frac{d-2}{2} - l_n \frac{d}{2}. \quad (\text{C.65})$$

From this formula, we recover that $[\lambda_0] = 0$, and if $\mathcal{O}_1 = \varphi^2$, then $[\lambda_1] = 2$, which we recognize as the mass squared term. The mass dimensions of these coupling constants are independent of d . However, the coupling constant for the interaction term

$$-\frac{1}{4!}\lambda_3\varphi^4 \quad (\text{C.66})$$

has mass dimensions $[\lambda_3] = d - 4(d - 2)/2 = 4 - 2d$. Our goal now is to exchange the bare coupling constants λ_n with renormalized ones, λ_n^r , and remove the divergent terms proportional to $(d - 4)^{-m}$. We can always define the renormalized coupling constants as dimensionless, i.e., $[\lambda_n^r] = 0$, by measuring them in units of a mass scale. We therefore write

$$\lambda_n = \mu^{4-D_n} \left[\lambda_n^r + \sum_{m=1} \frac{a_m(\lambda_n^r)}{(d-4)^m} \right], \quad (\text{C.67})$$

where we have introduced the dimensionful parameter μ to ensure that λ_n has the correct mass dimension for the action integral to stay dimensionless. The functions a_m are then determined to each order in perturbation theory by calculating Feynman diagrams. As μ again is arbitrary, λ_4' should not depend on this parameter. In this case, we chose the same renormalization scale as we did when regulating the one-loop integral. This is only for our own convenience. This means that if we change $\mu \rightarrow \mu'$, then λ_i^r and a_m must adjust to compensate and keep λ_n constant [88].

The vacuum energy term absorbs the divergence in the one-loop contribution to the free energy density. It is

$$\lambda_4\mathcal{O}_4 = \lambda_4 := m^4\lambda_4'. \quad (\text{C.68})$$

Using the expansion in terms of the renormalized coupling, we have,

$$\lambda_4' = \mu^{-2\epsilon} \left[\lambda_4^r + \frac{1}{2\epsilon} a_1(\lambda_4^r) + \dots \right], \quad (\text{C.69})$$

where $d = 4 - 2\epsilon$. After adding Eq. (C.68) to the Lagrangian of the free scalar, the temperature-independent free energy density becomes

$$\mathcal{F}_0 \sim -\mu^{-2\epsilon} \frac{1}{4} \frac{m^4}{(4\pi)^2} \left[\frac{1}{\epsilon} + \frac{3}{2} + \ln \frac{\tilde{\mu}^2}{m^2} + 4(4\pi)^2 \left(\lambda_4^r + \frac{1}{2\epsilon} a_1(\lambda_4^r) \right) \right], \quad \epsilon \rightarrow 0. \quad (\text{C.70})$$

Thus, if we choose $a_1 = -8(4\pi)^2 + \mathcal{O}(\lambda_4^r)$, and define $\lambda_4^r = 4(4\pi)^2 \lambda_4^r$, we are able to cancel the divergence, and may take the limit $\epsilon \rightarrow 0$ safely. The free energy is now

$$\mathcal{F} = -\frac{1}{4} \frac{m^4}{(4\pi)^2} \left(\frac{3}{2} + \lambda_4^r + \ln \frac{\tilde{\mu}^2}{m^2} \right) + \frac{T^4}{2\pi^2} \int dx x^2 \ln \left(1 - \exp \left\{ -\sqrt{x^2 + \beta^2 m^2} \right\} \right). \quad (\text{C.71})$$

Notice that all choices we have made up until now, such as defining $\lambda_4 = m^4\lambda_4'$ and using the same renormalization scale μ , have no impact on this result. Different choices would force us to define λ_4^r and a_4 differently, leaving us with the same result.

C.4 *Interacting scalar field

We now study a scalar field with a $\lambda\varphi^4$ interaction term. We write the Lagrangian in the form

$$\mathcal{L} = \mathcal{L}^{(0)} + \mathcal{L}^{(I)}, \quad \mathcal{L}^{(0)} = \frac{1}{2} \partial_\mu \varphi \partial^\mu \varphi - m^2 \varphi^2, \quad \mathcal{L}^{(I)} = -\frac{\lambda}{4!} \varphi^4. \quad (\text{C.72})$$

$\mathcal{L}^{(I)}$ is called the interaction term and makes it impossible to exactly solve for the partition function. Instead, we turn to perturbation theory. The canonical partition function in this theory is

$$Z = \text{Tr} \left\{ e^{-\beta \hat{H}} \right\} = \int_S \mathcal{D}\varphi \exp \left\{ - \int_\Omega dX \left(\mathcal{L}_E^{(0)} + \mathcal{L}_E^{(I)} \right) \right\} = \int_S \mathcal{D}\varphi e^{-S_0} e^{-S_I}. \quad (\text{C.73})$$

Here, S_0 and S_I denote the Euclidean action due to the free and interacting Lagrangian, respectively. The domain of integration S is again periodic field configurations $\varphi(\beta, \vec{x}) = \varphi(0, \vec{x})$. We may write the free energy as

$$-\beta F = \ln \left[\int_S \mathcal{D}\varphi e^{-S_0} \sum_n \frac{1}{n!} (-S_I)^n \right] = \ln Z_0 + \ln Z_I, \quad (\text{C.74})$$

where Z_0 is the partition function of the free theory. The correction to the partition function is thus given by

$$Z_I = \sum_{n=0}^{\infty} \frac{(-1)^n}{n!} \langle S_I^n \rangle_0, \quad (\text{C.75})$$

where

$$\langle A \rangle_0 = \frac{\int_S \mathcal{D}\varphi A e^{-S_0}}{\int_S \mathcal{D}\varphi e^{-S_0}}. \quad (\text{C.76})$$

To evaluate expectation values of the form $\langle \varphi(X_1) \dots \rangle_0$, we introduce the partition function with a source term

$$Z[J] = \int_S \mathcal{D}\varphi \exp \left\{ -\frac{1}{2} \int_{\Omega} dX \varphi (-\partial_E^2 + m^2) \varphi + \int_{\Omega} dX J \varphi \right\}. \quad (\text{C.77})$$

Thermal propagators are the generalization of the time-ordered two-point functions $\langle T\{\varphi(x)\varphi(y)\} \rangle$ of the vacuum formalism. For some differential operator D^{-1} , the thermal propagator is defined as

$$D^{-1}D(X, Y) = \beta \delta(X - Y). \quad (\text{C.78})$$

The Fourier transformed propagator is, assuming $D(X, Y) = D(X - Y, 0)$,

$$\begin{aligned} \tilde{D}(K, K') &= \frac{1}{V\beta^3} \int_{\Omega} dX dY D(X, Y) \exp \{ -i[X \cdot K + Y \cdot K'] \} \\ &= \frac{1}{V\beta^3} \int_{\Omega} dX' dY' D(X', 0) \exp \left\{ -i[X' \cdot \frac{1}{2}(K - K') + Y \cdot (K + K')] \right\} \\ &= \frac{1}{V\beta^2} \tilde{D}(K) \delta(K + K'), \end{aligned} \quad (\text{C.79})$$

where

$$\tilde{D}(K) = \int dX e^{iK \cdot X} D(X, 0). \quad (\text{C.80})$$

We write the thermal propagator of the free field as $D_0(X, Y)$. With this, we may complete the square,

$$Z[J] = Z[0] \exp \left\{ \frac{1}{2} \int_{\Omega} dX dY J(X) D_0(X, Y) J(Y) \right\} = Z[0] \exp \{ W[J] \}. \quad (\text{C.81})$$

We can now write

$$\langle \varphi(X) \varphi(Y) \rangle_0 = \frac{1}{Z[0]} \frac{\delta}{\delta J(X)} \frac{\delta}{\delta J(Y)} Z[J] \Big|_{J=0} = D_0(X, Y). \quad (\text{C.82})$$

This generalizes to higher-order expectation values,

$$\langle \varphi(X_i) \dots \varphi(X_n) \rangle_0 = \frac{1}{Z[0]} \left(\prod_{i=1}^n \frac{\delta}{\delta J(X_i)} \right) Z[J] \Big|_{J=0}, \quad (\text{C.83})$$

Using Wick's theorem, as described in section 3.1, the expectation values we are evaluating can be written

$$\begin{aligned} \langle S_I^m \rangle_0 &= \left(-\frac{\lambda}{4!} \right)^m \int_{\Omega} dX_1 \dots dX_m \langle \varphi^4(X_1) \dots \varphi^4(X_m) \rangle_0 \\ &= \left(-\frac{\lambda}{4!} \right)^m \int_{\Omega} dX_1 \dots dX_m \sum_{\{a,b\}} \langle \varphi(X_{a(1)}) \varphi(X_{b(1)}) \rangle_0 \dots \langle \varphi(X_{a(2m)}) \varphi(X_{b(2m)}) \rangle_0, \end{aligned}$$

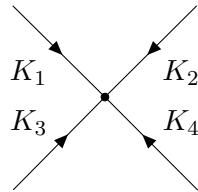
where X_i for $i > m$ is defined to equal X_j , where $j = i \bmod m$. More simply, $X_{m+i} = X_i$. The functions a, b represents a possible pairing, as described in section 3.1. Inserting the Fourier expansions of the field gives

$$\begin{aligned}
\langle S_I^m \rangle_0 &= \left(-\frac{\lambda}{4!} \right)^m \int_{\Omega} dX_1 \dots dX_m (V\beta)^2 \int_{\tilde{\Omega}} dK_1 \dots dK_{2m} \sum_{\{a,b\}} \exp \left\{ i \sum_{i=1}^m X_i \cdot K_i \right\} \\
&\quad \times \langle \varphi(K_{a(1)}) \varphi(K_{b(1)}) \rangle_0 \dots \langle \varphi(K_{a(2m)}) \varphi(K_{b(2m)}) \rangle_0 \\
&= \left(-\frac{\lambda}{4!} \right)^m \frac{(V\beta)^{2m} \beta^m}{(V\beta^2)^{2m}} \int_{\tilde{\Omega}} dK_1 \dots dK_{2m} \sum_{\{a,b\}} \prod_{i=1}^m \delta \left(\sum_{j=0}^3 K_{i+jm} \right) \\
&\quad \times \tilde{D}(K_{a(1)}) \delta(K_{a(1)} + K_{b(1)}) \dots \tilde{D}(K_{a(2m)}) \delta(K_{a(2m)} + K_{b(2m)}) \\
&= \left(-\frac{\lambda\beta}{4!} \right)^m \prod_{i=1}^{2m} \int_{\tilde{\Omega}} \left(dK_i \frac{1}{\beta} \tilde{D}(K_i) \right) \prod_{i=1}^m \delta \left(\sum_{j=0}^3 K_{i+jm} \right) \sum_{\{a,b\}} \prod_{n=1}^{2m} \delta(K_{a(n)} + K_{b(n)}).
\end{aligned}$$

Here we have used that $V\beta^2 \tilde{D}_0(K, P) = \tilde{D}_0(K) \delta(P+K)$, where $\tilde{D}_0(K)$ is the thermal propagator for the free field. In this case, it is

$$\tilde{D}_0(K) = \tilde{D}_0(\omega_n, \vec{k}) = \frac{1}{\omega_k^2 + \omega_n^2}. \quad (\text{C.84})$$

This expectation value can be represented graphically using Feynman diagrams. The thermal $\lambda\varphi^2$ -theory gets the prescription

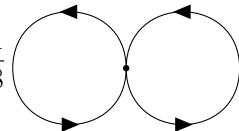


$$= -\lambda\beta\delta \left(\sum_i K_i \right), \quad (\text{C.85})$$



$$= \frac{1}{\beta} D_0(K). \quad (\text{C.86})$$

Lastly, one has to integrate over internal momenta and divide by the symmetry factor of the diagram s , which is described in detail in [40]. Calculating $\langle S_I^n \rangle_0$ boils down to the sum of all possible Feynman diagrams with n vertices. The first example is



$$\langle S_I \rangle_0 = \frac{1}{8} \quad (\text{C.87})$$

In section 3.1, we saw that the sum of all vacuum diagrams is the exponential of the sum of all *connected* diagrams. If we include a rule of dividing diagrams by factor βV , then the free energy density of the interacting theory is given by

$$\mathcal{F} = -\frac{\ln Z_0}{V\beta} + \sum (\text{all connected diagrams}). \quad (\text{C.88})$$

C.5 *Fermions

The derivation of the fermionic path integral is similar to the scalar one, but with some slight but important differences. If ψ and $\bar{\psi}$ are fermionic spinor fields, relevant relations are [87]

$$\mathbb{1} = \int \mathcal{D}\psi \mathcal{D}\bar{\psi} \exp \left\{ - \int dX \bar{\psi} \psi \right\} |\psi\rangle \langle \psi|, \quad (\text{C.89})$$

$$Z = \text{Tr} \{ \hat{\rho} \} = \int \mathcal{D}\psi \mathcal{D}\bar{\psi} \exp \left\{ - \int dX \bar{\psi} \psi \right\} \langle -\psi | e^{i\beta \hat{H}} | \psi \rangle, \quad (\text{C.90})$$

$$\langle \bar{\psi} | \psi \rangle = \exp \left\{ \int dX \bar{\psi} \psi \right\}. \quad (\text{C.91})$$

The anti-periodic nature of fermion-fields, as mentioned in section C.2, is due to these differences. We can verify them by studying the properties of the thermal Greens function. The thermal Greens function may be written

$$D(X_1, X_2) = D(\vec{x}, \vec{y}, \tau_1, \tau_2) = \text{Tr} \left\{ e^{-\beta H} T_\tau [\psi(\tau_1, \vec{x}) \bar{\psi}(\tau_2, \vec{y})] \right\}. \quad (\text{C.92})$$

Here, T_τ is the imaginary-time-ordering operator, which sorts fields just as the regular time-ordering operator, only with respect to τ instead of t . In the same way that $i\hat{H}$ generates the time translation of a quantum field operator through $\hat{\psi}(x) = \hat{\psi}(t, \vec{x}) = e^{it\hat{H}} \hat{\psi}(0, \vec{x}) e^{-it\hat{H}}$, the imaginary-time formalism implies the relation $\hat{\psi}(X) = \hat{\psi}(\tau, \vec{x}) = e^{\tau\hat{H}} \hat{\psi}(0, \vec{x}) e^{-\tau\hat{H}}$. Using $\mathbb{1} = e^{\tau\hat{H}} e^{-\tau\hat{H}}$ and the cyclic property of the trace, we show that, assuming $\beta > \tau > 0$,

$$\begin{aligned} D(\vec{x}, \vec{y}, \tau, 0) &= \frac{1}{Z} \text{Tr} \left\{ e^{-\beta\hat{H}} T_\tau [\psi(\tau, \vec{x}) \bar{\psi}(0, \vec{y})] \right\} \\ &= \frac{1}{Z} \text{Tr} \left\{ T_\tau [e^{-\beta\hat{H}} e^{\beta\hat{H}} \bar{\psi}(0, \vec{y}) e^{-\beta\hat{H}} \psi(\tau, \vec{x})] \right\} \\ &= \frac{1}{Z} \text{Tr} \left\{ e^{-\beta\hat{H}} T_\tau [\psi(\vec{y}, \beta) \bar{\psi}(\tau, \vec{x})] \right\} = \nu D(\vec{x}, \vec{y}, \tau, \beta) \end{aligned}$$

This implies that $\psi(0, x) = \nu \psi(\beta, \psi)$, where $\nu = \pm 1$ for bosons and fermions respectively, which shows that bosons are periodic in time, as stated earlier, while fermions are anti-periodic.

The Lagrangian density of a free Dirac fermion is

$$\mathcal{L} = \bar{\psi} (i\partial - m) \psi. \quad (\text{C.93})$$

This Lagrangian is invariant under the transformation $\psi \rightarrow e^{-i\alpha} \psi$, which by Nöther's theorem results in a conserved current

$$j^\mu = \frac{\partial \mathcal{L}}{\partial(\partial_\mu \psi)} \delta \psi = \bar{\psi} \gamma^\mu \psi. \quad (\text{C.94})$$

The canonical momentum corresponding to ψ is

$$\pi = \frac{\partial \mathcal{L}}{\partial(\partial_0 \psi)} = i\bar{\psi} \gamma^0, \quad (\text{C.95})$$

and the Hamiltonian density is

$$\mathcal{H} = \pi \dot{\psi} - \mathcal{L} = \bar{\psi} (-i\gamma^i \partial_i + m) \psi \quad (\text{C.96})$$

In the grand canonical ensemble, we substitute $\mathcal{H} \rightarrow \mathcal{H} - \mu \bar{\psi} \gamma^0 \psi$. The Euclidian Lagrangian is then

$$\mathcal{L}_E = -\pi \dot{\psi} + \mathcal{H}(\psi, \pi) - \mu \bar{\psi} \gamma^0 \psi = \bar{\psi} [\gamma^0 (\partial_\tau - \mu) - i\gamma^i \partial_i + m] \psi, \quad (\text{C.97})$$

The partition function for this system is then [87]

$$\begin{aligned} Z &= \int \mathcal{D}\psi \mathcal{D}\bar{\psi} \exp \left\{ - \int_{\Omega} dX \bar{\psi} [\gamma_0(\partial_{\tau} - \mu) - i\gamma^i \partial_i + m] \psi \right\} \\ &= C \int \mathcal{D}\psi \mathcal{D}\bar{\psi} e^{-\langle \bar{\psi}, D^{-1} \psi \rangle} = C \det(D^{-1}). \end{aligned}$$

In the second line, we have inserted the Fourier expansion of the field, as defined in section C.2, and changed variable of integration, as we did for the scalar field. We then used the Grassmann version of the Gaussian integral [9],

$$\int d\bar{\theta}_i d\theta_i \exp \{ -\theta_i A_{ij} \theta_j \} = \det(A). \quad (\text{C.98})$$

The linear operator in this case is

$$D^{-1} = i\gamma^0(-i\partial_{\tau} + i\mu) - (-i\gamma^i)\partial_i + m = \beta[i\tilde{\gamma}_a k_a + m]. \quad (\text{C.99})$$

This equality must be understood as an equality between linear operators, which are represented in different bases. We introduced the notation $k_a = (\omega_n + i\mu, k_i)$ and use the Euclidean gamma matrices $\tilde{\gamma}_i$, as defined in subsection A.2.1. We use the fact that

$$\det(i\tilde{\gamma}_a k_a + m) = \det(\gamma^5 \gamma^5) \det(i\tilde{\gamma}_a k_a + m) = \det[\gamma^5(i\tilde{\gamma}_a k_a + m)\gamma^5] = \det(-i\tilde{\gamma}_a k_a + m),$$

Let $\tilde{D}^{-1} = \beta[-i\tilde{\gamma}_a k_a + m]$, which means we can write

$$Z = \sqrt{\det(D^{-1}) \det(\tilde{D}^{-1})} = \sqrt{\det(D^{-1} \tilde{D}^{-1})} = \det[\mathbb{1} \beta^2 (k_a k_a + m^2)]^{1/2}, \quad (\text{C.100})$$

where we have used the anti-commutation rule for the Euclidean gamma-matrices, $\{\tilde{\gamma}_a, \tilde{\gamma}_b\} = 2\delta_{ab}$. It is important to keep in mind that the determinant here refers to linear operators on the space of spinor functions. Thus,

$$\begin{aligned} \ln(Z) &= \ln \left\{ \det[\mathbb{1} \beta^2 (k_a k_a + m^2)]^{1/2} \right\} = \frac{1}{2} \text{Tr} \left\{ \ln[\mathbb{1} \beta^2 (k_a k_a + m^2)] \right\} \\ &= 2V \int_{\tilde{\Omega}} dK \ln \{ \beta^2 [(\omega_n + i\mu)^2 + \omega_k^2] \}. \end{aligned} \quad (\text{C.101})$$

In the last step, we used the fact that the matrix within the logarithm is diagonal. The matrix part of the trace is therefore trivial. Using the fermionic version of the thermal sum from subsection C.3.1 gives the answer

$$\mathcal{F} = -\frac{2}{\beta} \int \frac{d^3 k}{(2\pi)^3} \left[\beta \omega_k + \ln \left(1 + e^{-\beta(\omega_k - \mu)} \right) + \ln \left(1 + e^{-\beta(\omega_k + \mu)} \right) \right]. \quad (\text{C.102})$$

We see again that the temperature-independent part of the integral diverges, and must be regulated. There are two temperature-dependent terms, one from the particle and one from the anti-particle.

Appendix D

Code

All code used in this thesis, as well as the L^AT_EX code, figures used, and more is open source and available at the online repository <https://github.com/martkjoh/master>.

D.1 Integrating the TOV equations

For numerical integration of the TOV equations, we use SciPy's `integrate.solve_ivp`.¹ Equations of state are evaluated either as explicit functions if a closed-form is available or as an interpolating function is created using a spline without smoothing. All code is written using dimensionless variables, and setting $k_1 = k_2 = k_3$. The continuity equation and the TOV equation then read, from Eq. (4.51) and Eq. (4.52),

$$\frac{d\tilde{m}}{d\tilde{r}} = 3\tilde{r}^2\tilde{u}, \quad \frac{d\tilde{p}}{d\tilde{r}} = -\frac{1}{\tilde{r}^2} (\tilde{p} + \tilde{u}) (3\tilde{r}^3\tilde{p} + \tilde{m}) \left(1 - \frac{2\tilde{m}}{\tilde{r}}\right)^{-1}. \quad (\text{D.1})$$

As $r \rightarrow 0$, parts of the TOV equation approach a 0/0-limit, and we must make use of an approximation for numeric evaluation. The Taylor-expansion of the mass function around $\tilde{r} = 0$ is

$$\tilde{m}(r) = \tilde{m}(0) + \tilde{m}'(0)\tilde{r} + \frac{1}{2!}\tilde{m}''(0)\tilde{r}^2 + \frac{1}{3!}\tilde{m}'''(0)\tilde{r}^3 + \mathcal{O}(\tilde{r}^4). \quad (\text{D.2})$$

One of the boundary conditions is $\tilde{m}(0) = 0$. We then use the differential equation for \tilde{m} , Eq. (4.37), to find

$$\tilde{m}'(0) = 0, \quad \tilde{m}''(0) = 0, \quad \tilde{m}'''(0) = 6k_2\tilde{u}_0, \quad (\text{D.3})$$

where $\tilde{u}_0 = \tilde{u}(r=0)$. We get an approximation of the TOV equation for $\tilde{r} \ll 1$ by substituting the \tilde{m} for its Taylor expansion and including only the leading-order term, which gives

$$\frac{d\tilde{p}}{d\tilde{r}} \sim -\tilde{r} (\tilde{p} + \tilde{u}) (3\tilde{p} + \tilde{u}_0) (1 - 2\tilde{u}_0\tilde{r}^2)^{-1}, \quad r \rightarrow 0. \quad (\text{D.4})$$

For the Newtonian approximation to the TOV equation, we get

$$\frac{d\tilde{p}}{d\tilde{r}} = -\frac{\tilde{u}\tilde{m}}{\tilde{r}^2} \sim -\tilde{u}\tilde{u}_0\tilde{r}, \quad r \rightarrow 0. \quad (\text{D.5})$$

¹Reference available at: https://docs.scipy.org/doc/scipy/reference/generated/scipy.integrate.solve_ivp.html.

D.2 Symbolic calculations in χ PT

Symbolic calculations in χ PT, such as the expansion of the Lagrangian in powers of φ/f , were done using the open-source, Python-based CAS software SageMath,² and Jupyter notebooks.³ The calculations presented in this thesis, in addition to expansions of \mathcal{L}_4 to second order, can be found in the online repository, at https://github.com/martkjoh/master/tree/main/power_expansion.

D.3 Spherically symmetric metric

The calculations in Chapter 4 were done using the pure Python CAS system SymPy,⁴ in combination with a Jupyter notebook. The full `.ipynb` file with executable code is available in the online repository, at <https://github.com/martkjoh/master/blob/main/scripts/TOV/TOV.ipynb>. Below is some of the code, which illustrates the main functions and their outputs.

²<https://www.sagemath.org/>

³<https://jupyter.org/>

⁴<https://www.sympy.org>

1 Metric $g_{\mu\nu}$ for spherically symmetric spacetime

```
[8]: t, r, th, ph = symbols("t, r, \\theta, \\phi")
x1 = r * cos(ph) * sin(th)
x2 = r * sin(ph) * sin(th)
x3 = r * cos(th)

one = Rational(1)
eta = sp.diag(one, -one, -one, -one)
var = (t, r, th, ph)
J = Matrix([t, x1, x2, x3]).jacobian(var)
g = np.array(simplify(J.T * eta * J))

a = sp.Function("\\alpha", real=True)(r)
b = sp.Function("\\beta", real=True)(r)
g[0, 0] *= exp(2 * a)
g[1, 1] *= exp(2 * b)
g_inv = get_g_inv(g)

print_matrix(g)
print_matrix(g_inv)
```

$$\begin{bmatrix} e^{2\alpha(r)} & 0 & 0 & 0 \\ 0 & -e^{2\beta(r)} & 0 & 0 \\ 0 & 0 & -r^2 & 0 \\ 0 & 0 & 0 & -r^2 \sin^2(\theta) \end{bmatrix}$$

$$\begin{bmatrix} e^{-2\alpha(r)} & 0 & 0 & 0 \\ 0 & -e^{-2\beta(r)} & 0 & 0 \\ 0 & 0 & -\frac{1}{r^2} & 0 \\ 0 & 0 & 0 & -\frac{1}{r^2 \sin^2(\theta)} \end{bmatrix}$$

```
[9]: C = Christoffel(g, g_inv, var)
c = print_christoffel(C, var)
```

$$\Gamma_{\mu\nu}^t = \begin{bmatrix} 0 & \frac{d}{dr}\alpha(r) & 0 & 0 \\ \frac{d}{dr}\alpha(r) & 0 & 0 & 0 \\ 0 & 0 & 0 & 0 \\ 0 & 0 & 0 & 0 \end{bmatrix}$$

$$\Gamma_{\mu\nu}^r = \begin{bmatrix} e^{2\alpha(r)}e^{-2\beta(r)}\frac{d}{dr}\alpha(r) & 0 & 0 & 0 \\ 0 & \frac{d}{dr}\beta(r) & 0 & 0 \\ 0 & 0 & -re^{-2\beta(r)} & 0 \\ 0 & 0 & 0 & -re^{-2\beta(r)}\sin^2(\theta) \end{bmatrix}$$

$$\Gamma_{\mu\nu}^\theta = \begin{bmatrix} 0 & 0 & 0 & 0 \\ 0 & 0 & \frac{1}{r} & 0 \\ 0 & \frac{1}{r} & 0 & 0 \\ 0 & 0 & 0 & -\sin(\theta)\cos(\theta) \end{bmatrix}$$

$$\Gamma_{\mu\nu}^\phi = \begin{bmatrix} 0 & 0 & 0 & 0 \\ 0 & 0 & 0 & \frac{1}{r} \\ 0 & 0 & 0 & \frac{\cos(\theta)}{\sin(\theta)} \\ 0 & \frac{1}{r} & \frac{\cos(\theta)}{\sin(\theta)} & 0 \end{bmatrix}$$

```
[10]: Rie = Riemann_tensor(C, var)
Ricci = contract(Rie, num_idx=4, upper=1, idx=(0, 2))

for i in range(4):
    print_scalar(Ricci[i, i].factor())
```

$$\frac{\left(r\left(\frac{d}{dr}\alpha(r)\right)^2 - r\frac{d}{dr}\alpha(r)\frac{d}{dr}\beta(r) + r\frac{d^2}{dr^2}\alpha(r) + 2\frac{d}{dr}\alpha(r)\right)e^{2\alpha(r)}e^{-2\beta(r)}}{r}$$

$$-\frac{r\left(\frac{d}{dr}\alpha(r)\right)^2 - r\frac{d}{dr}\alpha(r)\frac{d}{dr}\beta(r) + r\frac{d^2}{dr^2}\alpha(r) - 2\frac{d}{dr}\beta(r)}{r}$$

$$-\left(r\frac{d}{dr}\alpha(r) - r\frac{d}{dr}\beta(r) - e^{2\beta(r)} + 1\right)e^{-2\beta(r)}$$

$$-\left(r\frac{d}{dr}\alpha(r) - r\frac{d}{dr}\beta(r) - e^{2\beta(r)} + 1\right)e^{-2\beta(r)}\sin^2(\theta)$$


```
[11]: R = contract(Ricci, g_inv=g_inv, upper=0).simplify()
print_scalar(R)
```

$$\frac{2 \left(r^2 \left(\frac{d}{dr} \alpha(r) \right)^2 - r^2 \frac{d}{dr} \alpha(r) \frac{d}{dr} \beta(r) + r^2 \frac{d^2}{dr^2} \alpha(r) + 2r \frac{d}{dr} \alpha(r) - 2r \frac{d}{dr} \beta(r) - e^{2\beta(r)} + 1 \right) e^{-2\beta(r)}}{r^2}$$

```
[12]: G = Ricci - Rational(1, 2) * R * g
for i in range(4):
    G[i, i] = G[i, i].simplify().factor()
print_scalar(G[i, i])
```

$$\frac{\left(2r \frac{d}{dr} \beta(r) + e^{2\beta(r)} - 1 \right) e^{2\alpha(r)} e^{-2\beta(r)}}{r^2}$$

$$\frac{2r \frac{d}{dr} \alpha(r) - e^{2\beta(r)} + 1}{r^2}$$

$$r \left(r \left(\frac{d}{dr} \alpha(r) \right)^2 - r \frac{d}{dr} \alpha(r) \frac{d}{dr} \beta(r) + r \frac{d^2}{dr^2} \alpha(r) + \frac{d}{dr} \alpha(r) - \frac{d}{dr} \beta(r) \right) e^{-2\beta(r)}$$

$$r \left(r \left(\frac{d}{dr} \alpha(r) \right)^2 - r \frac{d}{dr} \alpha(r) \frac{d}{dr} \beta(r) + r \frac{d^2}{dr^2} \alpha(r) + \frac{d}{dr} \alpha(r) - \frac{d}{dr} \beta(r) \right) e^{-2\beta(r)} \sin^2(\theta)$$

1.0.1 Stress-energy tensor $T_{\mu\nu}$ for perfect fluid

```
[13]: p = sp.Function("p")(r)
u = sp.Function("u")(r)

UU = np.zeros((4, 4), dtype=sp.Rational)
UU[0, 0] = exp(2 * a)

T = (p + u) * UU - p * g
for i in range(4):
    T[i, i] = T[i, i].simplify()
print_matrix(T)
```

$$\begin{bmatrix} u(r)e^{2\alpha(r)} & 0 & 0 & 0 \\ 0 & p(r)e^{2\beta(r)} & 0 & 0 \\ 0 & 0 & r^2p(r) & 0 \\ 0 & 0 & 0 & r^2p(r)\sin^2(\theta) \end{bmatrix}$$

2 Einstein's field equations

$$R_{\mu\nu} - \frac{1}{2}Rg_{\mu\nu} = 8\pi GT_{\mu\nu}$$

```
[14]: G_newton = sp.Symbol("G")

eq = []
for i in range(len(G)):
    eq.append((G[i, i] - 8 * pi * G_newton * T[i, i]).simplify())

# Some manual simplification
Rtt = sp.Symbol("R_{\\theta} \\theta}")
eq[0] = eq[0] * r**2 / exp(2 * a)/exp(-2*b) * (-1)
eq[1] = eq[1] * r**2 * (-1)
eq[2] = eq[2] / r / exp(-2*b)
eq[3] = eq[3].subs(eq[2], Rtt)
for i in range(len(G)):
    print_eq(eq[i].simplify())
```

$$8\pi Gr^2u(r)e^{2\beta(r)} - 2r\frac{d}{dr}\beta(r) - e^{2\beta(r)} + 1 = 0$$

$$8\pi Gr^2p(r)e^{2\beta(r)} - 2r\frac{d}{dr}\alpha(r) + e^{2\beta(r)} - 1 = 0$$

$$-8\pi Grp(r)e^{2\beta(r)} + r\left(\frac{d}{dr}\alpha(r)\right)^2 - r\frac{d}{dr}\alpha(r)\frac{d}{dr}\beta(r) + r\frac{d^2}{dr^2}\alpha(r) + \frac{d}{dr}\alpha(r) - \frac{d}{dr}\beta(r) = 0$$

$$R_{\theta\theta}re^{-2\beta(r)}\sin^2(\theta) = 0$$

Define $e^{2\beta} = [1 - 2Gm(r)/r]^{-1}$

```
[15]: m = sp.Function("m", Real=True)(r)
      f = (1 - 2 * G_newton * m / r)**(-1)
      eq1 = (eq[0] * exp(- 2 * a)).simplify().subs(b, Rational(1, 2) * log(f)).
      ↪simplify().expand().simplify()
      s = sp.solve(eq1, m.diff(r))
      eq1 = m.diff(r) - s[0]
```

Use $\nabla_\mu T^{\mu r} = 0 \Rightarrow (p + \rho)\partial_r \alpha = -\partial_r p$.

```
[16]: eq2 = (eq[1] * r**2).subs(exp(2 * b), f).simplify()
      s = sp.solve(eq2, a.diff(r))
      eq2 = a.diff(r) - s[0]
      eq2 = ((a.diff(r) - s[0]).subs(a.diff(r), - p.diff(r) / (p + u))*(p + u)).
      ↪simplify()
      s = sp.solve(eq2, p.diff(r))
      eq2 = p.diff(r) - s[0].factor()
```

The TOV-equation and equation for $m(r)$, both expressions are equal to 0.

```
[17]: print_eq(eq1)
      print_eq(eq2)
```

$$-4\pi r^2 u(r) + \frac{d}{dr} m(r) = 0$$

$$\frac{G(4\pi r^3 p(r) + m(r))(p(r) + u(r))}{r(-2Gm(r) + r)} + \frac{d}{dr} p(r) = 0$$

Bibliography

- [1] S. Weinberg. “Phenomenological Lagrangians”. In: *Physica A: Statistical Mechanics and its Applications* 96.1 (Apr. 1979), pp. 327–340. ISSN: 0378-4371. DOI: 10.1016/0378-4371(79)90223-1.
- [2] S. M. Carroll. *Spacetime and Geometry: An Introduction to General Relativity*. First. Cambridge University Press, Aug. 2019. ISBN: 978-1-108-48839-6 978-1-108-77038-5. DOI: 10.1017/9781108770385.
- [3] P. C. Hemmer. *Termisk fysikk*. Trondheim: Tapir, 2002. ISBN: 978-82-519-1739-1.
- [4] D. Prialnik. *An Introduction to the Theory of Stellar Structure and Evolution*. Cambridge University Press, July 2000. ISBN: 978-0-521-65937-6.
- [5] J. O. Andersen and P. Kneschke. *Bose-Einstein Condensation and Pion Stars*. July 2018. arXiv: 1807.08951.
- [6] B. B. Brandt et al. “New Class of Compact Stars: Pion Stars”. In: *Phys. Rev. D* 98.9 (Nov. 2018), p. 094510. ISSN: 2470-0010, 2470-0029. DOI: 10.1103/PhysRevD.98.094510. arXiv: 1802.06685.
- [7] S. Carignano et al. “Scrutinizing the Pion Condensed Phase”. In: *Eur. Phys. J. A* 53.2 (Feb. 2017), p. 35. ISSN: 1434-601X. DOI: 10.1140/epja/i2017-12221-x.
- [8] S. M. Carroll. *The World of Everyday Experience, in One Equation*. Jan. 2013. URL: <https://www.preposterousuniverse.com/blog/2013/01/04/the-world-of-everyday-experience-in-one-equation/> (visited on 05/19/2022).
- [9] M. D. Schwartz. *Quantum Field Theory and the Standard Model*. Cambridge University Press, Dec. 2013. ISBN: 9781108985031. DOI: 10.1017/9781139540940.
- [10] D. Griffiths. *Introduction to Elementary Particles*. Physics Textbook. Weinheim: Wiley, 2008. ISBN: 978-3-527-61847-7.
- [11] M. Krämer. *The Standard Model of Particle Physics*. Cern, July 2017. URL: https://indico.cern.ch/event/632201/attachments/1491025/2317647/mkraemer_CERN_2017_SM4.pdf.
- [12] F. J. Dyson. “Divergence of Perturbation Theory in Quantum Electrodynamics”. In: *Phys. Rev.* 85.4 (Feb. 1952), pp. 631–632. DOI: 10.1103/PhysRev.85.631.
- [13] M. Flory, R. C. Helling, and C. Sluka. *How I Learned to Stop Worrying and Love QFT*. Jan. 2012. DOI: 10.48550/arXiv.1201.2714. arXiv: 1201.2714 [hep-th, physics:math-ph].
- [14] R. Penco. “An Introduction to Effective Field Theories”. In: *arXiv:2006.16285 [hep-th]* (June 2020). arXiv: 2006.16285 [hep-th].
- [15] S. Weinberg. “On the Development of Effective Field Theory”. In: *EPJ H* 46.1 (Mar. 2021), p. 6. ISSN: 2102-6467. DOI: 10.1140/epjh/s13129-021-00004-x.
- [16] K. Fukushima and T. Hatsuda. “The Phase Diagram of Dense QCD”. In: *Rep. Prog. Phys.* 74.1 (Dec. 2010), p. 014001. ISSN: 0034-4885. DOI: 10.1088/0034-4885/74/1/014001.

- [17] A. Andronic et al. “Hadron Production in Ultra-Relativistic Nuclear Collisions: Quarkyonic Matter and a Triple Point in the Phase Diagram of QCD”. In: *Nuclear Physics A* 837.1 (June 2010), pp. 65–86. ISSN: 0375-9474. DOI: 10.1016/j.nuclphysa.2010.02.005.
- [18] G. Baym et al. “From Hadrons to Quarks in Neutron Stars: A Review”. In: *Rep. Prog. Phys.* 81.5 (Mar. 2018), p. 056902. ISSN: 0034-4885. DOI: 10.1088/1361-6633/aaae14.
- [19] R. Hagedorn. “Hadronic Matter near the Boiling Point”. In: *Nuovo Cimento A (1965-1970)* 56.4 (Aug. 1968), pp. 1027–1057. ISSN: 1826-9869. DOI: 10.1007/BF02751614.
- [20] N. Cabibbo and G. Parisi. “Exponential Hadronic Spectrum and Quark Liberation”. In: *Physics Letters B* 59.1 (Oct. 1975), pp. 67–69. ISSN: 0370-2693. DOI: 10.1016/0370-2693(75)90158-6.
- [21] S. Borsányi et al. “Is There Still Any Tcmystery in Lattice QCD? Results with Physical Masses in the Continuum Limit III”. In: *J. High Energ. Phys.* 2010.9 (Sept. 2010), p. 73. ISSN: 1029-8479. DOI: 10.1007/JHEP09(2010)073.
- [22] K. Adcox et al. “Formation of Dense Partonic Matter in Relativistic Nucleus–Nucleus Collisions at RHIC: Experimental Evaluation by the PHENIX Collaboration”. In: *Nuclear Physics A. First Three Years of Operation of RHIC* 757.1 (Aug. 2005), pp. 184–283. ISSN: 0375-9474. DOI: 10.1016/j.nuclphysa.2005.03.086.
- [23] B. B. Back et al. “The PHOBOS Perspective on Discoveries at RHIC”. In: *Nuclear Physics A. First Three Years of Operation of RHIC* 757.1 (Aug. 2005), pp. 28–101. ISSN: 0375-9474. DOI: 10.1016/j.nuclphysa.2005.03.084.
- [24] M. Troyer and U.-J. Wiese. “Computational Complexity and Fundamental Limitations to Fermionic Quantum Monte Carlo Simulations”. In: *Phys. Rev. Lett.* 94.17 (May 2005), p. 170201. DOI: 10.1103/PhysRevLett.94.170201.
- [25] D. T. Son and M. A. Stephanov. “QCD at a Finite Isospin Density: From the Pion to Quark-Antiquark Condensation”. In: *Phys. Atom. Nuclei* 64.5 (May 2001), pp. 834–842. ISSN: 1562-692X. DOI: 10.1134/1.1378872.
- [26] J. B. Kogut and D. K. Sinclair. “Quenched Lattice QCD at Finite Isospin Density and Related Theories”. In: *Phys. Rev. D* 66.1 (July 2002), p. 014508. DOI: 10.1103/PhysRevD.66.014508.
- [27] J. B. Kogut and D. K. Sinclair. “Lattice QCD at Finite Isospin Density at Zero and Finite Temperature”. In: *Phys. Rev. D* 66.3 (Aug. 2002), p. 034505. DOI: 10.1103/PhysRevD.66.034505.
- [28] J. B. Kogut and D. K. Sinclair. “Finite Temperature Transition for 2-Flavor Lattice QCD at Finite Isospin Density”. In: *Phys. Rev. D* 70.9 (Nov. 2004), p. 094501. DOI: 10.1103/PhysRevD.70.094501.
- [29] D. Sinclair and J. B. Kogut. “Searching for the Elusive Critical Endpoint at Finite Temperature and Isospin Density”. In: *Proceedings of XXIVth International Symposium on Lattice Field Theory — PoS(LAT2006)*. Vol. 32. SISSA Medialab, Dec. 2006, p. 147. DOI: 10.22323/1.032.0147.
- [30] B. B. Brandt, G. Endrődi, and S. Schmalzbauer. “QCD at Finite Isospin Chemical Potential”. In: *EPJ Web Conf.* 175 (2018), p. 07020. ISSN: 2100-014X. DOI: 10.1051/epjconf/201817507020.
- [31] B. B. Brandt, G. Endrődi, and S. Schmalzbauer. “QCD Phase Diagram for Nonzero Isospin-Asymmetry”. In: *Phys. Rev. D* 97.5 (Mar. 2018), p. 054514. DOI: 10.1103/PhysRevD.97.054514.
- [32] B. B. Brandt and G. Endrődi. “Reliability of Taylor Expansions in QCD”. In: *Phys. Rev. D* 99.1 (Jan. 2019), p. 014518. DOI: 10.1103/PhysRevD.99.014518.

- [33] B. Brandt and G. Endrodi. “QCD Phase Diagram with Isospin Chemical Potential”. In: *Proceedings of 34th Annual International Symposium on Lattice Field Theory — PoS(LAT-TICE2016)*. Vol. 256. SISSA Medialab, Mar. 2017, p. 039. DOI: 10.22323/1.256.0039.
- [34] D. T. Son and M. A. Stephanov. “QCD at Finite Isospin Density”. In: *Phys. Rev. Lett.* 86.4 (Jan. 2001), pp. 592–595. DOI: 10.1103/PhysRevLett.86.592.
- [35] M. G. Alford et al. “Color Superconductivity in Dense Quark Matter”. In: *Rev. Mod. Phys.* 80.4 (Nov. 2008), pp. 1455–1515. DOI: 10.1103/RevModPhys.80.1455.
- [36] F. Hajkarim et al. “Effects of the QCD Equation of State and Lepton Asymmetry on Primordial Gravitational Waves”. In: *Phys. Rev. D* 99.10 (May 2019), p. 103527. DOI: 10.1103/PhysRevD.99.103527.
- [37] M. M. Wygas et al. “Cosmic QCD Epoch at Nonvanishing Lepton Asymmetry”. In: *Phys. Rev. Lett.* 121.20 (Nov. 2018), p. 201302. ISSN: 0031-9007, 1079-7114. DOI: 10.1103/PhysRevLett.121.201302. arXiv: 1807.10815.
- [38] V. Vovchenko et al. “Pion Condensation in the Early Universe at Nonvanishing Lepton Flavor Asymmetry and Its Gravitational Wave Signatures”. In: *Phys. Rev. Lett.* 126.1 (Jan. 2021), p. 012701. DOI: 10.1103/PhysRevLett.126.012701.
- [39] J. M. Lee. *Introduction to Smooth Manifolds*. Springer Science & Business Media, 2003. ISBN: 978-0-387-95448-6.
- [40] M. E. Peskin and D. V. Schroeder. *An Introduction to Quantum Field Theory*. Reading, USA: Addison-Wesley, 1995. ISBN: 978-0-201-50397-5.
- [41] S. Weinberg. *The Quantum Theory of Fields: Volume 1: Foundations*. Vol. 1. Cambridge: Cambridge University Press, 1995. ISBN: 978-0-521-67053-1. DOI: 10.1017/CB09781139644167.
- [42] S. Weinberg. *The Quantum Theory of Fields: Volume 2: Modern Applications*. Vol. 2. Cambridge: Cambridge University Press, 1996. ISBN: 978-0-521-55002-4. DOI: 10.1017/CB09781139644174.
- [43] T. Brauner. “Spontaneous Symmetry Breaking and Nambu-Goldstone Bosons in Quantum Many-Body Systems”. In: *Symmetry* 2.2 (Apr. 2010), pp. 609–657. ISSN: 2073-8994. DOI: 10.3390/sym2020609. arXiv: 1001.5212.
- [44] C. G. Callan et al. “Structure of Phenomenological Lagrangians. II”. In: *Phys. Rev.* 177.5 (Jan. 1969), pp. 2247–2250. DOI: 10.1103/PhysRev.177.2247.
- [45] S. Coleman, J. Wess, and B. Zumino. “Structure of Phenomenological Lagrangians. I”. In: *Phys. Rev.* 177.5 (Jan. 1969), pp. 2239–2247. DOI: 10.1103/PhysRev.177.2239.
- [46] L. A. Morrison. *Coleman-Callan-Wess-Zumino Construction*. July 2017. URL: http://scipp.ucsc.edu/~haber/archives/physics251_17/PHYS251_Presentation_L_Morrison.
- [47] G. Panico and A. Wulzer. “The Composite Nambu-Goldstone Higgs”. In: *arXiv:1506.01961 [hep-ph]* 913 (2016). DOI: 10.1007/978-3-319-22617-0. arXiv: 1506.01961 [hep-ph].
- [48] A. Pich. *Effective Field Theory with Nambu-Goldstone Modes*. Jan. 2020. arXiv: 1804.05664.
- [49] H. Watanabe and H. Murayama. “Effective Lagrangian for Nonrelativistic Systems”. In: *Phys. Rev. X* 4.3 (Sept. 2014), p. 031057. ISSN: 2160-3308. DOI: 10.1103/PhysRevX.4.031057. arXiv: 1402.7066.
- [50] S. Scherer. *Introduction to Chiral Perturbation Theory*. Oct. 2002. arXiv: hep-ph/0210398.
- [51] J. Gasser and H. Leutwyler. “Chiral Perturbation Theory to One Loop”. In: *Annals of Physics* 158.1 (Nov. 1984), pp. 142–210. ISSN: 0003-4916. DOI: 10.1016/0003-4916(84)90242-2.

- [52] J. Gasser and H. Leutwyler. “Chiral Perturbation Theory: Expansions in the Mass of the Strange Quark”. In: *Nuclear Physics B* 250.1 (Jan. 1985), pp. 465–516. ISSN: 0550-3213. DOI: 10.1016/0550-3213(85)90492-4.
- [53] H. Leutwyler. “On the Foundations of Chiral Perturbation Theory”. In: *Annals of Physics* 235.1 (Oct. 1994), pp. 165–203. ISSN: 0003-4916. DOI: 10.1006/aphy.1994.1094.
- [54] N. K. Glendenning. *Compact Stars: Nuclear Physics, Particle Physics and General Relativity*. Springer Science & Business Media, Dec. 2012. ISBN: 978-1-4684-0491-3.
- [55] J. B. Hartle. *Gravity: An Introduction to Einstein’s General Relativity*. June 2021. DOI: 10.1017/9781009042604.
- [56] S. Weinberg. *Gravitation and Cosmology: Principles and Applications of the General Theory of Relativity*. New York: Wiley, 1972. ISBN: 978-0-471-92567-5.
- [57] C. W. Misner, K. S. Thorne, and J. A. Wheeler. *Gravitation*. Dec. 2009. ISBN: 978-0-691-17779-3.
- [58] J. R. Oppenheimer and G. M. Volkoff. “On Massive Neutron Cores”. In: *Phys. Rev.* 55.4 (Feb. 1939), pp. 374–381. DOI: 10.1103/PhysRev.55.374.
- [59] R. C. Tolman. *Relativity, Thermodynamics, and Cosmology*. The International Series of Monographs on Physics. Oxford: Clarendon Press, 1934.
- [60] S. Chandrasekhar. “The Highly Collapsed Configurations of a Stellar Mass. (Second Paper.)” In: *Monthly Notices of the Royal Astronomical Society* 95.3 (Jan. 1935), pp. 207–225. ISSN: 0035-8711. DOI: 10.1093/mnras/95.3.207.
- [61] H. J. Lane. “On the Theoretical Temperature of the Sun, under the Hypothesis of a Gaseous Mass Maintaining Its Volume by Its Internal Heat, and Depending on the Laws of Gases as Known to Terrestrial Experiment”. In: *American Journal of Science* s2-50.148 (July 1870), pp. 57–74. ISSN: 0002-9599, 1945-452X. DOI: 10.2475/aj.s2-50.148.57.
- [62] J. O. Andersen. *Introduction to Statistical Mechanics*. Akademika forlag, 2012. ISBN: 978-82-321-0105-4.
- [63] J. I. Kapusta and C. Gale. *Finite-Temperature Field Theory: Principles and Applications*. Second. Cambridge Monographs on Mathematical Physics. Cambridge: Cambridge University Press, 2006. ISBN: 978-0-521-82082-0. DOI: 10.1017/CB09780511535130.
- [64] C. E. Rhoades and R. Ruffini. “Maximum Mass of a Neutron Star”. In: *Phys. Rev. Lett.* 32.6 (Feb. 1974), pp. 324–327. DOI: 10.1103/PhysRevLett.32.324.
- [65] S. Chandrasekhar. “Dynamical Instability of Gaseous Masses Approaching the Schwarzschild Limit in General Relativity”. In: *Phys. Rev. Lett.* 12.4 (Jan. 1964), pp. 114–116. DOI: 10.1103/PhysRevLett.12.114.
- [66] K. S. Thorne. “The General-Relativistic Theory of Stellar Structure and Dynamics”. In: *pp 166-280 of High-Energy Astrophysics. Gratton, L. (ed.). New York and London, Academic Press, 1966.* (Oct. 1968). URL: <https://www.its.caltech.edu/~kip/index.html/PubScans/II-12.pdf> (visited on 02/11/2022).
- [67] G. Ecker. “Chiral Perturbation Theory”. In: *Progress in Particle and Nuclear Physics* 35 (Jan. 1995), pp. 1–80. ISSN: 01466410. DOI: 10.1016/0146-6410(95)00041-G. arXiv: hep-ph/9501357.
- [68] H. W. Fearing and S. Scherer. “Extension of the Chiral Perturbation Theory Meson Lagrangian to Order p^6 ”. In: *Phys. Rev. D* 53.1 (Jan. 1996), pp. 315–348. DOI: 10.1103/PhysRevD.53.315.
- [69] R. Urech. “Virtual Photons in Chiral Perturbation Theory”. In: *Nuclear Physics B* 433.1 (Jan. 1995), pp. 234–254. ISSN: 05503213. DOI: 10.1016/0550-3213(95)90707-N. arXiv: hep-ph/9405341.

- [70] P. Adhikari, J. O. Andersen, and P. Kneschke. “Two-Flavor Chiral Perturbation Theory at Nonzero Isospin: Pion Condensation at Zero Temperature”. In: *Eur. Phys. J. C* 79.10 (Oct. 2019), p. 874. ISSN: 1434-6044, 1434-6052. DOI: 10.1140/epjc/s10052-019-7381-4. arXiv: 1904.03887.
- [71] G. Ecker et al. “The Role of Resonances in Chiral Perturbation Theory”. In: *Nuclear Physics B* 321.2 (July 1989), pp. 311–342. ISSN: 0550-3213. DOI: 10.1016/0550-3213(89)90346-5.
- [72] J. B. Kogut and D. Toublan. “QCD at Small Nonzero Quark Chemical Potentials”. In: *Phys. Rev. D* 64.3 (July 2001), p. 034007. DOI: 10.1103/PhysRevD.64.034007.
- [73] M. K. Johnsrud and J. O. Andersen. *To Be Published*.
- [74] P. Adhikari, J. O. Andersen, and M. A. Mojahed. “Quark, Pion and Axial Condensates in Three-Flavor Finite Isospin Chiral Perturbation Theory”. In: *Eur. Phys. J. C* 81.5 (May 2021), p. 449. ISSN: 1434-6052. DOI: 10.1140/epjc/s10052-021-09212-7.
- [75] R. Dashen. “Chiral $SU(3) \otimes SU(3)$ as a Symmetry of the Strong Interactions”. In: *Phys. Rev.* 183.5 (July 1969), pp. 1245–1260. DOI: 10.1103/PhysRev.183.1245.
- [76] T. Das et al. “Electromagnetic Mass Difference of Pions”. In: *Phys. Rev. Lett.* 18.18 (May 1967), pp. 759–761. DOI: 10.1103/PhysRevLett.18.759.
- [77] S. Weinberg. “Precise Relations between the Spectra of Vector and Axial-Vector Mesons”. In: *Phys. Rev. Lett.* 18.13 (Mar. 1967), pp. 507–509. DOI: 10.1103/PhysRevLett.18.507.
- [78] P. A. Zyla et al. “Review of Particle Physics”. In: *Progress of Theoretical and Experimental Physics* 2020.8 (Aug. 2020), p. 083C01. ISSN: 2050-3911. DOI: 10.1093/ptep/ptaa104.
- [79] J. Bijnens and G. Ecker. “Mesonic Low-Energy Constants”. In: *Annual Review of Nuclear and Particle Science* 64.1 (2014), pp. 149–174. DOI: 10.1146/annurev-nucl-102313-025528.
- [80] M. Jamin. “Flavour-Symmetry Breaking of the Quark Condensate and Chiral Corrections to the Gell-Mann–Oakes–Renner Relation”. In: *Physics Letters B* 538.1 (June 2002), pp. 71–76. ISSN: 0370-2693. DOI: 10.1016/S0370-2693(02)01951-2.
- [81] M. A. Mojahed. “Two-Flavor Chiral Perturbation Theory at Finite Isospin beyond Leading Order”. Master’s Thesis. NTNU, 2020. URL: <https://ntnuopen.ntnu.no/ntnu-xmlui/handle/11250/2785552>.
- [82] P. Adhikari, J. O. Andersen, and M. A. Mojahed. “Condensates and Pressure of Two-Flavor Chiral Perturbation Theory at Nonzero Isospin and Temperature”. In: *Eur. Phys. J. C* 81.2 (Feb. 2021), p. 173. ISSN: 1434-6052. DOI: 10.1140/epjc/s10052-021-08948-6.
- [83] H. Abuki, T. Brauner, and H. J. Warringa. “Pion Condensation in a Dense Neutrino Gas”. In: *Eur. Phys. J. C* 64.1 (Aug. 2009), p. 123. ISSN: 1434-6052. DOI: 10.1140/epjc/s10052-009-1121-0.
- [84] V. I. Borodulin, R. N. Rogalyov, and S. R. Slabospitskii. *CORE 3.1 (Compendium of Relations, Version 3.1)*. Mar. 2017. arXiv: 1702.08246.
- [85] J. S. R. Chisholm. “Change of Variables in Quantum Field Theories”. In: *Nuclear Physics* 26.3 (Aug. 1961), pp. 469–479. ISSN: 0029-5582. DOI: 10.1016/0029-5582(61)90106-7.
- [86] S. Kamefuchi, L. O’Raifeartaigh, and A. Salam. “Change of Variables and Equivalence Theorems in Quantum Field Theories”. In: *Nuclear Physics* 28.4 (Dec. 1961), pp. 529–549. ISSN: 0029-5582. DOI: 10.1016/0029-5582(61)90056-6.
- [87] M. Laine and A. Vuorinen. *Basics of Thermal Field Theory: A Tutorial on Perturbative Computations*. 2016. ISBN: 978-3-319-31933-9. DOI: 10.1007/978-3-319-31933-9. arXiv: 1701.01554.
- [88] G. ’t Hooft. “Dimensional Regularization and the Renormalization Group”. In: *Nuclear Physics B* 61 (Sept. 1973), pp. 455–468. ISSN: 0550-3213. DOI: 10.1016/0550-3213(73)90376-3.